

# Spatio-temporal variation of fine and coarse mode carbonaceous aerosols in the National Capital Region

Thesis submitted to the Jawaharlal Nehru University  
in partial fulfillment of the requirements  
for the award of the degree of

DOCTOR OF PHILOSOPHY

NABA HAZARIKA



SCHOOL OF ENVIRONMENTAL SCIENCES

JAWAHARLAL NEHRU UNIVERSITY

NEW DELHI-110067, INDIA

2017



जवाहरलाल नेहरू विश्वविद्यालय  
Jawaharlal Nehru University  
SCHOOL OF ENVIRONMENTAL SCIENCES

New Delhi-110067

Tele. 011-26704303, 4304

*CERTIFICATE*


This is to certify that the work titled “Spatio-temporal variation of fine and coarse mode carbonaceous aerosols in the National Capital Region”, submitted to the School of Environmental Sciences, Jawaharlal Nehru University, New Delhi (India), in partial fulfillment of the requirements for the award of the degree of **Doctor of Philosophy**. This work is original and has not been submitted in part or full for any other degree or diploma of any other Institution or University.


  
Naba Hazarika

*(Student)*

  
Dr. Arun Srivastava

*(Supervisor)*

  
Dr. ARUN SRIVASTAVA  
Assistant Professor  
School of Environmental Sciences  
Jawaharlal Nehru University  
New Delhi-110067, India

  
Prof. Saumitra Mukherjee

  
प्रो.सौमित्र मुखर्जी / Prof. S. Mukherjee  
डीन / Dean  
पर्यावरण विज्ञान संस्थान  
School of Environmental Sciences  
जवाहरलाल नेहरू विश्वविद्यालय,  
Jawaharlal Nehru University  
नई दिल्ली-110067/New Delhi-110067

*Dedicated to.....*

*My Parents, Teachers*

*&*

*Jawaharlal Nehru University*

## *Acknowledgements*

*“All praise for the Almighty, the ultimate being”*

*I wish to express my eternal feelings to those, whose strong support and motivation made possible to present my research work in the form of thesis.*

*First of all, I would like to express my deepest sense of gratitude and special thanks to my supervisor Dr. Arun Srivastava, who believed in, encouraged and supported my efforts and provided intellectual stimulation, continuing exhilarating and sagacious guidance throughout the present study. His scholarly suggestions, prudent admonitions, immense interest, constant help, and affectionate behaviour have been a beacon of light for me. His cordial behaviour, humble attitude, generous mood, friendly nature, cooperativeness, and magnanimity are some of the exquisite traits which I would certainly like to cherish and emulate.*

*I sincerely thank Prof. S. Mukherjee, Dean of the School of Environmental Sciences for providing me an opportunity to work and avail the necessary departmental facilities during the course of this work and, sincerely, thank also goes to Ex. Deans Prof. K. G. Saxena, Prof. S. Bhattacharya, Prof. A. K. Attri and Prof. I. S. Thakur for the same. I feel grateful to Prof. V. K. Jain, for his help, guidance, and fruitful discussions during the entire work,*

*I would also like to thank my Doctoral Committee Members, Dr. P. Rajamoni and Dr. S. Sreekrish for giving inspiration, suggestions and support which helped in improving the quality of the research work,*

*I would like to convey special thanks to Vikas Kamal, Arunangshu Das, Sunita Maharia, Jitender K. Jakhar and Khalid Anwar for their immense help and contribution during the various steps of the entire work. Continuous support and help provided by Vikas Kamal and Sunita Maharia (for their valuable contribution in making figures) will remain worth mentioning. Dr. Ajai Kumar and Sandeep Sarpal of the Advanced Instrumentation Research Facility (AIRF) are duly acknowledged for their technical assistance. Special thank goes to Arunangshu Das for his collaborative contribution during various steps of analyses. Thanks are also go to Prof. M. S. M. Rawat, Dr. S. Bisht and Dr. V. Shridhar for their timely help in the analytical processes.*

*I am thankful to all the faculty members specially Prof. A. L. Ramanathan, Prof. U. Kulshrestha and Prof. J. Behari (Retired) of the school for their valuable suggestions during the work. I am also thankful to the CIF (specially Dr. P. D. Gaikwad, B. D. Sharma, Nitin Gedan, R. Bhardwaj and Rashmi Sinha) and office staffs of the School of Environmental Sciences (specially Mr. M. P. Guite, Mr. Umasankar, Mr. M. K. Prabhakar, Mr. Amrik Singh, Mrs. Raj Dulari, Mr. Vinod K. Chaudhary and Miss. Lalita Joshi) for providing me the necessary research and administrative facilities. I overwhelmingly acknowledge the services rendered by Anil Sharma for providing necessary chemicals and supporting materials in the entire research work.*

*I wish to express my gratitude to the Council of Scientific and Industrial Research, India for providing financial assistance in the research work. Financial assistance partially supported by the Jawaharlal Nehru University is also appreciated.*

*No words would be enough for expressing my gratitude towards my lab members for their immense support all throughout the tenure of my Ph.D., I am thankful to Sunita Maharia, Himanshu Lal, Rajesh Kushwaha, Bipasha Ghosh, Dudun Mehta, Anshul Srivastava, Richa Verma, Sumant Srivastava and Akash K. Singh whom support and humorous moments have created a very pleasant environment.*

*I am thankful to my classmates and colleagues Disha Sharma, Shivesh Berwal, Purnima Bhardwaj, Vinay P. Singh, Alok Pandey, Monoj Singh, Yogendra Singh and Hemant S. Shekhwat for their motivation and moral support. I would like to thank my M.Sc classmates and colleagues Vikas Kamal, Virendra B. Singh, Amit Kumar, Deepika Srivastava, Sapna Chourasiya, Yashpal Meena, Devendra S. Bikundia, Shyam Ranjan and Gyan P. Gupta for their constructive suggestions, and timely help in overcoming numerous problems.*

*I would specially like to mention the company of my colleagues Chandrashekar A. Vishwakarma, Neelesh Lodhi, Subhash Chandra and Abhishek Kumar for their wise counsel and scholarly guidance.*

*Words alone cannot express my gratitude I owe to my friends, Keshab A. Pegu, Owahedur Zaman, Nitul Dutta, Mitra Nath Khanikar, Mintu Sharma and Ajay Chakraborty who have stood by me in all circumstances. A special word of thank to all these friends specially Panjal P. Barua, Promod Singh, Monoj Das, Ankur J. Bhuyan, Tarun Gogoi, Jahidul Dewan, Kuheli Das, Partha P. Borah, Rintu Borah, Shyamjyoti Saikia, Bhaswati Das, Gautam Das, Nijara Deka and Chandramoni Bhattarai whose friendship is really an achievement in my life.*

*I cannot get through without mentioning my family members, villagers and all the well-wishers from my area of the district with the almighty who established a great courage, confidence, patience in me and firm determination for fulfilling my dreams. With gratitude and reverence, I would like to admire my parents who answered to all I needed, tolerated my idiosyncrasies and boosted my morale for the successful completion of the project. Words fall short to express my appreciation for my spouse (Parishmita Hazarika), sisters and brothers whose unconditional love have always cherished in hard times.*

*Regret and regards to those who have been close enough to be mentioned but not included by name in this acknowledgement. I also expect their grant of forgiveness and acknowledge their help and support.*

*Naba Hazarika*

# Contents

	<i>Page no.</i>
Certificate	
Acknowledgement	
List of tables	i
List of figures	iii
List of Abbreviations	vi
<i>Chapter 1 Introduction</i>	1
<i>Chapter 2 Materials and methods</i>	29
2.1. Study area	29
2.2.1. Sampling sites description	30
2.2. Instrumentation	32
2.2.1 Samplings	34
2.2.2 Analyses	38
2.2.3 Reagents and chemicals	39
2.2.4 Analytical quality assessments	39
2.2.5 Extraction processes and PAHs determination	40
2.3. Software used in the analytical processes	44
2.4. Chronic health risk assessments of PAHs	45
2.4.1 Cancer risk assessment of PAHs	48
<i>Chapter 3 Results and discussion</i>	50
3.1. Spatio-temporal variation of carbonaceous species and PAHs through the application of GIS	50

3.1.1. Contribution of TC, EC and OC at various sites and in different seasons	57
3.1.2. Seasonal variation of PAHs throughout the analyses	61
3.1.3. Ring wise distribution of PAHs across the sites	66
3.1.4. Variation of concentration of PAHs in fine (< 2.5 µm) and coarse (> 2.5 µm) mode aerosols across the sites	70
3.2. Relationships among different parameters, and the species	75
3.2.1. Relationship between PMs and meteorological parameters	75
3.2.2. Relationship between PMs associated with fine and coarse particles	75
3.2.3. Relationship plot between carbon and PAHs	76
4.1. Source apportionment of PAHs throughout the season	81
4.1.1 Application of molecular diagnostic ratio (MDR) and carbonaceous ratio, for source identification of PAHs and carbonaceous species	90
5.1. Health risk assessment of PAHs	100
5.2. Correlation matrices among PAHs and carbonaceous species	108
<i>Conclusions</i>	116
<i>References</i>	119
<i>Appendices</i>	
<i>Publications</i>	



## List of Tables

	<i>Page no.</i>
Table 1.1	19
Brief summary of carbonaceous aerosols from few literatures Published in the international scenario (2000 to 2017)	
Table 1.2	20
Summary of PAHs carried out throughout the international scenario with covering few literatures published from 2000 to 2017	
Table 2.1	31
Details of sampling sites and its geographical coordinates	
Table 2.2	34
Brief specifications of the impactors	
Table 2.3	42
PAHs standard (before the analyses of the samples in the first phase) along with the parameters such as Retention time, Area, Area % etc	
Table 2.4	44
PAHs standard (before the analyses of the samples in the second phase) along with the parameters such as Retention time, Area, Area % etc	
Table 2.5	47
Details of the sixteen US EPA priority PAHs and their some important physico chemical properties	
Table 2.6	48
Summary of the sixteen US EPA priority PAHs, its RfD (oral), RfC (inhalation), slope factor (oral) and inhalation unit risk as according to the IRIS, CalEPA and the WHO/TEF value based on a toxicity equivalent factor from the WHO or US EPA	
Table 3.1	63
Average concentration of PAHs (ng/m <sup>3</sup> ) and carbonaceous species (μg/m <sup>3</sup> ) throughout the seasons of the study	
Table 3.2	78
Correlation matrix between meteorological parameters with PMs	
Table 4.1	85
PCA for PAHs in monsoon season	
Table 4.2	85
PCA for PAHs in autumn season	
Table 4.3	86
PCA for PAHs in winter season	
Table 4.4	86
PCA for PAHs in spring season	
Table 4.5	87
PCA for PAHs in summer season	
Table 4.6	87
PCA for PAHs throughout the analyses	
Table 4.7	94
Ratio of PAHs congeners (MDR), and carbonaceous species for source identification in the monsoon season	
Table 4.8	95
Ratio of PAHs congeners (MDR), and carbonaceous species for source identification in the autumn season	
Table 4.9	96
Ratio of PAHs congeners (MDR), and carbonaceous species for source identification in the winter season	

Table 4.10	Ratio of PAHs congeners (MDR), and carbonaceous species for source identification in the spring season	97
Table 4.11	Ratio of PAHs congeners (MDR), and carbonaceous species for source identification in the summer season	98
Table 4.12	Ratio of PAHs congeners (MDR), and carbonaceous species for source identification throughout the years	99
Table 5.1 (a)	Average HQ of PAHs in the monsoon season	103
Table 5.1 (b)	Average ILCR of PAHs in the monsoon season	103
Table 5.2 (a)	Average HQs of PAHs in the autumn season	104
Table 5.2 (b)	Average ILCR of PAHs in the autumn season	104
Table 5.3 (a)	Average HQs of PAHs in the winter season	105
Table 5.3 (b)	Average ILCR of PAHs in the winter season	105
Table 5.4 (a)	Average HQs of PAHs in the spring season	106
Table 5.4 (b)	Average ILCR of PAHs in the spring season	106
Table 5.5 (a)	Average HQs of PAHs in the summer season	107
Table 5.5 (b)	Average ILCR of PAHs in the summer season	107
Table 5.6	Correlation matrix of PAHs and carbonaceous load in the monsoon season	110
Table 5.7	Correlation matrix of PAHs and carbonaceous load in the autumn season	111
Table 5.8	Correlation matrix of PAHs and carbonaceous load in the winter season	112
Table 5.9	Correlation matrix of PAHs and carbonaceous load in the spring season	113
Table 5.10	Correlation matrix of PAHs and carbonaceous load in the summer season	114
Table 5.11	Correlation matrix of PAHs and carbonaceous load throughout the study	115

## List of Figures

		<i>Page no.</i>
Fig. 2.1	Sampling sites of the National Capital Region (NCR), India	32
Fig. 2.2	(a) Outlook of Dekati PM <sub>10</sub> impactor, (b) The stages of the impactor are shown separately (from left-hand side: > 10, 2.5-10, 1-2.5, and <1 μm)	33
Fig. 2.3	(a) Outlook of Sioutas five-stage cascade impactor, (b) The stages of the impactor are shown separately (from the left-hand side: <0.25, 0.25-0.50, 0.50-1.0, 1.0-2.5 and >2.5 μm)	33
Fig. 2.3 (a)	Wind rose during the sampling period of Monsoon (July-Sept).	35
Fig. 2.3 (b)	Wind rose during the sampling period of Autumn (Oct & Nov).	35
Fig. 2.3 (c)	Wind rose during the sampling period of Winter (Dec & Jan).	36
Fig. 2.3 (d)	Wind rose during the sampling period of Spring (Feb & Mar)	36
Fig. 2.3 (e)	Wind rose during the sampling period of Summer (Apr - Jun).	37
Fig. 2.3 (f)	Wind rose during the sampling period of 2014-15.	37
Fig. 2.4	Chromatogram of the PAHs standard (for the first phase samples)	42
Fig. 2.5	Chromatogram of the PAHs standard (for the second phase samples)	43
Fig. 3.1	Spatial variation of TC throughout the seasons of the study period	53
Fig. 3.2	Spatial variation of EC throughout the seasons of the study period	54
Fig. 3.3	Spatial variation of OC throughout the seasons of the study period	55
Fig. 3.4	Spatial variation of PAHs throughout the seasons of the study period	56
Fig. 3.5	Carbonaceous load with sites and size ranges of particles in the monsoon season	59
Fig. 3.6	Carbonaceous load with sites and size ranges of particles in the autumn season	59
Fig. 3.7	Carbonaceous load with sites and size ranges of particles in the winter season	59
Fig. 3.8	Carbonaceous load with sites and size ranges of particles in the spring season	60
Fig. 3.9	Carbonaceous load with sites and size ranges of particles in the summer season	60
Fig. 3.10	Variation of carbonaceous load with sites throughout the study	60
Fig. 3.11	PAHs distribution in the monsoon season with sites	64
Fig. 3.12	PAHs distribution in the autumn season with sites	64
Fig. 3.13	PAHs distribution in the winter season with sites	64
Fig. 3.14	PAHs distribution in the spring season with sites	65
Fig. 3.15	PAHs distribution in the summer season with sites	65

Fig. 3.16	Total (average) PAHs distribution throughout the sites	65
Fig. 3.17	Ring wise distribution of PAHs in the a. monsoon and b. autumn seasons throughout the sites	67
Fig. 3.18	Ring wise distribution of PAHs in the a. winter and b. spring seasons throughout the sites	68
Fig. 3.19	Ring wise distribution of PAHs in the a. summer and b. throughout the sites	69
Fig. 3.20	Concentration variation of PAHs with < 2.5 and > 2.5 $\mu\text{m}$ at the site CPL	73
Fig. 3.21	Concentration variation of PAHs with < 2.5 and > 2.5 $\mu\text{m}$ at the site FBD	73
Fig. 3.22	Concentration variation of PAHs with < 2.5 and > 2.5 $\mu\text{m}$ at the site GBD	73
Fig. 3.23	Concentration variation of PAHs with < 2.5 and > 2.5 $\mu\text{m}$ at the site GGN	74
Fig. 3.24	Concentration variation of PAHs with < 2.5 and > 2.5 $\mu\text{m}$ at the site JNU	74
Fig. 3.25	Average concentration of PAHs with < 2.5 and > 2.5 $\mu\text{m}$ throughout the study	74
Fig. 3.26	PMs relationship with a. Temperature ( $^{\circ}\text{C}$ ), b. Relative humidity (%), c. Wind speed (Km/hr) and d. Dew point ( $^{\circ}\text{C}$ )	77
Fig. 3.27	Regressions among PMs ( $\mu\text{g}/\text{m}^3$ ) in < 2.5 and > 2.5 $\mu\text{m}$ with seasons (a-e) and throughout the study period (f)	79
Fig. 3.28	Regressions between the a. mean EC vs OC, b. TC vs EC, c. OC vs TC, and d. $\Sigma\text{PAHs}$ vs TC, OC and EC throughout the study	80
Fig. 4.1	Percentage contribution of PCs in the a. monsoon, b. autumn and c. winter seasons	88
Fig. 4.1	Percentage contribution of PCs in the d. spring, e. summer and f. average	89
Fig. 5.1	ILCR associated with < 2.5 and > 2.5 $\mu\text{m}$ in the monsoon season	103
Fig. 5.2	ILCR associated with < 2.5 and > 2.5 $\mu\text{m}$ in the autumn	104
Fig. 5.3	ILCR associated with < 2.5 and > 2.5 $\mu\text{m}$ in the winter season	105
Fig. 5.4	ILCR associated with < 2.5 and > 2.5 $\mu\text{m}$ in the spring season	106
Fig. 5.5	ILCR associated with < 2.5 and > 2.5 $\mu\text{m}$ in the summer season	107
Fig A1	Biplots between a. PC1 vs PC2, b. PC1 vs PC3, c. PC1 vs PC4 and d. PC2 vs PC3 in the monsoon season	i
Fig A2	Biplots between a. PC1 vs PC2, b. PC1 vs PC3, c. PC1 vs PC4 and d. PC2 vs PC3 in the autumn season	ii
Fig A3	Biplots between a. PC1 vs PC2, b. PC1 vs PC3, c. PC1 vs PC4 and d. PC2 vs PC3 in the winter season	iii
Fig A4	Biplots between a. PC1 vs PC2, b. PC1 vs PC3, c. PC1 vs PC4 and d. PC2 vs	

	PC3 in the spring season	iv
Fig A5	Biplots between a. PC1 vs PC2, b. PC1 vs PC3, c. PC1 vs PC4 and d. PC2 vs PC3 in the summer season	v
Fig A6	Biplots between a. PC1 vs PC2, b. PC1 vs PC3, c. PC1 vs PC4 and d. PC2 vs PC3 throughout the study period	vi

## Abbreviations

IARC	International Agency for Research on Cancer
Acen	Acenaphthene
Acnp	Acenaphthylene
AMS-PMF	Aerosol mass spectrometer- positive matrix factorization method
Anth	Anthracene
AQI	Air Quality Index
ATSDR	Agency for Toxic Substances and Disease Registry
BaAn	Benzo[a]anthracene
BaPn	Benzo[a]pyrene
BbFn	Benzo[b]fluoranthrene
BghiP	Benzo[ghi]perylene
BkFn	Benzo[k]fluoranthrene
BW	Average body weight
CalEPA	California Environmental Protection Agency
CCPI	Climate Change Performance Index
CDi	Chronic Daily Intake Dose
CF	Conversion factor
Chr	Chrysene
CPCB	Central Pollution Control Board
CPL	Connaught Place
DahA	Dibenzo[a,h]anthracene
ED	Duration of exposure
EF	Frequency of exposure

ENSO	El Niño-Southern Oscillation
EPI	Environmental Performance Index
FBD	Faridabad
Flun	Fluoranthene
Fluo	Fluorene
GBD	Ghaziabad
GC/FID	Gas Chromatography/ Flame Ionization Detector
GC/MS	Gas Chromatography/ Mass Spectrometry
GGN	Gurgaon
GIS	Geographical Information System
HAPs	Hazardous air pollutants
HI	Hazard Index
HPLC	High Performance Liquid Chromatography
HQ	Hazard Quotient
IcdP	Indeno[1,2,3-cd]pyrene
IDW	Inverse Distance Weighted
ILCR	Incremental Lifetime Cancer Risk
IMPROVE:	Interagency Monitoring of Protected Visual Environments
IR	Rate of inhalation and/or the rate of ingestion
IRIS	Integrated Risk Information System
JNU	Jawaharlal Nehru University
MDR	Molecular Diagnostic Ratio
MSTFA	[N-Methyl-N-(trimethylsilyl) trifluoroacetamide]
NAAQS	National Ambient Air Quality Standards
NAMP	National Air Quality Monitoring Programme

NCR	National Capital Region
NCT	National Capital Territory
Npth	Naphthalene
PAHs	Polycyclic Aromatic Hydrocarbons
PCA	Principal Component Analysis
Phtn	Phenanthrene
PMCAMx	A three dimensional regional chemical transport model
Pym	Pyrene
RAIS	Risk Assessment Information System
RfC	Chronic Inhalation Reference Concentration
RfD	Chronic Oral Reference Dose
SEARCH	Southeastern Aerosol Research and Characterization project
TEF	Toxic Equivalency Factor
TMDO/TMO	Thermal Manganese Dioxide Oxidation
TOA	Thermal Optical Carbon Analyzer
TOR	Thermal Optical Reflectance
TOT	Thermal Optical Transmittance
UNFCC	United Nations Framework Convention on Climate Change
US EPA	United States Environmental Protection Agency
VOCs	Volatile Organic Compounds
WHO	World Health Organization



## *Chapter 1 Introduction*

In the present scenario, due to continuous growth of urbanization and industrialization processes, the trend of increasing pattern of pollution have been given importance for their crucial role in the global environment. Pollutants of various form cause diverse health effects on human. This peril has got attention of various governmental/non-governmental agencies and other sectors and/or organizations. The economic growth and consumers are responsible for increasing pollutants of different categories. As far as concerning air pollution, the International Agency for Research on Cancer (IARC); a cancer agency of the World Health Organization (WHO), declares outdoor air pollutant as group I carcinogen (IARC, 2013). Although, natural processes are responsible for negligible amounts of particulate emission but, anthropogenic activities have a crucial role in the emission of pollutants. In 20<sup>th</sup>-21<sup>st</sup> centuries, some air pollution episodes provide a valuable attention among the civilizations such as Belgium in 1930 (Meuse Valley fog; resulted from industrial pollution and climatic condition), US in 1939 (severe smog at St. Louis due to coal burning), Los Angles in 1940 (Photochemical smog), US in 1948 (Donora smog, an air inversion phenomena), London in 1952 (Great smog, due to the emission of sulphur dioxide from coal fired power stations), China in 2013 (dense wave of smog, where fine particles rose to 1000  $\mu\text{g}/\text{m}^3$ ), India in 2016 (Great smog in Delhi) etc.

Public participation regarding understanding air pollution was raised in most of the developing and developed countries (Valavanidis et al., 2008). Environmental degradation due to anthropogenic activities plays an important role in India also. It is also reported that most of the populations living in urban environment face some diseases (non-communicable diseases). Vineis et al., (2014) reported a commentary on non-communicable diseases behind the responsible environmental factors and their impacts on epigenetic over globalization. Environmental exposures, which have a major contribution on human health, have under-recognized contribution toward non-communicable diseases too (Norman et al., 2013). Non-communicable diseases results 60% of all death across the world, where women are more prone to death (<http://www.wecf.eu>). 60% of the 31.3% Indian population living in urban areas suffered from non-communicable diseases such as cardiovascular complications, chronic lung diseases, stroke, injuries, accidents, cancer and diabetes during the period 2000 to 2012 (WHO, 2014). But, all of these non-communicable diseases are not basically related to environmental condition in nature. About 8 to 10% cardiovascular diseases have been established to link with

air pollution and occupation (Norman et al., 2013). In India, about 5.8 million inhabitants die every year due to non-communicable diseases, where one in every four persons is below the age of 70 years (WHO, 2015). Cardiovascular diseases, due to various factors over the two decades on the National Capital Region, India have been well reported by Prabhakaran et al., (2017).

The deterioration of environment related to the pollution and global warming are one of the consequences of climate change. Major evidences of climate change are global warming as a result of greenhouse effects, temperature rising, sea-level rising, melting of glacier/polar ice caps, and other drastic changes of weather. The other seasonal events linked with climatic phenomena such as El Niño, La Niña and El Niño-Southern Oscillation (ENSO) associated with equatorial pacific have also covered a global history. The Intergovernmental Panel on Climate Change (IPCC) produces reports on climate that supports the United Nations Framework Convention on Climate Change (UNFCCC). According to the United States Environmental Protection Agency (US EPA), regarding the greenhouse gases emissions; China contributes the highest followed by United States, European Union, India, Russia, Japan and the rest of other countries. Similar trend was also observed for the emission of CO<sub>2</sub> of the countries from China to Japan in 2016 (<https://www.statista.com>). Though various factors contribute the changing environment, the major global environmental issues which are faced by the civilizations are related to diverse aspects of climatic phenomena such as pollution, degradation of environment and resource depletion etc. As far as the Environmental Performance Index (EPI) is concerned in 2016, India ranks 141 with score 53.58 out of the total 180 countries, where Finland ranks first in this index released at the World Economic Forum. According to the report of the Germanwatch and Climate Action Network, Europe in 2017; the climate change performance index (CCPI) of India possesses 20<sup>th</sup> rank.

In case of air pollution, gases and the particulate matters suspended in various forms/phases such as solid, liquid etc. play a major role. The distribution of particulate pollutants in the atmosphere are called aerosol, is defined as suspended particulate matters. These particulate pollutants may be primary or secondary and cover a broad size ranges (from ultrafine to super coarse). Secondary particles which are newly formed can be in diameter  $\leq 1 \times 10^{-3}$  to  $2 \times 10^{-3}$   $\mu\text{m}$ , while re-suspension of dust (coarse dust) and sea salt particles can be  $\geq 100$   $\mu\text{m}$ . But, very large particles have short existence in the atmosphere (WHO, 2006). Primary air pollutants are emitted directly into air from factory (chimney) or the vehicle exhaust pipeline and through the re-suspension of contaminated dust by wind. But, the secondary air pollutants are formed in

the atmosphere itself. Ambient air pollution take place on a spatial scale ranges such as local (they are encountered only in appreciable concentrations close to the place where they are emitted, e.g., from specific industrial sources), urban (by vehicular/road traffic), regional (fine particles, i.e.,  $< 2.5 \mu\text{m}$  which transport long range) and hemispheric/global scale (such as greenhouse gases). Source wise, a more useful categorization of air pollutants are point sources (power stations), line sources (road vehicles and railways) and area sources (emissions from boilers). The emissions of particulate pollutants are related to the industrialization and vehicular transportations in urban areas.

The ambient (outdoor) particulate matters (PMs) ranges from 0.001 to 100  $\mu\text{m}$  in aerodynamic diameter, where the deposition pattern of particulate matters is different according to their size ranges such as nuclei mode ( $< 0.1 \mu\text{m}$ ), accumulation mode (between 0.1 and 1.0-2.5  $\mu\text{m}$ ) and coarse mode ( $> 1.0$  to 100  $\mu\text{m}$ ) respectively (Brook et al., 2003). The size segregated aerosols which can also be fractionated into fine ( $< 2.5 \mu\text{m}$ ) and coarse particles ( $> 2.5 \mu\text{m}$ ), can help in inference of emission sources and relative impacts on environment. In general, complex burning or combustion processes (fossil fuel, wastes and biomass burning) and industrial activities are responsible for the emission of fine particles whereas, mechanical processes govern coarser particles (Pant et al., 2016). It is believed that inhalation of fine fraction of aerosol ( $< 2.5 \mu\text{m}$  or  $\text{PM}_{2.5}$ ) is responsible for cardiopulmonary effects (Churg & Brauer, 1997; Brook et al., 2003; Pope & Dockery, 2006). US EPA's report represents that there are likely causal relationship between suspended particles with respiratory, cardiovascular morbidity and mortality (Laden et al., 2000; Russel & Brunekreef, 2009). Inhalable fine particles may travel deep into lungs whereas coarser particles may deposit on the upper respiratory tract (Lin et al., 2005). Besides fine and coarse fractions, attention on ultrafine particles ( $< 0.1 \mu\text{m}$ ) and their exposure issues have been given importance (Lin et al., 2005; Sioutas et al., 2005; Russel & Brunekreef, 2009; Delfino et al., 2010). Vehicles (mainly diesel operated) are responsible for emission of ultrafine to fine particles in the urban environment (Shirmohammadi et al., 2016). Finer particles possess specific higher surface areas and toxicity than the corresponding coarse particles (Lu et al., 2012).

Air pollutants that are major concern throughout the global scenario are the suspended particulate matters,  $\text{NO}_x$ ,  $\text{SO}_x$ ,  $\text{CO}$ ,  $\text{O}_3$  (ground level), polycyclic aromatic hydrocarbons (PAHs), volatile organic compounds (VOCs), hazardous air pollutants (HAPs) etc. The emission inventories as well as the air quality guidelines have been updated for the major components of

pollutants such as PMs, O<sub>3</sub>, NO<sub>x</sub> (mainly NO<sub>2</sub>) and SO<sub>x</sub> (mainly SO<sub>2</sub>). The outdoor pollutants are responsible to cause premature deaths due to the exposure of PM<sub>10</sub> which cause carcinogenicity, cardiovascular and respiratory diseases (WHO, 2016). It has also been reported that PM<sub>2.5</sub> are measured widely and routinely in the high-income countries whereas in the middle and low income countries the measurements are still to be taken (WHO, 2016). In India, the National Air Quality Monitoring Programme (NAMP), under the Central Pollution Control Board (CPCB, Government of India) measures the trends and status of ambient air quality in major town and cities. The four air pollutants namely: PM<sub>10</sub>, SPM, SO<sub>2</sub> and NO<sub>2</sub> have been regularly monitoring by NAMP at all the major locations/stations. Again, the National Ambient Air Quality Standards (NAAQS), under the CPCB (CPCB, 2009; Government of India) sets the standard levels of 12 major ambient air pollutants regarding industrial, rural, residential, ecologically sensitive and other areas. According to the NAAQS, the average concentration of PM<sub>2.5</sub> in annual and 24 hr standards are 40 and 60 µg/m<sup>3</sup> while, in case of PM<sub>10</sub> it is 60 and 100 µg/m<sup>3</sup>. A total of 8 major ambient air pollutants are included in the Air Quality Index (AQI) of India, which are categorized from good to severe (from 0-50 to 401-500) based on their likely health impacts.

The US EPA sets NAAQS for six major air pollutants (criteria pollutants), out of which particulate matters (such as PM<sub>2.5</sub> and PM<sub>10</sub>) are one of the major consideration. The important aspect of aerosol is urban and rural air quality and its associated health impacts. Size of PMs determines the chemistry of air quality and impacts on human health followed by making heterogeneous chemistry of mechanism in the environment (EPA, 1996; Seinfeld and Pandis, 1998, 2006). PMs results from short term (e.g. respiratory symptoms, lung inflammatory disorders, adverse effects on cardiovascular system, hospital admissions, mortality rate and increase in medication usage etc.) to long term health effects (e.g. reduction in lung function, increase in chronic obstructive pulmonary diseases, increase in lower respiratory symptoms, life expectancy reduction etc.) on human throughout the consequences of degradation of environment (WHO, 2006; Gurjar et al., 2010; Jimoda, 2012). According to the WHO in 2014, the air quality models reveals that about 92% population of the world lives at places where the level of air quality exceeds the prescribed limit of the annual mean concentration of PM<sub>2.5</sub> (10 µg/m<sup>3</sup>) (WHO, 2016). The carcinogenic nature of pollutants associated with particulate matters in the size ranges < 2.5 and < 10 µm (PM<sub>2.5</sub> and PM<sub>10</sub>) has covered a large chapter in the

chemistry of environment. It is also important to note that, the mechanism of PM<sub>2.5</sub> and PM<sub>10</sub> in relation to the human health is still unclear in the atmospheric chemistry (Harrison & Yin, 2000).

In case of the investigation of carbonaceous aerosol, particulate samples and their analyses have been carried out by researchers through various analytical methods/protocols. Research on carbonaceous species represents a vast diversity in the particulate aerosols, because they possess the largest fraction of the atmospheric aerosol (Gelencsér, 2005). The total carbon content (TC) is the composition of organic and elemental carbon (OC and EC). It is important to note that EC possess minor fractions of TC. As far as the thermal methods are concerned, the determinations of carbonaceous aerosols have been carried out in major pollution hot-spot cities. TC can be determined by elemental analysis. In the process of cloud nucleation, there is an important role of organic aerosol. The thermal method for the measurements of TC and EC was developed by Cachier et al., (1989), and later it was modified for low level aerosol samples by Lavanchy et al., (1999). Moreover, some thermal methods/protocols have been applied for the evaluation of particle bound carbonaceous species by various researchers so far (Megido et al., 2016).

Carbonaceous aerosols such as OC, EC fall in the classes of major air pollutants of interest associated with PMs of various form (TSP, PM<sub>2.5</sub> and PM<sub>10</sub>) emitted from dust storms, fuel burning (fossil fuel and biomass), biogenic sources, use of fertilizer and the conversion processes from gas to particle phases (IARC Monograph, 2016). In urban environment, PAHs and other carbonaceous pollutants are comparatively higher than rural inhabited area. It has also been reported that the dominant component of particulate matters emitted from diesel are EC and OC, whereas the PAHs can be considered as small quantity of OC emitted from diesel engine but are carcinogenic in nature (Lima et al., 2005; Ramanathan et al., 2007; Cheung et al., 2009; Bisht et al., 2015). Although, the carbonaceous materials disturb the earth radiation budget, the EC has the characteristic of positive radiative forcing by absorbing the incoming solar radiation (Xu et al., 2013; Panda et al., 2016), whereas the OC has the characteristic of scattering the Sun's radiation and responsible for negative radiative forcing which in turn affects the properties of aerosol and microphysical properties of clouds too (Jones et al., 2005). Although; the emission sources of carbonaceous components are different with respect to region and site specifications, but the fossil fuel combustion, incomplete combustion of biomass (such as wood, biogenic materials etc.) are the major responsible sources. Non-fossil related sources associated with particulate matters normally exceed 30% if biomass burning is not a responsible factor (Heal,

2014). The comparative studies of abundances of carbonaceous aerosols (mainly EC and OC fractions) in urban and residential sites have been conducted by various researchers where, significant change in concentration with season was observed (Vodička et al., 2015). The visibility and the air quality affected by aerosols are also a major concern these days (Křůmal et al., 2015). Tiwari et al., (2013) and Behera & Sharma (2015) reported that the overall contribution of carbonaceous aerosol regarding the PM mass possess 20% to 50% in urban atmosphere.

The chemistry of carbonaceous aerosol associated with particulate matters covers the global importance due to its crucial role comprising about 20% to 70% of atmospheric composition, which in turn affects the visibility by forming haze, and also causes environment heating and adverse health effects. Carbonaceous aerosols originating from man-made activities, biomass burning and forest fires in the south Asian atmosphere affects the air quality and climate, which further contributes about 50% of the total suspended particulate matters (TSPM) over the mid-latitude continental ambient atmosphere (Ram et al., 2008). EC leads aerosol induced global warming and also responsible for melting the Himalayan glaciers by depositing over ice/snow packs, while OC (can also be a mixture of organic compounds, e.g., PAHs, polychlorinated compounds, di-benzo derivatives/furans etc.), some of which are considerably carcinogenic in nature (Pachauri et al., 2013; Bisht et al., 2015).

PAHs or polyarenes and their derivatives represent major classes of organic compounds (Harvey, 1991). Probably, PAHs are the most widely distributed organic compounds which are potent carcinogen present in the environment. We expose daily to significant levels of PAHs in air we breathe, the food and water that we eat and drink. These ubiquitous compounds present in nature are thought to be having suspected carcinogenic and mutagenic characteristics (Ravindra et al., 2006). Determination of PAHs in the environmental particulate samples have been carried out for long through the extraction of appropriate organic solvents (by using organic solvents such as dichloromethane, hexane, acetone etc.) as according to the US EPA prescribed methods/protocols. After the extraction of PM filters, the observation made for PAHs estimation through various chromatographic techniques such as GC/MS (Gas Chromatography/ Mass Spectrometry), GC/FID (Gas Chromatography/ Flame Ionization Detector), HPLC (High Performance Liquid Chromatography) etc. have been well defined so far (Liu et al., 2001; Chang et al., 2006; Okuda et al., 2006; Liaud et al., 2015; Yan et al., 2015; Alves et al., 2016).

Both the natural and anthropogenic processes are responsible for the emission of PAHs in the environment. As far as the natural sources are concerned; volcanic eruptions, forest fires, erosion from ancient sediments and oil seeps from crude oil are the source contributors (Wang & Stout, 2010) whereas fossil fuel burning through various activities such as vehicular sources (diesel and gasoline combustion), industrial activities and coal burning; and biomass burning (wood burning) are the major anthropogenic sources of PAHs. Again, as according to temperature and the source of origin, PAHs can be classified into pyrogenic (hydrocarbons associated with combustion of fossil fuels such as petroleum, coal, coal tar and also from biomass burning), petrogenic (e.g., hydrocarbons emitted from rock deformation; hydrocarbons associated with petroleum including fuels, crude oil, lubricants and their derivatives) and biogenic (biological processes governed by microorganisms, phytoplankton/algae and plants or digenetic processes) respectively (Boehm, 2010; Wang & Stout, 2010; Stogiannidis & Laane, 2015; Abdel-Shafy & Mansour, 2016).

Spatial and temporal variations of particle phase carbonaceous load and PAHs have been carried out by various researchers throughout the globe (Narváez et al., 2008; Minguillón et al., 2008), some studies have focused the variation of size segregated particles with sites and season while some other studies have focused the variation in urban and rural areas respectively. Studies carried out for spatio-temporal variation of size differentiated particles (PM<sub>2.5</sub> and PM<sub>10</sub>) showed that OC and EC concentration were higher in PM<sub>10</sub> (Querol et al., 2008; Salvador et al., 2011). On the contrary, PM<sub>2.5</sub> was also found to be dominated by organic carbons than PM<sub>10</sub> in some cases (Chow et al., 1998). In most cases, the relative concentration of OC and EC were found to be higher in urban sites than rural (Chou et al., 2010; Zhang et al., 2012). Cao et al., (2007) observed the seasonal variation of OC and EC ( $\mu\text{g}/\text{m}^3$ ) in summer and winter, and found winter season to be possessed with higher carbonaceous concentration than summer season. In case of PAHs also, efforts have been made to observe the spatial and temporal variation in the major cities across the world like Zaragoza, Spain (Mastral et al., 2003), Menen, Belgium (Ravindra et al., 2007), Quito, Ecuador (Brachtel et al., 2009), Mexico City (Thornhill et al., 2008), New York City (Narváez et al., 2008). It was observed that the temporal variation of particle phase PAHs represented seasonal trend (Mastral et al., 2003). In comparison to the total concentration of PAHs, the monthly average concentration of PAHs in the winter months (December, January and February) was found to be higher (Ravindra et al., 2007). PAHs were observed in different concentrations with sites along with the significant diurnal variations (Brachtel et al., 2009).



Spatio-temporal variations of concentration of particulate PAHs (or atmospheric pollutants) not only represent its sources but also the trend of atmospheric processes that the particles undergo (Thornhill et al., 2008). Narváez et al., (2008) observed the spatial distribution of PAHs across the stationary sites and found decrease in concentration over the time period of the analyses.

The spatial distribution of particle bound species can be mapped through interpolating the software Geographical Information System (GIS) version (Briggs et al., 1997). In this regard, spatial and/or temporal variation of the species associated with PMs (such as PM<sub>2.5</sub> and PM<sub>10</sub>) have been observed to be reported from different cities/locations (Yu et al., 2004; Querol et al., 2008; Pistocchi et al., 2010; He et al., 2011; Anastasopoulos et al., 2012). In case of PAHs also, GIS based spatial distribution has been carried out on particulate samples at various cities (Noth et al., 2011; Inomata et al., 2013; Lee et al., 2016; Xu et al., 2016). The dynamic behavior of pollutants can be obtained by determining their spatial and temporal variations. This provides a very decisive approach in the major cities and sensitive sites, to prevent upcoming pollution, to assess health risks and to obtain good air quality (Cetin et al., 2017).

Particle bound species carried out for two years or more have been reported by various researchers so far (Halsall et al., 1994; Dab et al., 1996; Moon et al., 2008; Wang et al., 2010; Yang et al., 2010; Yang et al., 2011; Blanchard et al., 2014; Dubey et al., 2015; Xu et al., 2015b). PM bound species such as elements, PAHs and some other organic compounds are found to be carcinogenic. Toxicity or health risks are not only constraint with PMs, but the probable risks associated with humans have been observed to be linked with other species (such as O<sub>3</sub>, NO<sub>2</sub>, SO<sub>2</sub> etc.) also (WHO, 2016). The toxicological risk can be divided into two groups: non-carcinogenic and carcinogenic. The chronic health risks (in terms of hazard quotient; HQ) of species can be obtained by measuring the daily intake dose and from the chronic reference dose as according to the US EPA guidelines. IARC has established a programme on the evaluation of carcinogenic risk of individual chemicals to humans in 1969 (IARC Monographs, 2010). As far as PAHs are concerned, it has been observed that PAHs have potential risk on other species including animals and plants apart from humans (Kim et al., 2013). The carcinogenicity associated with PAHs has been developed by various organizations such as the WHO, Integrated Risk Information System (IRIS) under the US EPA, Agency for Toxic Substances and Disease Registry (ATSDR) etc. IARC has categorized the chemicals according to their carcinogenicity in different groups such as 1, 2A, 2B and 3; as carcinogen, probable carcinogen, possible carcinogen and not classified respectively. The categorization of carcinogenicity has also been

incorporated in the sixteen priority PAHs under the US EPA (IARC Monographs, 2016). As far as the priority PAHs are concerned, the compound Benzo(a)pyrene belongs to the group 1 carcinogen and Benzo[a]anthracene belongs to the group 2A under the IARC. Some of the US EPA priority PAHs are categorized into 2B group (Naphthalene, Chrysene, Benzo[b]fluoranthene, Benzo[k]fluoranthene, Indeno[1,2,3-cd]pyrene, Dibenz[a,h]anthracene), and some compounds are not discovered as carcinogenic hence are not incorporated into the IARC groups such as Acenaphthylene, Acenaphthene, Fluorene, Phenanthrene, Fluoranthene, Pyrene, and Benzo[ghi]perylene. The compound Anthracene is kept in group 3. There are three different exposure pathways of chemicals in human such as inhalation, ingestion and dermal respectively. Among all the exposure routes with respect to airborne PAHs, inhalation exposure has appeared to be the most potent and thus may cause lung cancer (Kim et al., 2013). Benzo(a)pyrene is the first PAHs discovered as carcinogen, which has potential to cause cancer in animals (Abdel-Shafy & Mansour, 2016).

In this study, from the literatures survey, excluding other species only the brief findings of results of the carbonaceous fractions (mainly TC, OC, and EC) and PAHs are highlighted. So far, many studies have been carried out pertaining to carbonaceous species and PAHs across the world some important are as follows:

Carbonaceous aerosols and PAHs associated with ambient atmosphere from rural and traffic sites of Ping Tung (Southern Taiwan, China) was studied by Chen et al., (1997) during September 1994-December 1995. They found ambient air of the traffic site, average concentration of OC and EC was 55.7 and 39.8  $\mu\text{g}/\text{m}^3$ . Concentration ratios OC/EC and TC/EC were decreased as the sampling height increased (height with 1.5 and 17 m at the traffic intersection point, 12 m at rural site respectively). Samplings carried out at height 1.5 m possessed with relatively higher concentration of both OC and EC. In  $\text{PM}_{10}$ , the contribution of TC (TC = OC+EC) and PAHs found to be > 93 %.

Fromme et al., (1998) carried out a study on carbonaceous species and PAHs in fine dust samples (< 10  $\mu\text{m}$ ) in Berlin during summer in 1995 and winter in 1996, emitted from inside a car and a sub-way train. From the car, during the sampling campaigns, the concentration of PAHs were 10.2 and 28.7  $\text{ng}/\text{m}^3$ , TC were 27.1 and 27.0  $\mu\text{g}/\text{m}^3$ , and EC were 14.1 and 8.2  $\mu\text{g}/\text{m}^3$  in summer and winter respectively; while, in the sub-way train during the seasons, the concentration of PAHs were 30.2 and 67.5  $\text{ng}/\text{m}^3$ , TC were 31.6 and 33.3  $\mu\text{g}/\text{m}^3$ , and EC were

10.9 and 6.9  $\mu\text{g}/\text{m}^3$  respectively. Among PAHs, in winter, the concentration of Benzo[a]pyrene was three to four folds higher than the summer season.

In view of practical importance due to the potential penetrating effects of fine particles in human health as well as its role in global climate, a winter time aerosol samples were collected in Albuquerque by Currie et al., (1999). In this study, the isotopic (unique), elemental/organic tracers and molecular markers were used for sources of aerosol. Koeber et al., (1999) carried out a study on carbon fractions and PAHs from PMs collected at Grosshadern and Luise-Kiesselbach-Platz, Germany during summer and winter in 1997. In his study, the derivatives of Benzo[a]pyrene diones (concentration ranges observed from 8.00 to 605.00  $\text{pg}/\text{m}^3$ ) were observed. Average concentration of TC (20.85  $\mu\text{g}/\text{m}^3$ ) and EC (9.70  $\mu\text{g}/\text{m}^3$ ) were found higher at Luise-Kiesselbach-Platz, than Grosshadern (TC; 5.99  $\mu\text{g}/\text{m}^3$  and EC; 2.09  $\mu\text{g}/\text{m}^3$ ).

Characterization of organic content associated with suspended particles of PM<sub>10</sub> fraction from an urban environment of Chile (Santiago) was carried out by Didyk et al., (2000) in 1991. They found average contribution of organic content (38%) was lower than other urban sites of pre regulatory levels (71%). PAHs of pyrogenic origins were formed by combustion processes such as petrochemicals and wood. The detection limit or precision for EC and OC was 0.2 and 0.1  $\mu\text{g}/\text{m}^3$  in the accuracy range of 4±6%. Total average suspended particles in PM<sub>10</sub> fraction were 250±88  $\mu\text{g}/\text{m}^3$ , where EC and OC concentrations were 30.6±20 and 52.4±20  $\mu\text{g}/\text{m}^3$ . These results confirmed that the values of EC and OC were higher by a factor 4-6 times of Los Angeles and in some urban areas of USA.

Distribution and concentrations of carbonaceous aerosols (EC and OC) associated with PM<sub>2.5</sub> and PM<sub>10</sub> were carried out at Kaohsiung, Taiwan by Lin & Tai, (2001) for the samples collected from November 1998 to April 1999. They observed that on average 21.2% of carbonaceous species were found in PM<sub>2.5</sub> and, while 18.1% was found in PM<sub>10</sub>. It was also observed that OC dominated the carbonaceous load, which contributed 70.4 and 72.2 % for TC in PM<sub>10</sub> and PM<sub>2.5</sub>. OC/EC ratios throughout the study were 2.6 (PM<sub>2.5</sub>) and 2.4 (PM<sub>10</sub>). This indicates the formation of secondary organic carbon (SOC) due to the gaseous precursor of the gas to particle conversion. In urban area of Kaohsiung, the minimum OC/EC ratios (1.53 and 1.61 for PM<sub>2.5</sub> and PM<sub>10</sub>) in all the samples were also used to obtain the SOC formation.

A study on carbonaceous species (EC and OC) in the atmospheric particles PM<sub>2.5</sub> and PM<sub>10</sub> in the Hong Kong city was carried out by Ho et al., (2002) for the samples collected during

the period from November 2000 to February 2001. In this study, mass ratios of  $PM_{2.5}/PM_{10}$  at three sites in Hong Kong were 0.53 (at Hok Tsui), 0.61 (at PolyU station) and 0.78 (at Kwun Tong station), which indicated the dominance of  $PM_{2.5}$  concentrations at rural and urban areas in Hong Kong. Maximum mean concentration of OC and EC ( $12.02$  and  $6.86 \mu\text{g}/\text{m}^3$ ) was found at PolyU station in  $PM_{10}$  among the sites; while in  $PM_{2.5}$ , maximum mean concentration of EC ( $7.95 \mu\text{g}/\text{m}^3$ ) at PolyU station and OC ( $10.16 \mu\text{g}/\text{m}^3$ ) at Kwun Tong station was observed. OC/EC ratio of  $PM_{2.5}$  and  $PM_{10}$  was  $< 2$  at the Kwun Tong and PolyU stations, while the ratio found to be exceeded at Hok Tsui station. Chemical characterization of fine particles emitted from wood of fireplace combustion in the southern US was carried out by Fine et al., (2002). In this study, OC and EC (wt %) were found higher in softwoods than hardwoods, and PAHs were not a major contributor of the combustion source. Fraser et al., (2002) carried out a study on particulate emission regarding fine particles from diesel operated heavy vehicle at Texas. In this study, significant variations was observed for particulate emission with respect to EC to TC, and the variation regarding PAHs was also found for petroleum biomarkers.

Total carbon content in terms of OC and black carbon (BC) associated with  $< 2.5$  and  $> 2.5 \mu\text{m}$  in 1999 and 2000 were carried out at urban and rural sites in Nairobi, at two towns of Meru and Nanyuki, Kenya by Gatari & Boman, (2003). Throughout the analyses showed that mean TC concentration was found higher two times in Nanyuki ( $14 \pm 2 \mu\text{g}/\text{m}^3$ ) than Meru ( $7 \pm 1 \mu\text{g}/\text{m}^3$ ), whereas observed BC concentration was found two times in Meru ( $1.4 \pm 0.1 \mu\text{g}/\text{m}^3$ ) than Nanyuki ( $0.72 \pm 0.06 \mu\text{g}/\text{m}^3$ ). Major sources of carbonaceous aerosols in Nairobi were the vehicular emission and burning of wastes. Similar interpretation were also drawn from the ratios of fine carbonaceous fractions such as BC/TC (0.05, 0.14 and 0.20 for the sites Nanyuki, Nairobi and Meru), OC/BC (4.3, 5.7 and 18 for the sites Meru, Nairobi and Nanyuki) and OC/TC (0.81, 0.86 and 0.93 for the sites Nairobi, Meru and Nanyuki) throughout the study.

The long term characterization of  $PM_1$ ,  $PM_{2.5}$  and  $PM_{10}$  was carried out for a span of 10 years (1993-2002) from the down wind of Leipzig, Melpitz in Germany by Spindler et al., (2004). In this study, an additional instrument/sampler was used weekly as  $PM_1$  collector for the determination of OC and EC content using a thermo-graphic processes. They observed that TC was 30% of the total  $PM_1$  mass. In this study, it was also observed that EC to TC percentage increased in summer during the period 1999-2002. TC was reduced in 2002 and the concentration of OC was heavily degraded than EC. During the period of summer, the weakly trend of the ratio of coarse to fine particles was higher by a factor 1.4 than winter ( $\sim 0.3$ ).

OC and EC were measured by different methods and/or techniques by various researchers from different institutions and organizations so far. Thermal Manganese Dioxide Oxidation and Thermal Optical Transmittance (TMDO and TOT) methods were applied by Park et al., (2005) for the determination of OC and EC in PM<sub>2.5</sub> from an urban site of Gwangju, Korea in 2001. Throughout this study, a good correlation was observed for TC between the said methods but, in case of EC, the observation made by TMDO was lower than the TOT method by about 20%, where relative bias and precision were 49.1% and 37.6% respectively. Air mass pathway and its effects during the sampling were found different from northwestern, western/southern and northeastern sites. Meanwhile, the different pathways of air mass were found responsible factor for variation of concentration of EC and OC levels.

Chemical characteristics and concentration variation PM bound species (such as elements, ionic species, oxides of N, S and C, and OC/EC) were studied at a down town and semi residential site in Beijing during August 2001 to September 2002 by Duan et al., (2006). Results of this study showed that the concentration of OC and EC were found higher during the winter (32.23 and 11.34  $\mu\text{g}/\text{m}^3$ ) than other seasons. Average concentration of OC and EC at the down town site were 22.86 and 10.26  $\mu\text{g}/\text{m}^3$ , while at semi residential site the concentration of OC and EC were 28.80 and 9.58  $\mu\text{g}/\text{m}^3$  respectively. Average ratio of OC/EC was found higher at both the sites in the winter and fall, but was comparatively lower in spring and summer. Comparatively, higher contribution of OC at the residential site represented residential cooking and heating.

Dry deposition of atmospheric aerosols in fine and coarse size range particles in relation to wet environment was carried out from different sites of Banyuls sur Mer, (Barcelona) during 2002-04 by Del Vento & Dachs, (2007). They found aerosol associated OC, EC and PAHs were measured in a particular months (March 2003) of the said period, where concentration of OC was in the range 5-11% when aerosols were deposited with sea water and other chemicals (Octanol, Linear alkyl benzene sulphonate etc.). The maximum deposition of EC was found 0.2%. In this study, the role of surface tension of water on aerosol deposition and PAHs was also covered. Aerosol ( $\text{mgm}^{-2}\text{d}^{-1}$ ) and PAHs ( $\text{ngm}^{-2}\text{d}^{-1}$ ) deposition with respect to octanol and surfactant ( $\text{mg}/\text{l}$ ) was observed. Maximum concentration of PAHs was found 1500 ng/g in December-2003.

Contribution of sources of carbonaceous aerosols of particulate matters (PM<sub>2.5</sub> and PM<sub>10</sub>) from three locations in the Tennessee valley region were studied by Ke et al., (2007) during

2001-2004. After analyses throughout this study, a total of eight sources were found with the help of chemical mass balance. Diesel emission ( $0.18 \mu\text{g}/\text{m}^3$ ), gasoline ( $0.35 \mu\text{g}/\text{m}^3$ ) and combustion of wood ( $0.92 \mu\text{g}/\text{m}^3$ ) were the main contributor of primary OC, where primary sources contributed 14%, 43% and 71% from the three sites respectively. In case of EC, wood burning ( $37\pm 33\%$ ) and diesel emission ( $66\pm 32\%$ ) was the major contributor. The concentration of PAHs (represented in  $\text{ng}/\text{m}^3$ ) was very low in comparison to EC and OC throughout the region.

To characterize chemical species (carbonaceous load, elements, ionic species and PAHs) adhered in  $\text{PM}_{2.5}$  from a background site of East Asia (Jeju Island), source apportionment through positive matrix factorization was carried out by Moon et al., (2008) during November 2001-August 2003. A total of fourteen probable sources were estimated for PM mass in this study. Natural sources contributed 20% of PM mass whereas, other primary man-made activities contributed approximately 34% particulate mass. Formation of secondary aerosol was responsible for major ionic and organic carbon which contributed approximately 39% of particulate mass. Carbonaceous (anthropogenic contribution) and secondary sources contributed > 50% of total particulate mass over all the seasons. Contribution of all the sources was highest in winter of February 2002 (~76%).

An investigation of  $\text{PM}_{2.5}$  bound organic species (OC, EC, n-Alkanes and PAHs) was carried out for the samples collected from the central eastern part, Golden town in British Columbia (due to numerous reported health effects of  $\text{PM}_{2.5}$ ) for a period of fifteen months during December 2005-February 2006 by Ding et al., (2009). They observed that PAHs contributed 1-65% mass of organic composition and its daily trend was 0.27 to  $100.24 \text{ ng}/\text{m}^3$ . OC/EC ratio and trend was also similar to  $\text{PM}_{2.5}$ . Though, no seasonal variation was observed for the organics, but significant levels during winter were observed. Good correlations between EC/petroleum biomarkers and EC/PAHs suggested a uniform source of emission such as vehicles (mainly motor vehicle) and space heater.

The chemical reactivity (redox potential) of OC/EC and PAHs associated with particulate matters ( $\text{PM}_{2.5}$  and ultrafine particles) was studied from an urban and a rural site of USA by Jeng (2010). It was observed that OC/EC and PAHs associated with ultrafine particles was higher than  $\text{PM}_{2.5}$ . Percent contribution of OC in ultrafine and  $\text{PM}_{2.5}$  were 59.7% and 22.8% respectively. Comparatively, higher redox potential of ultrafine particles was observed than  $\text{PM}_{2.5}$ . OC was the

abundant species in both the PM<sub>2.5</sub> and ultrafine mode particles after EC. Overall conclusion revealed that ultrafine particles were organic dominated, whereas PM<sub>2.5</sub> was dominated with inorganic species (elements).

Organic components along with sources, behaviors, temporal and spatial patterns were studied for the particulate matters confined to PM<sub>2.5</sub> from five sites of Metropolitan zones (Mexico valley) in 2006 by Amador-Muñoz et al., (2011). It was found throughout this study that organic matters (solvent extracted) and PM<sub>2.5</sub> were uniformly distributed regarding mass concentration (gravimetric) at all the valley sites. Concentration of targeted compounds was highest in dry period in comparison to rainy period. Fireworks and bonfires were the probable inputs of highest concentration of PM<sub>2.5</sub>, organic matters (OM) and PAHs. Among PAHs; Benzo[ghi]perylene was the dominant PAHs, but Fluoranthene and Anthracene were the most abundant nitro-dominated PAHs. OC, EC and Benzo[ghi]perylene were observed to be correlated with respect to dithiothreitol. OC determined by thermal analyses can be compared with solvent extracted OMs if it is divided by a factor 1.4 (Turpin and Lim, 2001).

Comparative study on carbonaceous species and PAHs in urban, rural and roadsides were carried out for size-segregated aerosols using low pressure impactor (LPI) from the three regions in Beijing, China by Duan et al., (2012). In this study, all the PAHs were observed to be enriched in fine size ranges of particles, i.e., in the accumulation mode, but in the nucleation mode the PAHs was absent due to the coagulation and higher concentration associated with fine particles. Correlation among OC, EC and PAHs was carried out for the estimation of related sources. Molecular Diagnostic Ratio (MDR) showed vehicular activities and burning of coal was the major emission sources of winter time PAHs. Grinding of debris of biomass was the probable sources of coarse OC. Fine EC were the output of pyrolysis of OC, but both man-made and natural processes were linked to EC.

Carbonaceous portion in size-differentiated particulate matters (viz., PM<sub>1</sub>, PM<sub>2.5</sub> and PM<sub>10</sub>) have been studied widely so far. Godec et al., (2012) studied the richness of carbonaceous load on the said fractions of particulate matters during the winter season in 2009 at Croatia. In this study, the average concentration of EC and OC were observed in the following trend of variation: PM<sub>10</sub> > PM<sub>2.5</sub> > PM<sub>1</sub>. The overall results revealed that in particle fraction average mass contribution of OC, EC and TC were PM<sub>10</sub> > PM<sub>2.5</sub> > PM<sub>1</sub>, PM<sub>2.5</sub> > PM<sub>10</sub> > PM<sub>1</sub> and PM<sub>10</sub> >

$PM_{2.5} > PM_1$ . Again, overall OC/EC ratio in the particulate fractions  $PM_1$ ,  $PM_{2.5}$  and  $PM_{10}$  was 5.4, 6.9 and 7.4 respectively.

The carbonaceous species associated with the TSPM from different urban and sub-urban sites of Dhaka, Bangladesh was observed by Salam et al., (2013). In this study, the average concentration of TC, OC and EC were found 81.2, 55.4 and 25.4  $\mu\text{g}/\text{m}^3$  in greater Dhaka, whereas the concentration of TC, OC and EC were less by a factor 52.25, 55.5 and 43.2 % respectively at suburban site than greater Dhaka. Here, OC contributed about 68% of TC, which might cause regional climate change and serious health impacts. In urban Dhaka, OC/EC ratio 2.17 represented the SOC formation rather than primary OC, whereas the ratio of sub-urban Dhaka (1.86) indicated primary source of OC.

The study of carbonaceous aerosols on size-differentiated particles has been playing an important role for the researchers in the atmospheric sciences. Spindler et al., (2013) carried out an investigation on  $PM_1$ ,  $PM_{2.5}$  and  $PM_{10}$  as well as its chemistry with season, and associated inflow of air mass from a rural site (Melpitz), Germany during the period 1992-2012. In this study, TC (component of OC and EC) were analyzed by two steps method (thermographic) through carbon analyzer. OC portion was vaporized at 650°C under nitrogen gas and was converted catalytically into  $\text{CO}_2$ . The retaining part (EC) was then converted into  $\text{CO}_2$  in presence of  $\text{O}_2$ . They observed that in  $PM_{10}$  EC concentration (along with calcium and sulphate) was decreased by 50%, 70% and 30% after 2003. In the north west and south east side of the region, different concentration of  $PM_1$ ,  $PM_{2.5}$  and  $PM_{10}$  was observed due to wind direction.

Emission of  $PM_{2.5}$  bound organic species was investigated at three sites in the southern US during 2006-10 by Blanchard et al., (2014). They observed significant correlations among OC, EC and non-polar organic compounds throughout the period of analyses. Among the organic species, a total of 32 PAHs were observed. All these observed/measured species were associated with specific types of emission that serve as tracers. Taiwo et al., (2014) reported a that fine particles emitted from industrial processes. In this study, besides elemental species, the major emission sources of OC/EC and PAHs were also reported. Carbonaceous pollutants (OC and EC) have been reported to be emitted from industrial activities, but PAHs are minor contributor of industrial emissions and also observed differ in various countries such as in UK, EU etc.

Atmospheric aerosols (TSP,  $PM_{2.5}$  and  $PM_{10}$ ) were collected for the observation of elemental loads, ionic species, OC and EC during heating and non-heating periods from August



2010 to June 2011 in Harbin, China by Huang & Wang, (2014). OC was found 2-5 times higher in heating period than the non-heating period, but EC was not found differ in these periods. In this study, during heating period the range of OC/EC ratio was 8 to 11; which was found much higher than the other Chinese cities (which was found 4 to 6). The major responsible sources concluded based on the Chemical mass balance (CMB) model were: vehicular traffic, coal burning, secondary organic carbon etc. It was also observed that before and after the heating period, crustal dust and industry (petrochemical) were predominant, whereas in the heating period coal burning and secondary sulphate were higher.

PM<sub>2.5</sub> bound carbonaceous aerosols (OC, EC) during regional biomass burning at Gosan, South Korea was observed by Nguyen et al., (2015). It was observed through the analyses that the concentration of EC and OC level was found higher and similar in trend in the pollution period than the strong Asian dust period, but the OC level was found reverse during the dust period. The concentration of OC in the strong Asian dust period was related to the biomass combustion (smoldering burning/combustion), but, in this period EC was decreased, OC and the ratio OC/EC were increased. OC/EC ratio confirmed biomass burning as a major factor of OC in the strong dust period. The SOC formed through long range atmospheric transport was also an important factor for OC at Gosan.

Effects of residential combustion processes on chemical species of particulate matters (collected on PM<sub>10</sub>) were carried out by Vicente et al., (2015) in Portugal. The analyzed OC and EC fractions in PM<sub>10</sub> showed that TC represented with weight 54-73% of mass regardless the types of wood and operating conditions throughout the study. OC was dominated in PM<sub>10</sub>, when higher loads were used into the chamber of combustion for two different fuels, i.e., pine (name: *Pinus pinaster*), and a beech (name: *Fagus sylvatica*). EC represented weight 8 – 35% of mass. Range of OC/EC was from 1.1 to 3.4 and 1.1 to 6.9 for beech and pine combustion respectively.

Vojtisek-Lom et al., (2015) carried out an analysis on polycyclic aromatic hydrocarbons (PAHs) emitted from diesel engine during the operation of bio-diesel and diesel fuels in Czech Republic. The relative contribution of carbonaceous loads was also covered, where genotoxicity associated with PAHs was observed on diesel and bio-diesel operated engines. In these analyses, it was concluded that the neat biodiesel had lower genotoxicity/carcinogenic PAHs than diesel under all operations. Emission of PAHs, carcinogenic PAHs and Benzo[a]pyrene were higher on diesel in comparison to bio-diesel operated engines under all conditions and/or operations.

Chemical characterization of particulate matters (in terms of OC, EC, PAHs, elements and ionic parameters), deposited from biomass fuel and ashes in the households from four villages of Nepal (southern central Himalaya of the Mt. Everest region) in June 2012 was carried out by Ielpo et al., (2016). In this study, outdoor deposited PMs was also analyzed. Biomass burning, residential cooking and ashes (chimney) were the major sources of indoor PMs. But, these emission sources significantly affected the outdoor PMs. Residential cooking and biomass burning were the major contributor of PAHs. OC concentration in indoor environment was found higher (two times) than the outdoor. PAHs were also found higher in indoor samples (particles and ashes) than outdoor. Biomass burning was the main source of PAHs at outdoor.

Source apportionment of PAHs in ambient atmosphere and concentration of OC and EC levels ( $\mu\text{g}/\text{m}^3$ ) in the particulate matters of size ranges  $\text{PM}_{2.5}$  and  $\text{PM}_{10}$  from the urban and traffic sites of northern Greece (Thessaloniki) was observed by Manoli et al., (2016) during the warm and cold periods of 2011-12. Here, average concentration of  $\text{PM}_{10}$  bound PAHs was in the range  $5.8 \text{ ng}/\text{m}^3$  (in the urban site) to  $9.3 \text{ ng}/\text{m}^3$  (traffic site). CMB apportionment on OC revealed that diesel vehicle, gasoline and wood burning were the important factors of emission.  $\text{PM}_{2.5}$  bound Benzo[a]pyrene associated with wood burning was in the range between  $7.0 \times 10^{-2}$  to  $8.0 \times 10^{-2} \text{ ng}/\text{m}^3$  in the traffic and urban background sites respectively. A study on the estimation of carbonaceous part (EC and OC) along with PAHs confined in  $\text{PM}_{2.5}$  in the summer and winter seasons from Guangzhou, China in 2012-13 was carried out by Wang et al., (2016). In this study, the source identification of carbonaceous portion was carried out through the CMB model; where vehicular transportations, combustion of coal and SOC were observed to be main factor of OC emission. Further, quality assurance (QA) and quality control (QC) processes were also followed for the quantification of  $\text{PM}_{2.5}$ .

The distribution pattern of carbonaceous species in  $\text{PM}_{2.5}$  and  $\text{PM}_{10}$  from three districts covering a total of six urban locations of the industrial city Baotou, northern China in 2014 was studied by Zhou et al., (2016). They observed that, the OC and EC content were observed in the same trend of variation in both the particles  $\text{PM}_{2.5}$  and  $\text{PM}_{10}$ , where a reverse trend was observed in the months of April and September in 2014. In this study, it was confirmed that the emission source of OC was same as  $\text{SO}_2$ , whilst the emission sources of EC was from vehicular exhaust and combustion processes. Correlations of EC and OC along with meteorological consequences implied that low relative humidity and high wind speeds were only the reducing factors of OC and EC in the months of January and November.

Cai et al., (2017) reported emissions of particulate constituents (OC, EC, PAHs and other organic parameters) associated with PM<sub>2.5</sub> from the Chinese vehicles. In this study, OC was found  $55.4 \pm 15.5\%$  mass of PM<sub>2.5</sub>. PAHs with > 5-rings were found to differ in diesel and gasoline vehicles, which distinguished the higher ring PAHs [Benzo(ghi)perylene and coronene] emitted from different types of fuels. In an another study, PMs collected on quartz fiber (used for TC and particulate phase PAHs estimations) and organic membrane (used for the observation of elemental load) filters emitted from heavy duty diesel engine were simultaneously carried out in China by Jin et al., (2017). In his study TC was found 90% of the total diesel particulate matter. It was also observed that the 3-rings PAHs contributed 66% mass of total PAHs followed by 4-rings (18%) and 2-rings PAHs (16%). Mitchell et al., (2017) reported the residential fuel combustion aspects between the UK and New Zealand; but models assumed that consumption of residential fuel to decrease (slightly) from 1990 to 2030 in New Zealand whereas, to increase in UK by a factor  $\sim 14$  in the same period. Xiong et al., (2017) carried out a study on PM<sub>2.5</sub> (associated carbonaceous constituents, ionic parameters, elemental load, PAHs), its source contributions along with the spatial and seasonal variations at three sites in Wuhan, China in 2011 and 2012. In this study, OC was observed to be emitted from different local emissions. Average total concentration of PAHs was found  $16.81 \pm 11.51 \text{ ng/m}^3$  in Wuhan, but in winter PAHs concentration was higher ( $26.92 \pm 12.34 \text{ ng/m}^3$ ) while it was lower in summer ( $5.08 \pm 3.44 \text{ ng/m}^3$ ).

Besides the literatures discussed so far, a brief summary of carbonaceous aerosols (TC, OC and EC) and PAHs reported by various researchers from the international scenario are given in the tabulated form (Tables 1.1 & 1.2). Only carbonaceous fractions and PAHs were highlighted from the literatures throughout both in the Tables 1.1 & 1.2.

**Table 1.1** Brief summary of carbonaceous aerosols from few literatures published in the international scenario (2000 to 2017).

Sample types	Observations	Methods	Country/city	Factors	References
TSP	TC, EC, OC	Carbon particulate monitor	Rome	Vehicular traffic	Avino et al., (2000)
PM <sub>2.5</sub>	OC, EC	<sup>a</sup> TMO	Korea	Anthropogenic and meteorological	Park et al., (2001)
PM <sub>2.5</sub>	TC, EC, OC	Elemental analyzer	Taiwan	Formation of SOC	Lin, (2002)
PM <sub>2.5</sub> & PM <sub>10</sub>	OC, EC	<sup>b</sup> TOR	China	Motor vehicle	Cao et al., (2003)
PM <sub>2.5</sub>	OC, EC	Thermal/optical carbon analyzer	Hong Kong	Indoor/outdoor	Ho et al., (2004)
PM <sub>2.5</sub>	OC, EC	<sup>c</sup> IMPROVE, <sup>d</sup> SEARCH	USA	Temporal and geographic variability	Yu et al., (2004)
PM <sub>2.5</sub>	OC, EC, WSOC	thermal/optical carbon analyzer	Nanjing	Coal combustion, vehicle, secondary aerosol, road/sea salt	Yang et al., (2005)
PM <sub>0.1-10</sub>	TC, BC	Elemental analyzer, Integrated sphere	Austria, Slovenia	Diesel exhaust,	Hitzenberger et al., (2006)
Soot-EC, Char-EC	EC, OC	TOR	USA	Diesel exhaust, gas, wood	Han et al., (2007)
Size-segregated particle	TC, OC, EC	Thermographic method	China	Transportation processes, industrial, domestic sources	Gnauk et al., (2008)
PM <sub>2.5</sub> , PM <sub>10</sub>	TC, EC, OC	<sup>e</sup> TOT	Spain	Industrial and domestic emission	De la Campa et al., (2009)
TSP, PM <sub>2.5</sub>	OC, EC	CHNS/O analyzer	Gdynia	Traffic intensity, industry, domestic heating	Lewandowska et al., (2010)
PM <sub>2.5</sub>	EC, OC	Carbon analyzer	China	Haze, domestic emission, transport mechanism	Hou et al., (2011)
PM <sub>10</sub>	TC, EC, OC	<sup>f</sup> TOA	Nordic	Anthropogenic, natural sources	Yttri et al., (2011)
PM <sub>2.5</sub>	TC, EC, OC	TOR	China	Atmospheric processes, downwind region	Huang et al., (2012)
PM <sub>1</sub> , PM <sub>2.5</sub>	OC, EC, BC	<sup>g</sup> AMS-PMF, OC/EC ratio method	China	Biomass burning, local sources	Huang et al., (2013)
PM <sub>2.5</sub>	OC, EC/BC	<sup>h</sup> PMCAMx	Europe	Wood combustion, pellet stoves	Fountoukis et al., (2014)
PM <sub>2.5</sub>	OC, EC	TOC/TOR	China	Biomass, coal, vehicle	Wang et al., (2015a)
PM <sub>2.5</sub>	OC, EC	T/OCR	Italy	Vehicle, biomass, wood	Pietrogrande et al., (2016)
PM <sub>2.5</sub>	OC, EC	Thermal analysis, IMPROVE	Hong Kong	Anthropogenic sources, personal activities	Fan et al., (2017)

<sup>a</sup>TMO: Thermal Manganese Dioxide Oxidation. <sup>b</sup>TOR: Thermal Optical Reflectance. <sup>c</sup>IMPROVE: Interagency Monitoring of Protected Visual Environments. <sup>d</sup>SEARCH: Southeastern Aerosol Research and Characterization project. <sup>e</sup>TOT: Thermal-optical transmission method. <sup>f</sup>TOA: Thermal Optical Carbon Analyzer. <sup>g</sup>AMS-PMF: Aerosol mass spectrometer- positive matrix factorization method.

<sup>h</sup>PMCAMx: a three dimensional regional chemical transport model

**Table 1.2** Summary of PAHs carried out throughout the international scenario with covering few literatures published from 2000 to 2017.

Sample types	Sampler used	Extraction process	Methods	ΣPAHs	Country/city	Responsible factors	References
PM <sub>&lt;0.32&gt;26</sub>	Cascade, rotary impactor,	C <sub>6</sub> H <sub>5</sub> (CH <sub>3</sub> )	GC-MS	10	Germany	Biogenic material, combustion sources	Kaupp & McLachlan, (2000)
Aerosol	High volume sampler	CH <sub>2</sub> Cl <sub>2</sub>	GC-MS	16	Macao	Vehicular traffic and residential heating	Shihua et al., (2001)
Aerosol	High volume sampler	(CH <sub>3</sub> ) <sub>2</sub> CO+C <sub>6</sub> H <sub>14</sub> + CH <sub>2</sub> Cl <sub>2</sub>	GC-MSD	20	Corpus Christi Bay	Dry/wet deposition, air-water gas exchange	Park et al., (2002)
PM <sub>2.5</sub> , PM <sub>10</sub>	Universal air sampler	CH <sub>2</sub> Cl <sub>2</sub> , petroleum ether (PE)	GC-MS	14	Chicago	Vehicular emission, industries	Vardar & Noll, (2003)
PM <sub>&lt;0.3&gt;7.4</sub>	High volume sampler	CH <sub>2</sub> Cl <sub>2</sub>	GC-MS	14	Gran Canaria	Vehicular emission, industries	Cancio et al., (2004)
PM <sub>10</sub>	High volume sampler	CH <sub>3</sub> CN	HPLC/FLD	13	Athens	Vehicular emission	Mantis et al., (2005)
PM <sub>&lt;0.49-&lt;10</sub>	Andersen Hi-Vol pumping	CH <sub>2</sub> Cl <sub>2</sub>	GC-MS	16	Guangzhou	Vehicular emission	Tang et al., (2006)
PM <sub>2.5</sub>	MOUDI	CH <sub>2</sub> Cl <sub>2</sub>	GC-MS	16	Korea	Vehicular activities, air stagnation.	Park et al., (2007)
PM <sub>2.5</sub> , TSP	Annular denuder, high volume sampler	CH <sub>2</sub> Cl <sub>2</sub>	HPLC	18	Korea	Vehicular traffic, industry, residential heating	Lee & Lee, (2008)
TSP	Medium-volume intelligent sampler	C <sub>6</sub> H <sub>12</sub> +C <sub>6</sub> H <sub>14</sub>	GC-MS	16	Beijing	Coal,, industry vehicle and gas	Zhang et al., (2009)
PM <sub>10</sub>	High volume sampler	CH <sub>3</sub> CN, CH <sub>3</sub> OH,	<sup>a</sup> UPLC-APCIToFMS	21	France	Seasonal	Mirivel et al., (2010)
Aerosol	GPS-11 (Thermo-Andersen Inc.)	(CH <sub>3</sub> ) <sub>2</sub> CO+C <sub>6</sub> H <sub>14</sub>	GC-MS	14	Turkey	Dry/wet deposition, air-soil gas exchange	Demircioglu et al., (2011)
Aerosol	Graseby Anderson	(CH <sub>3</sub> ) <sub>2</sub> CO+C <sub>6</sub> H <sub>14</sub>	GC-MS	11	Taiwan	Seasonal factors	Fang et al., (2012)
TSP	Air sampler	CH <sub>3</sub> CN	HPLC	16	Portugal	Seasonal and meteorological	Augusto et al., (2013)
PM <sub>1</sub> , PM <sub>2.5</sub> , PM <sub>10</sub>	Dekati PM <sub>10</sub> impactor	CH <sub>3</sub> CN	HPLC	16	France	Indoor emission	Liaud et al., (2014)
PM <sub>1</sub> , PM <sub>2.5</sub> , PM <sub>10</sub>	GRIMM monitor	CH <sub>3</sub> OH+CH <sub>2</sub> Cl <sub>2</sub>	GC-MS	16	Tehran	Mobile sources and gas	Hassanvand et al., (2015)
PM <sub>10</sub>	Air sampling apparatus	Multistage separation process	GC-MS	17	Portugal	Diesel vehicle, coal, wood	Albuquerque et al., (2016)
PM <sub>2.5</sub>	PM <sub>2.5</sub> sampler, PQ200	CH <sub>2</sub> Cl <sub>2</sub>	GC-MS	20	Taiwan	Unburned petroleum and traffic emission	Yang et al., (2017)

<sup>a</sup>UPLC-APCIToFMS: Ultra-performance liquid chromatographic atmospheric pressure chemical ionization time-of-flight mass spectrometric method

Study of PM bound carbonaceous species and PAHs, some of which have been carried out in the national scenario are discussed below. In this discussion, more emphasis are given on the studies carried out in northern India (mainly in the Delhi region) depending on the selected sites in this work.

Chemical species associated with PM<sub>10</sub> in urban (Cossipore) and rural (Kasba) sites of Kolkata during the period November 2003-November 2004 was studied by Karar & Gupta, (2007). In this study, PM<sub>10</sub> concentration was found higher at industrial site (maximum 401  $\mu\text{g}/\text{m}^3$ ) than the residential site (maximum 281  $\mu\text{g}/\text{m}^3$ ). Quantitative estimation carried out through PCA for the species (carbonaceous load, PAHs, metallic and ionic species) indicated that in the residential site; dumping of solid waste, vehicular activities, coal burning, cooking and crustal dust were the major emission factors of PM<sub>10</sub>; while in the industrial site, the sources of PM<sub>10</sub> was vehicular activities, coal burning, industry (electroplating), tyre wear and minor contribution of secondary aerosol formation. Approximately, 13% and 7% sources contributed from rural and industrial sites could not be linked due to source marker limitations.

Sources and temporal variations of carbonaceous species (OC and EC) from two sites of high altitude, western India (Mt. Abu) and north India (Manora Peak) were carried out by Ram et al., (2008). Throughout this analyses, abundances of both the species were observed two to three times higher in Manora Peak than Mt. Abu, where minimum concentration was found during April-August and maximum in winter (December to March). OC/EC ratio at both the sites was also compared and found higher than the urban sites. Low EC and higher OC/EC ratio were due to the dominance of OC derived from crop waste burning. Total average carbonaceous aerosol contribution to TSP was approximately 24% at Manora Peak and 15% at Mt. Abu. SOC contributed to OC focused its significant role related to the absorption and scattering of carbonaceous species on the regional scale.

The fine and coarse mode particulate carbonaceous fractions were carried out in urban atmosphere covering three sites from south, west and north parts of Delhi for the monsoon and post-monsoon period during June 2003-November 2003 by Singh et al., (2008). It was found that, the concentration of OC ( $\mu\text{g}/\text{m}^3$ ) in fine particles was found in the range from 25.61 (south) to 33.31 (north), while in coarse particles it was 31.11 (south) to 36.31 (west), and PM<sub>10</sub> contributed 56.73 to 68.55  $\mu\text{g}/\text{m}^3$ . In case of EC ( $\mu\text{g}/\text{m}^3$ ), in fine particles it was in the range

from 6.24 to 14.83 and in coarse particles it was 7.63 to 23.67, but PM<sub>10</sub> contributed 13.87 to 38.49 µg/m<sup>3</sup>. In this study, the average concentration of PM<sub>10</sub> was found 247.1±126.0 µg/m<sup>3</sup> throughout the study.

PAHs emitted from diesel fuel exhaust was carried out at service stations in Agra, India by Rajput & Lakhani, (2009). In this study, after investigation it was found that PAHs of low molecular weight were higher ( $4.40 \times 10^2 - 1.70 \times 10^3$  mg/l) and found dominant than other PAHs of high molecular weight in diesel fuels. On the contrary, high molecular weight PAHs were observed to be dominant in exhaust emissions. From this study, it was concluded that the emission of PAHs was found different with respect to both the diesel and exhaust emissions due to combustion processes. The ratio of PAHs in terms of output/input was observed from emission factors and fuel concentration. Carcinogenicity associated with PAHs were also observed through Toxic Equivalency Factor (TEF), where Benzo[a]pyrene and (Indeno[1,2,3-cd]pyrene + Dibenzo[a,h]anthracene) possessed significant contribution in the exhaust among the PAHs. Among fuel PAHs and the emission factors, a negative correlation was found.

EC and OC associated with PM<sub>2.5</sub> and PM<sub>10</sub> at the major urban environments, characterized by heavy vehicular activities were studied during May 2005-January 2006 by Kumar & Deshmukh, (2010). In this study, the range of EC (14.4 to 48.8 µg/m<sup>3</sup>) was found higher than OC (1.7 to 9.2 µg/m<sup>3</sup>). The ratio of OC/EC varied in the range 0.09 – 0.31. Average range of concentration of PM<sub>2.5</sub> and PM<sub>10</sub> was 87 to 160 and 133 to 492 µg/m<sup>3</sup> respectively. During the months May to July, PM<sub>10</sub> concentration was higher (425 to 520 µg/m<sup>3</sup>), but the PM<sub>2.5</sub> percentage in PM<sub>10</sub> was lowest, whereas a reverse trend was observed in August. Higher PM<sub>2.5</sub> percent could be linked with diesel emission. Concentration of PM<sub>2.5</sub> was in the range 140 to 180 µg/m<sup>3</sup> during winter but, PM<sub>10</sub> was sharply rose which could be due to the crustal dust and other commercial activities. OC and EC accounted a total of 3.6 to 9.2% and 20 to 48% of PM<sub>2.5</sub> respectively.

Chemical species and their abundances associated with PM<sub>10</sub> were studied from three urban residential sites of Delhi in 2009 by Sarkar et al., (2010). Here, it was found that the concentration of EC level was found 41 µg/m<sup>3</sup>. Peak level of OC was due to the secondary processes of aerosol transportation. During the day of firework event of this study, the highest contribution of PM<sub>10</sub>, TC, OC and EC were 616.8, 117.87, 74.74 and 45.0 µg/m<sup>3</sup>, and while

PAHs were 44.3 ng/m<sup>3</sup> respectively. Except OC in the site Mayur Vihar, the other species (PM<sub>10</sub>, TC and EC) were dominated in the site Mithapur on the firework day. PAHs were correlated with transportations which represented vehicular emissions as the primary source. PM<sub>10</sub> values observed to be 3-6 times higher than the standard level of the NAAQS but, it was 6-12 times higher than 24 hr air quality standards (50 µg/m<sup>3</sup>) of the WHO.

Carbonaceous species emitted from biomass burning adhered with PM<sub>2.5</sub> at Patiala in the Indo Gangetic Plain was investigated by Rajput et al., (2011). Throughout this study, mass concentration due to burning of wheat residues for EC, OC and PAHs was 4 µg/m<sup>3</sup>, 15 µg/m<sup>3</sup> and 7 ng/m<sup>3</sup> whereas; from burning of paddy residues it was 7 µg/m<sup>3</sup>, 92 µg/m<sup>3</sup> and 40 ng/m<sup>3</sup>, which was 4 to 5 times higher than wheat residues. Concentrations of EC and OC during burning of paddy residues varied from 3.8 – 17.5 µg/m<sup>3</sup> and 34 - 188 µg/m<sup>3</sup>, but significantly the concentration ranges of EC (2.3 to 8.9 µg/m<sup>3</sup>) and OC (9.0 to 58.0 µg/m<sup>3</sup>) was lower when bio and fossil fuel burnings were dominated. Decrease of OC/EC ratio suggested the emission of EC from fossil fuel. Total PAHs varied from 3.3 to 47.9 ng/m<sup>3</sup> due to the combustion of bio- and fossil fuels. Particulate bound 5-ring PAHs were higher in concentration (ng/m<sup>3</sup>) than the corresponding 6, 4 and 3-ring PAHs. PAHs isomer ratios suggested distinct pattern of emission from burning of paddy, wheat residues and fossil fuel.

Satsangi et al., (2012) reported the concentration variation of OC and EC in TSP from a sub-urban site of Agra (Dayalbagh), in a one year investigation in the Indo-Gangetic Plain. In this study, EC and OC contributed to TSP was 1.5% and 11.8% respectively. Average concentration (annual) of EC was lower in comparison to OC, while average OC/EC ratio was also higher. The trend of EC and OC was found highest in winter followed by post-monsoon, summer and monsoon seasons. Correlations between OC and EC were also found excellent in the range from 0.92 to 0.97 at all the four seasons of the study period. Concentration of OC was approximately three times higher in all other seasons than monsoon. Total carbonaceous load contributed about 20.8±17.2%, where winter contributed highest than rest of other seasons.

Sources, variability and characterization of OC and EC were measured during winter 2010-2011 in Delhi by Tiwari et al., (2013). This study revealed that mass concentration of EC, OC and PM<sub>2.5</sub> was 10±5, 54±39 and 210±146 µg/m<sup>3</sup>. Total carbonaceous mass load to the PM<sub>2.5</sub> was approximately 46%, where OC/EC average ratio was 5±2. Secondary organic aerosol



accounted 37  $\mu\text{g}/\text{m}^3$  in December, and it was 14.6  $\mu\text{g}/\text{m}^3$  in February. Correlation of significant value 0.71 for both OC and EC implied common emission sources. Variation of concentration of OC in the winter season was found highest, namely in the month of December; followed by November, January and February. While, in case of EC; the highest concentration was obtained in November; followed by December, January and February. Biomass combustion and evening vehicular loads were the major emission factors for higher contribution of EC and OC in the months November and December.

Chemical characterization, abundances of carbonaceous load and PAHs associated with  $\text{PM}_{2.5}$  in the northeast Himalayan region was carried out in the period 2009-2010 by Rajput et al., (2013). This study showed that the concentration variation of  $\text{PM}_{2.5}$  over the region was observed to be varied in the range from 39 to 348  $\mu\text{g}/\text{m}^3$ . The corresponding ratio of OC/ $\text{PM}_{2.5}$  was found exceeded than the upwind region of Indo Gangetic Plain. Total concentration of PAHs ranged from 4 to 46  $\text{ng}/\text{m}^3$ , with highest trend of variation. The ratio of OC/EC was also found higher with factor 10 to 15 in the region in comparison to the fossil fuel origin. The ratio of PAHs isomer reaffirmed that biogenic emission in the form of biomass combustion was the dominant sources over the region. Overall concentrations of PAHs ( $\text{ng}/\text{m}^3$ ); and OC, WSOC and EC ( $\mu\text{g}/\text{m}^3$ ) over the northeast Himalayan region were 14.1; and 35.4, 23.3 and 5.3 respectively. The transport mechanism of carbonaceous species (EC, OC and PAHs) was related to the cloud condensation nuclei and radiative forcing.

Rajput et al., (2014) carried out an investigation on carbonaceous aerosols adhered into  $\text{PM}_{2.5}$  originated from biomass burning and compared the ratio of isomers in the Indo Gangetic Plain of northern India. In this study, burning activities (poor and open burning) of the agricultural residues were the main source of emission of carbonic pollutants in the atmosphere. Isomer ratios of PAHs were observed for a period of two years in the site "Patiala", which were accounted from two different activities of biomass burning. PAHs with heavier rings (4 to 6 ring PAHs) were dominated the lighter rings (2 to 3 ring PAHs). Including the radio-carbon and molecular markers; diagnosis ratios were also used for the characterization of origin of sources such as: isomer of PAHs,  $\text{K}^+/\text{EC}$ ,  $\text{K}^+/\text{OC}$ ,  $\text{OC}/\text{EC}$  and  $\text{WSOC}/\text{OC}$ . Chemical proxies,  $\text{WSOC}/\text{OC}$  and  $\text{OC}/\text{EC}$  was significantly higher due to different combustion processes of biomass burning.

Variation of organic, inorganic and/or ionic compositions associated with PM<sub>10</sub> was carried out in urban environment of Delhi in 2010 by Sharma et al., (2014). This study showed that maximum chemical constituents and variation of strong PM<sub>10</sub> mass concentration was found in the winter season (36.1±11.6 µg/m<sup>3</sup> of OC, 9.64±2.56 µg/m<sup>3</sup> of EC and 213.1±14.9 µg/m<sup>3</sup> of PMs), whilst it was lower in the rainy season (14.72±6.95 µg/m<sup>3</sup> of OC, 3.35±1.45 µg/m<sup>3</sup> of EC and 134.7±39.9 µg/m<sup>3</sup> of PMs). The ratio of Cl<sup>-</sup>/EC and K<sup>+</sup>/EC with the corresponding values 0.59 and 0.28 indicated the role of biomass burning of PM<sub>10</sub>. The average contribution of the total mass concentration of PM<sub>10</sub> was found as: 21.7% secondary aerosol, 20.7% soil dust, 17.4% fossil fuel burning, 17% vehicular activities and 14.3% biomass combustion revealed by positive matrix factorization.

Emission sources of PM<sub>10</sub> bound particulate species were carried out in six Indian megacities/cities covering the sites Delhi, Kanpur, Mumbai, Chennai, Bengaluru and Pune by Gargava & Rajagopalan, (2015). In this study, CMB8 model was used to observe the contribution of sources for the major chemical species namely: carbonaceous portions, metals/metalloids and ions. PM<sub>10</sub> concentration was found in the order: Delhi > Mumbai > Bengaluru > Pune > Chennai > Kanpur. From 13.5 to 37% TC associated with PM<sub>10</sub> was related to burning and paved road dust. Delhi and Kanpur had the highest carbonaceous fractions; while in Kanpur, industrial monitoring sites recorded maximum carbonaceous load and PM<sub>10</sub>. In this study, it was concluded that PM<sub>10</sub> levels was found to exceed the limits of the NAAQS under the CPCB in 2009. Variation of carbonaceous load and its relative contribution with source can also be obtained and/or compared from other sites of the Indo Gangetic Plain, which has been observed so far (Rajput & Sarin, 2014; Ram & Sarin, 2015; Sharma et al., 2015; Singh et al., 2015).

Chemical characterization of PM<sub>2.5</sub>, at a polluted site in New Delhi was carried out by Pant et al., (2015a), in the winter and summer time 2013. Along with other species (elements, anhydrosaccharides, ions, and molecular markers); EC, OC and PAHs concentrations were compared in both the summer and winter seasons throughout this study. All the observed species were found to be dominated in winter season. In winter season, concentration of PM<sub>2.5</sub> exceeded the 24 hourly recommended limits of NAAQS, but in summer also the concentration was found higher in some occasions. EC and OC observed to be emitted from common sources such as biomass burning and vehicular traffic in both the season. The mean concentration of EC and OC

in summer season was 7.77 and 17.6  $\mu\text{g}/\text{m}^3$ , while in winter season it was 46.3 and 104.4  $\mu\text{g}/\text{m}^3$  respectively. Comparative study on chemical species adhered with suspended particulates have been carried out between the megacities New Delhi and Xi'an (Li et al., 2014a), and New Delhi and Birmingham (Pant et al., 2015b). Xi'an registered higher amount of suspended pollutants than New Delhi, whereas Birmingham experienced relatively higher elemental concentration and source contribution (in %) in comparison to New Delhi. Similarly, comparative results of dust originated chemical species have also found between the countries like India (at New Delhi and Bangaluru) and Vietnam (at Duong Kuang and Hanoi), carried out by Tue et al., (2014).

A study of carbonaceous pollutants associated with  $\text{PM}_{2.5}$  in two polluted cities of north India (Kanpur and Agra) was carried out during the year 2011-2012 by Villalobos et al., (2015). In this study, in the winter and summer seasons, average concentration of carbonaceous aerosols was found  $33\pm 21$  and  $23\pm 16$   $\mu\text{g}/\text{m}^3$  in the sites Kanpur and Agra respectively. Strong seasonal variation was observed in winter and summer seasons, where winter had the highest level of carbonaceous pollutants. Five predominant sources were found to be responsible for carbonaceous aerosols through organic tracers by applying CMB model. Monthly average concentration of PAHs was higher in Agra than Kanpur for the months December to April, whereas the carbonaceous portion (EC, OC and WSOC) contributed same pattern of variation which accounted highest in winter and lowest in summer throughout the study.

Coal mine area is also one of the major contributors of particulate emission in Indian environment. Roy et al., (2016) carried out a study on carbonaceous load, metals/metalloids and anionic species adhered into  $\text{PM}_{10}$  at the coalfield of Jharia, India during 2011-12. In this study, monitoring of air has been carried out as according to the prescribed protocol/methods available in CPCB/NAAQS, India. Average concentration of  $\text{PM}_{10}$  was highest in winter followed by post monsoon and summer season. Concentration of EC, OC and total carbonic aerosol (TCA) were 238.0, 19.5 and  $\sim 279$   $\mu\text{g}/\text{m}^3$  respectively. During the study period, OC/EC ratio was obtained 0.08. PAHs were analyzed through GC-MS, which contributed  $2.45\pm 0.82$   $\mu\text{g}/\text{m}^3$ . Meanwhile, mean concentration of organic OM (in  $\mu\text{g}/\text{m}^3$ ) and TCA/ $\text{PM}_{10}$  was 41 and 0.78 respectively.

Carbon rich aerosols namely: EC, OC, WSOC and along with the water soluble inorganic ionic species in  $\text{PM}_{2.5}$  and  $\text{PM}_{10}$  were measured from two cities of the western India (Jodhpur and Ahmedabad) in 2011 by Sudheer et al., (2016). In  $\text{PM}_{10}$  samples, carbon isotopic composition

( $\delta^{13}\text{C}$ ) was determined to obtain TC. In Ahmedabad, 80% EC was confined in  $\text{PM}_{2.5}$ , whereas in Jodhpur, 70% EC of  $\text{PM}_{10}$  was confined in  $\text{PM}_{2.5}$ . In Ahmedabad, an average concentration of 52% OC was associated with  $\text{PM}_{2.5}$ , but in Jodhpur, 80% OC was associated with  $\text{PM}_{10}$ . Both the organic carbon parts showed correlation with  $\text{K}^+$ , but not with EC, which in turn indicated biogenic contribution of OC. TC content in  $\text{PM}_{2.5}$ ,  $\text{PM}_{2.5-10}$  and  $\text{PM}_{10}$  in Jodhpur was 7.5, 32.6 and  $40.1 \mu\text{g}/\text{m}^3$ ; while in Ahmedabad it was 4.2, 3.3 and  $7.5 \mu\text{g}/\text{m}^3$  respectively. It was concluded that, a total of 80% OM in Jodhpur was associated with  $\text{PM}_{2.5-10}$ , whereas it was about 48% in Ahmedabad.

The air quality of the capital of India (Delhi) has been degraded and recorded as one of the most polluted cities in the world. Besides the sensitive and urban sites of the capital, the neighboring satellite towns/cities (National Capital Region) have also experienced higher atmospheric pollution due to industries, vehicular transportations as a result of complex anthropogenic activities (Hazarika & Srivastava, 2017). Though the exposure of PMs in terms of fine (Pant et al., 2017; Tyagi et al., 2017), and fine and coarse particles (Kumar et al., 2017a) have been studied throughout the capital region, the pollution scenario regarding carbonaceous load (Jaiprakash & Habib, 2017; Tyagi et al., 2017) and PAHs (Hazarika et al., 2017) have also been investigated. The implementation of odd-even trial on car also showed that the average hourly concentrations of  $\text{PM}_{2.5}$  and  $\text{PM}_{10}$  was reduced by  $\sim 74\%$  during the major trial hours; whereas daily mean concentrations of  $\text{PM}_{2.5}$  and  $\text{PM}_{10}$  was observed to be increased three times than the non-trial days (Kumar et al., 2017b).

In view of the literatures published throughout the world so far, the present investigation was an attempt to understand and estimate the carbonaceous aerosols and PAHs adhered into the particulate matters of different size ranges (fine and coarse particles). Required techniques/protocols were followed to determine the carbonaceous fractions (e.g., Lin and Tai, 2001; Dan et al., 2004; Duan et al., 2004; Duan et al., 2006; See & Balasubramanian, 2008; Sarkar et al., 2010; Sachdeva et al., 2013; Huang & Wang, 2014; Padhi et al., 2016) and PAHs (Li et al., 2014b; Liu et al., 2014; Wang et al., 2015b; Yan et al., 2015; Hazarika et al., 2017) from size differentiated particulate matters. In the light of the above discussions, to carry out the chemical characterization of PM bound carbonaceous load and PAHs, for the samples collected from five different sites in the National Capital Region, Delhi were undertaken with the following objectives:

1. To determine the carbonaceous load and their spatio-temporal variation on the proposed sites of locations.
2. To determine the contribution of carbonaceous load and PAHs in fine and coarse mode aerosols.
3. To carry out the source apportionment of the carbonaceous material.
4. To determine the influence of meteorological parameters on organic pollutants using appropriate statistical tool.
5. To determine the correlation between various fractions of organic aerosols.

The thesis is organized as follows: after introduction in the first chapter, the methodology about the proposed work followed during the experiments and/or analyses is provided in Chapter 2. In Chapter 3, spatio-temporal variations of carbonaceous species and PAHs are discussed. In this chapter, seasonal variation of carbonaceous species, ring wise distribution PAHs, relative variation of the particulate species with fine and coarse particles, the role of meteorological parameters on PMs, and regressions among the species are also covered. The source identification of carbonaceous load and PAHs are covered in Chapter 4. Health risk assessments of PAHs are described in Chapter 5. In this chapter, the correlation matrices among PAHs and carbonaceous species are also included. The conclusions part of the study are given after Chapter 5.

## *Chapter 2 Materials and methods*

### [2.1] Study area

The present work was carried out in the National Capital Region (NCR) of India. NCR of India comprises the whole National Capital Territory (NCT) of Delhi, which covers New Delhi as well as the three adjoining states namely: Haryana (in the northwest of Delhi), Rajasthan (in the southwest of Delhi), and Uttar Pradesh (in the southeast of Delhi). Delhi, the capital of India, is recognized as a city of one of the major problems of pollution in the globe according to the researchers and WHO, (2014). As far as the area is concerned, the capital (the National Capital Territory of India) shares 0.04% area in the nation, having with almost equal length and width (32 and 30 miles respectively). According to the 2011 census, entire capital experiences a home of dense populations, with growth of ~ 21% during 2001-11. The capital region is separated into the following three parts; the ridge (Aravalli ridge part), flood-plain of Yamuna (alluvial soil is covered throughout) and the part of plain. Latitudinal and longitudinal coordinates of the capital are 28.60° N and 77.10° E with an elevation of approximately 216 m (mean) of the sea level. Semi-arid climate is the characteristic of the capital, bears the sub-tropical belt with approximately 714 mm of unreliable rainfall during the monsoon months (July and August). A notable range of temperature variation in the capital has been observed in the winter and summer seasons. In winter it is found the lowest in the month of January of approximately  $\leq 1$  to 2°C (lowest ever recorded -2.2°C on 11<sup>th</sup> January, 1967), and in summer the maximum temperature reaches from 45 to 48°C in June. The capital experiences an annual average wind speed of 1–2 m/s (Srivastava and Jain, 2007a,b; Srivastava et al., 2008, 2009). A total of five different seasons can be seen in Delhi within the year, these are summer (April, May and June), monsoon (July, August and September), autumn (October and November), winter (December and January) and spring (February and March) respectively. Climate of Delhi is governed by two major winds: South west and western disturbances. At most of the seasons, the wind direction predominantly prevails from the west to the northwest, excluding the monsoon season, where it directs to the south west from the south. A comparatively higher pollutant load has been found and/or recorded in the winter season due to the temperature inversion and low mixing height (Hazarika et al., 2015).

The area of the NCR region covers approximately 58,332 km<sup>2</sup> at present; where inhabiting populations of more than 46 million are established according to the census, 2011. The rainfall pattern shows that the NCR have faced an average of three months in a year, the

monsoon/rainy months are only the input of the recharge of ground water. As far as the whole area is concerned, NCR covers two major geomorphic sections; these are the alluvial plain (covered by quartzitic ridge, belongs to the Indo Gangetic plains) and the flood-plain covered by passing across three major rivers: Yamuna, Ganga and Hindon. Southern and the south-western parts of the NCR are absence of any eternal rivers. Average rainfall of the NCR region varies in the range from 300 mm (western parts) to 850 mm (in the parts of north and north-eastern). Regarding the total area of the NCR, maximum temperature of the region has been found about 47°C in the summer months (from May to June), while the minimum temperature varies in the range from 7 to 21°C in the winter months (mainly January). In general, air is dry in majority of the NCR parts within the year, where dust induced aerosol originated due to rapid industrialization in some of the capital region, e.g., Faridabad (Pathak et al., 2013). Winds are light in winter and post-monsoon seasons whilst, these are strengthening during the months of monsoon and summer seasons, but prevailing winds of southeasterly and easterly are predominated in the monsoon season, again winter is associated with western disturbances.

### **[2.1.1] Sampling sites description**

The required samplings of size-differentiated particulate matters were done at five different sites in the NCR. Two sites were covered from Delhi. First site, the Connaught Place (characterized as urban/traffic site), is situated in the northern central part of Delhi, experiences very frequent with dense vehicular transportation and a famous financial, business and commercial locations of the capital, connects major busy roads such as Janpath, Panchkuian road, Barakhamba road, Minto road etc. This site is pride of the capital and accounts top heritage structure of New Delhi. Second, the Jawaharlal Nehru University is an urban, institutional cum residential area in the southwest Delhi. This area can also be characterized as sensitive and receptor site. It covers a broad acre of vegetation of natural origin. This site is located far away from the influence of industrial and other anthropogenic activities, but it is bordered by the three roads with enormous vehicular frequency. Ongoing building construction from 2009 onwards contributed dust-induced aerosol inside the campus.

From other parts of the NCR, three sites were covered: Faridabad, Ghaziabad and Gurgaon (also known as Gurugram). Faridabad is characterized by hub of major industrial site



leading one of the largest city (situated in the south east region of Haryana), in the vicinity of the Yamuna river. This site has the characteristic climate of hot semi-arid with an average rainfall of about 540 mm. Ghaziabad, is also popular as gateway of the state of Uttar Pradesh (situated in the east of Uttar Pradesh), is an industrial site which is connected by periphery roads and the network of railways. The meteorological parameters such as relative humidity (RH), temperature variation and rainfall patterns are almost similar to the capital. Gurgaon, is situated in the south west of Haryana, having annual average rainfall of about 710 mm. Day to day rapid growth of urbanization lead the city prone to the industrial, commercial and financial hub. The proposed sampling sites of the NCR are provided in Fig 2.1. Geographic locations along with code used for the individual sites are given in Table 2.1.

**Table 2.1** Details of sampling sites and its geographical coordinates

<b>Monitoring sites</b>	<b>Latitude</b>	<b>Longitude</b>	<b>Sites code</b>	<b>Description of sites</b>
Connaught Place	28.63°N	77.21°E	CPL	Commercial, business, financial
Faridabad	28.40°N	77.31°E	FBD	Commercial, industrial
Ghaziabad	28.66°N	77.45°E	GBD	Heavy transportation, industrial
Gurgaon	28.45°N	77.02°E	GGN	Business, heavy transportation
Jawaharlal Nehru University	28.54°N	77.16°E	JNU	Residential, Institutional, receptor

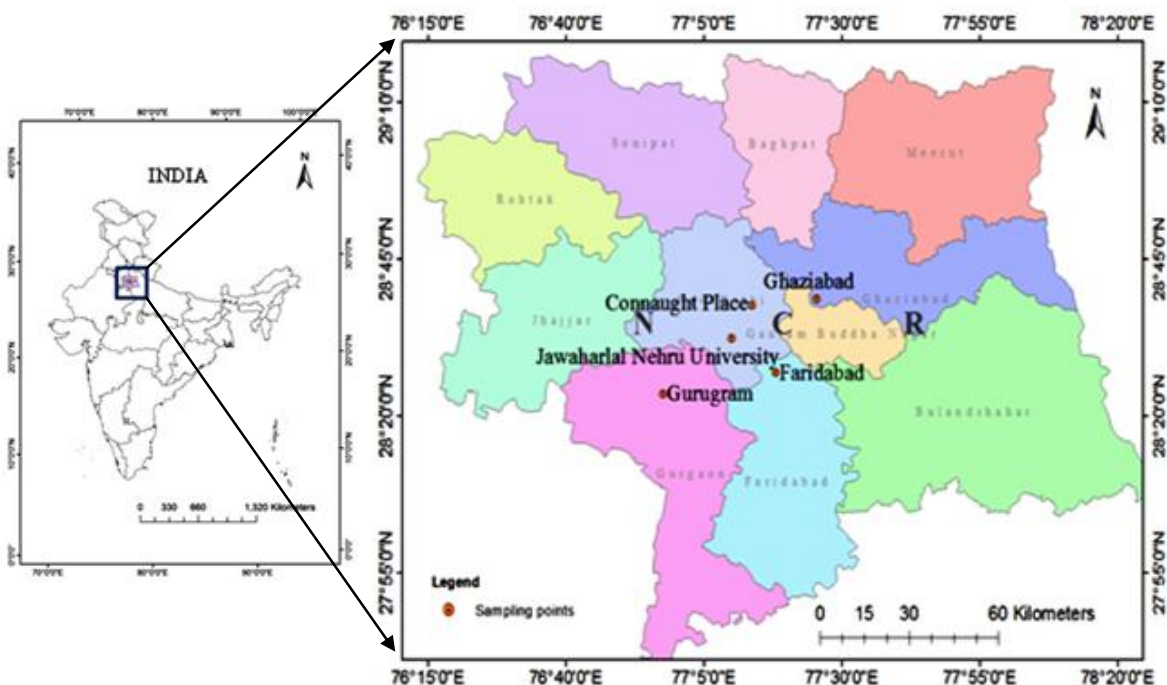


**Fig 2.1** Sampling sites of the National Capital Region (NCR), India

## [2.2] Instrumentation

The instruments used for sampling were “Dekati PM<sub>10</sub> impactor” (www.dekati.fi, Dekati Ltd. Finland, a three-stage cascade impactor) and “Sioutas cascade impactor” (www.skinc.com, Cat. no. 225-370). The instruments were kept on the rooftop of the buildings of the respective sites and run for twenty four hours. The samplers; Dekati PM<sub>10</sub> and Sioutas cascade impactors have characteristics to differentiate the particles into various size fractions as according to their design. The impactor “Dekati PM<sub>10</sub>” was used to collect the size-differentiated particulate matters: > 10, 2.5-10, 1-2.5 and < 1 μm; whereas, the “Sioutas cascade impactor”, a five stage sampler used to collect/deposit particulate matters of size ranges > 2.5, 1.0 to 2.5, 0.50 to 1.0, 0.25 to 0.50 and < 0.25 μm. According to the specifications of the samplers, “Dekati PM<sub>10</sub> impactor” was run at a flow rate of 30 L/min and “Sioutas five stage cascade impactor” optimized at a flow rate 9 L/min for twenty four hours at all the sites. The concentrations of the carbons and quantified PAHs are shown by taking averages throughout the study periods. Samples were collected on the recommended filters for both of the samplers/impactors. Verification of some samples collected through the high volume sampler (for PM<sub>10</sub> sampling) was also employed in the carbonaceous analyses. The samplers outlook (Dekati PM<sub>10</sub> and

Sioutas cascade impactors), which were used simultaneously during the whole sampling campaign and the deposition sizes are given in Figs 2.2 & 2.3. Brief specifications of these two instruments are also provided in Table 2.1.

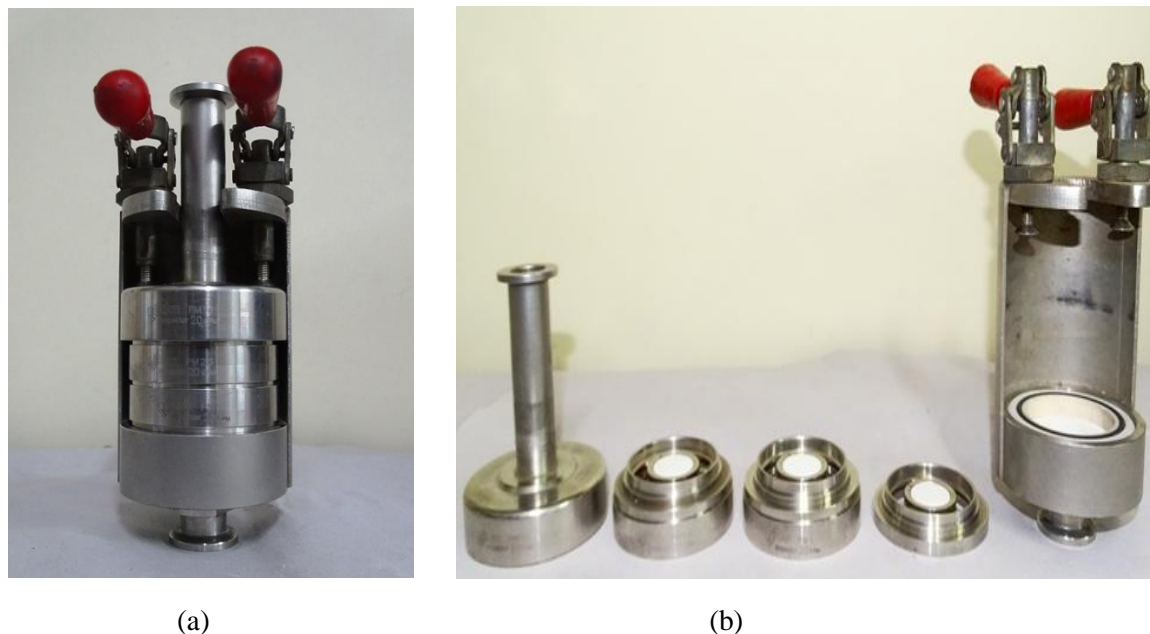


**Fig 2.2** (a) Outlook of Dekati PM<sub>10</sub> impactor, (b) The stages of the impactor are shown separately (from left-hand side: > 10, 2.5-10, 1-2.5, and < 1 μm)

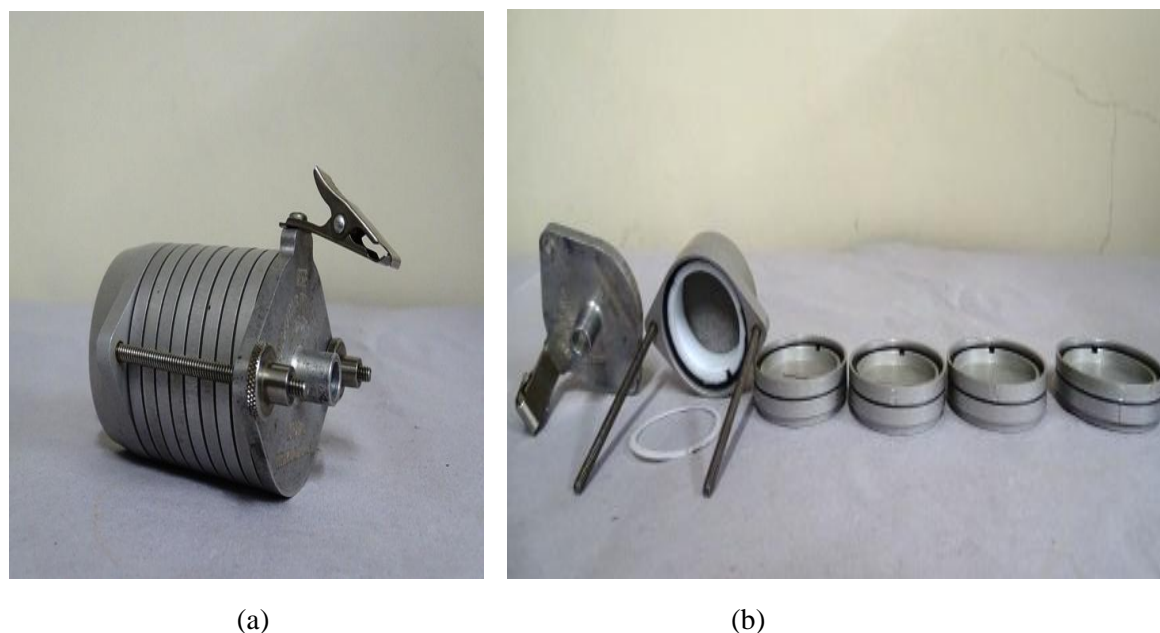


**Fig 2.3** (a) Outlook of Sioutas five-stage cascade impactor, (b) The stages of the impactor are shown separately (from the left-hand side: < 0.25, 0.25-0.50, 0.50-1.0, 1.0-2.5 and > 2.5 μm)

**Table 2.2** Brief specifications of the impactors:

<b>Features</b>	<b>Dekati PM<sub>10</sub> impactor</b>	<b>Sioutas five stage cascade impactor</b>
Recommended filters	Quartz/glass /aluminium/polycarbonate, teflon	Polytetrafluoroethylene
Flow rate	10/30 Lmin <sup>-1</sup>	9 Lmin <sup>-1</sup>
Particle size ranges (µm)	<1, 1-2.5, 2.5-10, >10	<0.25, 0.25-0.50, 0.50-1.0, 1.0-2.5, >2.5
Cut points (µm)	1, 2.5 and 10	0.25, 0.50, 1.0 and 2.5
Filter size (mm)	25 and 47	25 and 37
Temperature (Max <sup>m</sup> )	200°C	240°C
Weight (Kg)	2.4	0.159
Dimensions	76×180 mm	8.6×5.6 cm
Materials of construction	Stainless steel	Anodized aluminium, Buna-N, Acrylic

### [2.2.1] Samplings

The size-differentiated samples of particulate matters were collected on pre-weighted recommended Whatman glass/quartz fiber and PTFE filters, and preserved carefully in the refrigerator for the investigation of adhered carbonaceous loads along with PAHs according to the prescribed protocol. The size ranges of the impactors are grouped as fine or < 2.5 µm (the size ranges 1-2.5 and < 1 µm for Dekati PM<sub>10</sub> impactor and 1.0 - 2.5, 0.50 - 1.0, 0.25 - 0.50 and < 0.25 µm for Sioutas cascade impactor) and coarse mode or > 2.5 µm (size ranges > 10 and 2.5-10 µm for Dekati PM<sub>10</sub> impactor and > 2.5 µm for Sioutas cascade impactor) particles respectively throughout the results.

The wind rose pattern during the sampling period of 2014-15 with season wise is also given in Fig. 2.3 (a-f). Since, similar sampling protocol was followed in the second phase at all the sites throughout the year 2015-16, hence the wind rose pattern for the first phase (2014-15) was only shown in the present work. The meteorological parameters during the sampling period were noted by using the Envirometer, from Fisher Scientific (Enviro-Meter<sup>TM</sup>, 02-401-5) and, were also taken from the website: <http://wunderground.com>.

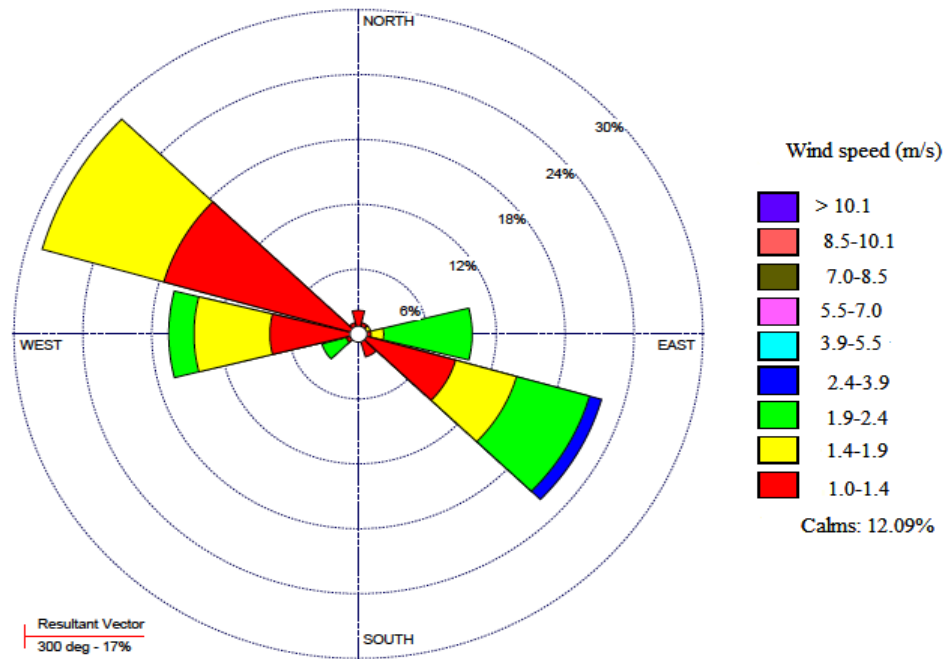


**Fig 2.3 (a)** Wind rose during the sampling period of Monsoon (July-Sept). Dates: 03-07-2014 to 30-09-2014; Calm winds 12.09%; Avg. wind speed 1.24 m/s. Date: 11-08-2016 (WRPLOT view, Lakes Environmental software).

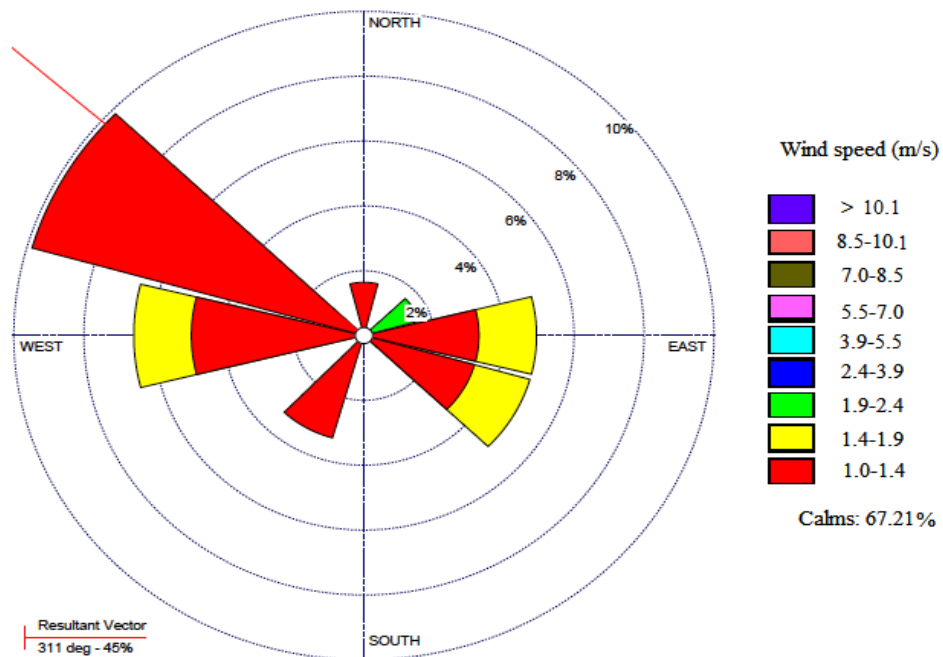


**Fig 2.3 (b)** Wind rose during the sampling period of Autumn (Oct & Nov). Dates: 02-10-2014 to 29-11-2014; Calm winds 67.21%; Avg. wind speed 0.38 m/s; Date: 11-08-2016 (WRPLOT view, Lakes Environmental software).

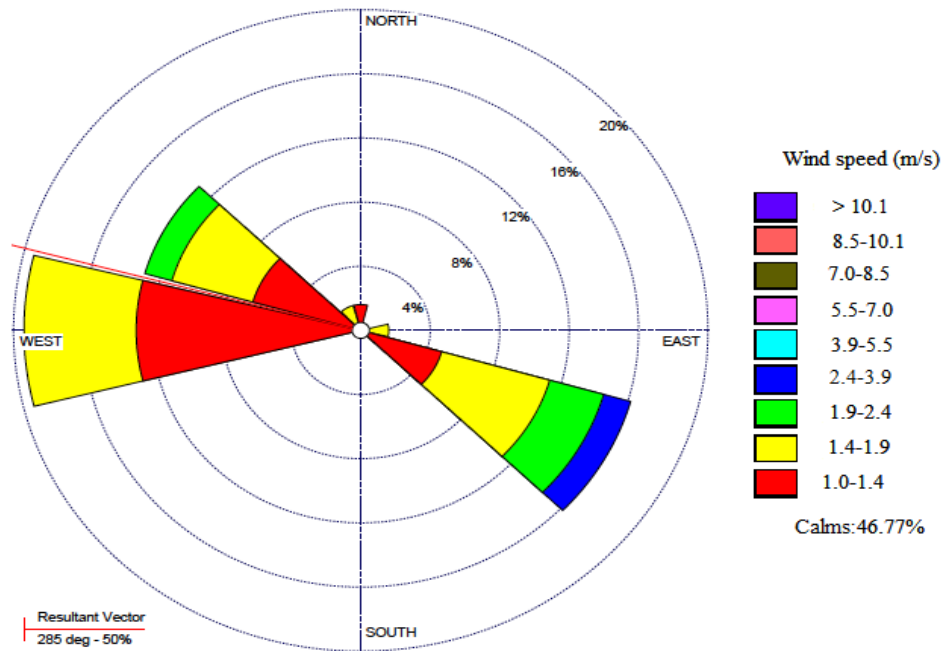


**Fig 2.3 (c)** Wind rose during the sampling period of Winter (Dec & Jan). Dates: 01-12-2014 to 31-01-2015; Calm winds 46.77%; Avg. wind speed 0.73 m/s; Date: 11-08-2016 (WRPLOT view, Lakes Environmental software).

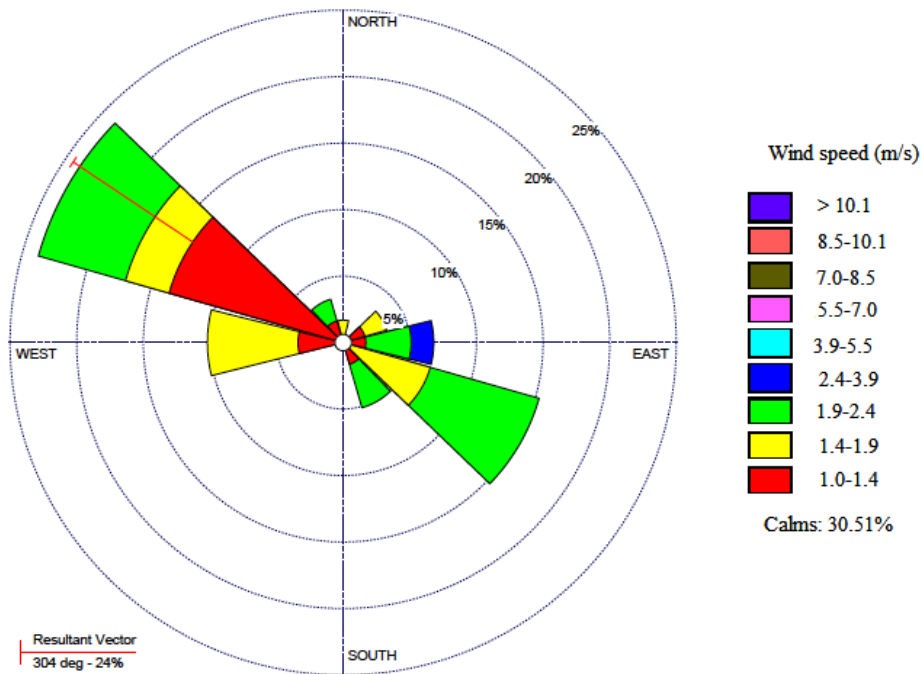


**Fig 2.3 (d)** Wind rose during the sampling period of Spring (Feb & Mar). Dates: 01-02-2015 to 31-03-2015; Calm winds 30.51%; Avg. wind speed 1.09 m/s; Date: 11-08-2016 (WRPLOT view, Lakes Environmental software).

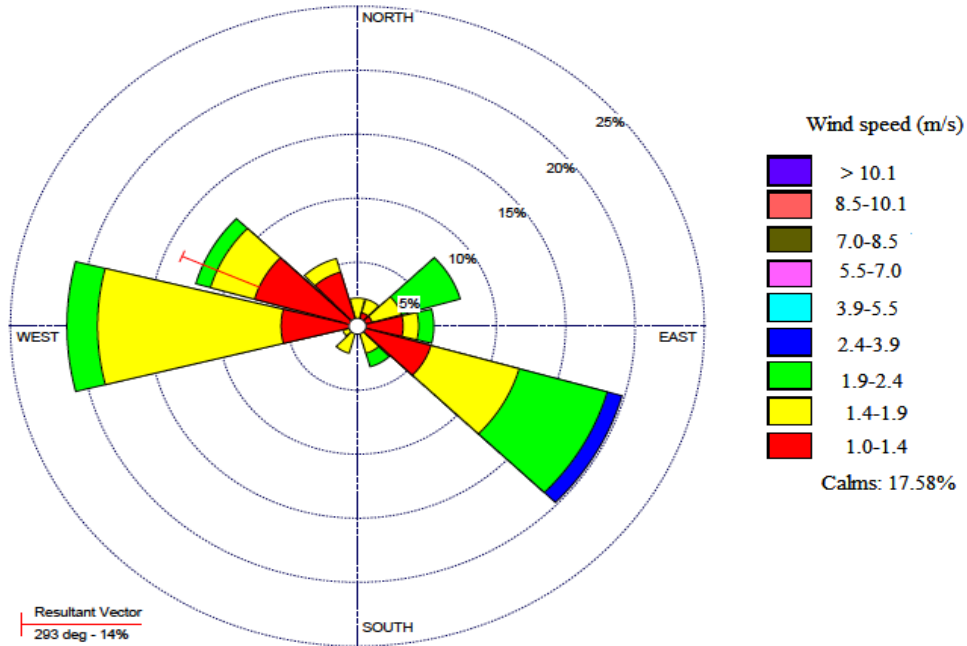


**Fig 2.3 (e)** Wind rose during the sampling period of Summer (Apr - Jun). Dates: 02-04-2015 to 30-06-2015; Calm winds 17.58%; Avg. wind speed 1.22 m/s; Date: 11-08-2016 (WRPLOT view, Lakes Environmental software).

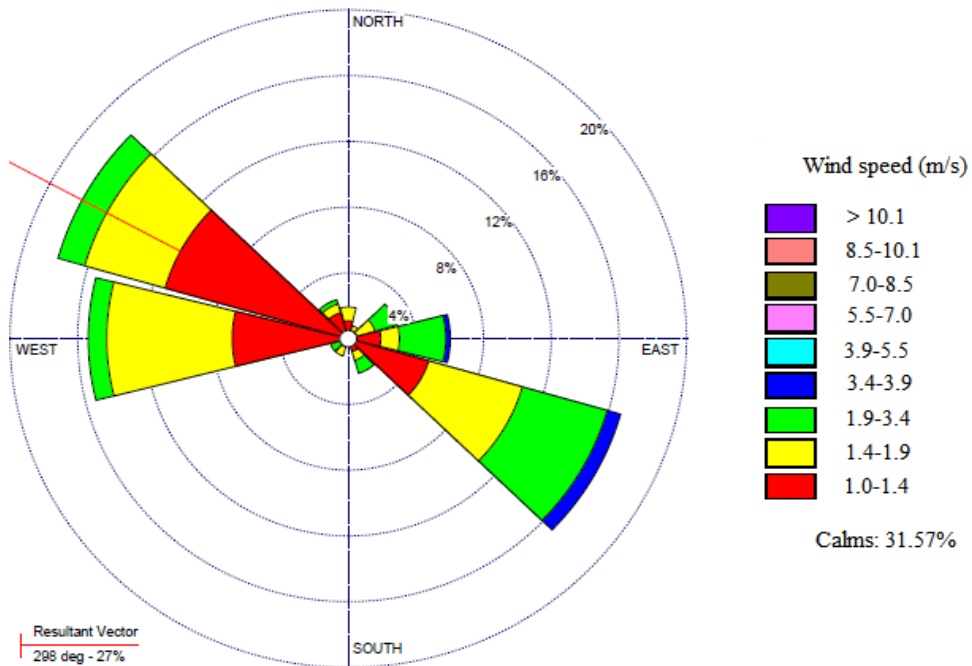


**Fig 2.3 (f)** Wind rose during the sampling period of 2014-15. Dates: 03-07-2014 to 29-07-2015; Calm winds 31.57%; Avg. wind speed 0.98 m/s; Date: 11-08-2016 (WRPLOT view, Lakes Environmental software). During the whole sampling campaign, precipitation was 0.0 mm.

### [2.2.2] Analyses

The analyses of TC and EC were carried out on the basis of the previous studies (Cachier et al., 1989; Duan et al., 2004; Duan et al., 2006; See & Balasubramanian, 2008; Sarkar et al., 2010). CHNS analyzer (Euro EA3000, Euro Vector and Thermo Scientific 2000 Flush) was used to observe the TC from glass fiber filters afterwards another part of filters were treated by heating at 350°C for about 100 min to remove the organic compounds/contents which thereafter were used for the determination of elemental carbon (EC). Further, OC was calculated by subtracting TC from EC throughout the analyses. Helium (He) was used as the carrier gas with flow rate of ~ 100 ml/min. Evolved CO<sub>2</sub> was separated in a chromatography column and carried out through a thermal conductivity detector. Standards used for calibration were Acetanilide and L-cystine. Again, after proper handling and preserving of quartz/teflon filters; these filters were used for the estimation of PAHs through the GC-MS (Shimadzu Gas Chromatograph-Mass Spectrometry; GCMS-QP2010). Quantification of some samples were also carried out with Gas Chromatography-Flame Ionization Detector (GC-FID, 5700 Nucon Gas Chromatography) and Agilent Gas Chromatograph (7890A) fitted with the mass spectrometry triple quadruple system. The sampler, “Sioutas five-stage cascade impactor” could satisfactorily be used for the analyses of PAHs, but not for the carbonaceous loads whereas, “Dekati PM<sub>10</sub> impactor” could be used for both the carbonaceous fractions and PAHs respectively. In case of Dekati PM<sub>10</sub> impactor, only the particle size range < 1, 2.5-10, and > 10 μm (due to relatively homogeneous deposition in comparison to the size range 1-2.5 μm) gave good outputs of TC and EC.

Although various approaches have been made to study the carbonaceous loads and PAHs from particulate emissions, the measurements made by these impactors are well defined for the carbonaceous fractions using Dekati PM<sub>10</sub> impactor (Kourtchev et al., 2005; Geng et al., 2009a,b) and Sioutas cascade impactor (Ono-Ogasawara et al., 2011; Huboyo et al., 2011; Kam et al., 2012; Hasheminassab et al., 2013). Similarly for PAHs also; Dekati PM<sub>10</sub> impactor (Booyens et al., 2015) and Sioutas five stage cascade impactor (Martins et al., 2012; Blomqvist et al., 2014; Xu et al., 2015a) have been used.



### [2.2.3] Reagents and chemicals

The deuterated internal PAHs standard used in this study were Acenaphthene-D10; Chrysene-D12; Naphthalene-D8; Phenanthrene-D10 and Perylene-D12. For the authentication of results, EPA 610 Polynuclear Aromatic Hydrocarbons mixture was used as standard, these were Naphthalene (Npth), Acenaphthylene (Acnp), Acenaphthene (Acen), Fluorene (Fluo), Phenanthrene (Phtn), Anthracene (Anth), Fluoranthene (Flun), Pyrene (Pyrn), Benzo[a]anthracene (BaAn), Chrysene (Chrn), Benzo[b]fluoranthrene (BbFn), Benzo[k]fluoranthrene (BkFn), Benzo[a]pyrene (BaPn), Indeno[1,2,3-cd]pyrene (IcdP), Dibenzo[a,h]anthracene (DahA) and Benzo[ghi]perylene (BghiP). Solvents used in the extraction processes were dichloromethane or DCM (CH<sub>2</sub>Cl<sub>2</sub>) and n-hexane (C<sub>6</sub>H<sub>14</sub>) from Fisher Scientific International Inc. The compound MSTFA [N-Methyl-N-(trimethylsilyl) trifluoroacetamide] for GC derivatization was used for identification of silylated compounds.

### [2.2.4] Analytical quality assessments

The instruments (carbon analyzer) were checked and calibrated routinely during the analyses, and the field blank filters were run to obtain background accuracy. Analyses were carried out for blank filters also, and the result was corrected for average concentrations of the blanks, which was observed to be on an average 1.23 and 0.5 µg/m<sup>3</sup> for TC and EC respectively. Relative standard deviations of the replicates were 7% and 9% for TC and EC respectively.

In case of PAHs, the instruments used were calibrated using the standards. Linear calibration curves with concentration range was observed, where linear regression coefficients R<sup>2</sup> > 0.83 was found for data of least-squares fit. Analyses were carried out in duplicates to ensure the precision of the samples. Relative standard deviations of the replicates were less than 12 %. To determine the bias of analyses; field blanks and reagent blanks were also analyzed. Out of the total peaks observed throughout the samples, only sixteen peaks of the priority PAHs were noted for obtaining concentrations of PAHs by comparing the areas of the compounds. Recoveries of PAHs were observed by spiking the samples with the internal standards. Efficiency of recoveries of the PAHs in the first phase was in the range from 75 to 86 %. In the second phase, the

regression co-efficient  $R^2 > 0.97$  was found for data of least square fit, while recoveries were in the range of 77% to 102%.

#### **[2.2.5] Extraction processes and PAHs determination**

Methylene chloride or DCM (with minimum assay 99.5% for GC, from Fisher Scientific International Inc.) was taken as solvent for the extraction of the particulate filters for the sample in first phase. An aliquot of 10 ml of the solvent was added in each of the filters of different size ranges (from “Dekati PM<sub>10</sub>”; one portion from  $< 1 \mu\text{m}$ , while a portion of deposition part from  $> 1 \mu\text{m}$  of the filters was used, and from “Sioutas impactor”; only the particle deposition part was used) followed by sonication for one hr at about 10°C. 10 ml of the solvent (CH<sub>2</sub>Cl<sub>2</sub>) was added again into the supernatant solvent and the process was repeated to obtain the final volume 30 ml for each of the sample extract. The volume was reduced to concentrate to become 2 ml using speed vacuum (Thermo Fisher Scientific). Each extract of the particulate sample was further divided into two parts. In the 1<sup>st</sup> part, a 3  $\mu\text{l}$  out of 1.5 ml volume was injected to the GC-column for the detection of apolar hydrocarbons/ compounds. Again, in the rest of 0.5 ml of the extract, 0.5 ml of neat MSTFA for GC derivatization, from Sigma Aldrich was added for the observation of polar silylated compounds as according to Orasche et al., (2011).

In the first phase, PAHs analyses were carried out through the instrument Shimadzu Gas Chromatograph 2010, attached with single quadruple MS (GCMS-QP2010; Shimadzu. Corp.), and GC-FID, 5700 Nucon Gas Chromatograph. Fused silica column [low polarity phase; products of Restek chromatography: Rtx®-5MS (30m×0.25mm×0.25 $\mu\text{m}$ , crossbond @diphenyl dimethyl polysiloxane)] was used for the detection of PAHs. The extracts of the sample which are consequently transferred into vials, were vortexed well for about 5 minutes and finally kept for 1/2 hr in a water bath for at about 60°C. A volume of 3  $\mu\text{l}$  sample was injected to the column. Peaks of the PAHs, and its identifications and calibrations were observed through retention times and the areas with comparing the prescribed standard. The priority and/or targeted compounds were identified with calibration and were also verified throughout the libraries available in the GC-MS section namely; WILEY 8 and NIST 11. During the GC operation, oven temperature (column) was set initially at 80°C, where the holding time was 2 min. Temperature of ramp was first applied 5°C/min to reach 250°C of the ultimate temperature. Temperature of the column was

set at 260°C for an interval of 5 minutes to remove all the weakly bound compounds and/or derivatives. 10°C ramp was put to reach the final temperature of 280°C. At 280°C, a period of 15 minutes was set to diminish further any other strongly bounded compounds, derivatives and/or reagents for the column. During the time of injection, the injector temperature in split less mode was 260°C (i.e., linear velocity; flow control) with the split ratio 10.0 and the inlet pressure was 90.5 KPa. Total flow, column flow, linear velocity and purge flow (septum) were 16.3 ml/min, 1.2 ml/min, 40.9 cm/sec and 3.00 ml/min respectively. Again, for mass spectrometry (MS), 230°C was ion source temperature; 4.5 min was solvent cut time and the interface temperature was 270°C. Micro scan width was 0 u. Scan was started at 5 minutes and continued till 49.99 minutes with the total program period of 50.75 min. Helium was used as carrier gas. MS was set in fully scan mode and accordingly the detection results were noted and observed. Temperature of quadruple was fixed at 200°C, and as detector the quadruple mass spectrum was applied. Chromatogram obtained through Shimadzu GCMS-QP2010, after running PAHs standard (external) is given below in Fig. 2.4 and the peak report total ion chromatogram (TIC) of the standard is also given in Table 2.3 (Snapshot before running the samples in the first phase). Again, for the samples of the second phase; chromatogram obtained after running PAHs standard is given in Fig. 2.5 and the peak report of the standard is also shown in Table 2.4. In this phase, the solvents DCM/n-hexane (1:1) were used for the extraction of quartz fibre filters; PAHs were analysed by using Shimadzu Gas Chromatograph attached with single quadruple MS (GCMS-QP2010) and Agilent Gas Chromatograph (7890A) fitted with the triple quadruple mass spectrometry. In the second phase, the following major programmes were followed: inlet pressure 95 KPa, injection volume 2.0 µl, GC programme time 55.00 min and scan was performed as acq. mode. The peaks of the samples of the targeted/priority compounds were matched with the retention times of the standard. Concentrations of the monitored compounds were obtained through the area of the compounds, comparing with the area of the authentic standard. The monitored compounds were identified with calibration and the verification was also carried out through the libraries NIST 14, NIST 14s, and Wiley mass spectral databases.

## GC-MS Laboratory: AIRF Analysis Report



Analyzed by : SAjai Kumar\$  
 Analyzed : 4/26/2016 4:30:22 PM  
 Sample Type : SEssential oils\$  
 Sample Name : PAHs standard  
 Method File : D:\GCMS Method\Method\Extract.qgd

Chromatogram PAHs standard D:\GCMS DATA\SES\Dr. Arun Srivastava\Naba\PAHs standard.qgd

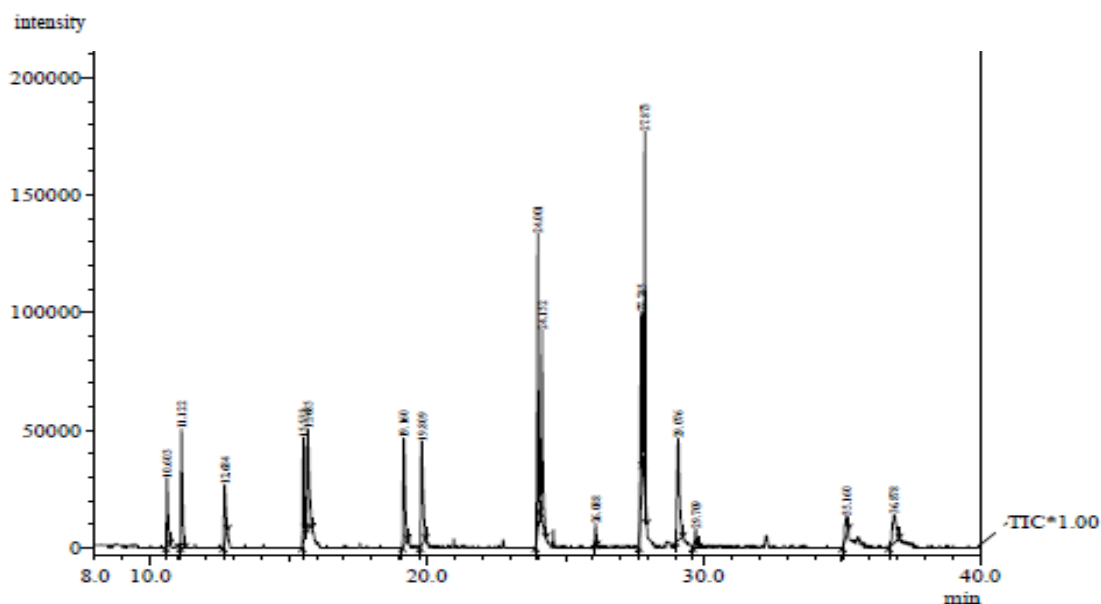


Fig 2.4 Chromatogram of the PAHs standard (for the first phase samples)

**Table 2.3** PAHs standard (before the analyses of the samples in the first phase) along with the parameters such as Retention time, Area, Area % etc.

Peak Report TIC				
Peak#	R.Time	Area	Area%	Name
1	10.603	109634	3.59	Naphthalene
2	11.122	196274	6.43	Acenaphthylene
3	12.684	106231	3.48	Acenaphthene
4	15.533	132853	4.35	Fluorene
5	15.685	230289	7.54	Phenanthrene
6	19.160	204864	6.71	Anthracene
7	19.809	225000	7.37	Fluoranthene
8	24.001	335397	10.98	Pyrene
9	24.152	293188	9.60	Benzo[a]anthracene
10	26.088	19429	0.64	Chrysene
11	27.745	268768	8.80	Benzo[b]fluoranthene
12	27.873	453406	14.84	Benzo[k]fluoranthene
13	29.076	272133	8.91	Benzo[a]pyrene
14	29.709	35020	1.15	Indeno[1,2,3-cd]pyrene
15	35.160	56654	1.85	Dibenzo[a,h]anthracene
16	36.878	115549	3.78	Benzo[ghi]perylene
		3054689	100.00	

# GC-MS Laboratory: AIRF Analysis Report

## Sample Information



Analyzed by : \$Admn.\$  
Analyzed : 10-11-2016 17:13:41  
Sample Type : \$Organic\$  
Sample Name : PAHs standard  
Method File : D:\GCMS\GCMS METHOD\SES\Naba.qgm

Chromatogram PAHs standard D:\GCMS DATA\SES\Dr. Arun Srivastava\Naba\PAHs standard.qgd

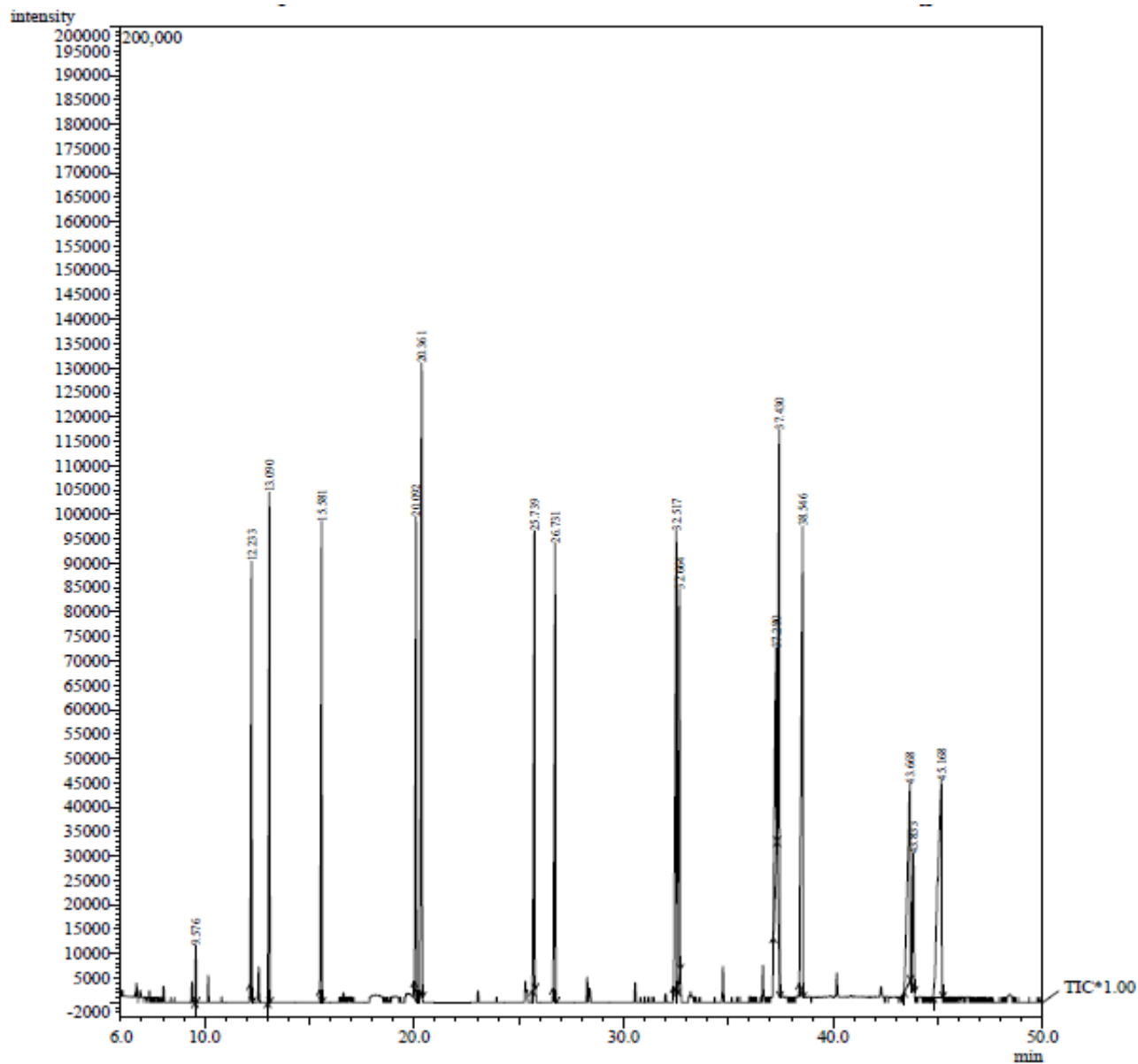


Fig 2.5 Chromatogram of the PAHs standard (for the second phase samples)

**Table 2.4** PAHs standard (before the analyses of the samples in the second phase) along with the parameters such as Retention time, Area, Area % etc.

Peak Report TIC				
Peak#	R. Time	Area	Area%	Name
1	9.576	24244	0.45	Acenaphthylene
2	12.233	253105	4.69	Acenaphthene
3	13.090	325747	6.04	Anthracene
4	15.581	310203	5.75	Benzo[a]anthracene
5	20.092	322410	5.98	Benzo[b]fluoranthene
6	20.361	512326	9.49	Benzo[k]fluoranthene
7	25.739	324621	6.02	Benzo[g,h,i]perylene
8	26.731	343255	6.36	Benzo[a]pyrene
9	32.517	436870	8.10	Chrysene
10	32.664	260567	4.83	Dibenzo[a,h]anthracene
11	37.280	268338	4.97	Fluoranthene
12	37.430	424984	7.88	Fluorene
13	38.546	546907	10.14	Indeno[1,2,3-cd]pyrene
14	43.668	370170	6.86	Naphthalene
15	43.833	130523	2.42	Phenanthrene
16	45.168	541560	10.04	Pyrene
		5395830	100.00	

In the present investigation, sixteen US EPA priority PAHs were targeted to be observed, all the priority PAHs were found to be dominated throughout the proposed sites of the Delhi-NCR (except the compound Acenaphthene, which was abundant in the second phase samples). Hence, in this study, the average concentrations of Acenaphthene could be considered primarily as the representative of the samples of the second phase only. In lieu of these priority PAHs, few other PAHs were also observed to be associated with the size ranges < 0.25, 0.25–0.50, 0.50–1.0, and > 2.5  $\mu\text{m}$  (for Sioutas impactor) and for Dekati PM<sub>10</sub> impactor (< 1 and 1.0–2.5  $\mu\text{m}$ ).

### [2.3] Software used in the analytical processes

The spatial and temporal distribution of carbonaceous load and PAHs were carried out with the help of ArcGIS (Geographic Information System) software version 10.1. Some figures were plotted with the software Graph Pad Prism 5.0 (Graph Pad Software, Inc., San Diego, CA, USA) for PAHs associated with fine and coarse particles to obtain the concentration variations and risk assessments. Statistical software SPSS version 16.0 (SPSS, Inc., Chicago, IL, USA) was used to observe the correlations (Pearson correlation) of PMs ( $\mu\text{g}/\text{m}^3$ ) with meteorological parameters. In the source apportionment section, the principal component analyses (PCA) was applied through the statistical software XLSTAT version 7.5.2., where correlation matrices were also obtained after running the PCA for PAHs and carbonaceous load.

## [2.4] Chronic health risk assessments of PAHs

To observe the chronic health risk of the PAHs, the concentration of the PAHs were used to determine the Chronic Daily Intake Dose (CDi,  $\text{mg kg}^{-1}\text{day}^{-1}$ ), to quantify the Hazard Quotient (HQ) of the individual species followed by the assessment of Hazard Index (HI) as according to the prescribed methods provided by the Integrated Risk Information System (IRIS) under the United States Environmental Protection Agency (US EPA, 1989; 1997; 1998; 2012). Though, there are three different exposure pathways (inhalation, ingestion and dermal), only two pathways such as inhalation and ingestion are considered for children ( $\text{HQ}_C$ ) and adults ( $\text{HQ}_A$ ) in this study. CDi can be obtained by the following equation:

$$\text{CDi} = (\text{C} \times \text{IR} \times \text{EF} \times \text{ED}) / (\text{BW} \times \text{AL} \times \text{CF})$$

In this equation, C represents the concentration of the individual PAHs, IR is the rate of inhalation and/or the rate of ingestion (where, the inhalation rate for adult is around  $20 \text{ m}^3 \text{ day}^{-1}$  and for the children it is considered  $10 \text{ m}^3 \text{ day}^{-1}$ ). Again, the ingestion rate for adults is  $100 \text{ mg day}^{-1}$  and it is  $200 \text{ mg day}^{-1}$  for children. EF is the frequency of exposure ( $\text{day yr}^{-1}$ ), which is again considered as equivalent to  $350 \text{ days yr}^{-1}$  (for adults) due to the fifteen official leave days out of the year, i.e., 365 days. For children, EF is considered as  $180 \text{ days yr}^{-1}$ . ED is the duration of exposure, which is considered as 40 yrs for adults and it is 6 years for children, BW represents the average weight of body (in Kilograms), which is considered as 65 Kgs, since the adults average body weight (male/female) was considered, for children it is 15 years. AL indicates the average lifetime, which is 70 yrs for adults and 15 years for children. Here, the conversion factor (CF) is used ( $\text{mg ng}^{-1}$ ), since the concentrations of all the observed PAHs were expressed in  $\text{ng m}^{-3}$ . Similar types of observations have been carried out by various studies so far (Di Vaio et al., 2016; Chakraborty & Mondal, 2017).

The minute health risk of the pollutants depends on HQ, which in turn depends on HI of the observed PAHs, and it can be considered to be minute risk if the HQ value exceeds one. When  $\text{HQ} > 10.0$  then there would be potential health risk associated with that particular species. HQ can be calculated from CDi and RfD [chronic oral reference dose, ( $\text{mg kg}^{-1} \text{ day}^{-1}$ )]. RfD can

also be obtained from RfC (chronic inhalation reference concentration,  $\text{mg m}^{-3}$ ), inhalation rate and the average body weight as according to the information available at [www.rais.ornl.gov](http://www.rais.ornl.gov). HQ depends on CDi of the species; which in turn also depends on the concentration of the species and/or the RfD values.

$$\text{HQ} = \text{CDi}/\text{RfD}, \text{ and}$$

$$\text{RfD (inhalation)} = (\text{RfC} \times \text{rate of inhalation}) / \text{body weight}$$

$$\text{HI} = \Sigma \text{HQ}_i$$

The higher contribution of HQ is generally having greater chronic health risk. In this work, the prescribed/referred RfD values provided by the organizations such as: IRIS, and the Risk Assessment Information System (RAIS) were considered for the quantification of HQ, but not the calculated RfD value. Calculated RfD (inhalation) can be obtained only then, when the prescribed RfC value is available and which is possible only for Naphthalene. The detailed summary of physico chemical properties of the sixteen priority PAHs listed according to the US EPA are given in Table 2.5, whereas Table 2.6 covers the RfD ( $\text{mg Kg}^{-1}\text{day}^{-1}$ ), RfC ( $\text{mg m}^{-3}$ ), inhalation unit risk [ $(\mu\text{g m}^{-3})^{-1}$ ] and slope factor [ $(\text{mg kg}^{-1}\text{day}^{-1})^{-1}$ ] of the priority PAHs.



**Table 2.5** Details of the sixteen US EPA priority PAHs and their some important physico chemical properties

PAHs	No. of Rings	Cas No.	Molar mass (g mol <sup>-1</sup> )	MP (°C)	BP (°C)	Density (g cm <sup>-3</sup> )	Solubility(mg l <sup>-1</sup> )	*V.P (mm Hg)	*Group	Structure
Naphthalene	2	91-20-3	128.17	78.2	217.97	1.025 (at 20°C)	31	$8.89 \times 10^{-2}$	2B	C <sub>10</sub> H <sub>8</sub>
Acenaphthylene	3	208-96-8	152.2	91.8	280	0.8987	16.1	$2.90 \times 10^{-2}$	-	C <sub>12</sub> H <sub>8</sub>
Acenaphthene	3	83-32-9	154.21	93.4	279	1.024	3.8	$3.75 \times 10^{-3}$	-	C <sub>12</sub> H <sub>10</sub>
Fluorene	3	86-73-7	166.22	116-117	295	1.202	1.9	$3.24 \times 10^{-3}$	-	C <sub>13</sub> H <sub>10</sub>
Phenanthrene	3	85-01-8	178.23	101	332	1.18	1.1 or 1.6	$6.80 \times 10^{-4}$	-	C <sub>14</sub> H <sub>10</sub>
Anthracene	3	120-12-7	178.23	215.76	339.9	1.28	0.045	$2.55 \times 10^{-5}$	3	C <sub>14</sub> H <sub>10</sub>
Fluoranthene	4	206-44-0	202.26	110.8	375	1.252	0.265	$8.13 \times 10^{-6}$	-	C <sub>16</sub> H <sub>10</sub>
Pyrene	4	129-00-0	202.25	145-148	404	1.271 g ml <sup>-1</sup>	0.135	$4.25 \times 10^{-6}$	-	C <sub>16</sub> H <sub>10</sub>
Benzo[a]anthracene	4	56-55-3	228.29	158	138	1.19	0.011	$1.54 \times 10^{-7}$	2A	C <sub>18</sub> H <sub>12</sub>
Chrysene	4	218-01-9	228.29	254	448	1.274	0.0015	$7.80 \times 10^{-9}$	2B	C <sub>18</sub> H <sub>12</sub>
Benzo[b]fluoranthene	5	205-99-2	252.31	168	-	1.286	0.0015	$8.06 \times 10^{-8}$	2B	C <sub>20</sub> H <sub>12</sub>
Benzo[k]fluoranthene	5	207-08-09	252.32	217	-	1.286	0.0008	$9.59 \times 10^{-11}$	2B	C <sub>20</sub> H <sub>12</sub>
Benzo[a]pyrene	5	50-32-8	252.32	179	495	1.24	0.0002 - 0.0062	$4.89 \times 10^{-9}$	1	C <sub>20</sub> H <sub>12</sub>
Indeno[1,2,3-cd]pyrene	6	193-39-5	276.331	161-163	536	-	0.062	$1.40 \times 10^{-10}$	2B	C <sub>22</sub> H <sub>12</sub>
Dibenzo[a,h]anthracene	6	53-70-3	278.35	262	-	1.232	0.0005	$2.10 \times 10^{-11}$	2B	C <sub>22</sub> H <sub>14</sub>
Benzo[ghi]perylene	6	191-24-2	276.331	278	500	1.38	0.00026	$1.00 \times 10^{-10}$	-	C <sub>22</sub> H <sub>12</sub>

Density and Solubility (mg l<sup>-1</sup>; in water) are represented at the standard state, i.e., 25°C and 100 kPa. \*V.P (mm Hg) represents vapour pressure in mm Hg. \*Group signifies the categorization of carcinogenicity under the International Agency for Research on Cancer (IARC). Group 1 represents human carcinogen, 2A represents probable human carcinogen, 2B represents possibility to the human carcinogen and the group 3 is not classifiable as human carcinogen. Two parameters namely; solubility and vapour pressure can also be obtained at the Agency for Toxic Substances and Disease Registry (ATSDR, 2005), and also highlighted by Bojes & Pope, (2007). All these compounds are soluble in alcohol, diethyl ether, acetone, benzene, chloroform, carbon disulphide etc, but the solubility in water is very low. Density, solubility, thermal conductivity, and viscosity of majority of these compounds are also differ with different temperatures. Again, physical appearance and crystal structure are also different for majority of these compounds.

**Table 2.6** Summary of the sixteen US EPA priority PAHs, its RfD (oral), RfC (inhalation), slope factor (oral) and inhalation unit risk as according to the IRIS, CalEPA and the WHO/TEF value based on a toxicity equivalent factor from the WHO or US EPA

PAHs	RfD (mg kg <sup>-1</sup> day <sup>-1</sup> )	RfC (mg m <sup>-3</sup> )	Slope factor (mg kg <sup>-1</sup> day <sup>-1</sup> ) <sup>-1</sup>	Unit risk (μg m <sup>-3</sup> ) <sup>-1</sup>
Naphthalene	<sup>a</sup> 2.00 × 10 <sup>-2</sup>	<sup>a</sup> 3.00 × 10 <sup>-3</sup>	-	<sup>b</sup> 3.40 × 10 <sup>-5</sup>
Acenaphthylene	-	-	-	-
Acenaphthene	<sup>a</sup> 6.00 × 10 <sup>-2</sup>	-	-	-
Fluorene	<sup>a</sup> 4.00 × 10 <sup>-2</sup>	-	-	-
Phenanthrene	-	-	-	-
Anthracene	<sup>a</sup> 3.00 × 10 <sup>-1</sup>	-	-	-
Fluoranthene	<sup>a</sup> 4.00 × 10 <sup>-2</sup>	-	-	-
Pyrene	<sup>a</sup> 3.00 × 10 <sup>-2</sup>	-	-	-
Benzo[a]anthracene	-	-	<sup>c</sup> 1.00 × 10 <sup>-1</sup>	<sup>c</sup> 6.00 × 10 <sup>-5</sup>
Chrysene	-	-	<sup>c</sup> 1.00 × 10 <sup>-3</sup>	<sup>c</sup> 6.00 × 10 <sup>-7</sup>
Benzo[b]fluoranthene	-	-	<sup>c</sup> 1.00 × 10 <sup>-1</sup>	<sup>c</sup> 6.00 × 10 <sup>-5</sup>
Benzo[k]fluoranthene	-	-	<sup>c</sup> 1.00 × 10 <sup>-2</sup>	<sup>c</sup> 6.00 × 10 <sup>-6</sup>
Benzo[a]pyrene	-	-	<sup>a</sup> 1.00 × 10 <sup>0</sup>	<sup>a</sup> 6.00 × 10 <sup>-4</sup>
Indeno[1,2,3-cd]pyrene	-	-	<sup>c</sup> 1.00 × 10 <sup>-1</sup>	<sup>c</sup> 6.00 × 10 <sup>-5</sup>
Dibenzo[a,h]anthracene	-	-	<sup>c</sup> 1.00 × 10 <sup>0</sup>	<sup>c</sup> 6.00 × 10 <sup>-4</sup>
Benzo[ghi]perylene	-	-	-	-

<sup>a</sup>Source: Integrated Risk Information System (IRIS),

<sup>b</sup>Source: California Environmental Protection Agency (CalEPA),

<sup>c</sup>Source: World Health Organization/Recommended Toxicity Equivalence Factors (WHO/TEF),

“-”: Values are not available or not recommended so far.

### [2.4.1] Cancer risk assessment of PAHs

Attempts were made to carry out the Incremental Lifetime Cancer Risk (ILCR) associated with inhalation exposure for adults and children, which represents the probability of carcinogenicity for an individual over the lifetime (here, it is 70 yrs for adults and for children it is 15 yrs) consequences of exposure potential of the carcinogen.

ILCR can be calculated as:

$$\text{ILCR} = \text{CDi} \times \text{SF}_o$$

Where,  $CDi$  is the Chronic Daily Intake Dose ( $mg\ kg^{-1}day^{-1}$ ) and  $SF_o$  is the oral slope factor (per  $mg\ kg^{-1}day^{-1}$ ). Hence, ILCR is a unit less parameter.

Again, inhalation slope factor ( $SF_i$ ) can also be calculated as (RAIS, [www.rais.ornl.gov](http://www.rais.ornl.gov); Vuković et al., 2014):

$$SF_i = (UR \times BW)/IR$$

Although, a large number of compound are estimated to be carcinogenic, but due to the complexity for interpretation/estimation of the carcinogenicity, the risk for all species (such as metals/metalloids and organic compounds) has not been confirmed by the IRIS. The information concerning the carcinogenicity and unit risks can also be obtained from the website of the US EPA through IRIS ([www.epa.gov/iris/](http://www.epa.gov/iris/)), CalEPA and WHO/TEF [informations are also available at the RAIS ([www.rais.ornl.gov](http://www.rais.ornl.gov)). Majority of these informations regarding the carcinogenicity are also found to be initially developed by the WHO/TEF (value based on a toxicity equivalent factor from the WHO or US EPA). In this study, the cancer risks of PAHs are observed through the inhalation unit risk of the respective compounds.

It is important to observe whether the carcinogenic risk of inhalation for the PAHs (Npth, Chrn, BaAn, BaPn, BbFn, BkFn, IcdP and DahA) fall in the range of ILCR, i.e.,  $10^{-6}$  to  $10^{-4}$ . The risk of carcinogenicity, which is related to the value of ILCR, can be regarded as potential risk if the values fall within the range of ILCR. If it is  $> 10^{-4}$  then it indicates potentially high risk and when it is  $\leq 10^{-6}$  then it is considered as virtual safety for that particular species. The excess risk of inhalation of the PAHs: Npth, Chrn, BaAn, BbFn, BkFn, BaPn and DahA can only be observed due to its availability of unit risk values. ILCR associated with particulate bound PAHs have been carried out by various researchers so far (Bortey-Sam et al., 2013; Vuković et al., 2014; Li et al., 2016a; Lu et al., 2016; Singh & Gupta, 2016). Level of risk of carcinogenicity depends on concentration and on the prescribed unit risk of the individual compound and/or species. Among the PAHs, BaPn come under group 1 carcinogen (according to the IARC category) and the PAHs such as Npth, Chrn, BbFn, BkFn, IcdP and DahA belong to 2B category except BaAn, which is recognized as 2A category under the IARC.

## *Chapter 3 Results and discussion*

**[3.1] Spatio-temporal variation of carbonaceous species and PAHs through the application of GIS software**

Carbonaceous aerosols, and a total of sixteen priority PAHs as according to the United States Environmental Protection Agency (US EPA) were targeted to observe the spatial and temporal variations in the present work. Many approaches have been made to observe spatio-temporal variation of PM bound pollutants (Wong et al., 2004; Denby et al., 2005; Noth et al., 2011; Righini et al., 2014; Lee et al., 2016), similarly, in this study also, an attempt was made to construct the spatio-temporal variation maps of the carbonaceous species (such as TC, EC, OC) and PAHs with season, by taking the averages of the total concentrations throughout the periods, which have been prepared by applying Inverse Distance Weighted (IDW) approach in Spatial Analyst extension of ArcGIS software version 10.1 For pollution mapping, the spatial analyses and overlays techniques from GIS provides powerful tool (Briggs et al., 1997). Different approaches of spatial regression models also able to exploit pollutants data unlike interpolation methods (Jerrett et al., 2005; Hoek et al., 2008; Martín et al., 2010). The advent of modeling and GIS methods for the exposure assessment (intraurban exposure) has emerged at that time when chronic health risks has become interested (Jerrett et al., 2005). GIS can be used to visualize the spatially distributed concentrations of particulate bound species, which further can be used for exposure models to identify the pollution variation within a small area (Jerrett et al., 2005). Both the temporal and spatial variability were observed to be significant through this model. It has been reported that PM and associated pollutants are dependent on various factors such as local climatic conditions, topography, sources of emission etc. Thus, the representation of pollutants with geo statistical model could improve the monitoring tool with wide range of applications such as riskiness and epidemiological studies too (Lai et al., 2013). This strategy can build a versatile and useful tool in the exposure of analyses and also the probable risks of pollutants (Lee et al., 2016). In this study, the spatial and temporal changes of carbonaceous species and PAHs carried out through GIS in the proposed sites of Delhi-NCR are explained below:

Variation of TC ( $\mu\text{g}/\text{m}^3$ ) showed that GBD site recorded the highest concentration throughout the study, while JNU recorded the lowest (Fig 3.1). In monsoon season, it is clear that GBD experiences higher load of TC followed by CPL, FBD, JNU and GGN. During autumn an

opposite pattern of variation of TC was observed for the sites CPL, FBD, GGN and JNU except the site GBD; where GBD possessed the highest abundances of TC and JNU possessed the lowest. The overall pattern of spatial changes in the autumn revealed that GBD had the highest contribution of TC followed by FBD, CPL, GGN and JNU. During winter, GBD was observed to have high abundances of TC after FBD, GGN, CPL and JNU. In spring, again similar pattern of relative abundances of TC was observed for all the sites as was in the autumn and winter seasons. The order of relative contribution of TC in spring was found as:  $GBD > FBD > GGN > CPL > JNU$ . In the summer season, again GBD had the highest concentration of TC followed by FBD, CPL, GGN and JNU.

Spatio-temporal variation of EC ( $\mu\text{g}/\text{m}^3$ ) showed that GBD recorded the highest concentration throughout the analyses followed by FBD, CPL, GGN and JNU (Fig 3.2). Similar to TC, variation of EC showed that GBD region had the highest contribution all-round the years, whereas at JNU the relative concentrations was found lowest. In the monsoon season, it is clear from Fig. 3.2 that GBD experiences higher load of EC followed by CPL, FBD, GGN and JNU. In autumn season, an opposite trend of EC was observed among the sites CPL, FBD and GGN; where relative abundances of EC was found as:  $JNU < CPL < GGN < FBD < GBD$ . In case of the winter season; CPL and JNU experienced comparatively lower amount of EC than the rest of other sites. In this season, the relative contribution of EC was found highest for that of GBD, whereas it was the lowest for JNU. The overall contribution of EC in winter showed that GBD had the highest load followed by GGN, FBD, CPL ~ JNU. In spring, the relative abundances of EC for CPL, FBD and GGN was observed almost equivalent, where JNU possessed lowest amount among all the sites and GBD had the highest contribution. During summer season, JNU and GGN possessed relatively lower abundances of EC than the other sites. In this season, the following trend was observed:  $JNU < GGN < FBD < CPL < GBD$ .

Variation of OC ( $\mu\text{g}/\text{m}^3$ ) showed that GBD recorded the highest abundances of OC throughout the seasons of the study period among all the sites (Fig 3.3). In monsoon season, the trend of variation of OC was observed similar to EC, where GBD experienced relatively higher abundances and JNU experienced lower abundances of OC. The order of spatial changes in the monsoon season was:  $GBD > CPL > FBD > JNU > GGN$ . In case of the autumn season, GBD and FBD experienced comparatively higher contribution of OC. In this season, the relative contribution of OC was found highest for GBD followed by FBD, CPL, GGN and JNU. In

winter, again GBD was observed to be highly abundant of OC after FBD, CPL, GGN and JNU. The overall result of OC showed that GBD had the highest load and the rest of other sites possessed lower amount. In spring, in comparison to winter an opposite pattern of relative abundances of OC was observed between the sites GGN and CPL. Relative abundances of OC in spring was found as: JNU < CPL < GGN < FBD < GBD. It was observed that GBD had the highest contribution followed by CPL, FBD, GGN and JNU during summer, where relatively lower contributions of OC were observed at JNU and GGN. GBD experienced the highest contribution of OC and JNU experienced the lowest contribution of OC. The sites GBD, FBD and GGN are dominated by vehicles which run mainly on diesel and petrol, while in Delhi, Compressed Natural Gas (CNG) is widely used. The widespread use of diesel and gasoline vehicles may be the reason behind higher carbonaceous aerosols. Again, the nearby industrial activities have also been played an important role in the NCR sites, which in turn may also be the reason of higher carbons than Delhi.

Seasonal variation for PAHs ( $\text{ng/m}^3$ ) showed that GBD site recorded highest abundances throughout the periods followed by FBD, GGN, CPL and JNU (Fig 3.4). In monsoon season, a reverse trend of PAHs was observed between the sites FBD and GGN (in comparison to other seasons), where an overall order was found as: JNU < CPL < FBD < GGN < GBD. The spatial changes in the autumn season was found as similar to the variation in monsoon season except the sites FBD and GGN, where GBD experienced highest contribution of PAHs followed by FBD, GGN, CPL and JNU. In the winter season, again GBD was observed to be highly abundant of PAHs and JNU recorded the lowest. In this season, CPL was found to be with relatively lower contribution of PAHs than the autumn, but the overall trend of variation of PAHs showed similar to the autumn season with the following order GBD > FBD  $\geq$  GGN > CPL > JNU. In spring, a similar trend of abundances of PAHs was observed as in the autumn and winter. The order of PAHs in spring was found as: GBD > FBD > GGN > CPL > JNU. In the summer season, again similar pattern of variation of PAHs was observed; where the site GBD loaded with the highest amount of PAHs and JNU possessed the lowest. In this season also, the overall pattern of variation of PAHs was found similar to autumn, spring and winter seasons. JNU is rich in biodiversity in comparison to other sampling sites. Hence, effectively lower amounts of particulate pollutants under such environmental conditions are facilitated. Again, lower levels of pollutants in JNU might be due to the lack of anthropogenic activities than the other sites.

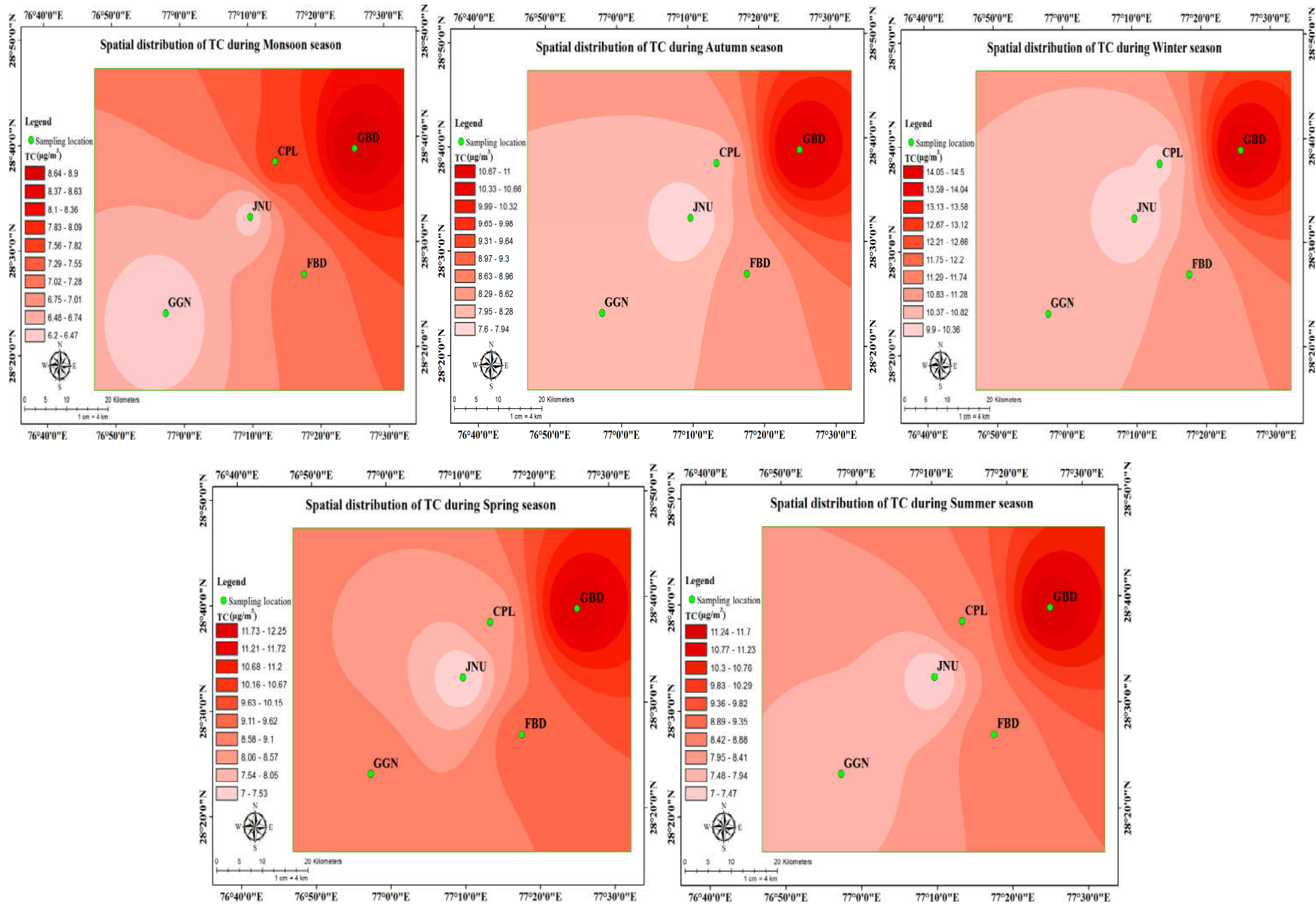


Fig 3.1 Spatial variation of TC throughout the seasons of the study period



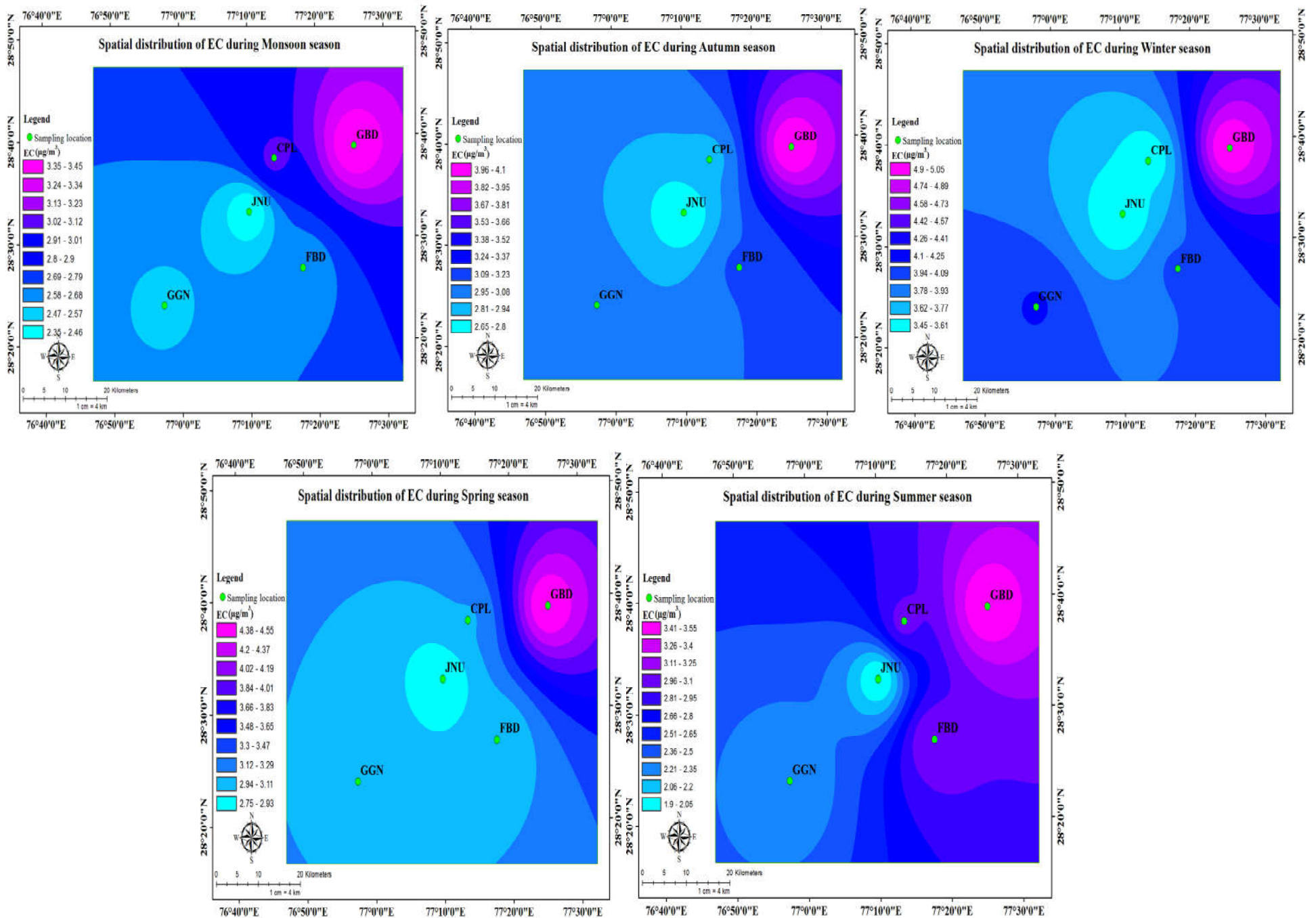
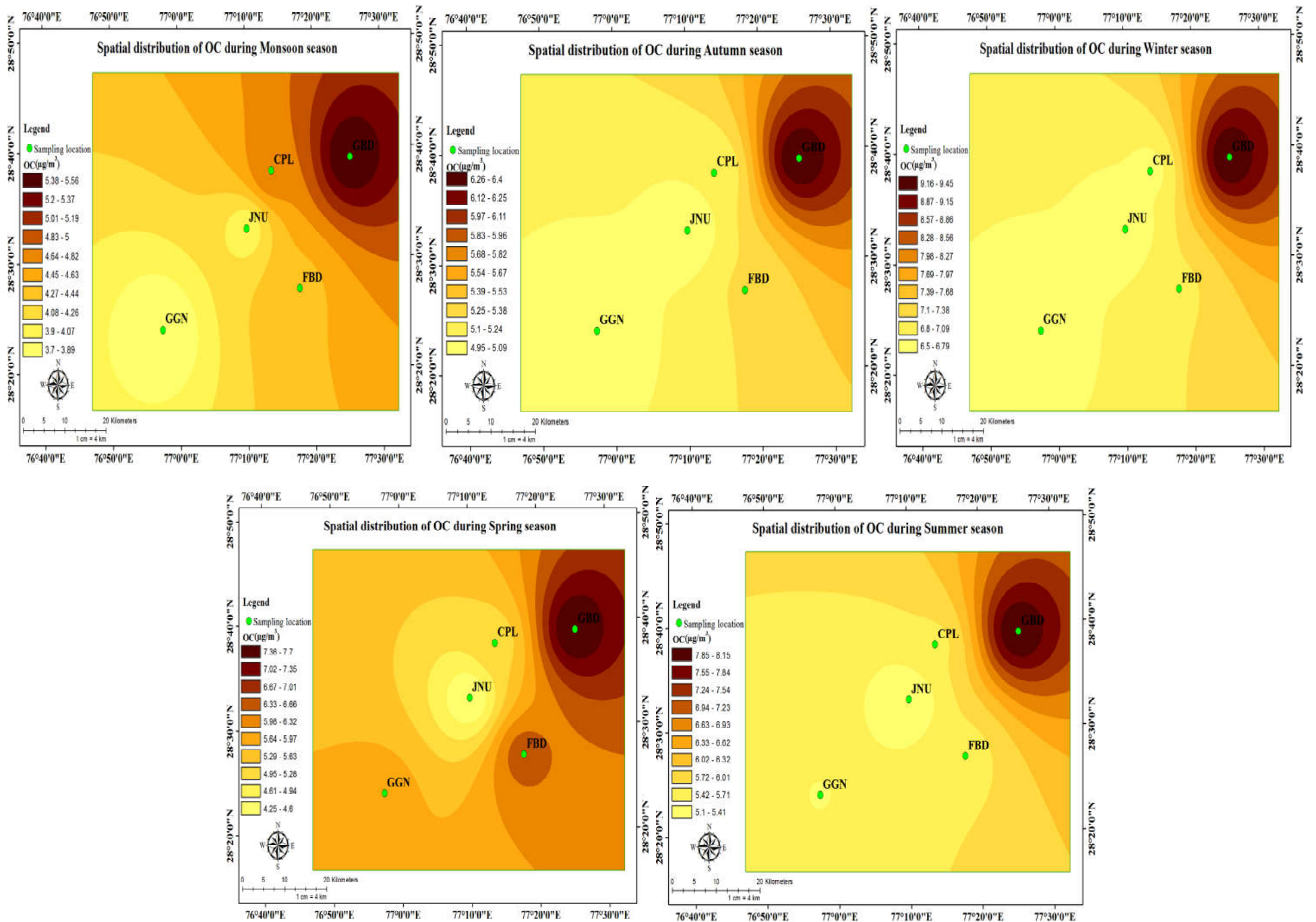


Fig 3.2 Spatial variation of EC throughout the seasons of the study period



**Fig 3.3** Spatial variation of OC throughout the seasons of the study period

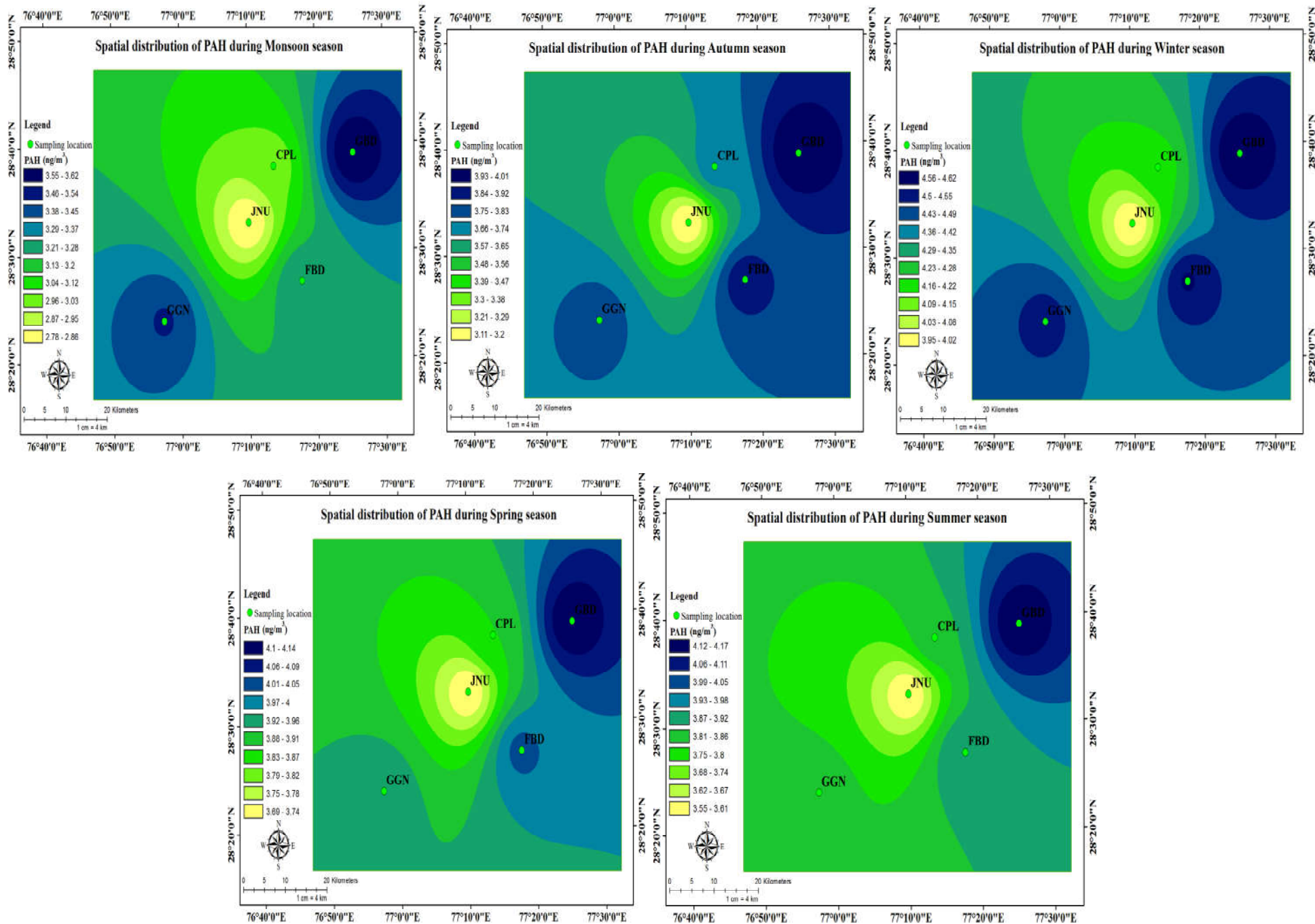


Fig 3.4 Spatial variation of PAHs throughout the seasons of the study period

### [3.1.1] Contribution of TC, EC and OC at various sites and in different seasons

The carbonaceous load with respect to TC, EC and OC were investigated across the season and sites associated with the size ranges of particles; fine ( $< 2.5 \mu\text{m}$ ) and coarse ( $> 2.5 \mu\text{m}$ ). It was observed that the higher average concentration ( $\mu\text{g}/\text{m}^3$ ) of TC, EC and OC were found in the fine particles, but in some cases coarse particles ( $> 2.5 \mu\text{m}$ ) was observed to be associated with higher amount of carbons. In this study, higher fractions of carbon were found to be associated with ultrafine, fine and coarse particles. Carbonaceous species have been studied in different size ranges or size segregated particles across the world at various monitoring sites (Kourtchev et al., 2005; Li et al., 2007; Geng et al., 2011). Studies carried out in different countries regarding size segregated particles revealed that relatively lower concentration of carbonaceous species have been observed to be associated with  $< 2.5 \mu\text{m}$  than the corresponding particles  $> 2.5 \mu\text{m}$  (Godec et al., 2012; Huang & Wang, 2014; Samara et al., 2014). On the contrary, some studies also reported the carbonaceous species associated with smaller size ranges (i.e.,  $< 2.5 \mu\text{m}$ ) exceeded than the corresponding coarse particles (Lin & Tai, 2001; Geng et al., 2009; Zhou et al., 2016). Meanwhile, studies carried out in different seasons showed that winter registered higher amount of carbons than the monsoon season (Duan et al., 2006; Cao et al., 2007; Yang et al., 2011; Samara et al., 2014; Satsangi et al., 2012; Sharma et al., 2014; Pant et al., 2015a; Villalobos et al., 2015; Roy et al., 2016), which is observed to be consistent with this work.

In all the seasons and at all the sites, TC was observed maximum followed by OC and EC throughout the study. In the monsoon season (Fig. 3.5), at the site GBD, the average concentration of carbons ( $\mu\text{g}/\text{m}^3$ ) was higher than the rest of other sites. Though, TC in fine fractions exceeded the corresponding coarse particles, but at the sites FBD and GGN; the concentrations were found higher in coarse fractions. The mean concentration of TC, EC and OC in the monsoon season was  $7.26 \pm 2.29$ ,  $2.80 \pm 0.95$  and  $4.48 \pm 1.17 \mu\text{g}/\text{m}^3$  respectively.

In the autumn season (Fig. 3.6), in fine particles, the mean concentration of TC was observed comparatively higher at all the sites except the site CPL; where higher concentration of TC was found in coarse particles. It was found that, the overall carbon load in autumn season was comparatively higher than the monsoon season. Mean concentration of carbon in this season was observed  $8.62 \pm 2.98$ ,  $3.15 \pm 1.04$  and  $5.33 \pm 1.55 \mu\text{g}/\text{m}^3$  for TC, EC and OC respectively

From Fig. 3.7, in winter, it was found that average concentration ( $\mu\text{g}/\text{m}^3$ ) of carbon was observed higher at all the sites than the monsoon and autumn seasons. Another major conclusion could be drawn is that the relative contribution of carbonaceous load regarding both the particles  $< 2.5$  and  $> 2.5$   $\mu\text{m}$  was found higher in winter season than the rest of other seasons. In this season, except the site JNU; all the sites possessed higher amount of carbons in fine particles than the corresponding coarse particles. The mean concentration of TC, EC and OC were  $11.26\pm 3.07$ ,  $4.01\pm 1.16$  and  $7.25\pm 2.17$   $\mu\text{g}/\text{m}^3$  respectively.

In the spring season (Fig. 3.8), mean concentration ( $\mu\text{g}/\text{m}^3$ ) of carbon was observed as  $9.15\pm 2.83$ ,  $3.29\pm 1.07$  and  $5.86\pm 1.61$  for TC, EC and OC respectively. Similar to other seasons, the higher amount of carbon was observed at the site GBD; whereas it was comparatively lower at JNU. In this season, at the site FBD, the concentration of carbonaceous load was found higher in coarse particles than the fine. At FBD; the OC possessed equivalent concentrations at both the fine and coarse fractions. At the site GBD, the average concentration of EC was found almost similar regarding both the fine and coarse fractions. Again, OC was found similar at GGN and JNU in coarse and fine particles respectively.

From Fig. 3.9, in summer season, it is clear that at sites CPL and GGN; coarse fractions registered the higher amount of carbon than the fine fractions. Relatively, similar amount of EC was observed in the coarse fractions at CPL and in fine fractions at FBD. Similarly, TC concentration was found similar at GGN in coarse fractions and at JNU in fine fractions. In this season, dust-storm might be the responsible factor for higher particulate loads. The average concentration of TC, EC and OC was  $8.73\pm 2.65$ ,  $2.75\pm 0.86$  and  $5.98\pm 1.73$   $\mu\text{g}/\text{m}^3$  respectively.

In Fig. 3.10, mean concentration of carbon was shown by considering concentrations of all the seasons, which was observed  $8.95\pm 2.97$ ,  $3.18\pm 0.93$  and  $5.76\pm 1.86$   $\mu\text{g}/\text{m}^3$  for TC, EC and OC respectively. Higher amount of carbon was found for GBD (TC  $11.69\pm 3.11$ , EC  $4.14\pm 1.19$  and OC  $7.45\pm 2.12$   $\mu\text{g}/\text{m}^3$ ) followed by FBD (TC  $8.91\pm 2.33$ , EC  $3.14\pm 0.94$  and OC  $5.76\pm 1.98$   $\mu\text{g}/\text{m}^3$ ), CPL (TC  $8.60\pm 2.81$ , EC  $3.11\pm 0.52$  and OC  $5.47\pm 1.83$   $\mu\text{g}/\text{m}^3$ ), GGN (TC  $8.25\pm 2.68$ , EC  $2.99\pm 0.71$  and OC  $5.27\pm 2.02$   $\mu\text{g}/\text{m}^3$ ) and JNU (TC  $7.57\pm 2.59$ , EC  $2.62\pm 0.67$  and OC  $4.95\pm 1.83$   $\mu\text{g}/\text{m}^3$ ). GBD had the highest amount of all the carbons, while GGN and JNU possessed lower concentration at all the seasons. Relatively, lower amount of carbons found at GGN than CPL might be due to the far off samplings from the busiest roadways and other activities.

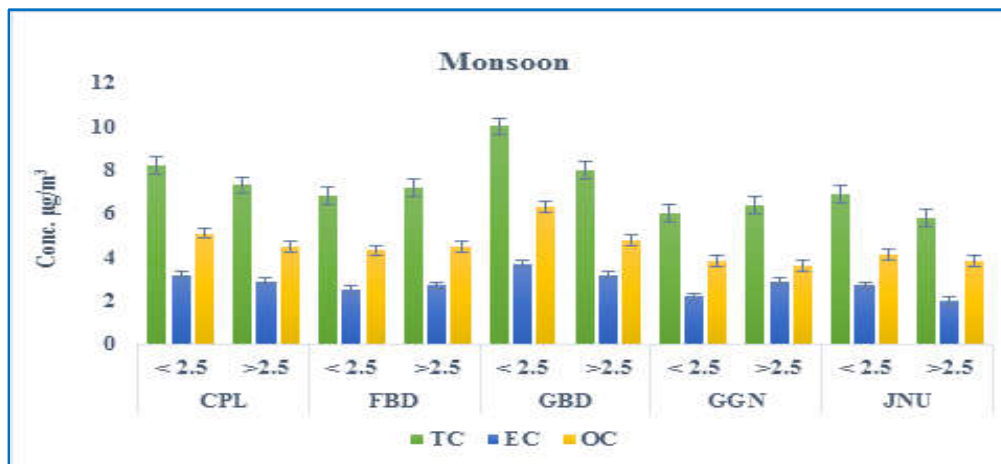


Fig. 3.5 Carbonaceous load with sites and size ranges of particles in the monsoon season

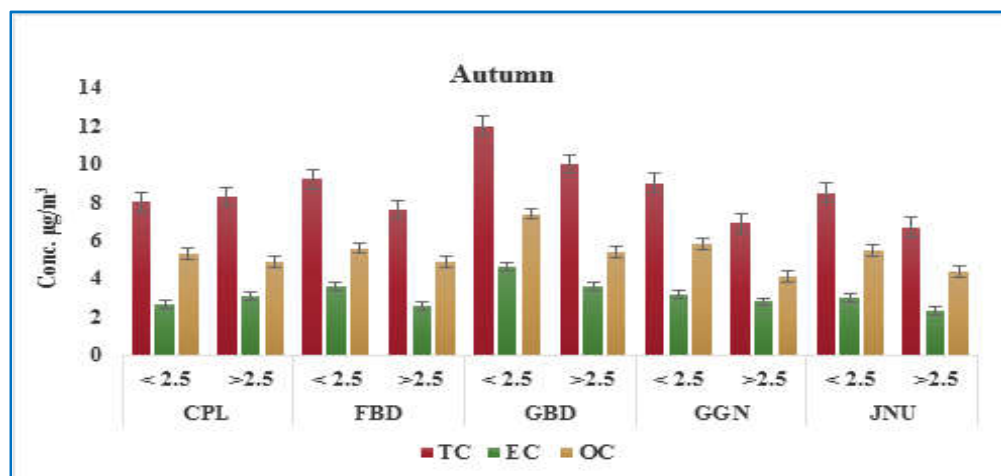


Fig. 3.6 Carbonaceous load with sites and size ranges of particles in the autumn season

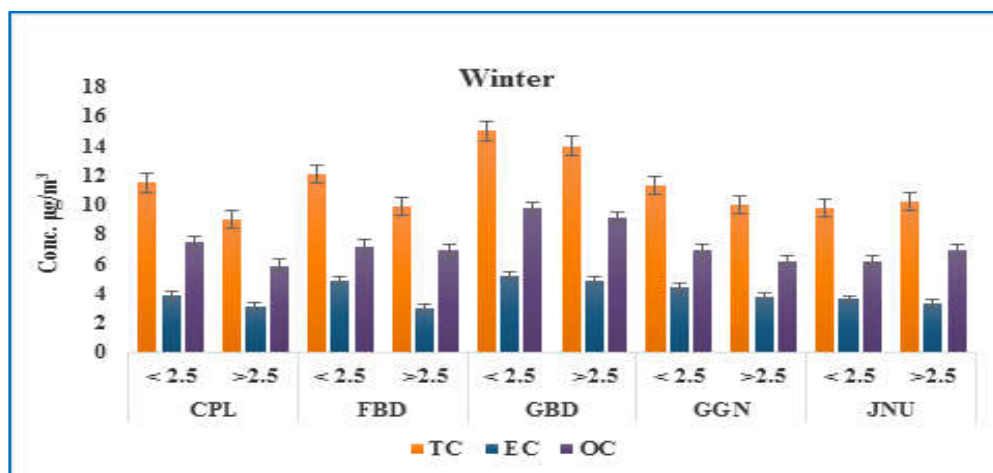
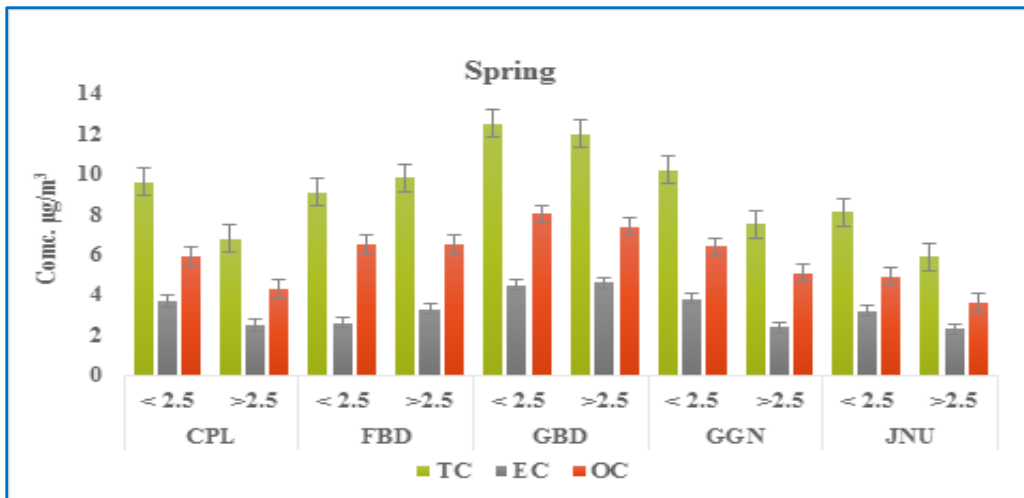
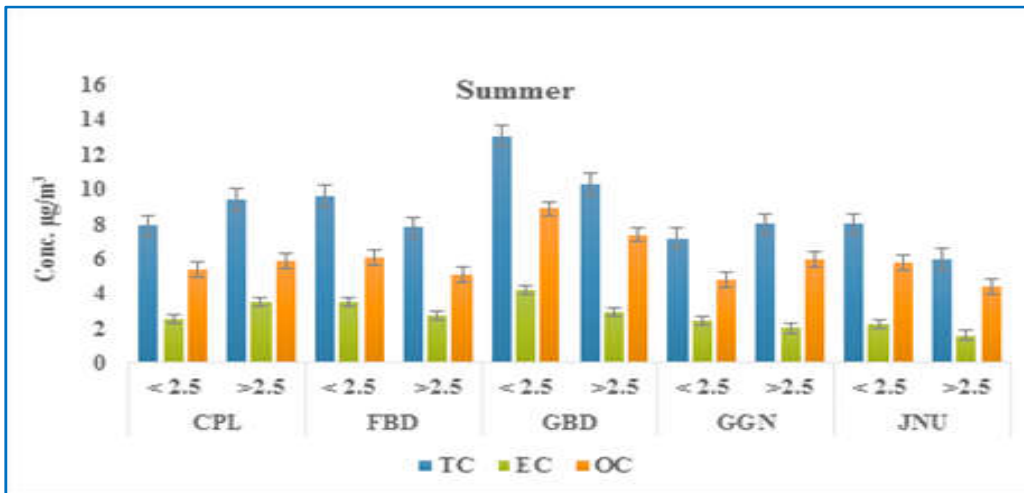


Fig. 3.7 Carbonaceous load with sites and size ranges of particles in the winter season



**Fig. 3.8** Carbonaceous load with sites and size ranges of particles in the spring season



**Fig. 3.9** Carbonaceous load with sites and size ranges of particles in the summer season

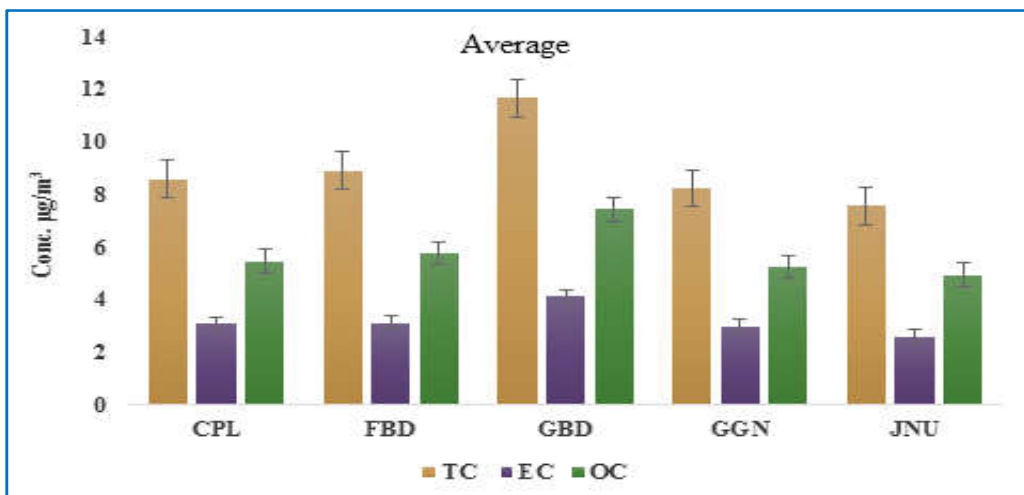


**Fig. 3.10** Variation of carbonaceous load with sites throughout the study

### [3.1.2] Seasonal variation of PAHs throughout the analyses

PAHs with seasonality have been reported at various monitoring sites (Li et al., 2006a; Pengchai et al., 2009; Wang et al., 2010; Tobiszewski & Namieśnik, 2012; Hoseini et al., 2016), where majority of studies have observed the significant seasonality between the winter and other seasons (Guo et al., 2003; Fon et al., 2007; Sitaras & Siskos, 2008; Martellini et al., 2012; Singla et al., 2012; Hasheminassab et al., 2013; Zhang et al., 2013; Wang et al., 2014; Dubey et al., 2015; Finardi et al., 2015; Pozo et al., 2015; Kim et al., 2016). In areas; where PAHs are emitted from industrial activities the concentration shows little seasonality, but significant seasonality is observed in areas where PAHs sources are related to commercial and residential heating (Kim et al., 2013). In this study, though relative seasonal variation of PAHs were observed, this might be due to the invariable vehicular and industrial activities throughout the NCR.

In the monsoon season (Table 3.1), it was observed that the mean concentration ( $\text{ng/m}^3$ ) of Npth ( $5.21 \pm 1.83$ ), Phtn ( $4.87 \pm 1.16$ ), Pym ( $5.10 \pm 1.68$ ), BaPn ( $5.25 \pm 1.29$ ), Chrn ( $4.15 \pm 1.18$ ), Flun ( $3.92 \pm 0.93$ ) and BaAn ( $3.68 \pm 1.23$ ) was found higher at all the sites in comparison to other PAHs. Acen ( $1.05 \pm 0.39$ ) was found with minimum concentration for all the sites and in all the seasons. The compounds BbFn ( $2.51 \pm 0.74$ ) and BkFn ( $2.54 \pm 0.73$ ) were distributed approximately in equal concentrations. Similarly, BghiP ( $2.28 \pm 0.80$ ) and DahA ( $2.24 \pm 0.96$ ) contributed almost equal concentrations. From Fig. 3.11; it could be inferred that the compounds Npth, Phtn, Pym and BaPn had higher concentrations followed by Chrn, Flun and BaAn; where the rest of other compounds possessed relatively lower concentrations with seasons.

In the autumn season, relatively higher trend of variation of concentration was observed for all the compounds in comparison to the monsoon season (Table 3.1). BaPn ( $7.49 \pm 2.46$ ) showed highest average concentration among all the PAHs and Acen ( $1.4 \pm 0.72$ ) possessed minimum average concentration ( $\text{ng/m}^3$ ) in the autumn season. Fig. 3.12 revealed that there was a linear trend of decrease in concentration for the compounds from Pym to BbFn. Again, the concentration of DahA was found higher than BghiP in this season.

During winter (Table 3.1), the mean concentration of PAHs was found higher than the rest of all other seasons. In contrast to the other two seasons (monsoon and autumn); the concentration of Phtn ( $6.53 \pm 2.18$ ), and Pym ( $6.52 \pm 2.29$ ), had almost parallel concentrations. In



this season, the maximum mean concentration was observed for BaPn ( $8.64 \pm 2.92$ ) followed by Npth ( $6.65 \pm 2.03$ ), Phtn ( $6.53 \pm 2.18$ ), Pyn ( $6.52 \pm 2.29$ ), Flun ( $5.14 \pm 1.42$ ) and then rest of the other PAHs. Similar to other seasons, the trend of decrease in concentrations were observed for the compounds from Npth to Anth (excluding Acen), and from Pyn to BkFn (Fig. 3.13).

In spring, the mean concentrations of Fluo ( $3.08 \pm 0.72$ ), Anth ( $3.11 \pm 0.92$ ) and BbFn ( $3.10 \pm 0.98$ ) were observed equivalent, where a similar trend of decrease in concentration for the PAHs from BaPn ( $7.82 \pm 2.95$ ) to Acen ( $1.25 \pm 0.30$ ) was observed (Table 3.1). But, the relative concentration of Acen was found comparatively higher in spring ( $1.25 \pm 0.30$ ) and winter ( $1.55 \pm 0.44$ ) seasons. In this season (spring), the average concentrations of Fluo, Anth, BbFn and DahA were observed almost parallel (Fig. 3.14). The variation of concentrations of rest of other PAHs was found to possess similar trend with other seasons.

In summer (Table 3.1), it was found that the concentration of Phtn ( $6.12 \pm 1.68 \text{ ng/m}^3$ ) exceeded slightly than Npth ( $5.91 \pm 2.10 \text{ ng/m}^3$ ). Though mean concentration variation of PAHs was observed to be following similar trend as observed in other seasons, but the overall PAHs concentration was found similar to the spring and autumn seasons (Fig. 3.15). The concentration of Acen ( $1.16 \pm 0.46 \text{ ng/m}^3$ ) was also found almost constant in all the seasons. Meanwhile, Acen possessed lowest average concentration at all the sites and season.

Fig. 3.16 shows the mean concentrations of all PAHs ( $\text{ng/m}^3$ ) throughout the study. The relative higher concentration of PAHs was observed for the compounds BaPn, Npth, Phtn Pyn, Flun and Chrn. Among the PAHs; Acen and IcdP possessed lower concentrations [Table 3.1]. It was seen that the compounds Acnp, Fluo and BbFn distributed equally throughout the analyses. From Table 3.1; it was clear that the average concentration of PAHs were higher in winter, whereas it was lower in the monsoon season. The annual average concentration of PAHs were found in the following order: Acen ( $1.29 \pm 0.38$ ) < IcdP ( $1.89 \pm 0.46$ ) < BghiP ( $2.56 \pm 0.87$ ) < DahA ( $2.87 \pm 0.85$ ) < Anth ( $2.93 \pm 0.81$ ) < Acnp ( $3.04 \pm 1.06$ ) ~ Fluo ( $3.06 \pm 0.73$ ) < BbFn ( $3.08 \pm 0.99$ ) < BkFn ( $3.14 \pm 0.82$ ) < BaAn ( $3.83 \pm 1.23$ ) < Chrn ( $4.52 \pm 1.25$ ) < Flun ( $4.76 \pm 1.27$ ) < Phtn ( $5.78 \pm 1.38$ ) < Pyn ( $5.85 \pm 1.76$ ) < Npth ( $5.89 \pm 2.06$ ) < BaPn ( $7.42 \pm 2.18$ ). Again, in case of carbonaceous load also, monsoon registered lower concentrations while winter comparatively registered higher load. The low temperature and low mixing height in winter might be the responsible factor for higher amounts of trapping particles, whereas the rainfall might be the deciding factor for lower amount of pollutants in the monsoon season.

**Table 3.1** Average concentration of PAHs (ng/m<sup>3</sup>) and carbonaceous species (µg/m<sup>3</sup>) throughout the seasons of the study.

Seasons→	Monsoon	Autumn	Winter	Spring	Summer	Average
Particulate species↓						
Npth	5.21±1.83	5.64±1.78	6.65±2.03	6.06±1.94	5.91±2.10	5.89±2.06
Phtn	4.87±1.16	5.35±1.97	6.53±2.18	5.98±1.72	6.12±1.68	5.78±1.38
Acnp	2.33±0.80	2.80±1.03	3.90±1.26	2.94±0.99	3.15±1.39	3.04±1.06
Acen	1.05±0.39	1.40±0.72	1.55±0.44	1.25±0.30	1.16±0.46	1.29±0.38
Fluo	2.57±0.74	2.93±0.79	3.58±0.96	3.08±0.72	3.00±0.69	3.06±0.73
Anth	2.40±0.55	2.86±1.01	3.27±0.74	3.11±0.92	2.91±1.09	2.93±0.81
Pyrn	5.10±1.68	6.09±2.07	6.52±2.29	5.61±1.77	5.74±1.98	5.85±1.76
Flun	3.92±0.93	4.76±1.58	5.14±1.42	4.98±1.04	4.88±1.21	4.76±1.27
Chrn	4.15±1.18	4.35±1.43	4.91±1.48	4.60±0.97	4.56±1.32	4.52±1.25
BaAn	3.68±1.13	3.62±1.22	4.08±1.56	3.81±1.05	3.75±1.16	3.83±1.23
BbFn	2.51±0.75	2.84±1.06	3.92±1.35	3.10±0.98	2.97±1.05	3.08±0.99
BkFn	2.54±0.73	3.04±0.90	3.76±1.14	3.16±0.86	3.12±0.78	3.14±0.82
BaPn	5.25±1.29	7.49±2.46	8.64±2.92	7.82±2.95	7.80±2.67	7.42±2.18
BghiP	2.28±0.80	2.45±0.92	2.83±0.89	2.63±0.97	2.41±1.02	2.56±0.87
DahA	2.24±0.96	2.71±0.81	3.33±0.78	2.99±0.78	3.18±0.95	2.87±0.85
IcdP	1.54±0.28	1.93±0.52	2.28±0.69	1.85±0.55	1.70±0.32	1.89±0.46
TC	7.26±2.29	8.62±2.98	11.26±3.07	9.15±2.83	8.73±2.65	8.95±2.97
EC	2.80±0.95	3.15±1.04	4.01±1.16	3.29±1.07	2.75±0.86	3.18±0.93
OC	4.48±1.17	5.33±1.55	7.25±2.17	5.86±1.61	5.98±1.73	5.76±1.86

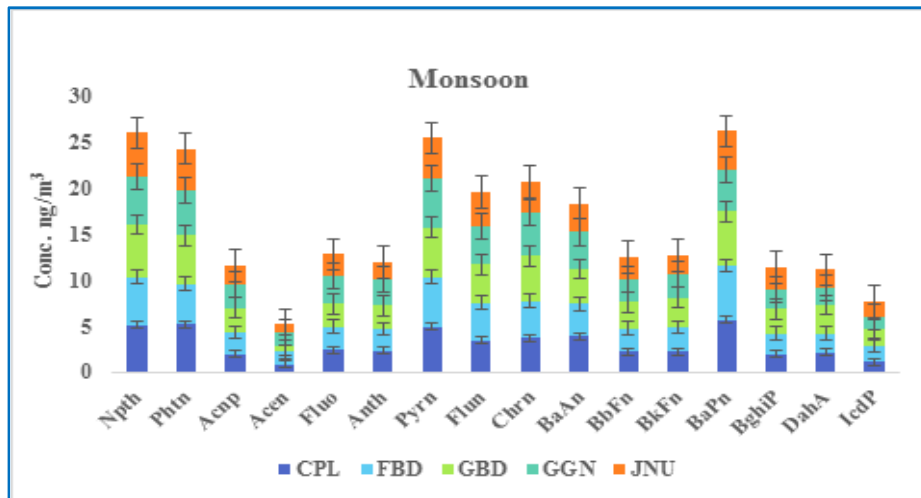


Fig. 3.11 PAHs distribution in the monsoon season with sites

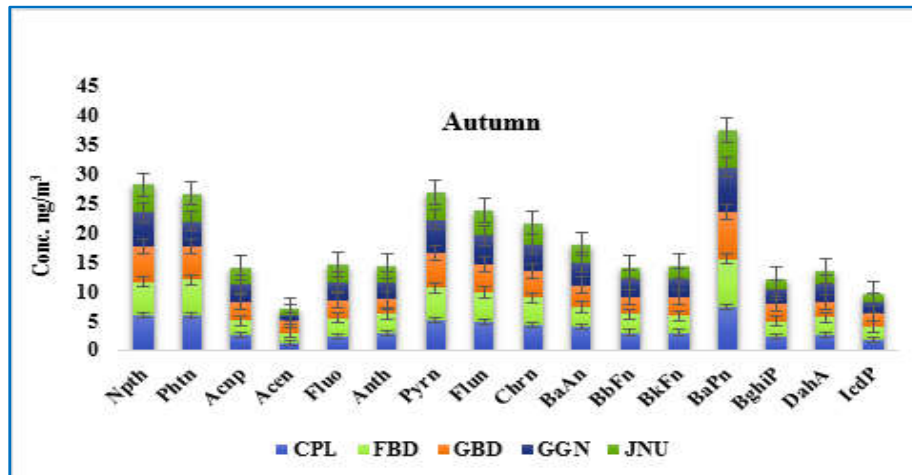


Fig. 3.12 PAHs distribution in the autumn season with sites

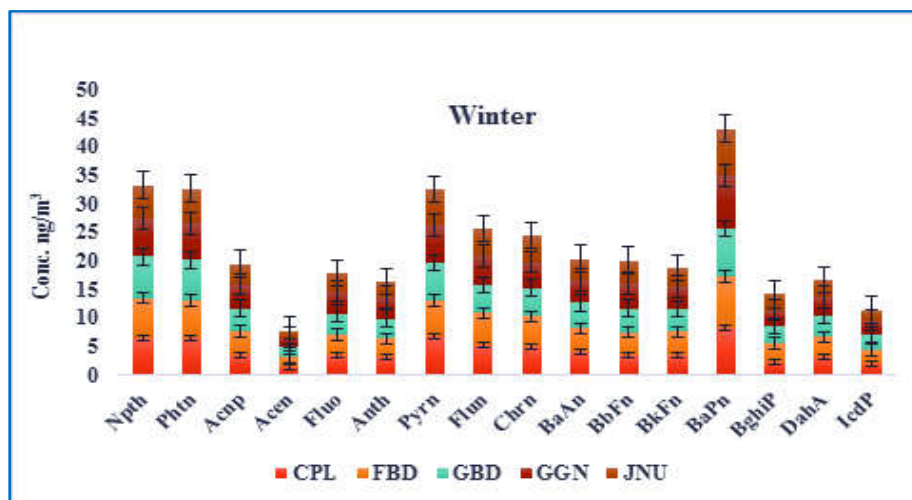


Fig. 3.13 PAHs distribution in the winter season with sites

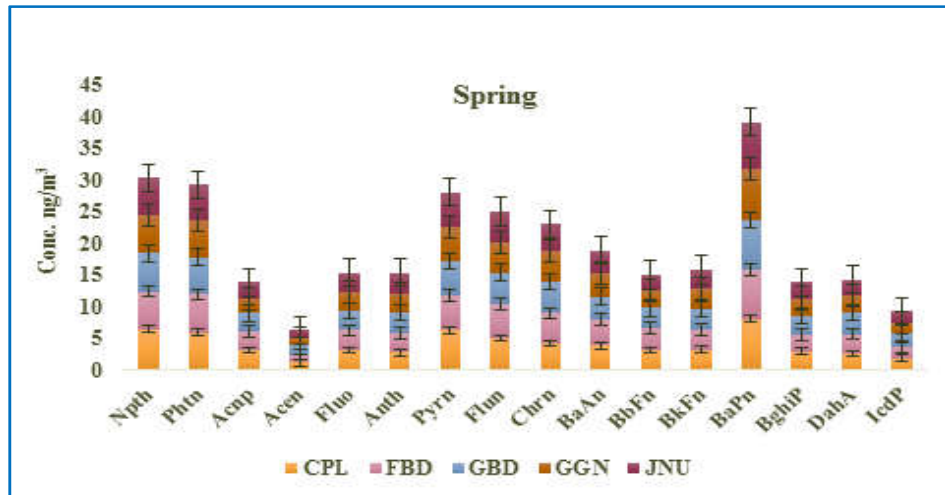


Fig. 3.14 PAHs distribution in the spring season with sites

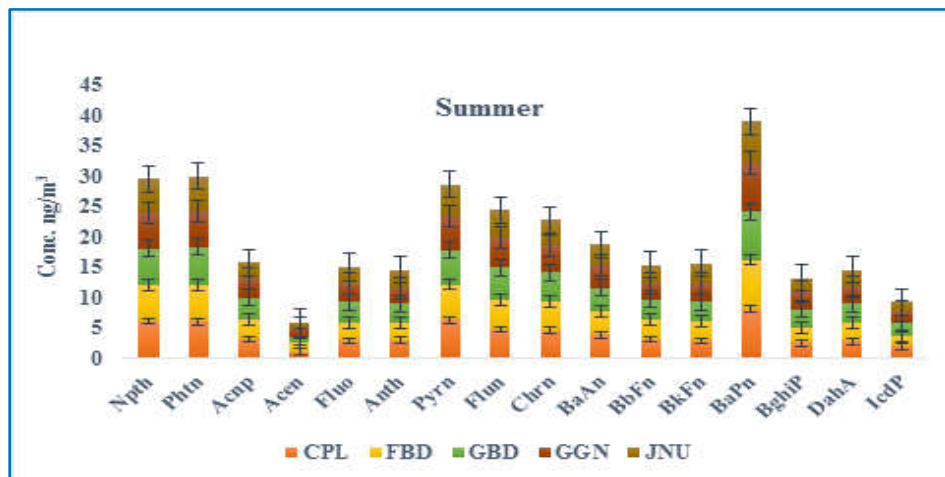


Fig. 3.15 PAHs distribution in the summer season with sites

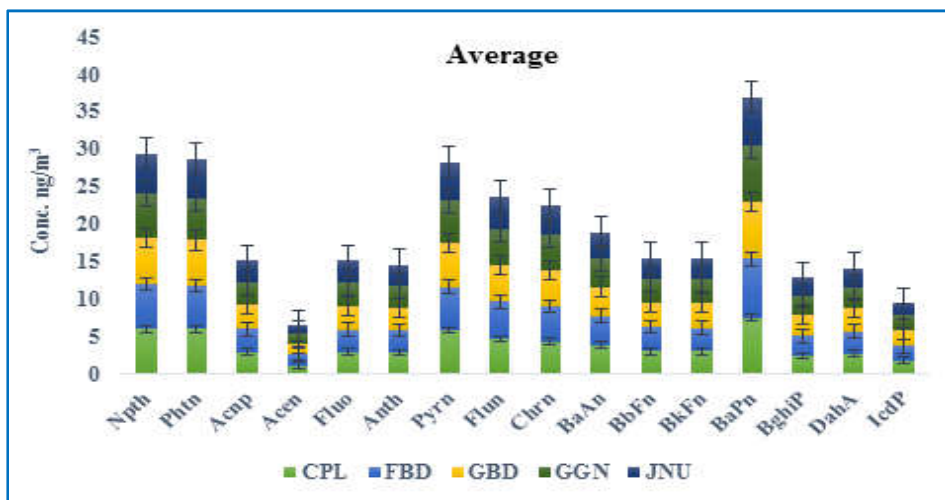
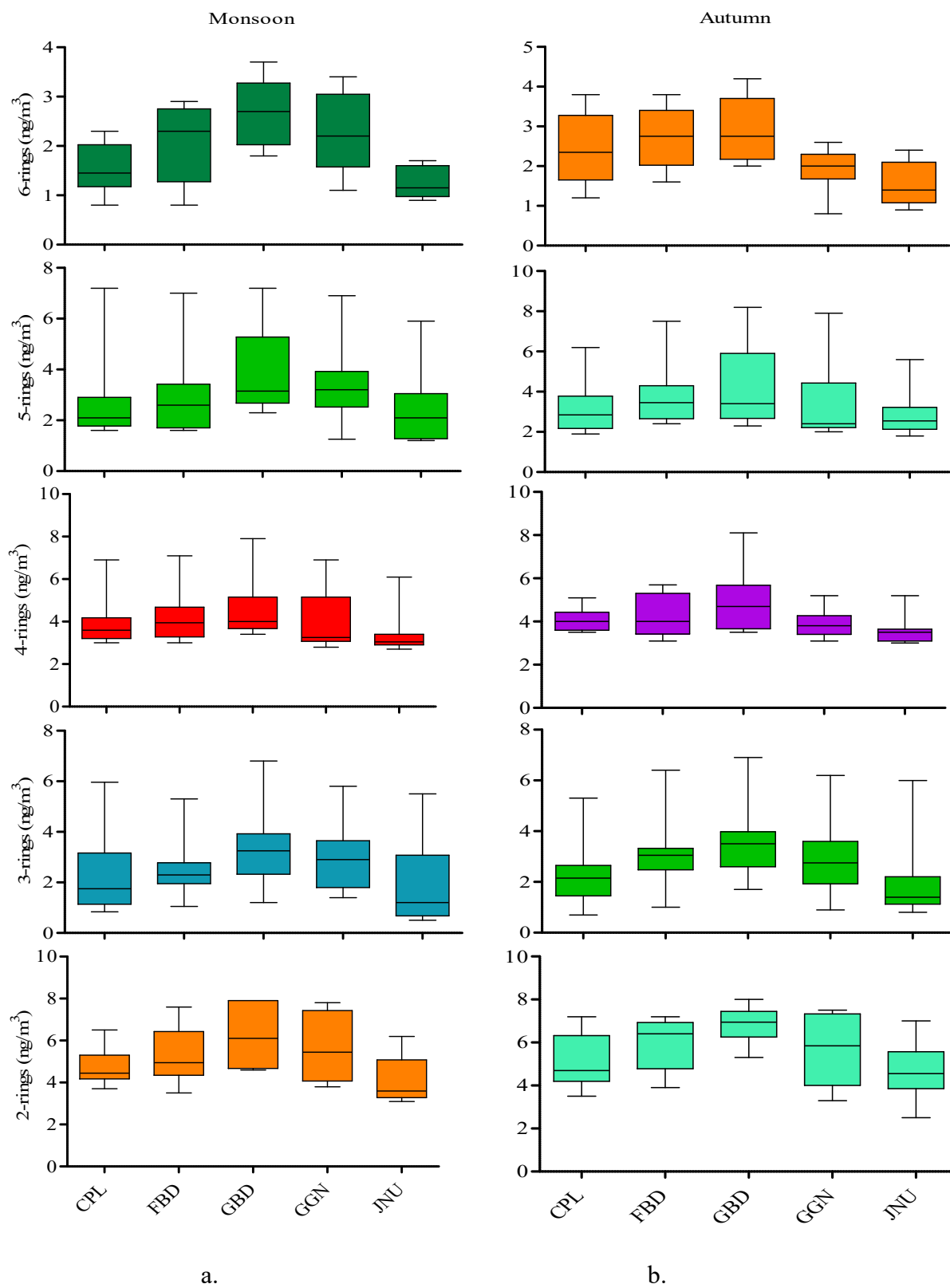


Fig. 3.16 Total (average) PAHs distribution throughout the sites

### [3.1.3] Ring wise distribution of PAHs across the sites

The PAHs of having different rings and their relative distribution at all the sites with seasons and throughout the study period are given in Figs. 3.17-3.19. It was observed that the site GBD possessed higher concentrations of all the rings of PAHs in comparison to other sites irrespective of seasons, whereas JNU possessed lower concentrations across the seasons. The 2-rings PAH (i.e., Np<sub>th</sub>) was found in higher concentrations at all the sites and size ranges of particles, for which the average concentration across the seasons was comparatively found higher. Higher concentrations of Np<sub>th</sub> was also observed (compared to other priority PAHs) in other studies such as at Tampa Bay, Florida USA (Poor et al., 2004) and at Assiut, Egypt (Abdallah & Atia, 2014). In this work, similar to Np<sub>th</sub>; Pht<sub>n</sub> (3-rings), Pyr<sub>n</sub> (4-rings) and BaP<sub>n</sub> (5-rings) possessed relatively higher amount across the seasons. But, the average concentration of PAHs with respect to 3-rings (Pht<sub>n</sub>, Acn<sub>p</sub>, Acn, Fluo and Anth), 4-rings (Pyr<sub>n</sub>, Flun, Chr<sub>n</sub> and BaAn), 5-rings (BbFn, BkFn and BaP<sub>n</sub>) and 6-rings (BghiP, DahA and IcdP) possessed almost similar variation regarding the sites and seasons. The priority PAHs under the US EPA guidelines; their concentrations and variations regarding different rings have been well observed by various researchers so far (Vardar & Noll, 2003; Poor et al., 2004; Kaur et al., 2013; Singh et al., 2013; Abdallah & Atia, 2014; Hassine et al., 2014; Jin et al., 2014; Villar-Vidal et al., 2014; Wu et al., 2014; Yin et al., 2015; Szabó et al., 2015; Albuquerque et al., 2016).

From Figs 3.17-3.19, it can be concluded that the trend of variation of concentration regarding all the PAHs of different rings showed different contributions. Monsoon (Fig. 3.17 a) possessed relatively lower concentration of all PAHs regarding all the rings (2 to 6 rings), whereas the winter (Fig. 3.18 a) possessed higher concentrations of all rings of PAHs. Relatively, moderate concentrations regarding ring wise distribution were observed for the rest of three seasons namely autumn (Fig. 3.17 b), spring (Fig. 3.18 b) and summer seasons (Fig. 3.19 a). Fig. (3.19 b) shows the average distribution of PAHs from 2 to 6 rings throughout the period of study. The average percentage contribution of PAHs (from Fig. 3.19 b) with respect to all rings for the sites CPL, FBD, GBD, GGN and JNU was found in the following order: GBD (23 %) > FBD (21 %) > GGN (20%) ~ CPL (19 %) > JNU (17 %).



**Fig. 3.17** Ring wise distribution of PAHs in the a. monsoon and b. autumn seasons throughout the sites

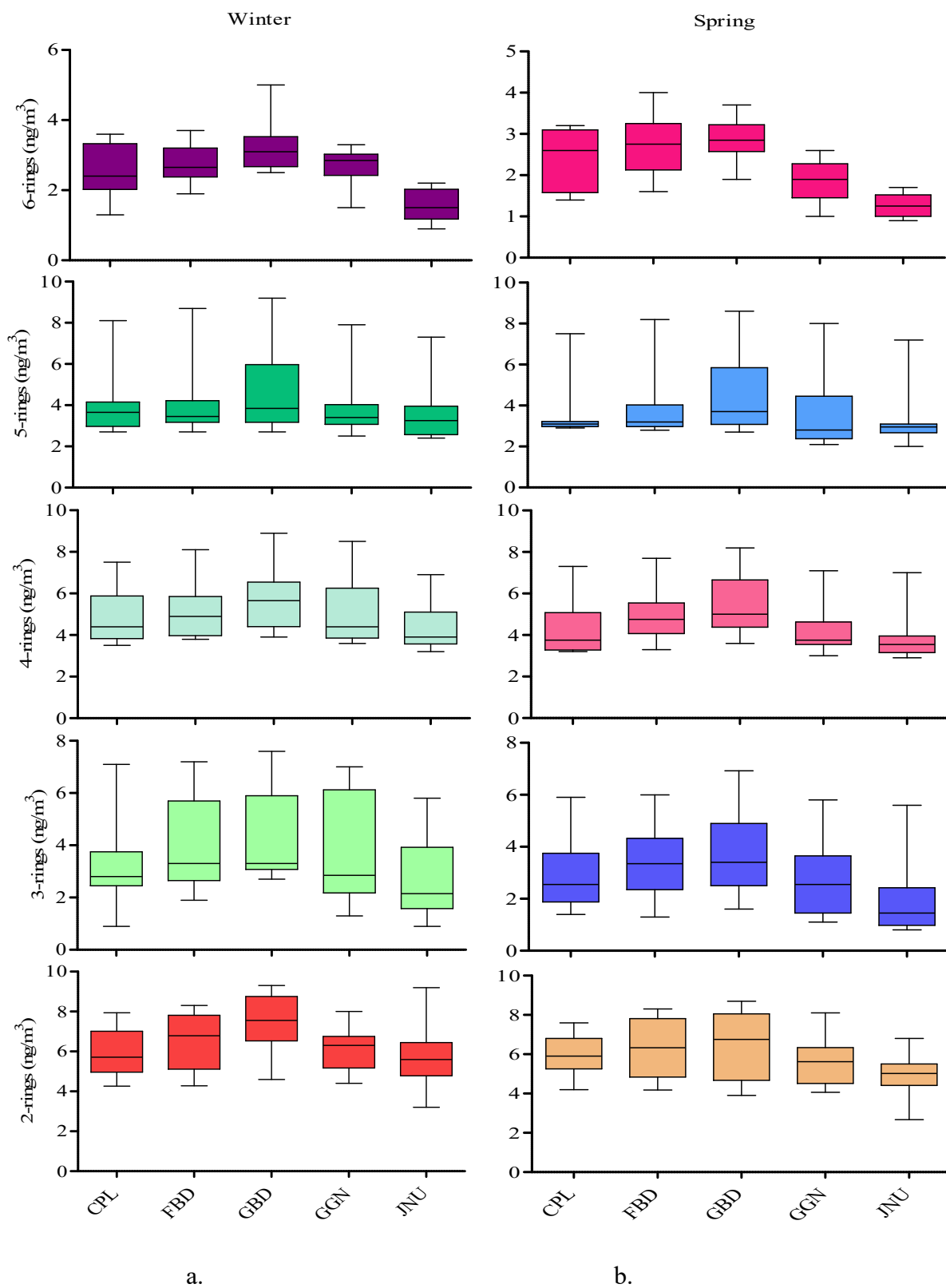


**Fig. 3.18** Ring wise distribution of PAHs in the a. winter and b. spring seasons throughout the sites

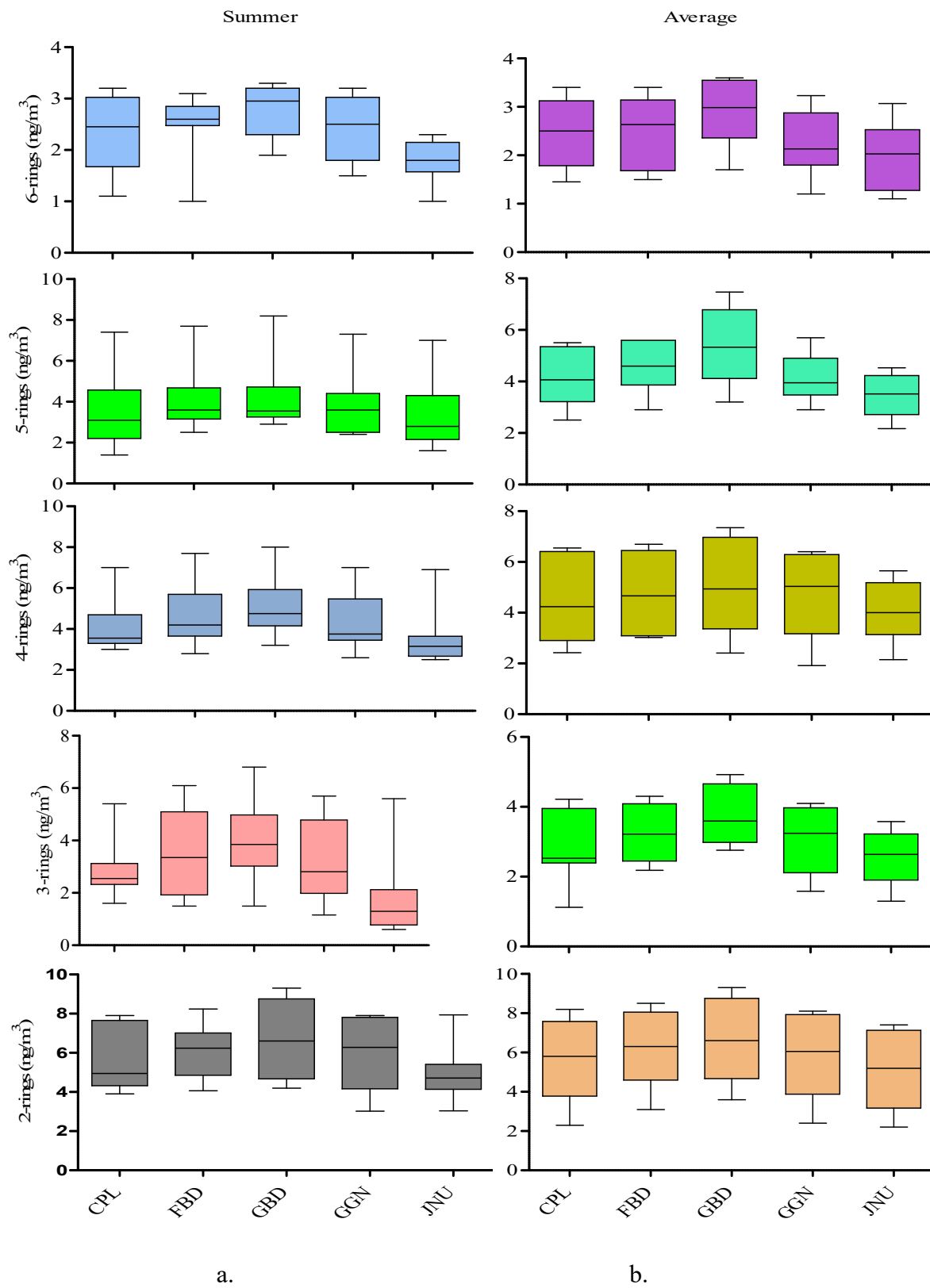


**Fig. 3.19** Ring wise distribution of PAHs in the a. summer and b. throughout the site



#### **[3.1.4] Variation of concentration of PAHs in fine (< 2.5 µm) and coarse (> 2.5 µm) mode aerosols across the sites**

PAHs associated with fine and coarse particles have been studied widely (Guo et al., 2003; Bourotte et al., 2005; Slezakova et al., 2013; Teixeira et al., 2013; Liaud et al., 2014; Booyens et al., 2015; Roy et al., 2017). Some studies observed that the concentrations of particle bound PAHs was found higher in finer particles or in the back up stages filters (Kameda et al., 2005; Blomqvist et al., 2014; Xu et al., 2015a; Lin et al., 2016; Sarti et al., 2017), which is found consistent with this study. It is clear from the Figs. (3.20-3.25) that the concentration of PAHs in fine particles (< 2.5 µm) exceeded the concentration adhered in coarse particles (> 2.5 µm), which is too consistent with the previous studies (Martins et al., 2012; Booyens et al., 2015).

In Fig 3.20, the concentration variation of sixteen priority PAHs associated with the size ranges fine and coarse are shown for the sites CPL. It was noted that at all the sites, fine particulate bound carbonaceous species dominated the coarse bound particles in terms of concentration and traceability. The concentrations of BaPn (in fine  $8.56 \pm 2.48 \text{ ng/m}^3$ ; and in coarse  $6.46 \pm 1.87 \text{ ng/m}^3$ ) and Pym (in fine  $8.28 \pm 3.45 \text{ ng/m}^3$ ; and in coarse  $3.4 \pm 1.43 \text{ ng/m}^3$ ) were observed higher than other priority PAHs. After BaPn and Pym; Npth (in fine  $7.76 \pm 2.46 \text{ ng/m}^3$ ; and in coarse  $4.28 \pm 1.37$ ), Phtn (in fine  $6.94 \pm 1.38 \text{ ng/m}^3$ ; and in coarse  $4.98 \pm 0.49 \text{ ng/m}^3$ ), Flun (in fine  $5.8 \pm 1.57 \text{ ng/m}^3$ ; and in coarse  $3.58 \pm 1.07 \text{ ng/m}^3$ ), Chrn (in fine  $5.6 \pm 1.79 \text{ ng/m}^3$ ; and in coarse  $3.06 \pm 1.26 \text{ ng/m}^3$ ) and BaAn (in fine  $5.02 \pm 1.61 \text{ ng/m}^3$ ; and in coarse  $2.74 \pm 0.62 \text{ ng/m}^3$ ) accounted comparatively higher concentrations among all other PAHs. Acen (in fine  $1.44 \pm 0.42 \text{ ng/m}^3$ ; and in coarse  $0.84 \pm 0.25 \text{ ng/m}^3$ ) and IcdP (in fine  $2.1 \pm 0.45 \text{ ng/m}^3$ ; and in coarse  $1.46 \pm 0.29 \text{ ng/m}^3$ ) possessed lower concentrations among all the PAHs.

In FBD (Fig. 3.21), the highest average concentration was observed for BaPn ( $8.78 \pm 2.57 \text{ ng/m}^3$  in fine and  $6.84 \pm 1.38 \text{ ng/m}^3$  in coarse) and Acen ( $1.76 \pm 0.48 \text{ ng/m}^3$  in fine and  $1.22 \pm 0.29 \text{ ng/m}^3$  in coarse) possessed lower amount among all the PAHs. The relative concentrations of some PAHs were found higher in this area than CPL. In comparison to the site CPL, the concentration of Fluo ( $3.82 \pm 1.42 \text{ ng/m}^3$  in fine and  $2.24 \pm 1.12 \text{ ng/m}^3$  in coarse) and IcdP ( $2.42 \pm 0.69 \text{ ng/m}^3$  in fine and  $1.46 \pm 0.28 \text{ ng/m}^3$  in coarse) were found higher. In fine particles, Anth ( $3.72 \pm 1.05 \text{ ng/m}^3$ ) and DahA ( $3.72 \pm 1.08 \text{ ng/m}^3$ ) were found equally abundant. In coarse

particles, the compounds Fluo ( $2.24 \pm 1.12 \text{ ng/m}^3$ ) and Anth ( $2.24 \pm 0.85 \text{ ng/m}^3$ ) were found in similar concentrations.

It was observed that, the site GBD loaded with higher concentration of carbonaceous load and PAHs, and in contrast, JNU was found with lower load of carbonaceous species and PAHs throughout the seasons. The concentration of BaPn ( $8.68 \pm 2.75$  and  $6.48 \pm 1.56 \text{ ng/m}^3$  in fine and coarse particles respectively) at GBD was found comparatively similar to the other sites (Fig. 3.22). But, the overall concentration of PAHs was observed to exceed than other sites with respect to  $< 2.5$  and  $> 2.5 \mu\text{m}$  in this sites. The concentration of Pyn ( $8.71 \pm 3.04$  and  $2.94 \pm 1.12 \text{ ng/m}^3$  in fine and coarse particles respectively) was found higher than the concentration of Npht with respect to fine particles. After BaPn, the concentrations of Npht ( $8.30 \pm 2.91$  and  $4.18 \pm 1.82 \text{ ng/m}^3$  in fine and coarse respectively) and Phtn ( $7.24 \pm 1.65$  and  $4.90 \pm 1.09 \text{ ng/m}^3$  in fine and coarse particles respectively) were found higher at the site GBD. IcdP also ( $2.52 \pm 0.44$  and  $1.90 \pm 0.23 \text{ ng/m}^3$  in fine and coarse respectively) was found comparatively highly concentrated than the sites CPL and FBD. Hazarika & Srivastava (2017) found similar concentration variations of PAHs at the site GBD. This could be due to the nearby industrial activities and heavy vehicular transportations, where particulate components might have highly dispersed in the surrounding areas. It is also important to mention that the areas experience with higher vehicular and industrial activities possess higher carbonaceous aerosols (Hazarika et al., 2017). Besides the concentration in fine particles, concentration of some PAHs such as BghiP ( $3.60 \pm 1.04$  and  $2.14 \pm 0.43 \text{ ng/m}^3$  in fine and coarse particles respectively) and DahA ( $3.88 \pm 1.23$  and  $2.56 \pm 0.94 \text{ ng/m}^3$  in fine and coarse particles respectively) were found higher in coarse particles in comparison to the sites CPL and FBD.

At site GGN (Fig. 3.23), the concentration of BaPn ( $8.68 \pm 3.06$  and  $6.34 \pm 1.65 \text{ ng/m}^3$  in fine and coarse particles respectively) was found almost equal to the sites CPL and FBD. In fine particles; Acnp ( $4.06 \pm 1.43$  and  $2.02 \pm 0.46 \text{ ng/m}^3$  in fine and coarse particles respectively) and BkFn ( $4.02 \pm 1.18$  and  $2.34 \pm 0.39 \text{ ng/m}^3$  in fine and coarse particles respectively) possessed similar concentrations. Similar to the other sites, Acen ( $1.78 \pm 0.62$  and  $0.9 \pm 0.13 \text{ ng/m}^3$  in fine and coarse respectively) and IcdP ( $2.16 \pm 0.43$  and  $1.54 \pm 0.24 \text{ ng/m}^3$  in fine and coarse particles respectively) contributed lower concentrations among all the PAHs. In fine particles, the concentration of BaAn ( $5.0 \pm 1.66 \text{ ng/m}^3$ ) was observed as similar to the concentration obtained at

CPL and FBD. Pynr ( $8.36\pm 3.06$  and  $3.03\pm 0.97$  ng/m<sup>3</sup> in fine and coarse particles respectively) was found second abundant PAHs after BaPn throughout the analyses at all the seasons at GBD.

Fig. 3.24 shows the mean concentration of PAHs at JNU. Though, the overall contribution of PAHs was found lower at this site, but the trend of variation across the study found similar to other sites. At this site, regarding both fine and coarse particles, the concentration of BaPn ( $7.46\pm 2.73$  and  $5.72\pm 2.08$  ng/m<sup>3</sup> in fine and coarse respectively) was found comparatively lower than the rest of other sites. Again, with respect to fine particles, the concentration of Pynr ( $7.57\pm 2.99$  ng/m<sup>3</sup>) was found comparatively higher than BaPn ( $7.46\pm 2.30$  ng/m<sup>3</sup>). Activities such as industrial, vehicular and other anthropogenic role are very limited in the area of JNU in comparison to the other active sites/areas, hence crustal re-suspension and other pyrogenic activities might be the major contribution of PAHs (Yadav et al., 2013; Hazarika et al., 2017). Concentration of IcdP ( $2.17\pm 0.70$  and  $1.16\pm 0.31$  ng/m<sup>3</sup> in fine and coarse particles) was found similar to the concentration of IcdP at GGN in fine particles. Acen ( $1.14\pm 0.43$  and  $0.82\pm 0.24$  ng/m<sup>3</sup> in fine and coarse respectively) and IcdP were found with lower concentrations among all the PAHs.

Fig. 3.25 shows the mean concentration of PAHs across the study. The overall concentration variations of PAHs were found from  $0.98\pm 0.30$  ng/m<sup>3</sup> for Acen (the lowest in fine particles) to  $8.43\pm 2.46$  ng/m<sup>3</sup> for BaPn (the highest; associated with fine particles) throughout the study. PAHs adhered with fine particles were higher, while PAHs with the particles bounded to coarse were lower concentrations. Since, fine particles adheres more pollutants because of high surface to volume ratio than coarse, which might be the results of higher amount of PAHs. Among all the priority PAHs; the compounds Phtn ( $7.01\pm 1.78$  ng/m<sup>3</sup> in fine; and  $4.49\pm 1.17$  ng/m<sup>3</sup> in coarse particles), Npth ( $7.82\pm 2.72$  ng/m<sup>3</sup> in fine; and  $3.97\pm 1.03$  ng/m<sup>3</sup> in coarse particles), Pynr ( $8.27\pm 2.68$  ng/m<sup>3</sup> in fine; and  $3.07\pm 0.98$  ng/m<sup>3</sup> in coarse particles) and BaPn ( $8.43\pm 2.46$  ng/m<sup>3</sup> in fine; and  $6.37\pm 1.50$  ng/m<sup>3</sup> in coarse particles) were found to be highly abundant regarding fine particles throughout the analyses. In case of fine particles, concentrations of PAHs were found with the following order: BaPn > Pynr > Npth > Phtn > Flun > Chrn > BaAn > Acnp > BbFn > BkFn > Fluo > Anth > DahA > BghiP > IcdP > Acen. Again, the variations of concentrations of PAHs with respect to coarse particles were found in the following order: BaPn > Phtn > Npth > Flun > Chrn > Pynr > BaAn > Fluo > BkFn > BbFn > Anth > DahA > Acnp > BghiP > IcdP > Acen.

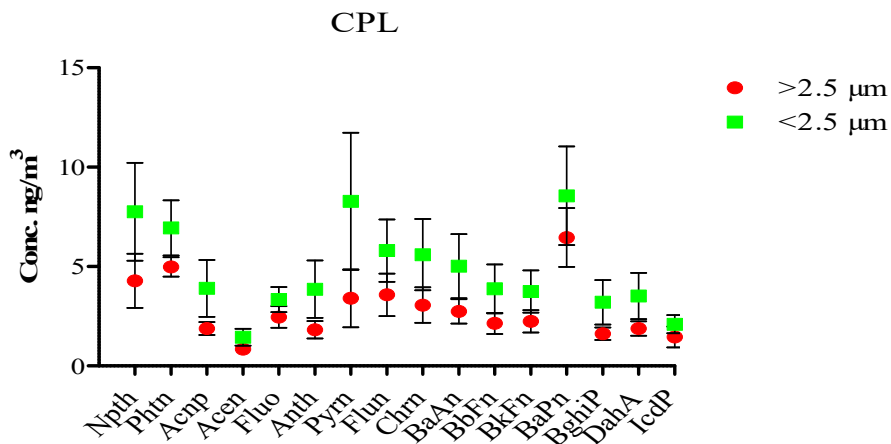


Fig. 3.20 Concentration variation of PAHs with < 2.5 and > 2.5 μm at the site CPL

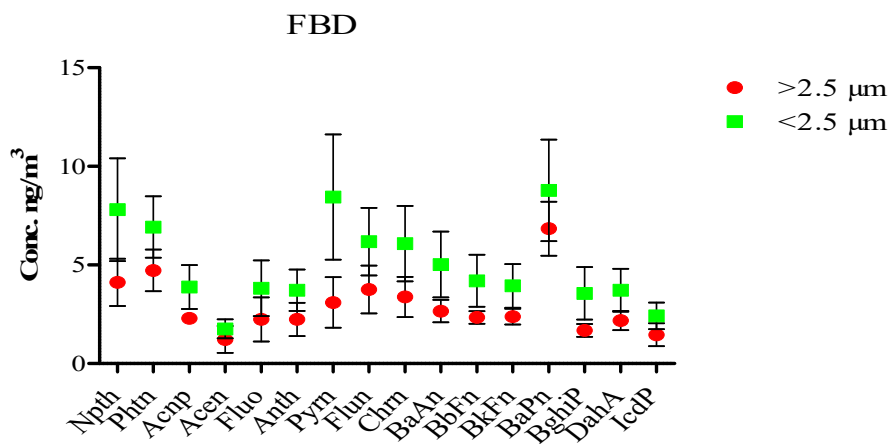


Fig. 3.21 Concentration variation of PAHs with < 2.5 and > 2.5 μm at the site FBD

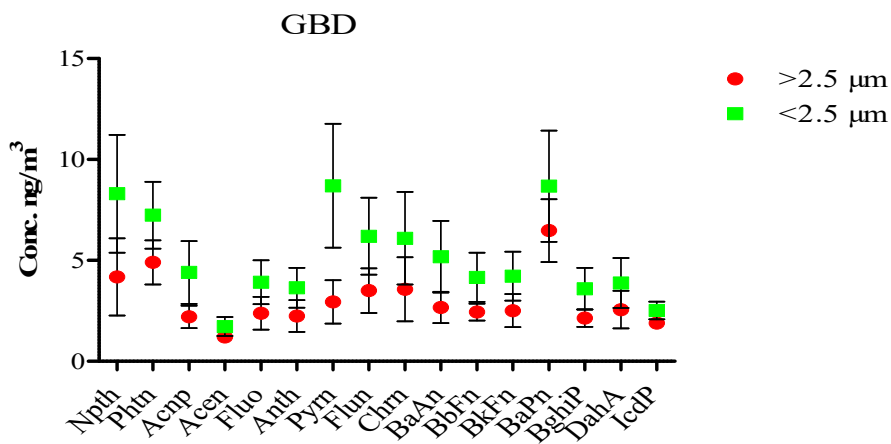


Fig. 3.22 Concentration variation of PAHs with < 2.5 and > 2.5 μm at the site GBD

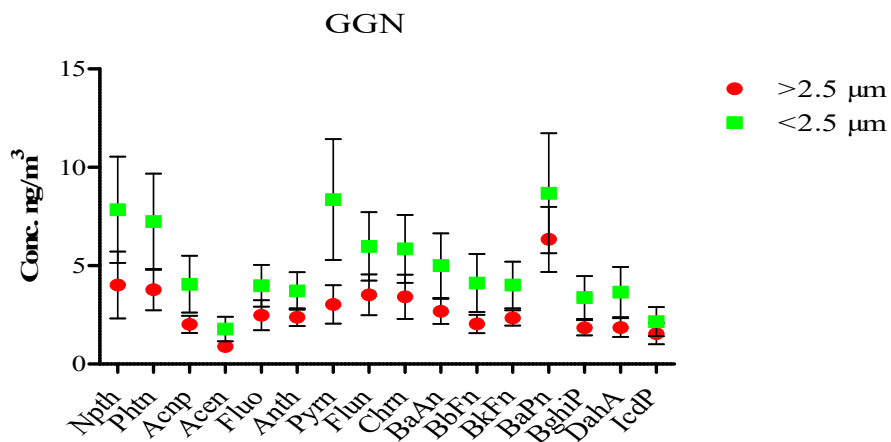


Fig. 3.23 Concentration variation of PAHs with < 2.5 and > 2.5 μm at the site GGN

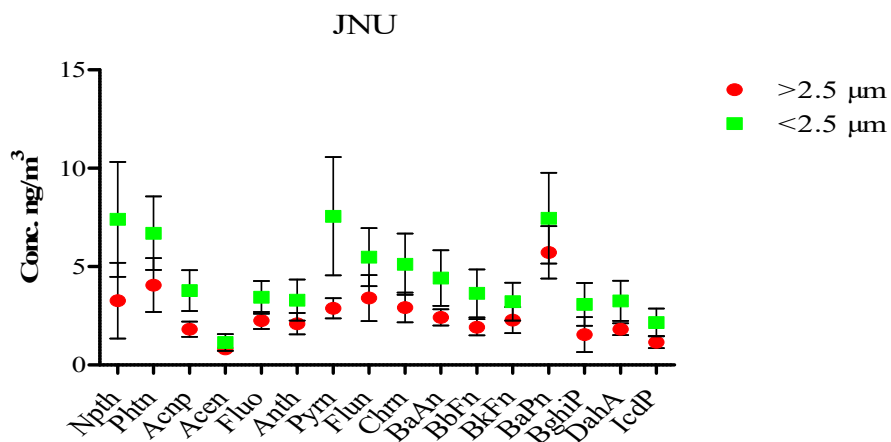


Fig. 3.24 Concentration variation of PAHs with < 2.5 and > 2.5 μm at the site JNU

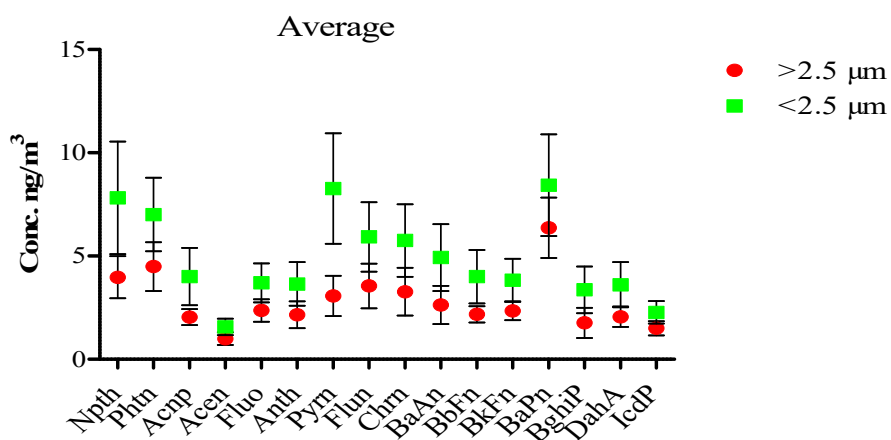


Fig. 3.25 Average concentration of PAHs with < 2.5 and > 2.5 μm throughout the study

### **[3.2] Relationships among different parameters, and the species**

#### **[3.2.1] Relationship between PMs and meteorological parameters**

Fig. 3.26 shows the regression analyses of particulate matters [PMs ( $\mu\text{g}/\text{m}^3$ )] with respect to temperature ( $^{\circ}\text{C}$ ), relative humidity (RH, %), wind speed (Km/hr) and dew point ( $^{\circ}\text{C}$ ) across the years at the study sites. PMs, and its relationships with meteorological parameters have been reported by various researchers so far (Gupta et al., 2006; Sharma et al., 2007; Singla et al., 2012). PMs concentrations were found higher in the winter season, while it was comparatively lower in the monsoon season. Rest of the other seasons registered considerably moderate concentrations of PMs. The concentration of PMs was taken averages of all the seasons and consequently regression was plotted against the meteorological parameters (Fig. 3.26). Regression of best fit was plotted with PMs, and it was found that with respect to temperature ( $^{\circ}\text{C}$ ), it is negatively co-related; i.e.,  $R^2 = 0.64$  (Fig. 3.26 a). But, in case of RH (%), the regression with PMs was observed to be positively related (Fig. 3.26 b;  $R^2 = 0.44$ ). Again, the negative relations between PMs with wind speed ( $R^2 = 0.09$ ; Fig. 3.26 c) and, PMs with dew point ( $R^2 = 0.03$ ; Fig. 3.26 d) were observed. The correlation matrices obtained between the meteorological parameters and PMs are also given in Table 3.2. Role of dew point temperature on PM have also been reported (Schwartz, 1994a,b,c). The prevailing environmental conditions might have governed the correlations with PMs of the area of NCR.

#### **[3.2.2] Relationship between PMs associated with fine and coarse particles**

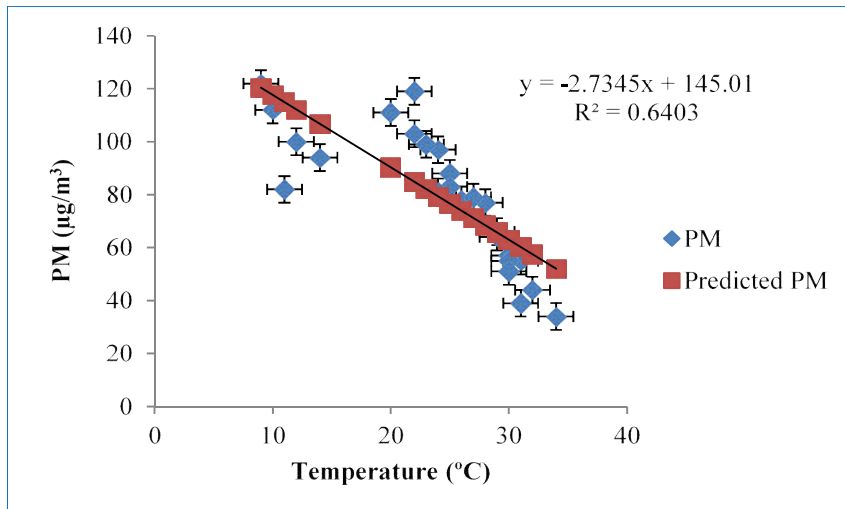
Abundances of PMs associated with fine and coarse particles ( $< 2.5 \mu\text{m}$  vs.  $> 2.5 \mu\text{m}$ ) show a linear increment throughout the seasons (Fig. 3.27). Similar to PMs with meteorological parameters (Fig. 3.26), the mean concentration of PMs associated with  $< 2.5 \mu\text{m}$  vs.  $> 2.5 \mu\text{m}$  was considered for the scatter plots. It was observed that significant linear increment among all the size ranges of particles ( $< 2.5$  and  $> 2.5 \mu\text{m}$ ) are the indicative of common emission/exposure sources in the Delhi-NCR (Fig. 3.27 a-f). PMs associated with  $< 2.5 \mu\text{m}$  was higher than  $> 2.5 \mu\text{m}$ . Gupta et al., (2006) observed significant relationships between PMs associated with  $< 2.5$  and  $> 2.5 \mu\text{m}$ . Similar result was obtained by Pant et al., (2015a) in Delhi where  $\text{PM}_{2.5}$  concentrations were higher during the winter, and it was lower in monsoon season. Studies

carried out in Delhi capital region reported that  $PM_{2.5}$  concentrations have exceeded the prescribed limit of Indian NAAQS (Tiwari et al., 2013; Trivedi et al., 2014). A significant linear correlation was found for all the PMs adhered with  $< 2.5$  and  $> 2.5 \mu m$  at all the seasons of the study; such as in monsoon (Fig. 3.27 a;  $R^2 = 0.62$ ), autumn (Fig. 3.27 b;  $R^2 = 0.82$ ), winter (Fig. 3.27 c;  $R^2 = 0.77$ ), spring (Fig. 3.27 d;  $R^2 = 0.81$ ), summer (Fig. 3.27 e;  $R^2 = 0.74$ ) and throughout the analyses (Fig. 3.27 f;  $R^2 = 0.84$ ).

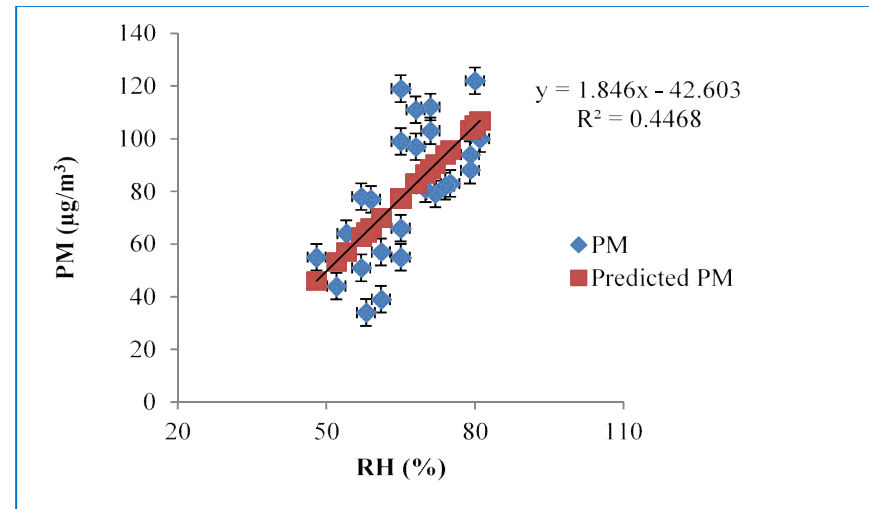
### [3.2.3] Relationship plot between carbon and PAHs

Fig. 3.28 (a, b and c) shows scatter plots of EC vs. OC, TC vs. EC and, OC vs. TC; which were made by taking mean concentrations of TC, EC and OC throughout seasons of the study periods. Linear increment/correlation was observed for EC vs. OC (Fig. 3.28 a;  $R^2 = 0.34$ ) [which was found relevant to the summer season observed by Ji et al., (2016), and in Delhi relatively higher significant values were observed ( $R^2 = 0.53$ , Sharma et al., 2014;  $R^2 = 0.843$ , Sharma et al., 2016)], and TC vs. EC (Fig. 3.28 b;  $R^2 = 0.85$ ). Similarly, positive relation was also obtained between OC vs. TC (Fig. 3.28 c;  $R^2 = 0.33$ ). Yang et al., (2010) observed significant correlation between OC and EC at Toronto and Beijing, China. The significant linear correlation between OC and EC indicates similar emission sources such as vehicular frequencies, and poorer correlation might be the source of secondary organic aerosols under favorable conditions followed by photochemical reactions and also the mechanisms associated with gas to particle conversions (Sharma et al., 2016). From the relation of OC and EC, the possible common emission sources such as vehicular traffic and biomass burning has already been established in New Delhi by Pant et al., (2015a).

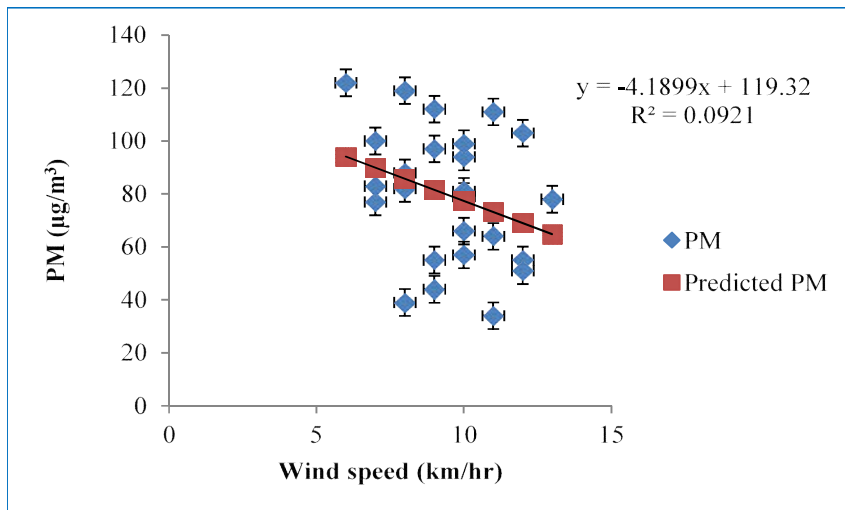
Fig. 3.28 d shows the regression of  $\Sigma PAHs$  with carbon (TC, EC and OC) by considering the average values of all the five seasons. Positive correlation was observed for  $\Sigma PAHs$  vs. TC ( $R^2 = 0.56$ ) and  $\Sigma PAHs$  vs. EC ( $R^2 = 0.67$ ); but a comparatively low significant but positive relation was observed between  $\Sigma PAHs$  vs. OC ( $R^2 = 0.35$ ). Arnott et al., (2005) observed the significant relations ( $R^2 = 0.75$ ) between PAHs and EC originated from vehicular sources or fossil fuel combustion. Similarly, significant relationship among PAHs and EC associated with biomass burning were also reported (Li et al., 2009; Rajput et al., 2013). Han et al., (2009) observed that dust derived  $PM_{10}$  bound PAHs and OC showed good relationship ( $R^2 = 0.87$ ).



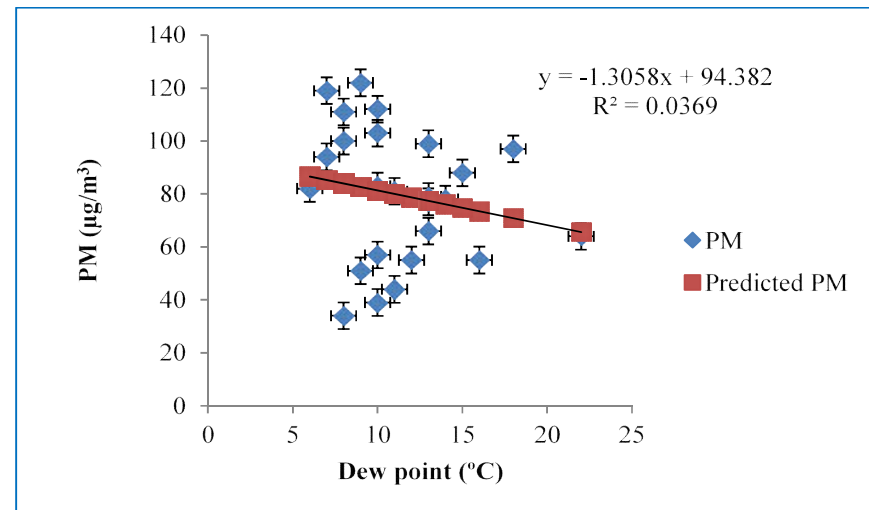
a.



b.



c.



d.

**Fig 3.26** PMs relationship with a. Temperature ( $^{\circ}\text{C}$ ), b. Relative humidity (%), c. Wind speed (Km/hr) and d. Dew point ( $^{\circ}\text{C}$ )



**Table 3.2** Correlation matrix between meteorological parameters with PMs

		Temperature (°C)	RH (%)	Dew point (°C)	Wind speed (Km/hr)	PMs (µg/m <sup>3</sup> )
<b>Temperature (°C)</b>	Pearson Correlation	1	-0.754**	0.418*	0.401*	-0.800**
	Sig. (2-tailed)		0.000	0.037	0.047	0.000
<b>RH (%)</b>	Pearson Correlation	-0.754**	1	-0.316	-0.410*	0.668**
	Sig. (2-tailed)	0.000		0.124	0.042	0.000
<b>Dew point (°C)</b>	Pearson Correlation	0.418*	-0.316	1	0.252	-0.192
	Sig. (2-tailed)	0.037	0.124		0.224	0.357
<b>Wind speed (Km/hr)</b>	Pearson Correlation	0.401*	-0.410*	0.252	1	-0.303
	Sig. (2-tailed)	0.047	0.042	0.224		0.140
<b>PMs (µg/m<sup>3</sup>)</b>	Pearson Correlation	-0.800**	0.668**	-0.192	-0.303	1
	Sig. (2-tailed)	0.000	0.000	0.357	0.140	

\*\* . Correlation is significant at the 0.01 level (2-tailed).

\* . Correlation is significant at the 0.05 level (2-tailed).

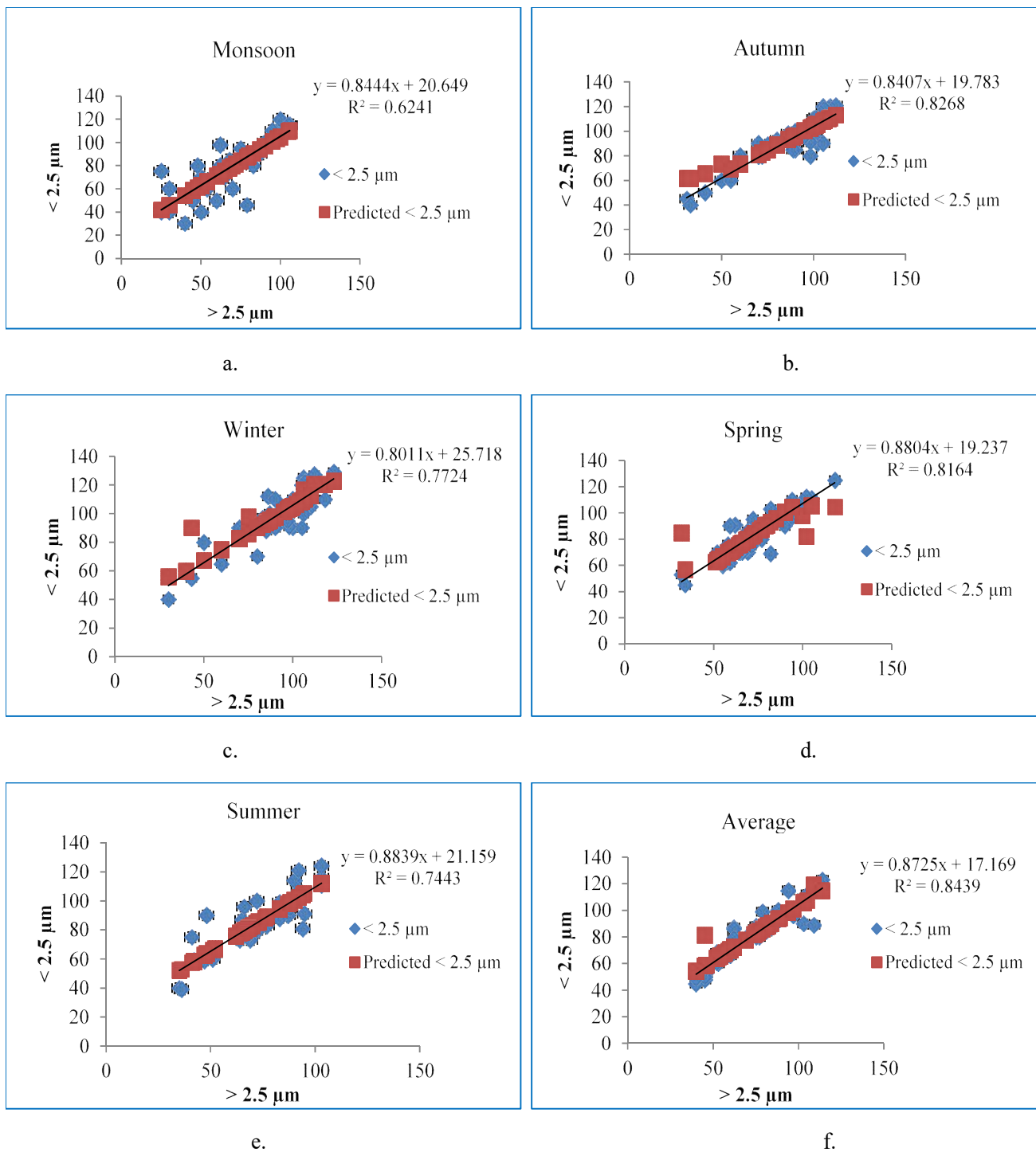
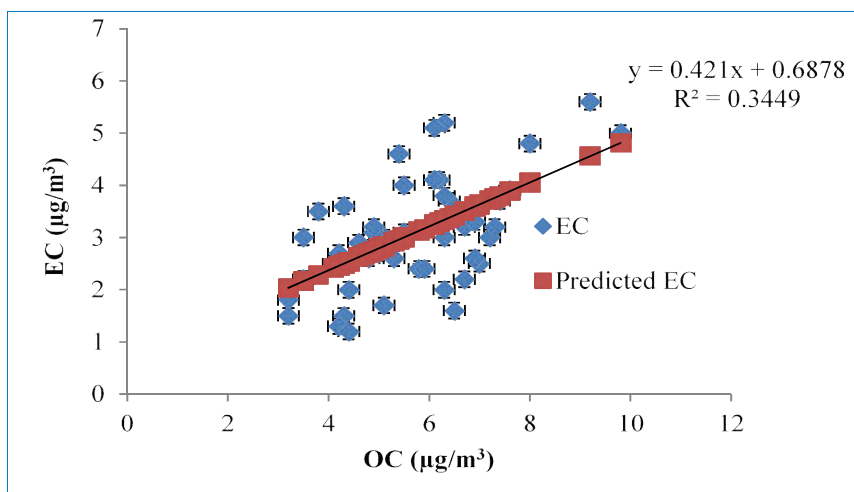
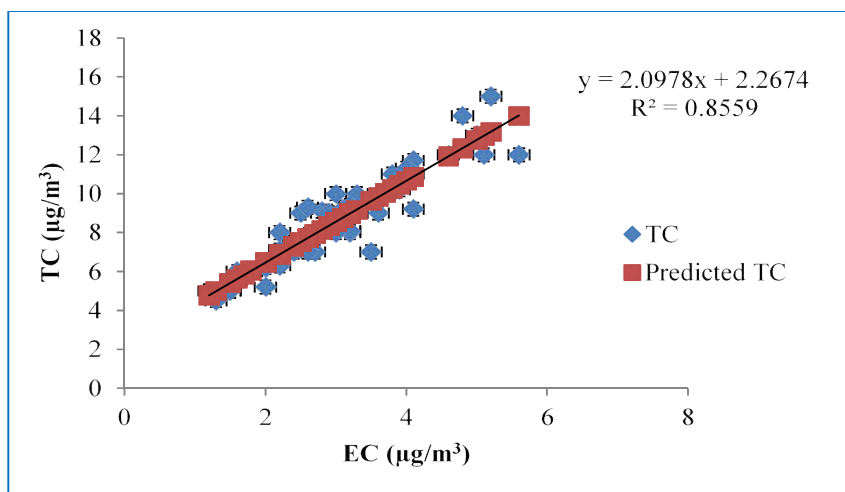


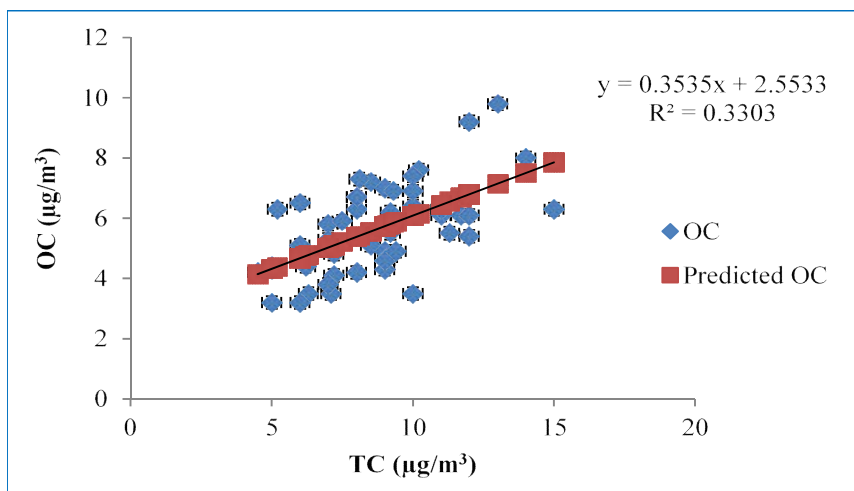
**Fig 3.27** Regressions among PMs ( $\mu\text{g}/\text{m}^3$ ) in  $< 2.5$  and  $> 2.5$   $\mu\text{m}$  with seasons (a-e) and throughout the study period (f)



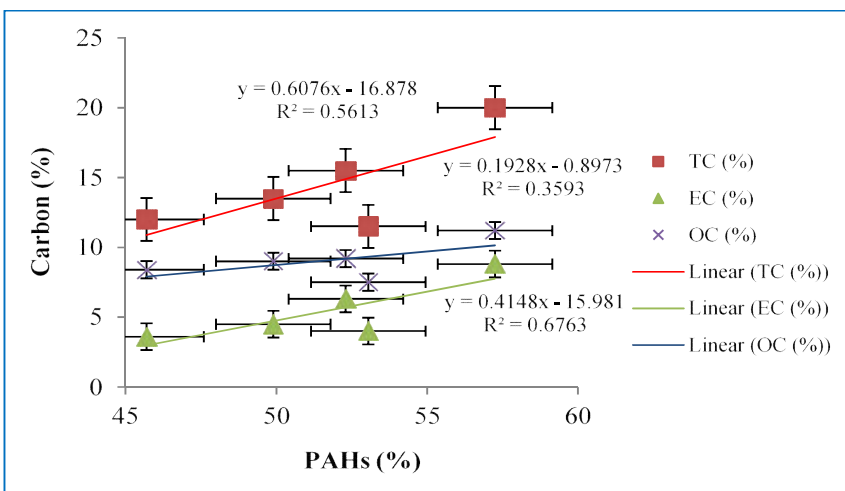
a.



b.



c.



d.

**Fig 3.28** Regressions between the a. mean EC vs OC, b. TC vs EC, c. OC vs TC, and d.  $\Sigma$ PAHs vs TC, OC and EC throughout the study

**[4.1] Source apportionment of PAHs throughout the season**

Source apportionments of PAHs were carried out by applying the Principal Component Analysis (PCA) through the statistical software version XLSTAT 7.5.2. PCA is a statistical technique, which is applicable to a set of variables/parameters in order to reduce their dimensionality. PCA represents the replacement of a wide set of inter correlated parameters/variables with smaller numbers of independent variables. The variables (i.e., principal components) are derived from the original parameters/variables (Thurston & Spengler, 1985). Sources of PAHs have been established by various studies in different parts of the country (Kulkarni & Venkataraman, 2000; Ray et al., 2008; Agarwal et al., 2009; Sarkar & Khillare, 2011; Gupta et al., 2011; Masih et al., 2012; Hussain et al., 2015; Hazarika et al., 2017) and in the world (Duval & Friedlander, 1981; Khalili et al., 1995; Simcik et al., 1999; Fang et al., 2006). The probable sources are vehicular activities (diesel, gasoline and natural gas), coal and biomass burning along with incomplete combustion of oil/organic materials from industries. Though, there are possibilities of miscellaneous sources of emission of PAHs primarily from vehicular, industrial activities, coal and biomass burning; but only the major expected sources of individual PAHs in a combined manner are shown throughout PC1-PC4 in Tables (4.1-4.6). Similar conclusion was also drawn in the percentage contribution of different sources in Figs. 4.1-4.2.

In Table 4.1 (monsoon season); the components of the groups (PC1, PC2, PC3 and PC4) of PAHs with higher loadings are given with their expected emission sources (below the respective Table). The corresponding Eigen values are 6.09, 3.88, 2.00 and 1.12 whereas; the cumulative percentages 36.57%, 49.89%, 61.94% and 75.98% for the components PC1-PC4 respectively. The percentage variances for PC1-PC4 are 36.57%, 19.25%, 10.04% and 3.03% respectively. The first component (PC1) is associated with Npth (0.749), Phth (0.694), Anth (0.627), Flun (0.651), Chrn (0.564), BkFn (0.872) and BaPn (0.560) indicating vehicular activities (diesel and gasoline) are the major sources (Ravindra et al., 2006; Han et al., 2009; Liu et al., 2015; Li et al., 2016b). PC2 is dominated by Npth (0.646), Acnp (0.504), Flun (0.732), BaAn (0.618) and IcdP (0.521); this could be ascribed as gasoline emission and coal combustion (Wang et al., 2008; Sarkar & Khillare, 2011; Di Vaio et al., 2016), while for the component PC3;

Acen (0.725), Pyn (0.545), BbFn (0.669), BaPn (0.677) and DahA (0.524) could be the indicator of miscellaneous sources such as diesel, gasoline and coal burning (Wang et al., 2008; Jamhari et al., 2014; Sarkar & Khillare, 2011, 2013). The fourth component (PC4) indicated more tracers from gasoline, natural gas and coal burning of the compounds Fluo (0.533), Chrn (0.648) and BghiP (0.651) (Dallarosa et al., 2005; Wang et al., 2008; Kong et al., 2010).

In autumn season (Table 4.2); the percentage variance for PC1-PC4 are 40.63%, 21.17%, 8.34% and 4.12% respectively. The Eigen values are 8.17, 3.65, 2.32 and 1.01; the cumulative percentages 40.63%, 52.65%, 68.89% and 78.55% for PC1-PC4 respectively. PC1 comprised Npth (0.787), Acnp (0.689), Fluo (0.703), Pyn (0.587), Chrn (0.603), and BaPn (0.641) which could be referred as vehicular activities (diesel and gasoline) and combustions processes (Ravindra et al., 2006; Wang et al., 2008; Wang et al., 2014; Liu et al., 2015). For the component PC2; Acen (0.697), Flun (0.620), Chrn (0.790), BkFn (0.532) and DahA (0.771) attributed vehicular emission (mainly diesel) and coal combustion (Hong et al., 2007; Sharma et al., 2007; Kong et al., 2010). In case of PC3; the compounds Phtn (0.735), Anth (0.616), BaAn (0.512) and BghiP (0.655) might be the sources of gasoline, diesel and natural gas (Ravindra et al., 2006; Fon et al., 2007; Sharma et al., 2007; Mohanraj et al., 2011; Pongpiachan et al., 2015). PC4 comprised Npth (0.583), Pyn (0.712) and BbFn (0.619); which could be emitted from diesel vehicle, coal and biomass burning (Simcik et al., 1999; Dallarosa et al., 2005; Wang et al., 2014).

In Table 4.3 (winter season); the percentage variance of the components PC1-PC4 are obtained as 34.05%, 16.24%, 6.15% and 2.97% respectively. The corresponding Eigen values are 6.52, 3.28, 1.93 and 1.14; and the cumulative percentages 34.05%, 47.69%, 64.05% and 76.21% for PC1-PC4 respectively. PC1 explained high loadings of Phtn (0.862), Acnp (0.571), Flun (0.657), BaAn (0.526), BbFn (0.598), BaPn (0.617) and IcdP (0.868). These compounds suggested the emission mainly from vehicular diesel and natural gas (Fon et al., 2007; Jamhari et al., 2014). The higher loadings of the compounds Npth (0.685), Fluo (0.887), Pyn (0.582) and BkFn (0.699) in PC2 might be the exposure of diesel exhaust and wood combustion (Ravindra et al., 2006; Han et al., 2009; Kong et al., 2010), and in PC3; the higher loadings of Acen (0.732), Chrn (0.538), BaAn (0.872) and BghiP (0.783) might have linked with the gasoline and diesel emission (Ravindra et al., 2006; Sharma et al., 2007). Again, the higher loaded PAHs in PC4 such as Phtn (0.729), Anth (0.781), and DahA (0.837) could come from diesel emission and coal combustion (Ravindra et al., 2006; Sharma et al., 2007; Pongpiachan et al., 2015).

In Table 4.4 (for the spring months); the percentage variance for the groups of components (PC1 PC2, PC3 and PC4) are 38.41%, 17.16%, 9.07% and 3.25% respectively. The corresponding Eigen values are 7.68, 4.07, 2.91 and 1.85 whereas; the cumulative percentages are 38.41%, 53.77%, 67.35% and 77.47% for PC1-PC4 respectively. The first component (PC1) is dominated by Npth (0.977), Acnp (0.879), Pym (0.880), BkFn (0.682), BghiP (0.523) and IcdP (0.616); which could be characterized by vehicular sources (primarily diesel) (Ravindra et al., 2006). PC2 is associated with Phtn (0.873), Fluo (0.522), Chrn (0.593), and DahA (0.643). These PAHs (in PC2) might be associated with gasoline and wood burning (Ravindra et al., 2006; Kong et al., 2010). PC3 accounted the compounds Npth (0.658), Anth (0.530), and BbFn (0.542); which could also be attributed from diesel and coal burning (Ravindra et al., 2006; Kong et al., 2010; Silva et al., 2010). The fourth component (PC4) is loaded with Acen (0.557), Flun (0.608) and BaPn (0.597). These PAHs could be the tracer of vehicular activities (primarily gasoline) and coal burning (Duval & Friedlander, 1981; Khalili et al., 1995; Ravindra et al., 2006; Sarkar & Khillare, 2011; Liu et al., 2015).

In summer season (Table 4.5); the Eigen values for the corresponding groups are 6.15, 2.87, 1.72 and 1.01 whereas; the percentage variance are 32.56%, 13.50%, 5.63% and 2.21%; again the cumulative percentages are 32.56%, 45.25%, 58.16% and 71.13% for PC1-PC4 respectively. Species having high loadings in PC1 are Npth (0.682), Phtn (0.561), Acnp (0.716), Pym (0.769), Flun (0.642), BkFn (0.551) and BaPn (0.558); which might be the sources of vehicular activities and gaseous emission (Aldabe et al., 2012; Sarkar et al., 2013; Jamhari et al., 2014; Wang et al., 2014). PC2 accounted high loadings of Npth (0.601), Anth (0.528), Flun (0.537), BbFn (0.613), BaPn (0.562) and BghiP (0.516). Hence, PC2 could be represented as gasoline vehicle and coal combustion (Ravindra et al., 2006; Kong et al., 2010; Jamhari et al., 2014). Acnp (0.627) and Chrn (0.655) loaded with PC3 may come from automobile (mainly gasoline) exhaust (Hussain et al., 2015); again Acen (0.518) and BaAn (0.648) in PC4 could be the tracer of biomass and natural gas emissions (Fon et al., 2007; Wang et al., 2014).

Table 4.6 represents the PCA carried out throughout the analyses of PAHs. For the components PC1–PC4, the corresponding Eigen values 8.46, 3.67, 1.56 and 1.04; and cumulative percentages are 37.12%, 48.26%, 61.67% and 79.64% respectively. The percentage variance of the components (PC1, PC2, PC3 and PC4) are 37.12%, 12.15%, 8.41% and 3.96% respectively. PC1 explained high loadings of Npth (0.850), Phtn (0.549), Fluo (0.533), Pym (0.687), BaAn

(0.674) *BbFn* (0.821) and *BaPn* (0.508). These PAHs might be indicator of vehicular sources (Guo et al., 2003; Ravindra et al., 2006; Han et al., 2009; Sarkar & Khillare, 2011; Liu et al., 2015). *Acen* (0.658), *Flun* (0.617), *Chrn* (0.591) and *DahA* (0.588) loaded in PC2 suggesting the sources of gasoline vehicle (Fang et al., 2004; Sarkar & Khillare, 2013). PC3 comprised the PAHs *Acnp* (0.597), *BkFn* (0.560) and *IcdP* (0.677); which could be linked with gasoline and wood combustion (Liu et al., 2015; Aldabe et al., 2012; Sarkar & Khillare, 2013). The compounds *Npth* (0.652) and *Anth* (0.637) in PC4 could be contributed from coal and wood burning (Ravindra et al., 2006; Han et al., 2009).

The percentage contributions of the components (PC1, PC2, PC3 and PC4) for all the seasons are given in Fig 4.1 (a-f). The percentage contributions of PC1-PC4 for the monsoon season possessed 37%, 29%, 22% and 12% respectively (Fig 4.1a). In the autumn season (Fig 4.1b), the corresponding contribution of PC1-PC4 found 34%, 28%, 24% and 14% respectively. The components PC1-PC4 contributed 36%, 29%, 23% and 12% in the winter season respectively (Fig 4.1c). In spring (Fig 4.1d), the percentages 37%, 28%, 22% and 13% were observed for PC1-PC4 respectively. In the summer season (Fig 4.1e), relative percentage contribution of PC1-PC4 was 36%, 28% 23% and 13% respectively. The mean contribution (Fig 4.1f) of the corresponding components (PC1-PC4) was 39%, 27%, 20% and 14% respectively.

The biplots of the components (PC1-PC4) between PC1 vs PC2, PC1 vs PC3, PC1 vs PC4 and PC2 vs PC3 for PAHs are given in appendices for all the seasons and throughout the study as the supplementary data (Figs. A1-A6). This technique is a useful tool for data analyses and for the investigation of response of different components/parameters on different environments. Matrices of rank two could be displayed as biplot, where a vector exists in each row and column, which reveals the inter-unit distances and the correlations among the variables also (Gabriel, 1971). This technique provides a graphical representation of pattern of interactions, which in turn allows the response of each parameter (Gabriel, 1971; Kempton, 1984). Relative contribution of principal components, depicted through biplots have been well defined so far (Legendre & Gallagher, 2001; Novembre & Stephens, 2008; Filzmoser et al., 2009; Škrbić & Đurišić-Mladenović, 2010; Melnyk et al., 2015). In case of PAHs also, biplot have been represented by various researchers (Golobočanin et al., 2004; Hengren et al., 2010; Wang et al., 2011; Sun et al., 2015; Potapova et al., 2016; Liu et al., 2017; Kang et al., 2017; Tongo et al., 2017).

**Table 4.1** PCA for PAHs in monsoon season

	PC1	PC2	PC3	PC4
Npth	0.749	0.646	-	-
Phtn	0.694	-	-	-
Acnp	-	0.504	-	-
Acen	-	-	0.725	-
Fluo	-	-	-	0.533
Anth	0.627	-	-	-
Pyrn	-	-	0.545	-
Flun	0.651	0.732	-	-
Chrn	0.564	-	-	0.648
BaAn	-	0.618	-	-
BbFn	-	-	0.669	-
BkFn	0.872	-	-	-
BaPn	0.560	-	0.677	-
BghiP	-	-	-	0.651
DahA	-	-	0.524	-
IcdP	-	0.521	-	-
Eigenvalue	6.096	3.889	2.007	1.125
% variance	36.579	19.258	10.049	3.035
Cumulative %	36.579	49.896	61.945	75.981
Probable sources	Diesel+ Gasoline	Gasoline+ Coal	Diesel+ Gasoline+ Coal	Gasoline +Natural gas +Coal

Values with ~ 0.5 or more are shown only

**Table 4.2** PCA for PAHs in autumn season

	PC1	PC2	PC3	PC4
Npth	0.787	-	-	0.583
Phtn	-	-	0.735	-
Acnp	0.689	-	-	-
Acen	-	0.697	-	-
Fluo	0.703	-	-	-
Anth	-	-	0.616	-
Pyrn	0.587	-	-	0.712
Flun	-	0.620	-	-
Chrn	0.603	0.790	-	-
BaAn	-	-	0.512	-
BbFn	-	-	-	0.619
BkFn	-	0.532	-	-
BaPn	0.641	-	-	-
BghiP	-	-	0.655	-
DahA	-	0.771	-	-
Eigenvalue	8.176	3.654	2.327	1.014
% variance	40.638	21.171	8.346	4.128
Cumulative %	40.638	52.651	68.897	78.556
Probable sources	Diesel+ Gasoline	Diesel +Coal	Diesel+ Gasoline +Natural gas	Diesel+ Coal+ Biomass



**Table 4.3** PCA for PAHs in winter season

	PC1	PC2	PC3	PC4
Npth	-	0.685	-	-
Phtn	0.862	-	-	0.729
Acnp	0.571	-	-	-
Acen	-	-	0.732	-
Fluo	-	0.887	-	-
Anth	-	-	-	0.781
Pyrn	-	0.582	-	-
Flun	0.657	-	-	-
Chrn	-	-	0.538	-
BaAn	0.526	-	0.872	-
BbFn	0.598	-	-	-
BkFn	-	0.699	-	-
BaPn	0.617	-	-	-
BghiP	-	-	0.783	-
DahA	-	-	-	0.837
IcdP	0.868	-	-	-
Eigenvalue	6.523	3.281	1.930	1.147
% variance	34.054	16.245	6.153	2.973
Cumulative %	34.054	47.692	64.05	76.210
Probable sources	Diesel+ Natural gas	Diesel+ Wood	Gasoline+ Diesel	Diesel+ Coal

Values with ~ 0.5 or more are shown only

**Table 4.4** PCA for PAHs in spring season

	PC1	PC2	PC3	PC4
Npth	0.977	-	0.658	-
Phtn	-	0.873	-	-
Acnp	0.879	-	-	-
Acen	-	-	-	0.557
Fluo	-	0.522	-	-
Anth	-	-	0.530	-
Pyrn	0.880	-	-	-
Flun	-	-	-	0.608
Chrn	-	0.593	-	-
BaAn	-	-	-	-
BbFn	-	-	0.542	-
BkFn	0.682	-	-	-
BaPn	-	-	-	0.597
BghiP	0.523	-	-	-
DahA	-	0.643	-	-
IcdP	0.616	-	-	-
Eigenvalue	7.681	4.072	2.911	1.857
% variance	38.415	17.167	9.073	3.251
Cumulative %	38.415	53.775	67.325	77.473
Probable sources	Diesel	Gasoline+ Wood	Diesel+ Coal	Gasoline +Coal

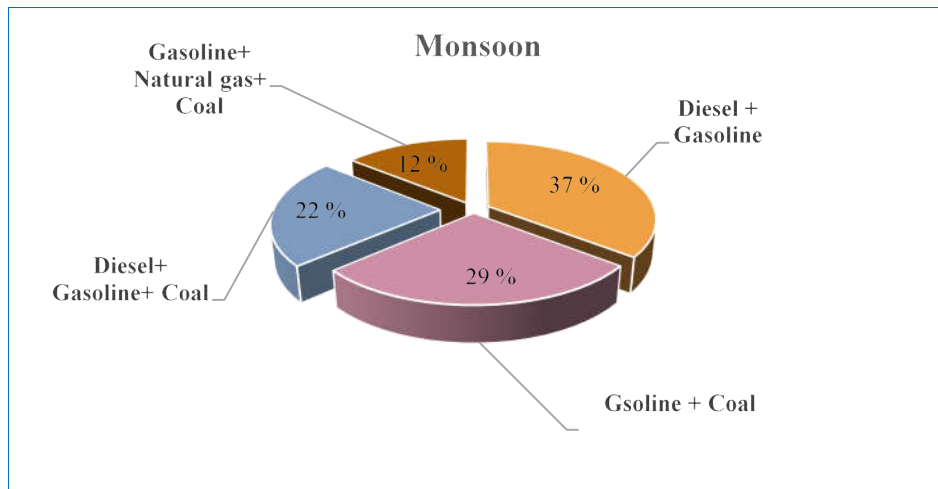
**Table 4.5** PCA for PAHs in summer season

	PC1	PC2	PC3	PC4
Npth	0.682	0.601	-	-
Phtn	0.561	-	-	-
Acnp	0.716	-	0.627	-
Acen	-	-	-	0.518
Fluo	-	-	-	-
Anth	-	0.528	-	-
Pyrn	0.769	-	-	-
Flun	0.642	0.537	-	-
Chrn	-	-	0.655	-
BaAn	-	-	-	0.648
BbFn	-	0.613	-	-
BkFn	0.551	-	-	-
BaPn	-	0.562	-	-
BghiP	-	0.516	-	-
DahA	0.558	-	-	-
Eigenvalue	6.154	2.874	1.723	1.012
% variance	32.561	13.50	5.634	2.211
Cumulative %	32.561	45.258	58.163	71.134
Probable sources	Diesel+ Gasoline +Natural gas	Gasoline+ Coal	Gasoline	Biomass+ Natural gas

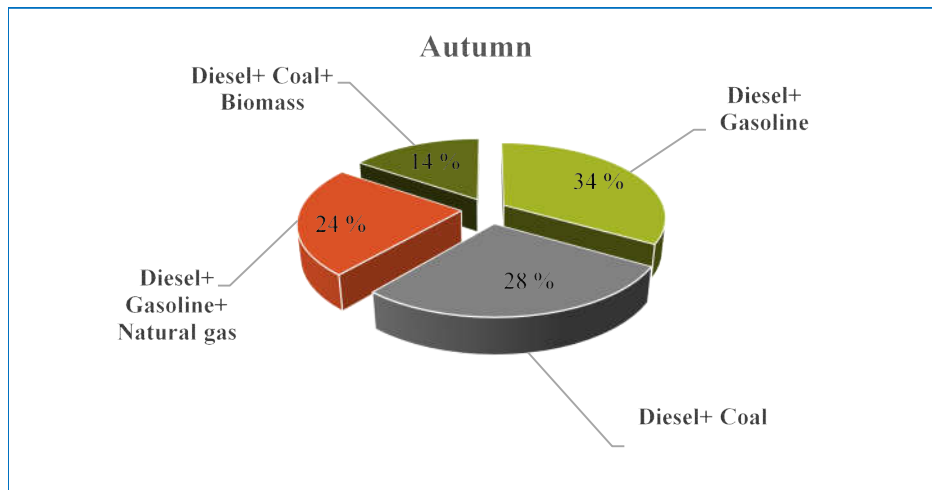
Values with ~ 0.5 or more are shown only

**Table 4.6** PCA for PAHs throughout the analyses

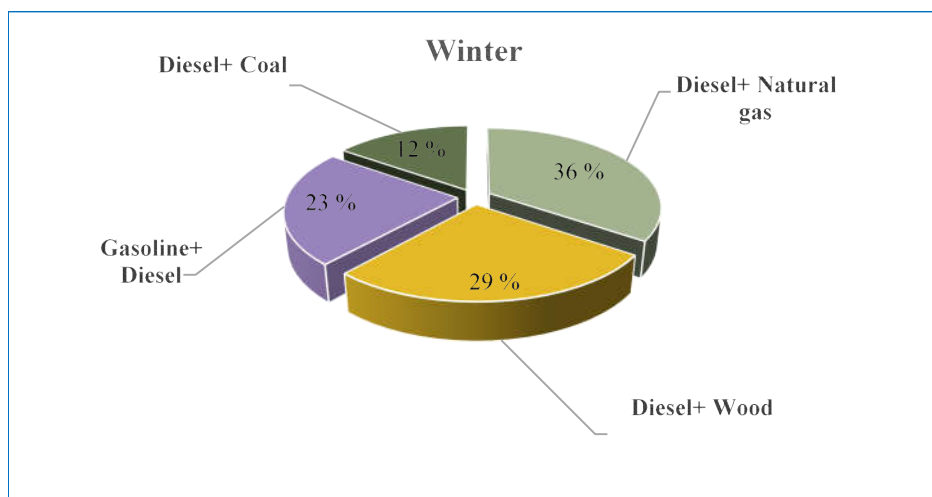
	PC1	PC2	PC3	PC4
Npth	0.850	-	-	0.652
Phtn	0.549	-	-	-
Acnp	-	-	0.597	-
Acen	-	0.658	-	-
Fluo	0.533	-	-	-
Anth	-	-	-	0.637
Pyrn	0.687	-	-	-
Flun	-	0.617	-	-
Chrn	-	0.591	-	-
BaAn	0.674	-	-	-
BbFn	0.821	-	-	-
BkFn	-	-	0.560	-
BaPn	0.508	-	-	-
BghiP	-	-	-	-
DahA	-	0.588	-	-
IcdP	-	-	0.677	-
Eigenvalue	8.466	3.673	1.563	1.045
% variance	37.126	12.153	8.419	3.967
Cumulative %	37.126	48.260	61.679	79.646
Probable sources	Diesel +Gasoline	Diesel+ Gasoline+ Coal	Gasoline+ Wood	Coal+ Wood



a.

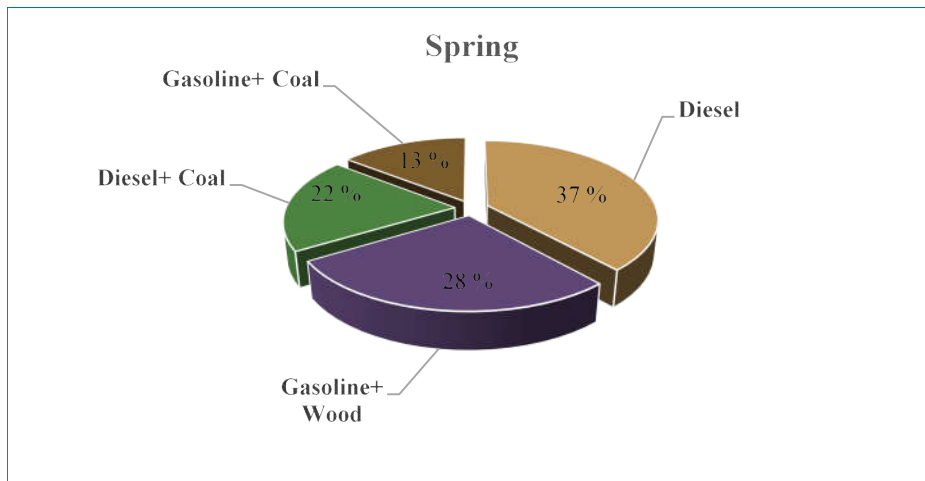


b.

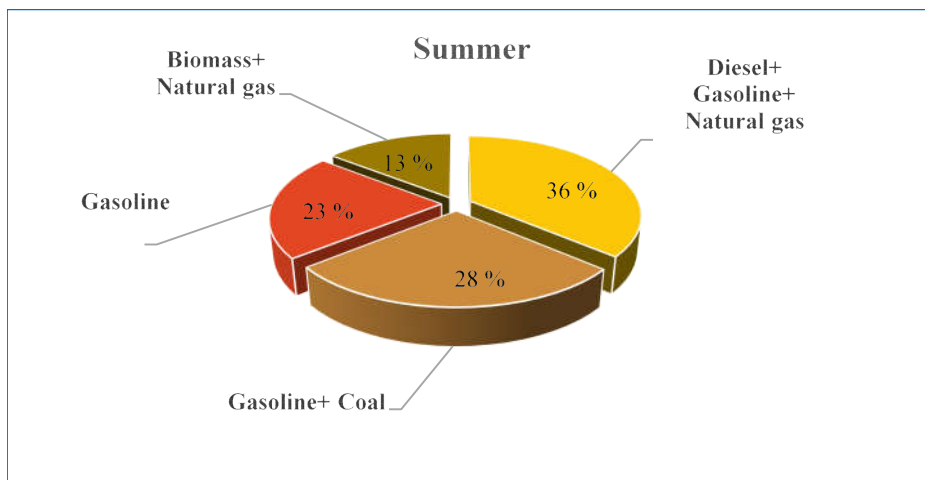


c.

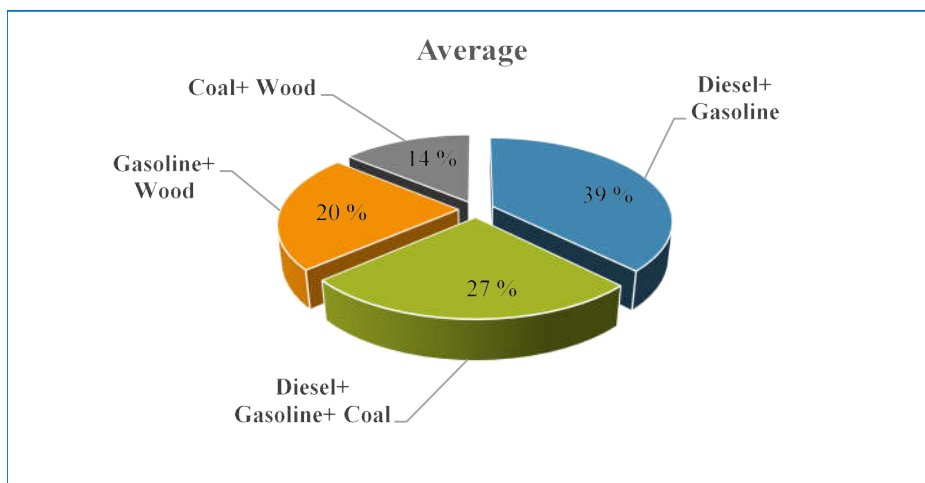
**Fig.4.1** Percentage contribution of PCs in the a. monsoon, b. autumn and c. winter seasons



d.



e.



f.

**Fig.4.1** Percentage contribution of PCs in the d. spring, e. summer and f. average

#### **[4.1.1] Application of molecular diagnostic ratio (MDR) and carbonaceous ratio, for source identification of PAHs and carbonaceous species**

Source identification of PAHs and carbonaceous species were also attempted to observe through diagnostic ratios for both the fine and coarse ( $< 2.5 \mu\text{m}$  and  $> 2.5 \mu\text{m}$ ) size ranges of particles of the PAHs congener: Anth/(Anth+Phtn), BaAn/BaAn+Chrn, BaAn/Chrn, BaPn/BghiP, BaPn/(BaPn+Chrn), Flun/(Flun+Pyrn), Flun/Pyrn, BbFn/BkFn, IcdP/BghiP and, OC/EC are given in Tables 4.7 to 4.11; while the diagnostic ratios of PAHs, and the ratios of carbonaceous species throughout the years was given in Table 4.12. In these Tables, the corresponding emission sources were attributed based on the previous studies carried out in different parts of the country and across the world (References are provided in Tables).

In the monsoon season (Table 4.7), the ratio found for the PAHs congener Anth/(Anth+Phtn), in fine and coarse particles were 0.32 and 0.34, which were attributed to come from pyrogenic sources (Pies et al., 2008; Abdallah & Atia, 2014). Combustion /burning activities could be linked from the ratio of BaAn/(BaAn+Chrn) (0.49 and 0.44 for fine and coarse mode particles) (Duan et al., 2012; Galarneau, 2008). Ratio of BaAn/Chrn (0.95 for fine and 0.79 for coarse particles respectively) indicated the emissions from vehicular frequencies (gasoline) and wood burning (Simcik et al., 1999; Dickhut et al., 2000, Fang et al., 2004; Fon et al., 2007). Oil and coal burning could be assessed from the ratio of BaPn/BghiP in both the modes of particles (2.07 and 2.73 for fine and coarse respectively) (Simcik et al., 1999). Ratio of BaPn/(BaPn+Chrn) (0.55 for fine and 0.57 for coarse particles) inferred the vehicular emission; i.e. gasoline and diesel (Khalili et al., 1995; Kaur et al., 2013). The ratio of the congener Flun/(Flun+Pyrn) for fine and coarse particles (0.63 and 0.47) suggested the contribution from vehicular (diesel, natural gas and gasoline) activities (Kavouras et al., 2001; Mandalakis et al., 2002; Fang et al., 2004; Albuquerque et al., 2016). Flun/Pyrn ratio (0.71 for fine and 0.88 for coarse particles) could be assessed from petrogenic emission (Baumard et al., 1998; Abdallah & Atia, 2014). Ratio of BbFn/BkFn (1.04 for fine and 0.91 for coarse particles) might have linked with diesel vehicle and wood burning (Rogge et al., 1993a; Dickhut et al., 2000; Kaur et al., 2013). The ratio of the congener IcdP/BghiP for fine and coarse particles (0.64 and 0.46) could be established from wood burning (Dickhut et al., 2000; Fang et al., 2004). The carbonaceous ratio OC/EC (1.45 for fine and 2.06 for coarse particles) could be linked with vehicular sources

and coal burning (Watson et al., 2001; Gonçalves et al., 2011). The petrogenic sources could be the responsible factors at the site JNU, whereas pyrogenic and petrogenic sources might be the responsible factor for the sites CPL, FBD, GBD and GGN (Hazarika & Srivastava, 2017).

In case of the autumn season (Table 4.8), the ratio of Anth/(Anth+Phtn) in fine and coarse particles were 0.35 and 0.29, which were attributed to be linked from diesel and other pyrogenic sources. Ratio of BaAn/(BaAn+Chrn) (0.45 and 0.41 for fine and coarse mode particles) could be used for identifying mainly coal burning and other combustion sources. Wood burning indicated the emission of BaAn/Chrn (0.84 for fine, and 0.82 for coarse particles respectively). Oil and coal burning indicated the probable sources of the corresponding ratio BaPn/BghiP in both the modes of particles (2.69 and 3.75 for fine and coarse respectively). BaPn/(BaPn+Chrn) (0.61 for fine and 0.67 for coarse particles) could be established to be linked with vehicular emission (gasoline and diesel). The different ratio of the congener Flun/(Flun+Pyrn) for fine and coarse particles (0.43 and 0.57) can be associated with gasoline emission. Ratio of Flun/Pyrn (0.75 for fine 1.30 for coarse particles) could be linked with petrogenic and pyrogenic emissions. The ratio of BbFn/BkFn (1.06 for fine and 0.88 for coarse particles) can be linked with gasoline and wood burning. Diesel and wood burning could be the source of the PAHs congener IcdP/BghiP for fine and coarse particles (0.72 and 0.92). The ratio of OC/EC (1.8 for fine and 1.73 for coarse particles) can be established to be emitted from vehicular activities and combustion processes (Salam et al., 2003; Satsangi et al., 2012).

In Table 4.9, for winter season, ratio of Anth/(Anth+Phtn), 0.30 and 0.33 in fine and coarse particles, suggesting to be the sources of fossil fuel burning/pyrogenic emission. Ratio of BaAn/(BaAn+Chrn) (0.47 and 0.43 for fine and coarse mode particles) revealed the link of petrogenic and pyrogenic emissions. The ratio of BaAn/Chrn (0.88 for fine and 0.74 for coarse particles respectively) indicated the emission from wood burning. The corresponding ratio of BaPn/BghiP in both the modes of particles (2.8 and 3.49 for fine and coarse respectively) might be from burning of coal. Vehicular emission (automobile exhaust) could be the responsible factor that can be established from the ratio of BaPn/(BaPn+Chrn) (0.62 for fine and 0.66 for coarse particles). Ratio of Flun/(Flun+Pyrn) for fine and coarse particles (0.41 and 0.52) could be the representation of fuel burning (gasoline and diesel). The ratio of the congener Flun/Pyrn (0.68 for fine, 1.07 for coarse particles) indicated the dominant sources of pyrogenic and petrogenic sources. The ratio of BbFn/BkFn (1.1 for fine and 1.02 for coarse particles), indicated the

potential sources of diesel burning and wood combustion. Ratio of *IcdP/BghiP* from the fine and coarse particles (0.78 and 0.84) could be linked to be emitted from wood, coal burning and smelters. The OC/EC ratio (1.7 for fine and 2.11 for coarse particles) signified the dominant sources of vehicular activities and combustion sources (Chen et al., 1997; Tiwari et al., 2013).

In case of the spring season (Table 4.10), emission from diesel and the combustion (pyrogenic) sources could be linked with the ratio of *Anth/(Anth+Phtn)*, 0.34 and 0.31 in fine and coarse particles. Ratio of *BaAn/(BaAn+Chrn)* (0.44 and 0.47 for fine and coarse mode particles) represented gasoline, and the emissions from coal and biomass combustions. Gasoline emission and biomass/wood burning indicated the probable sources of emission of *BaAn/Chrn* (0.79 for fine and 0.87 for coarse particles respectively). The ratio of *BaPn/BghiP* (2.49 and 1.75 for fine and coarse respectively) suggested the emission sources from oil and/or coal burning. From the ratio of *BaPn/(BaPn+Chrn)* (0.59 for fine and 0.69 for coarse particles); the corresponding value represented the origin of diesel and gasoline emissions. Fossil fuel burning and combustion sources could be established as responsible sources from the mean ratio of *Flun/(Flun+Pyrn)* (0.43 and 0.58) for fine and coarse particles. The petrogenic sources could be thought as the possible emission factor of *Flun/Pyrn* (0.74 for fine, 1.37 for coarse particles). *BbFn/BkFn* ratio (0.96 for fine and 0.93 for coarse particles) could be linked from the emission of diesel vehicle and wood burning. Ratio of *IcdP/BghiP* for fine and coarse particles (0.57 and 0.82) suggested the emission from wood combustion. OC/EC ratio (1.68 for fine and 1.92 for coarse particles) could be associated with vehicular sources and coal burning (Salam et al., 2003; Tiwari et al., 2013).

For the summer season (Table 4.11), the ratio of *Anth/(Anth+Phtn)*, 0.36 and 0.28 in fine and coarse particles, indicated the activities associated with combustion/pyrogenic sources from diesel and coal burnings. Ratio of *BaAn/(BaAn+Chrn)* (0.42 and 0.40 for fine and coarse mode particles) inferred the emissions due to the activities from combustion/burning of fuels (wood, coal). *BaAn/Chrn* (0.83 for fine and 0.80 for coarse particles respectively) referred the vehicular sources (gasoline) and contribution from biomass/wood combustion. Combustion of coal or oil burning could be the responsible sources of *BaPn/BghiP*, which can be established from the ratio in both the modes of particles (2.42 and 4.10 for fine and coarse respectively). Ratio of *BaPn/(BaPn+Chrn)* (0.60 for fine and 0.68 for coarse particles) indicated the emission sources of vehicular activities (diesel and gasoline). *Flun/(Flun+Pyrn)* ratio for fine and coarse particles

(0.41 and 0.56) could also be established as the contribution of fossil fuel and coal burnings. Ratio of Flun/Pyrn (0.70 for fine, 1.29 for coarse particles) could be associated with petrogenic output. Vehicular sources (mainly diesel) and biomass/wood burning might be the possible emission factor of BbFn/BkFn (1.06 for fine and 0.87 for coarse particles). Ratio of IcdP/BghiP for fine and coarse particles (0.59 and 0.92) represented the emission of wood burning. Fossil fuel burning could be associated with the ratio of OC/EC (1.96 for fine and 2.45 for coarse particles) (Safai et al., 2014; Behra & Sharma, 2015; Tiwari et al., 2016).

It was observed that the MDR of all the PAHs with seasons found in the range of in and around the literatures cited in the Tables (4.7 - 4.12) throughout the observation. Table 4.12 shows the MDR of mean PAHs throughout the years, where the PAHs congener Anth/(Anth+Phtn), 0.34 and 0.32 in fine and coarse particles, represented the sources of diesel burning and the emission from combustion/pyrogenic sources. Ratio of BaAn/(BaAn+Chrn) (0.46 and 0.45 for fine and coarse mode particles) inferred the significant emissions from the combustion of biofuels. Ratio of BaAn/Chrn (0.86 for fine, and 0.81 for coarse particles respectively) associated with the tracer of vehicular sources and biomass/wood burning. The results of the ratio BaPn/BghiP in both the modes of particles (2.5 and 3.6 for fine and coarse respectively) indicated significant sources of coal combustion and oil burning. Ratio of BaPn/(BaPn+Chrn) (0.59 for fine and 0.66 for coarse particles) revealed vehicular activities (diesel and gasoline) as the responsible sources of emission. The ratio of Flun/(Flun+Pyrn) (0.42 and 0.58) for fine and coarse particles could also be the source of vehicular activities. For the congener Flun/Pyrn (0.72 for fine, 1.16 for coarse particles) could be from petrogenic emission. Biomass/wood burning could be the sources of BbFn/BkFn (1.04 for fine and 0.93 for coarse particles), which were established from the corresponding ratios. Ratio of IcdP/BghiP for fine and coarse particles (0.68 and 0.85) indicated the emission from diesel and wood combustion. The ratio of TC/EC (2.68 and 3.32 in fine and coarse particles) could be associated with fossil fuel burning (Chen et al., 1997; Srinivas and Sarin, 2014). Again, OC/EC ratio (1.72 for fine and 2.31 for coarse particles) represented the close association of vehicular sources and coal combustion (Sudheer et al., 2016; Tiwari et al., 2016).



**Table 4.7** Ratio of PAHs congeners (MDR), and carbonaceous species for source identification in the monsoon season

Species ratio	Fine ranges	Coarse ranges	Literatures ranges	Probable sources	References
Anth/Anth+Phtn	0.32	0.34	< 0.1 petrogenic, > 0.1 pyrogenic	Pyrogenic	Pies et al., (2008); Abdallah & Atia, (2014)
BaAn/BaAn+Chrn	0.49	0.44	> 0.35 combustion, 0.46 coal combustion	Combustion processes	Galarneau, (2008); Duan et al., (2012)
BaAn/Chrn	0.95	0.79	0.66-0.92 wood combustion, 0.28-1.2 gasoline	Gasoline, wood	Simcik et al., (1999); Dickhut et al. (2000); Fang et al., (2004); Fon et al., (2007)
BaPn/BghiP	2.07	2.73	> 2 oil burning, 0.9-6.6 coal burning	Oil and coal burning	Simcik et al., (1999)
BaPn/BaPn+Chrn	0.55	0.57	0.49 gasoline, 0.73 diesel	Gasoline and diesel	Khalili et al., (1995); Kaur et al., (2013)
Flun/Flun+Pyrn	0.63	0.47	0.6-0.7 diesel, 0.49 natural gas, 0.4 gasoline	Diesel, natural gas and gasoline combustion	Kavouras et al., (2001); Mandalakis et al., (2002); Fang et al., (2004); Albuquerque et al., (2016)
Flun/Pyrn	0.71	0.88	< 1 petrogenic, > 1 pyrogenic	Petrogenic emission	Baumard et al., (1998); Abdallah & Atia, (2014)
BbFn/BkFn	1.04	0.91	1.07 diesel, 0.92 wood	Diesel and wood	Rogge et al., (1993a); Dickhut et al. (2000); Kaur et al., (2013)
IcdP/BghiP	0.64	0.46	< 1 wood	Wood burning	Dickhut et al. (2000); Fang et al., (2004)
OC/EC	1.45	2.06	1.1 vehicle, 2.7 coal	Vehicle and coal burning	Watson et al., (2001); Gonçalves et al., (2011)

**Table 4.8** Ratio of PAHs congeners (MDR), and carbonaceous species for source identification in the autumn season

Species ratio	Fine ranges	Coarse ranges	Literatures ranges	Probable sources	References
Anth/Anth+Phtn	0.35	0.29	Petroleum (< 0.1), combustion sources (> 0.1), and (0.35) diesel	Diesel and other combustion sources	Vasilakos et al., (2007); Han et al., (2011); Albuquerque et al., (2016); Lu et al., (2016)
BaAn/BaAn+Chrn	0.45	0.41	Petrogenic/pyrolytic emission (0.2-0.35), coal combustion (0.46)	Combustion sources (mainly coal)	Galarneau, (2008); Duan et al., (2012); Hu et al., (2012); Lu et al., (2016)
BaAn/Chrn	0.84	0.82	Wood combustion (0.70-0.90)	Emission from wood burning	Simcik et al., (1999); Hong et al., (2007)
BaPn/BghiP	2.69	3.75	Coal burning (0.9-6.6); oil burning (> 2)	Combustion of oil and coal	Daisey et al., (1979); Simcik et al., (1999); Hong et al., (2007)
BaPn/BaPn+Chrn	0.61	0.67	Gasoline (0.49), diesel (0.73)	Gasoline and diesel burning	Khalili et al., (1995); Kaur et al., (2013); Di Vaio et al., (2016)
Flun/Flun+Pyrn	0.43	0.57	Gasoline (0.40-0.60)	Gasoline combustion	Dallarosa et al., (2005)
Flun/Pyrn	0.75	1.30	Petrogenic (<1), pyrogenic (>1)	Combustion ( pyrogenic and petrogenic) sources	Baumard et al., (1998); Abdallah & Atia, (2014); Daso et al., (2016)
BbFn/BkFn	1.06	0.88	Wood (0.8-1.1), gasoline (1.1-1.5)	Burning of gasoline and wood	Dickhut et al., (2000); Hong et al., (2007)
IcdP/BghiP	0.72	0.92	Diesel emission (1), wood (<1)	Emission from diesel and wood burning	Caricchia et al., (1999); Dickhut et al., (2000); Fang et al., (2004); Abdallah & Atia, (2014)
OC/EC	1.8	1.73	Vehicular and burning activities (1.8)	Vehicular activities and combustion sources	Salam et al., (2003); Satsangi et al., (2012)

**Table 4.9** Ratio of PAHs congeners (MDR), and carbonaceous species for source identification in the winter season

Species ratio	Fine ranges	Coarse ranges	Literatures ranges	Probable sources	References
Anth/Anth+Phtn	0.30	0.33	Heavy fuel combustion (>0.1), petrogenic (<0.1)	Fuel combustion	Budzinski et al., (1997); Wang et al., (2008); Li et al., (2006b)
BaAn/BaAn+Chrn	0.47	0.43	Petrogenic (< 0.2), combustion (> 0.35)	Petrogenic and pyrogenic sources	Yunker et al., (2002); Jamhari et al., (2014)
BaAn/Chrn	0.88	0.74	Wood (0.79±0.13)	Wood burning	Simcik et al., (1999); Dickhut et al., (2000); Wang et al., (2008)
BaPn/BghiP	2.8	3.49	Coal/coke combustion (>1.25), coal burning (0.9-6.6)	Coal burning	Simcik et al., (1999); Akyüz and Çabuk, (2008); Ravindra et al., (2008); Pongpiachan et al., (2015)
BaPn/BaPn+Chrn	0.62	0.66	Automobile exhaust (0.53±0.10)	Emission from automobile exhaust	Rogge et al., (1993a, b); El-Mubarak et al., (2014)
Flun/Flun+Pyrn	0.41	0.52	Gasoline (0.4), diesel (0.6-0.7)	Combustion sources (gasoline and diesel)	Sicre et al., (1987); Simcik et al., (1999); Hong et al., (2007)
Flun/Pyrn	0.68	1.07	Pyrogenic (>1), petrogenic (<1)	Petrogenic and pyrogenic emission	Baumard et al., (1998); Neff et al., (2005); Abdallah & Atia., (2014)
BbFn/BkFn	1.1	1.02	Wood (0.92±0.16), diesel (1.26±0.19)	Burning of diesel and wood	Rogge et al., (1993a); Dickhut et al., (2000); Kaur et al., (2013); Wang et al., (2008)
IcdP/BghiP	0.78	0.84	Coal (1.09±0.33), smelters (1.03±0.15), wood burning (< 1)	Emission from coal, smelters processes, and wood burning	Dickhut et al., (2000); Fang et al., (2004); Wang et al., 2008)
OC/EC	1.7	2.11	1.1-1.6 traffic intersections, 1.6 combustion	Vehicular congestion and combustion processes	Chen et al., (1997); Tiwari et al., (2013)

**Table 4.10** Ratio of PAHs congeners (MDR), and carbonaceous species for source identification for the spring season

Species ratio	Fine ranges	Coarse ranges	Literatures ranges	Probable sources	References
Anth/Anth+Phtn	0.34	0.31	0.35 (Diesel), >0.1 (pyrogenic)	Diesel burning and other pyrogenic sources	Guo et al., (2003); Pies et al., (2008); Abdallah & Atia, (2014); Pongpiachan et al., (2015)
BaAn/BaAn+Chrn	0.44	0.47	0.43 (wood/biomass), 0.46 (coal burning), 0.49 (gasoline)	Gasoline, coal and biomass burning	Mantis et al., (2005); Vasilakos et al., (2007); Galarneau, (2008); Akyüz & Çabuk, (2009)
BaAn/Chrn	0.79	0.87	0.66-0.92 (wood burning), 0.28-1.2 (gasoline emission)	Gasoline, and wood burning	Simcik et al., (1999); Dickhut et al., (2000); Fang et al., (2004); Fon et al., (2007)
BaPn/BghiP	2.49	1.75	>2 (oil burning), 0.9-6.6 (coal burning)	Burning of oil and coal	Simcik et al., (1999)
BaPn/BaPn+Chrn	0.59	0.69	0.49 (gasoline), 0.73 (diesel)	Vehicular sources	Khalili et al., (1995); Kaur et al., (2013)
Flun/Flun+Pyrn	0.43	0.58	< 0.4 (petroleum), 0.4-0.5 (fossil fuel), > 0.5 (coal combustion)	Fossil fuel and coal combustion	Yunker et al., (2002); Lu et al., (2016)
Flun/Pyrn	0.74	1.37	<1 (petrogenic), >1 (pyrogenic)	Emissions from petrogenic and pyrogenic sources	Baumard et al., (1998); Abdallah & Atia, (2014)
BbFn/BkFn	0.96	0.93	1.07 (diesel), 0.92( wood)	Burning of wood	Rogge et al., (1993a); Dickhut et al., (2000); Kaur et al., (2013)
IcdP/BghiP	0.57	0.82	Wood burning (< 1)	Burning of wood	Dickhut et al., (2000); Fang et al., (2004)
OC/EC	1.68	1.92	1.6 (combustion sources), 1.8 (vehicular and burning activities)	Vehicular sources and burning processes	Salam et al., (2003); Tiwari et al., (2013)

**Table 4.11** Ratio of PAHs congeners (MDR), and carbonaceous species for source identification in the summer season

Species ratio	Fine ranges	Coarse ranges	Literatures ranges	Probable sources	References
Anth/Anth+Phtn	0.36	0.28	Coal burning (< 0.24), diesel emission (> 0.35)	Diesel and coal burning	Guo et al., (2003); Kong et al., (2010)
BaAn/BaAn+Chrn	0.42	0.40	Burning (>0.35), wood burning (0.43), coal burning (0.46)	Burning of wood, coal and other pyrogenic sources	Mantis et al., (2005); Galarneau, (2008); Duan et al., (2012); Pongpiachan et al., (2015)
BaAn/Chrn	0.83	0.80	Wood burning (0.66-0.92), gasoline emission (0.28-1.2)	Emissions from gasoline and wood	Simcik et al., (1999); Dickhut et al., (2000); Fang et al., (2004); Fon et al., (2007)
BaPn/BghiP	2.42	4.10	Burning of oil (>2), coal burning (0.9-6.6)	Coal and oil burning	Simcik et al., (1999)
BaPn/BaPn+Chrn	0.60	0.68	Gasoline (0.49), diesel (0.73)	Emissions from vehicular sources	Khalili et al., (1995); Kaur et al., (2013)
Flun/Flun+Pyrn	0.41	0.56	Fossil fuel (0.4-0.5), coal (>0.5)	Combustion processes (fossil fuel and coal)	Li et al., (2006b); Wang et al., (2008)
Flun/Pyrn	0.70	1.29	Pyrogenic (>1), petrogenic (<1)	Pyrogenic and petrogenic emissions	Baumard et al., (1998); Abdallah & Atia, (2014)
BbFn/BkFn	1.06	0.87	Wood burning (0.92), vehicular diesel (1.07)	Vehicular activities and wood burning	Rogge et al., (1993a); Dickhut et al., (2000); Kaur et al., (2013)
IcdP/BghiP	0.59	0.92	Wood burning (<1)	Wood burning	Dickhut et al., (2000); Fang et al., (2004)
OC/EC	1.96	2.45	Fossil fuel burning (<4)	Fossil fuel burning	Safai et al., (2014); Behra & Sharma, (2015); Tiwari et al., (2016)

**Table 4.12** Ratio of PAHs congeners (MDR), and carbonaceous species for source identification throughout the years

Species ratio	Fine ranges	Coarse ranges	Literatures ranges	Probable sources	References
Anth/Anth+Phtn	0.34	0.32	< 0.1 (petrogenic sources), > 0.1 (pyrogenic emission), (0.35) diesel	Pyrogenic sources and diesel burning	Pies et al., (2008); Abdallah & Atia, (2014); Albuquerque et al., (2016)
BaAn/BaAn+Chrn	0.46	0.45	0.43 (wood combustion), 0.46 (burning of coal)	Coal and wood burning	Mantis et al., (2005); Akyüz & Çabuk, (2008); Galarneau, (2008); Kong et al., (2010); Wang et al., (2015)
BaAn/Chrn	0.86	0.81	Wood (0.66-0.92), gasoline (0.28-1.2)	Emissions from gasoline and wood burning	Simcik et al., (1999); Dickhut et al., (2000); Fang et al., (2004); Fon et al., (2007)
BaPn/BghiP	2.5	3.6	Oil burning (> 2), coal burning (0.9-6.6)	Burning activities (oil and coal)	Simcik et al., (1999); Ravindra et al., (2008)
BaPn/BaPn+Chrn	0.59	0.66	Vehicular sources [Gasoline (0.49), diesel (0.73)]	Gasoline and diesel	Khalili et al., (1995); Kaur et al., (2013)
Flun/Flun+Pyrn	0.42	0.58	Gasoline (0.4), 0.57 (coal), diesel (0.6-0.7)	Diesel, gasoline and coal burning	Kavouras et al., (2001); Mandalakis et al., (2002); Fang et al., (2004); Galarneau, (2008); Wang et al., (2015)
Flun/Pyrn	0.72	1.16	Petrogenic emission (< 1), pyrogenic emission (> 1)	Petrogenic and pyrogenic emissions	Baumard et al., (1998); Abdallah & Atia, (2014)
BbFn/BkFn	1.04	0.93	Diesel burning (1.07), wood burning (0.92)	Wood and diesel burning	Rogge et al., (1993a); Dickhut et al., (2000); Kaur et al., (2013)
IcdP/BghiP	0.68	0.85	(1) Diesel, (< 1) wood burning	Emissions from diesel and wood burning	Dickhut et al., (2000); Fang et al., (2004); Ravindra et al., (2008)
TC/EC	2.68	3.32	Traffic intersection (2.6), burning activities (2.7)	Vehicular and burning processes	Chen et al., (1997); Srinivas and Sarin, (2014)
OC/EC	1.72	2.31	Domestic use of biofuel (> 1.1), vehicular traffic, industrial and biomass burning (1.6-9.2)	Vehicular activities and fuel burning	Sudheer et al., (2016); Tiwari et al., (2016)

The ratio of the PAHs (MDR), and the carbonaceous ratio throughout these tables (Tables 4.7 – 4.12) not representative of the exact/actual values of the literature ranges which were followed. But, the observed ratios for all the species are in and/or within/around the literature ranges, hence the probable sources were drawn depending on the literature ranges. Literatures are arranged year wise throughout these tables.

**[5.1] Health risk assessment of PAHs**

Following the US EPA guidelines, an attempt was made to observe the chronic health risk and cancer risk caused by PAHs. In this study, only Naphthalene has the available and/or prescribed RfC value, so the HQ values could be obtained from RfD, and also from the calculated RfD or RfC (inhalation) values. Hence, for Naphthalene both the RfD values such as chronic oral reference dose and the inhalation dose were calculated separately for the quantification of overall HQs. For the other PAHs, the HQs are the representative of ingestion exposure only. Toxicity associated with PAHs regarding chronic disorder (Li et al., 2010; Hu et al., 2013), and carcinogenicity (Xia et al., 2013; Di Vaio et al., 2016; Lu et al., 2016; Ke et al., 2017) have already been reported. HQs associated with children (HQ<sub>C</sub>) and adults (HQ<sub>A</sub>) along with the overall ILCR, regarding inhalation with respect to children (ILCR<sub>C</sub>) and adults (ILCR<sub>A</sub>) are discussed below.

The HQs obtained for the PAHs in the monsoon season was given in Table 5.1 (a). The quantified HQs for the compounds Npth, Acen, Fluo, Anth, Flun and Pynr was observed due to the availability of RfD (mg/Kg-day) values in the US EPA website. HQs of Npth, Acen, Fluo, Anth, Flun and Pynr for children was  $3.47 \times 10^{-4}$ ,  $1.91 \times 10^{-8}$ ,  $7.03 \times 10^{-8}$ ,  $8.75 \times 10^{-8}$ ,  $1.07 \times 10^{-7}$ , and  $1.86 \times 10^{-7}$ ; while for adults it was  $9.53 \times 10^{-4}$ ,  $3.69 \times 10^{-10}$ ,  $2.26 \times 10^{-8}$ ,  $2.81 \times 10^{-8}$ ,  $3.44 \times 10^{-8}$ , and  $5.97 \times 10^{-8}$  respectively. The HI (HI =  $\Sigma$ HQ<sub>i</sub>) of the species was  $3.47 \times 10^{-4}$  (children) and  $9.53 \times 10^{-4}$  (adults). From the value of HQs and HI, it can be concluded that no adverse health impact and no adverse significant non-carcinogenic risk associated with the PAHs was observed. The cancer risk assessment (inhalation) was also attempted to observe for the species of having unit risk [ $(\mu\text{g}/\text{m}^3)^{-1}$ ] such as BaAn, Chrn, BbFn, BkFn, BaPn, IcdP, DahA and Npth in the monsoon season (Table 5.1 b). The corresponding risk (ILCR) of the species were found as  $4.37 \times 10^{-8}$ ,  $5.19 \times 10^{-10}$ ,  $2.98 \times 10^{-8}$ ,  $3.02 \times 10^{-9}$ ,  $6.24 \times 10^{-7}$ ,  $1.83 \times 10^{-8}$ ,  $2.66 \times 10^{-7}$  and  $3.51 \times 10^{-8}$  for children; again  $1.21 \times 10^{-7}$ ,  $1.37 \times 10^{-9}$ ,  $8.27 \times 10^{-8}$ ,  $8.37 \times 10^{-9}$ ,  $1.73 \times 10^{-6}$ ,  $5.08 \times 10^{-4}$ ,  $7.38 \times 10^{-7}$  and  $9.77 \times 10^{-8}$  for adults respectively. From the risk values, it can be concluded that it falls within or below the range of ILCR (i.e.,  $10^{-6}$  to  $10^{-4}$ ), which can be represented as virtual safety for the particular PAHs. BaPn ( $1.73 \times 10^{-6}$  for adults) found to be high risk and Chrn (for children  $5.19 \times 10^{-10}$ ; and  $1.37 \times 10^{-9}$  for adults) found with lower risk in comparison to the other

PAHs. Again, the ILCR associated with fine and coarse particles ( $< 2.5$  and  $> 2.5 \mu\text{m}$ ) was also provided separately for this season in Fig. 5.1.

In case of the autumn season (Table 5.2a), the observed HQs of Npth, Acen, Fluo, Anth, Flun and Pynr for children were  $1.86 \times 10^{-4}$ ,  $2.55 \times 10^{-8}$ ,  $8.01 \times 10^{-8}$ ,  $1.04 \times 10^{-8}$ ,  $1.30 \times 10^{-7}$  and  $2.22 \times 10^{-7}$ ; while in case of adults the corresponding HQs were  $1.03 \times 10^{-4}$ ,  $8.19 \times 10^{-9}$ ,  $2.57 \times 10^{-8}$ ,  $3.34 \times 10^{-9}$ ,  $4.18 \times 10^{-8}$  and  $7.13 \times 10^{-8}$  respectively. HI of the species was  $1.86 \times 10^{-4}$  (children) and  $1.03 \times 10^{-4}$  (adults) respectively. Hence, it can be concluded that no adverse health impact and/or no adverse significant non-carcinogenic risk was found to be associated with the species. The compounds BaAn, Chr, BbFn, BkFn, BaPn, IcdP, DahA and Npth were considered for quantification of ILCR in the autumn season (Table 5.2b). In case of children, the corresponding cancer risk of the species was found as  $4.30 \times 10^{-8}$ ,  $5.17 \times 10^{-10}$ ,  $3.37 \times 10^{-8}$ ,  $3.61 \times 10^{-9}$ ,  $8.89 \times 10^{-7}$ ,  $2.29 \times 10^{-8}$ ,  $3.22 \times 10^{-7}$  and  $3.79 \times 10^{-8}$  respectively. Again, ILCR of the corresponding compounds for adults were  $1.19 \times 10^{-7}$ ,  $1.42 \times 10^{-9}$ ,  $9.35 \times 10^{-8}$ ,  $1.00 \times 10^{-8}$ ,  $2.47 \times 10^{-6}$ ,  $6.36 \times 10^{-8}$ ,  $8.93 \times 10^{-7}$  and  $1.06 \times 10^{-7}$ . Hence, ILCR (range;  $10^{-6}$  to  $10^{-4}$ ) represents virtual safety of the PAHs. Again, cancer risk associated with the particles  $< 2.5$  and  $> 2.5 \mu\text{m}$  are also given in Fig. 5.2, while average riskiness of BaPn (for adults  $2.47 \times 10^{-6}$ ) found to be higher and Chr (for children  $5.17 \times 10^{-10}$ ) found lower in comparison to other PAHs.

In winter season (Table 5.3a), in case of children, the HQs of the compounds Npth, Acen, Fluo, Anth, Flun and Pynr were  $4.39 \times 10^{-4}$ ,  $2.83 \times 10^{-8}$ ,  $9.79 \times 10^{-8}$ ,  $1.19 \times 10^{-8}$ ,  $1.41 \times 10^{-7}$  and  $2.38 \times 10^{-7}$  respectively. Again, in case of adults, HQs of the corresponding compounds were  $5.62 \times 10^{-4}$ ,  $9.07 \times 10^{-9}$ ,  $3.14 \times 10^{-8}$ ,  $3.83 \times 10^{-9}$ ,  $4.51 \times 10^{-8}$  and  $7.63 \times 10^{-8}$  respectively. HI was found to be  $4.39 \times 10^{-4}$  and  $5.62 \times 10^{-4}$  for children and adults respectively. Hence, no adverse health impact or significant non-carcinogenic risk found to be associated with the observed PAHs. Incremental lifetime cancer risk associated with children for the species BaAn, Chr, BbFn, BkFn, BaPn, IcdP, DahA and Npth; were estimated to be  $4.85 \times 10^{-8}$ ,  $5.83 \times 10^{-10}$ ,  $4.67 \times 10^{-8}$ ,  $4.45 \times 10^{-9}$ ,  $1.03 \times 10^{-6}$ ,  $2.71 \times 10^{-8}$ ,  $3.96 \times 10^{-7}$  and  $4.42 \times 10^{-8}$  respectively. ILCR associated with adults for the corresponding compounds was  $1.34 \times 10^{-7}$ ,  $1.62 \times 10^{-9}$ ,  $1.29 \times 10^{-7}$ ,  $1.24 \times 10^{-8}$ ,  $2.85 \times 10^{-6}$ ,  $7.51 \times 10^{-8}$ ,  $1.10 \times 10^{-6}$  and  $1.25 \times 10^{-7}$  respectively (Table 5.3 b). Hence, ILCR values showed the virtual safety for the compounds. Again, cancer risk assessment associated with  $< 2.5$  and  $> 2.5 \mu\text{m}$  are also provided in Fig. 5.3, but the average value of ILCR associated with children for Chr ( $5.83 \times 10^{-10}$ ) found with lower risk and, BaPn and DahA



associated with adults ( $2.85 \times 10^{-6}$  and  $1.10 \times 10^{-6}$ ); found to be comparatively higher risk than other PAHs.

In spring season (Table 5.4a), the observed HQs (for children and adults) of the compounds Npth ( $3.99 \times 10^{-4}$  and  $5.12 \times 10^{-4}$ ), Acen ( $2.28 \times 10^{-8}$  and  $7.31 \times 10^{-9}$ ), Fluo ( $8.42 \times 10^{-8}$  and  $2.70 \times 10^{-8}$ ), Anth ( $1.13 \times 10^{-8}$  and  $3.64 \times 10^{-9}$ ), Flun ( $1.36 \times 10^{-8}$  and  $4.37 \times 10^{-8}$ ) and Pym ( $2.05 \times 10^{-7}$  and  $6.56 \times 10^{-8}$ ) showed no adverse health impact and/or no adverse significant non-carcinogenic risk respectively. HI of the species found was  $3.99 \times 10^{-4}$  and  $5.12 \times 10^{-4}$ . The PAHs: BaAn, Chr, BbFn, BkFn, BaPn, IcdP, DahA and Npth were considered for quantification of ILCR (Table 5.4 b). The corresponding cancer risk (ILCR) of the species for children were found as  $4.53 \times 10^{-8}$ ,  $5.47 \times 10^{-10}$ ,  $3.69 \times 10^{-8}$ ,  $3.75 \times 10^{-9}$ ,  $9.29 \times 10^{-7}$ ,  $2.19 \times 10^{-8}$ ,  $3.55 \times 10^{-7}$  and  $4.80 \times 10^{-8}$ , while, for adults it was  $1.26 \times 10^{-7}$ ,  $1.51 \times 10^{-9}$ ,  $1.02 \times 10^{-7}$ ,  $1.04 \times 10^{-8}$ ,  $2.58 \times 10^{-6}$ ,  $6.09 \times 10^{-8}$ ,  $9.85 \times 10^{-7}$  and  $1.14 \times 10^{-7}$  respectively. It signified that ILCR falls within or below the recommended range (i.e.,  $10^{-6}$  to  $10^{-4}$ ). Riskiness of BaPn (for adults  $2.58 \times 10^{-6}$ ) and Chr (for children  $5.47 \times 10^{-10}$ ) possessed similar trend with other seasons. ILCR of the PAHs with  $< 2.5$  and  $> 2.5 \mu\text{m}$  for this season are given in Fig. 5.4.

Table 5.5a (in summer season) showed that HQs of the compounds Npth ( $3.90 \times 10^{-4}$  and  $4.99 \times 10^{-4}$ ), Acen ( $2.12 \times 10^{-8}$  and  $6.78 \times 10^{-9}$ ), Fluo ( $8.21 \times 10^{-8}$  and  $2.63 \times 10^{-8}$ ), Anth ( $1.06 \times 10^{-8}$  and  $3.40 \times 10^{-9}$ ), Flun ( $1.34 \times 10^{-7}$  and  $4.28 \times 10^{-8}$ ) and Pym ( $2.09 \times 10^{-7}$  and  $6.72 \times 10^{-8}$ ) for children and adults represented no adverse health impact and/or no adverse significant non-carcinogenic risk. The HI of the species was  $3.90 \times 10^{-4}$  (children) and  $4.99 \times 10^{-4}$  (adults). Similar to other seasons, the compounds BaAn, Chr, BbFn, BkFn, BaPn, IcdP and DahA were considered for the quantification of ILCR (Table 5.5b). The corresponding risk (ILCR) of the species (children and adults) was observed as ( $4.46 \times 10^{-8}$  and  $1.24 \times 10^{-7}$ ), ( $5.42 \times 10^{-10}$  and  $1.50 \times 10^{-9}$ ), ( $3.53 \times 10^{-8}$  and  $9.79 \times 10^{-8}$ ), ( $3.71 \times 10^{-9}$  and  $1.03 \times 10^{-3}$ ), ( $9.04 \times 10^{-7}$  and  $2.51 \times 10^{-6}$ ), ( $2.02 \times 10^{-8}$  and  $5.60 \times 10^{-8}$ ), ( $3.78 \times 10^{-7}$  and  $1.05 \times 10^{-6}$ ) and ( $3.98 \times 10^{-8}$  and  $1.11 \times 10^{-7}$ ) respectively. So, the riskiness of PAHs fall in the range of ILCR (i.e.,  $10^{-6}$  to  $10^{-4}$ ); which infers the virtual safety of the compounds. Similar to other seasons, cancer risk associated with fine and coarse particles ( $< 2.5$  and  $> 2.5 \mu\text{m}$ ) are also provided for this season in Fig. 5.5. But, Chr (for children  $5.42 \times 10^{-10}$ ) was found to be lower risk among the PAHs, and whereas BaPn and DahA ( $2.51 \times 10^{-6}$  and  $1.05 \times 10^{-6}$ ) for adults found comparatively higher risk among the observed PAHs.

**Table 5.1 (a)** Average HQ of PAHs in the monsoon season

PAHs	RfD (mg kg <sup>-1</sup> day <sup>-1</sup> )	RfC (mg m <sup>-3</sup> )	HQ <sub>C</sub>	HQ <sub>A</sub>
Npth	<sup>a</sup> 2.00 × 10 <sup>-2</sup>	<sup>a</sup> 3.00 × 10 <sup>-3</sup>	3.47 × 10 <sup>-4</sup>	9.53 × 10 <sup>-4</sup>
Acen	<sup>a</sup> 6.00 × 10 <sup>-2</sup>	-	1.91 × 10 <sup>-8</sup>	3.69 × 10 <sup>-10</sup>
Fluo	<sup>a</sup> 4.00 × 10 <sup>-2</sup>	-	7.03 × 10 <sup>-8</sup>	2.26 × 10 <sup>-8</sup>
Anth	<sup>a</sup> 3.00 × 10 <sup>-1</sup>	-	8.75 × 10 <sup>-9</sup>	2.81 × 10 <sup>-9</sup>
Flun	<sup>a</sup> 4.00 × 10 <sup>-2</sup>	-	1.07 × 10 <sup>-7</sup>	3.44 × 10 <sup>-8</sup>
Pym	<sup>a</sup> 3.00 × 10 <sup>-2</sup>	-	1.86 × 10 <sup>-7</sup>	5.97 × 10 <sup>-8</sup>
HI = ΣHQ <sub>i</sub>			3.47 × 10 <sup>-4</sup>	9.53 × 10 <sup>-4</sup>

**Table 5.1 (b)** Average ILCR of PAHs in the monsoon season

PAHs	Unit risk (μg m <sup>-3</sup> ) <sup>-1</sup>	SF <sub>O</sub> (mg kg <sup>-1</sup> day <sup>-1</sup> ) <sup>-1</sup>	SF <sub>C</sub> (mg kg <sup>-1</sup> day <sup>-1</sup> ) <sup>-1</sup>	SF <sub>A</sub> (mg kg <sup>-1</sup> day <sup>-1</sup> ) <sup>-1</sup>	ILCR <sub>C</sub>	ILCR <sub>A</sub>
BaAn	<sup>b</sup> 6.00 × 10 <sup>-5</sup>	<sup>b</sup> 1.00 × 10 <sup>-1</sup>	9.00 × 10 <sup>-5</sup>	1.95 × 10 <sup>-4</sup>	4.37 × 10 <sup>-8</sup>	1.21 × 10 <sup>-7</sup>
Chrn	<sup>b</sup> 6.00 × 10 <sup>-7</sup>	<sup>b</sup> 1.00 × 10 <sup>-3</sup>	9.00 × 10 <sup>-7</sup>	1.95 × 10 <sup>-6</sup>	5.19 × 10 <sup>-10</sup>	1.37 × 10 <sup>-9</sup>
BbFn	<sup>b</sup> 6.00 × 10 <sup>-5</sup>	<sup>b</sup> 1.00 × 10 <sup>-1</sup>	9.00 × 10 <sup>-5</sup>	1.95 × 10 <sup>-4</sup>	2.98 × 10 <sup>-8</sup>	8.27 × 10 <sup>-8</sup>
BkFn	<sup>b</sup> 6.00 × 10 <sup>-6</sup>	<sup>b</sup> 1.00 × 10 <sup>-2</sup>	9.00 × 10 <sup>-6</sup>	1.95 × 10 <sup>-5</sup>	3.02 × 10 <sup>-9</sup>	8.37 × 10 <sup>-9</sup>
BaPn	<sup>a</sup> 6.00 × 10 <sup>-4</sup>	<sup>a</sup> 1.00 × 10 <sup>0</sup>	9.00 × 10 <sup>-4</sup>	1.95 × 10 <sup>-3</sup>	6.24 × 10 <sup>-7</sup>	1.73 × 10 <sup>-6</sup>
IcdP	<sup>b</sup> 6.00 × 10 <sup>-5</sup>	<sup>b</sup> 1.00 × 10 <sup>-1</sup>	9.00 × 10 <sup>-5</sup>	1.95 × 10 <sup>-4</sup>	1.83 × 10 <sup>-8</sup>	5.08 × 10 <sup>-8</sup>
DahA	<sup>b</sup> 6.00 × 10 <sup>-4</sup>	<sup>b</sup> 1.00 × 10 <sup>0</sup>	9.00 × 10 <sup>-4</sup>	1.95 × 10 <sup>-3</sup>	2.66 × 10 <sup>-7</sup>	7.38 × 10 <sup>-7</sup>
Npth	<sup>c</sup> 3.40 × 10 <sup>-5</sup>	-	5.10 × 10 <sup>-5</sup>	1.11 × 10 <sup>-4</sup>	3.51 × 10 <sup>-8</sup>	9.77 × 10 <sup>-8</sup>

<sup>a</sup>Source: Integrated Risk Information System (IRIS),

<sup>b</sup>Source: WHO/TEF Value based on a toxicity equivalent factor from the WHO or US EPA

<sup>c</sup>Source: California Environmental Protection Agency (CalEPA)

The information regarding RfD, RfC, unit risk and SF<sub>O</sub> prescribed by the IRIS and WHO/TEF are also available at the Risk Assessment Information System (RAIS)

SF<sub>O</sub> is the oral slope factor. SF<sub>C</sub> and SF<sub>A</sub> are the corresponding slope factors (inhalation) for children and adults respectively

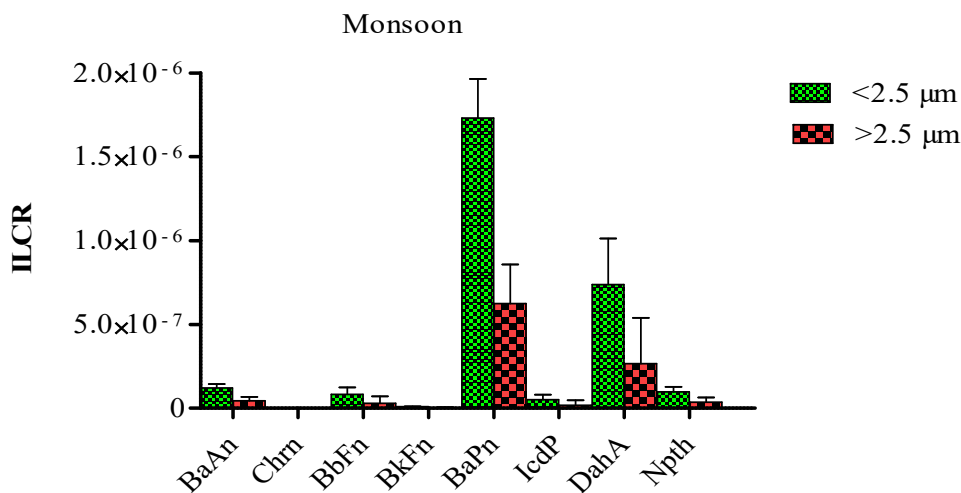


**Fig 5.1** ILCR associated with < 2.5 and > 2.5 μm in the monsoon season

**Table 5.2 (a)** Average HQs of PAHs in the autumn season

PAHs	RfD (mg kg <sup>-1</sup> day <sup>-1</sup> )	RfC (mg m <sup>-3</sup> )	HQ <sub>C</sub>	HQ <sub>A</sub>
Npth	<sup>a</sup> 2.00 × 10 <sup>-2</sup>	<sup>a</sup> 3.00 × 10 <sup>-3</sup>	1.86 × 10 <sup>-4</sup>	1.03 × 10 <sup>-4</sup>
Acen	<sup>a</sup> 6.00 × 10 <sup>-2</sup>	-	2.55 × 10 <sup>-8</sup>	8.19 × 10 <sup>-9</sup>
Fluo	<sup>a</sup> 4.00 × 10 <sup>-2</sup>	-	8.01 × 10 <sup>-8</sup>	2.57 × 10 <sup>-8</sup>
Anth	<sup>a</sup> 3.00 × 10 <sup>-1</sup>	-	1.04 × 10 <sup>-8</sup>	3.34 × 10 <sup>-9</sup>
Flun	<sup>a</sup> 4.00 × 10 <sup>-2</sup>	-	1.30 × 10 <sup>-7</sup>	4.18 × 10 <sup>-8</sup>
Pym	<sup>a</sup> 3.00 × 10 <sup>-2</sup>	-	2.22 × 10 <sup>-7</sup>	7.13 × 10 <sup>-8</sup>
HI = ΣHQ <sub>i</sub>			1.86 × 10 <sup>-4</sup>	1.03 × 10 <sup>-4</sup>

**Table 5.2 (b)** Average ILCR of PAHs in the autumn season

PAHs	Unit risk (μg m <sup>-3</sup> ) <sup>-1</sup>	SF <sub>O</sub> (mg kg <sup>-1</sup> day <sup>-1</sup> ) <sup>-1</sup>	SF <sub>C</sub> (mg kg <sup>-1</sup> day <sup>-1</sup> ) <sup>-1</sup>	SF <sub>A</sub> (mg kg <sup>-1</sup> day <sup>-1</sup> ) <sup>-1</sup>	ILCR <sub>C</sub>	ILCR <sub>A</sub>
BaAn	<sup>b</sup> 6.00 × 10 <sup>-5</sup>	<sup>b</sup> 1.00 × 10 <sup>-1</sup>	9.00 × 10 <sup>-5</sup>	1.95 × 10 <sup>-4</sup>	4.30 × 10 <sup>-8</sup>	1.19 × 10 <sup>-7</sup>
Chrn	<sup>b</sup> 6.00 × 10 <sup>-7</sup>	<sup>b</sup> 1.00 × 10 <sup>-3</sup>	9.00 × 10 <sup>-7</sup>	1.95 × 10 <sup>-6</sup>	5.17 × 10 <sup>-10</sup>	1.42 × 10 <sup>-9</sup>
BbFn	<sup>b</sup> 6.00 × 10 <sup>-5</sup>	<sup>b</sup> 1.00 × 10 <sup>-1</sup>	9.00 × 10 <sup>-5</sup>	1.95 × 10 <sup>-4</sup>	3.37 × 10 <sup>-8</sup>	9.35 × 10 <sup>-8</sup>
BkFn	<sup>b</sup> 6.00 × 10 <sup>-6</sup>	<sup>b</sup> 1.00 × 10 <sup>-2</sup>	9.00 × 10 <sup>-6</sup>	1.95 × 10 <sup>-5</sup>	3.61 × 10 <sup>-9</sup>	1.00 × 10 <sup>-8</sup>
BaPn	<sup>a</sup> 6.00 × 10 <sup>-4</sup>	<sup>a</sup> 1.00 × 10 <sup>0</sup>	9.00 × 10 <sup>-4</sup>	1.95 × 10 <sup>-3</sup>	8.89 × 10 <sup>-7</sup>	2.47 × 10 <sup>-6</sup>
IcdP	<sup>b</sup> 6.00 × 10 <sup>-5</sup>	<sup>b</sup> 1.00 × 10 <sup>-1</sup>	9.00 × 10 <sup>-5</sup>	1.95 × 10 <sup>-4</sup>	2.29 × 10 <sup>-8</sup>	6.36 × 10 <sup>-8</sup>
DahA	<sup>b</sup> 6.00 × 10 <sup>-4</sup>	<sup>b</sup> 1.00 × 10 <sup>0</sup>	9.00 × 10 <sup>-4</sup>	1.95 × 10 <sup>-3</sup>	3.22 × 10 <sup>-7</sup>	8.93 × 10 <sup>-7</sup>
Npth	<sup>c</sup> 3.40 × 10 <sup>-5</sup>	-	5.10 × 10 <sup>-5</sup>	1.11 × 10 <sup>-4</sup>	3.79 × 10 <sup>-8</sup>	1.06 × 10 <sup>-8</sup>

<sup>a</sup>Source: Integrated Risk Information System (IRIS),

<sup>b</sup>Source: WHO/TEF Value based on a toxicity equivalent factor from the WHO or US EPA

<sup>c</sup>Source: California Environmental Protection Agency (CalEPA)

The information regarding RfD, RfC, unit risk and SF<sub>O</sub> prescribed by the IRIS and WHO/TEF are also available at the Risk Assessment Information System (RAIS)

SF<sub>O</sub> is the oral slope factor. SF<sub>C</sub> and SF<sub>A</sub> are the corresponding slope factors (inhalation) for children and adults respectively

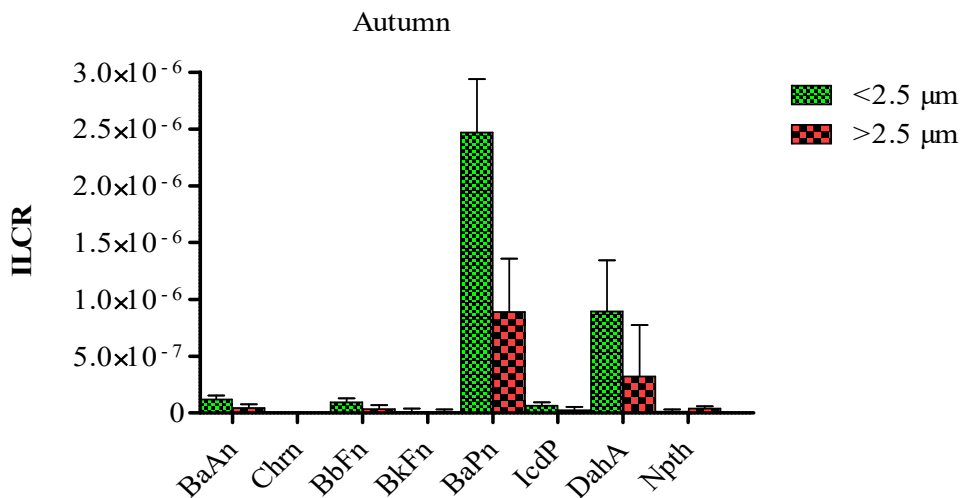


**Fig 5.2** ILCR associated with < 2.5 and > 2.5 μm in the autumn

**Table 5.3 (a)** Average HQs of PAHs in the winter season

PAHs	RfD (mg kg <sup>-1</sup> day <sup>-1</sup> )	RfC (mg m <sup>-3</sup> )	HQ <sub>C</sub>	HQ <sub>A</sub>
Npth	<sup>a</sup> 2.00 × 10 <sup>-2</sup>	<sup>a</sup> 3.00 × 10 <sup>-3</sup>	4.39 × 10 <sup>-4</sup>	5.62 × 10 <sup>-4</sup>
Acen	<sup>a</sup> 6.00 × 10 <sup>-2</sup>	-	2.83 × 10 <sup>-8</sup>	9.07 × 10 <sup>-9</sup>
Fluo	<sup>a</sup> 4.00 × 10 <sup>-2</sup>	-	9.79 × 10 <sup>-8</sup>	3.14 × 10 <sup>-8</sup>
Anth	<sup>a</sup> 3.00 × 10 <sup>-1</sup>	-	1.19 × 10 <sup>-8</sup>	3.83 × 10 <sup>-9</sup>
Flun	<sup>a</sup> 4.00 × 10 <sup>-2</sup>	-	1.41 × 10 <sup>-7</sup>	4.51 × 10 <sup>-8</sup>
Pym	<sup>a</sup> 3.00 × 10 <sup>-2</sup>	-	2.38 × 10 <sup>-7</sup>	7.63 × 10 <sup>-8</sup>
HI = ΣHQ <sub>i</sub>			4.39 × 10 <sup>-4</sup>	5.62 × 10 <sup>-4</sup>

**Table 5.3 (b)** Average ILCR of PAHs in the winter season

PAHs	Unit risk (μg m <sup>-3</sup> ) <sup>-1</sup>	SF <sub>O</sub> (mg kg <sup>-1</sup> day <sup>-1</sup> ) <sup>-1</sup>	SF <sub>C</sub> (mg kg <sup>-1</sup> day <sup>-1</sup> ) <sup>-1</sup>	SF <sub>A</sub> (mg kg <sup>-1</sup> day <sup>-1</sup> ) <sup>-1</sup>	ILCR <sub>C</sub>	ILCR <sub>A</sub>
BaAn	<sup>b</sup> 6.00 × 10 <sup>-5</sup>	<sup>b</sup> 1.00 × 10 <sup>-1</sup>	9.00 × 10 <sup>-5</sup>	1.95 × 10 <sup>-4</sup>	4.85 × 10 <sup>-8</sup>	1.34 × 10 <sup>-7</sup>
Chrn	<sup>b</sup> 6.00 × 10 <sup>-7</sup>	<sup>b</sup> 1.00 × 10 <sup>-3</sup>	9.00 × 10 <sup>-7</sup>	1.95 × 10 <sup>-6</sup>	5.83 × 10 <sup>-10</sup>	1.61 × 10 <sup>-9</sup>
BbFn	<sup>b</sup> 6.00 × 10 <sup>-5</sup>	<sup>b</sup> 1.00 × 10 <sup>-1</sup>	9.00 × 10 <sup>-5</sup>	1.95 × 10 <sup>-4</sup>	4.67 × 10 <sup>-8</sup>	1.29 × 10 <sup>-7</sup>
BkFn	<sup>b</sup> 6.00 × 10 <sup>-6</sup>	<sup>b</sup> 1.00 × 10 <sup>-2</sup>	9.00 × 10 <sup>-6</sup>	1.95 × 10 <sup>-5</sup>	4.45 × 10 <sup>-9</sup>	1.24 × 10 <sup>-8</sup>
BaPn	<sup>a</sup> 6.00 × 10 <sup>-4</sup>	<sup>a</sup> 1.00 × 10 <sup>0</sup>	9.00 × 10 <sup>-4</sup>	1.95 × 10 <sup>-3</sup>	1.03 × 10 <sup>-6</sup>	2.85 × 10 <sup>-6</sup>
IcdP	<sup>b</sup> 6.00 × 10 <sup>-5</sup>	<sup>b</sup> 1.00 × 10 <sup>-1</sup>	9.00 × 10 <sup>-5</sup>	1.95 × 10 <sup>-4</sup>	2.71 × 10 <sup>-8</sup>	7.51 × 10 <sup>-8</sup>
DahA	<sup>b</sup> 6.00 × 10 <sup>-4</sup>	<sup>b</sup> 1.00 × 10 <sup>0</sup>	9.00 × 10 <sup>-4</sup>	1.95 × 10 <sup>-3</sup>	3.96 × 10 <sup>-7</sup>	1.10 × 10 <sup>-6</sup>
Npth	<sup>c</sup> 3.40 × 10 <sup>-5</sup>	-	5.10 × 10 <sup>-5</sup>	1.11 × 10 <sup>-4</sup>	4.42 × 10 <sup>-8</sup>	1.25 × 10 <sup>-7</sup>

<sup>a</sup>Source: Integrated Risk Information System (IRIS),

<sup>b</sup>Source: WHO/TEF Value based on a toxicity equivalent factor from the WHO or US EPA

<sup>c</sup>Source: California Environmental Protection Agency (CalEPA)

The information regarding RfD, RfC, unit risk and SF<sub>O</sub> prescribed by the IRIS and WHO/TEF are also available at the Risk Assessment Information System (RAIS)

SF<sub>O</sub> is the oral slope factor. SF<sub>C</sub> and SF<sub>A</sub> are the corresponding slope factors (inhalation) for children and adults respectively

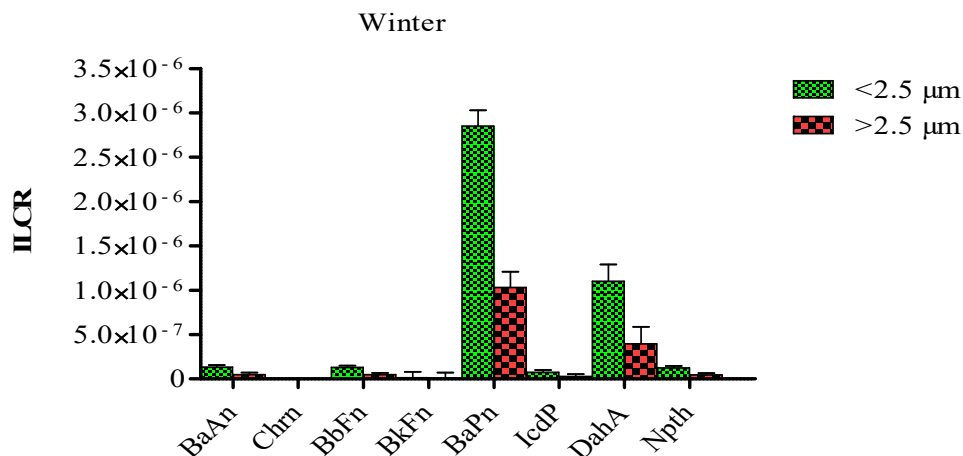


**Fig 5.3** ILCR associated with < 2.5 and > 2.5 μm in the winter season

**Table 5.4 (a)** Average HQs of PAHs in the spring season

PAHs	RfD (mg kg <sup>-1</sup> day <sup>-1</sup> )	RfC (mg m <sup>-3</sup> )	HQ <sub>C</sub>	HQ <sub>A</sub>
Npth	<sup>a</sup> 2.00 × 10 <sup>-2</sup>	<sup>a</sup> 3.00 × 10 <sup>-3</sup>	3.99 × 10 <sup>-4</sup>	5.12 × 10 <sup>-4</sup>
Acen	<sup>a</sup> 6.00 × 10 <sup>-2</sup>	-	2.28 × 10 <sup>-7</sup>	7.31 × 10 <sup>-9</sup>
Fluo	<sup>a</sup> 4.00 × 10 <sup>-2</sup>	-	8.42 × 10 <sup>-8</sup>	2.70 × 10 <sup>-8</sup>
Anth	<sup>a</sup> 3.00 × 10 <sup>-1</sup>	-	1.13 × 10 <sup>-8</sup>	3.64 × 10 <sup>-9</sup>
Flun	<sup>a</sup> 4.00 × 10 <sup>-2</sup>	-	1.36 × 10 <sup>-7</sup>	4.37 × 10 <sup>-8</sup>
Pym	<sup>a</sup> 3.00 × 10 <sup>-2</sup>	-	2.05 × 10 <sup>-7</sup>	6.56 × 10 <sup>-8</sup>
HI = ΣHQ <sub>i</sub>			3.99 × 10 <sup>-4</sup>	5.12 × 10 <sup>-4</sup>

**Table 5.4 (b)** Average ILCR of PAHs in the spring season

PAHs	Unit risk (μg m <sup>-3</sup> ) <sup>-1</sup>	SF <sub>O</sub> (mg kg <sup>-1</sup> day <sup>-1</sup> ) <sup>-1</sup>	SF <sub>C</sub> (mg kg <sup>-1</sup> day <sup>-1</sup> ) <sup>-1</sup>	SF <sub>A</sub> (mg kg <sup>-1</sup> day <sup>-1</sup> ) <sup>-1</sup>	ILCR <sub>C</sub>	ILCR <sub>A</sub>
BaAn	<sup>b</sup> 6.00 × 10 <sup>-5</sup>	<sup>b</sup> 1.00 × 10 <sup>-1</sup>	9.00 × 10 <sup>-5</sup>	1.95 × 10 <sup>-4</sup>	4.53 × 10 <sup>-8</sup>	1.26 × 10 <sup>-7</sup>
Chrn	<sup>b</sup> 6.00 × 10 <sup>-7</sup>	<sup>b</sup> 1.00 × 10 <sup>-3</sup>	9.00 × 10 <sup>-7</sup>	1.95 × 10 <sup>-6</sup>	5.47 × 10 <sup>-10</sup>	1.51 × 10 <sup>-9</sup>
BbFn	<sup>b</sup> 6.00 × 10 <sup>-5</sup>	<sup>b</sup> 1.00 × 10 <sup>-1</sup>	9.00 × 10 <sup>-5</sup>	1.95 × 10 <sup>-4</sup>	3.69 × 10 <sup>-8</sup>	1.02 × 10 <sup>-7</sup>
BkFn	<sup>b</sup> 6.00 × 10 <sup>-6</sup>	<sup>b</sup> 1.00 × 10 <sup>-2</sup>	9.00 × 10 <sup>-6</sup>	1.95 × 10 <sup>-5</sup>	3.75 × 10 <sup>-9</sup>	1.04 × 10 <sup>-8</sup>
BaPn	<sup>a</sup> 6.00 × 10 <sup>-4</sup>	<sup>a</sup> 1.00 × 10 <sup>0</sup>	9.00 × 10 <sup>-4</sup>	1.95 × 10 <sup>-3</sup>	9.29 × 10 <sup>-7</sup>	2.58 × 10 <sup>-6</sup>
IcdP	<sup>b</sup> 6.00 × 10 <sup>-5</sup>	<sup>b</sup> 1.00 × 10 <sup>-1</sup>	9.00 × 10 <sup>-5</sup>	1.95 × 10 <sup>-4</sup>	2.20 × 10 <sup>-8</sup>	6.19 × 10 <sup>-9</sup>
DahA	<sup>b</sup> 6.00 × 10 <sup>-4</sup>	<sup>b</sup> 1.00 × 10 <sup>0</sup>	9.00 × 10 <sup>-4</sup>	1.95 × 10 <sup>-3</sup>	3.55 × 10 <sup>-7</sup>	9.85 × 10 <sup>-7</sup>
Npth	<sup>c</sup> 3.40 × 10 <sup>-5</sup>	-	5.10 × 10 <sup>-5</sup>	1.11 × 10 <sup>-4</sup>	4.80 × 10 <sup>-8</sup>	1.14 × 10 <sup>-7</sup>

<sup>a</sup>Source: Integrated Risk Information System (IRIS),

<sup>b</sup>Source: WHO/TEF Value based on a toxicity equivalent factor from the WHO or US EPA

<sup>c</sup>Source: California Environmental Protection Agency (CalEPA)

The information regarding RfD, RfC, unit risk and SF<sub>O</sub> prescribed by the IRIS and WHO/TEF are also available at the Risk Assessment Information System (RAIS)

SF<sub>O</sub> is the oral slope factor. SF<sub>C</sub> and SF<sub>A</sub> are the corresponding slope factors (inhalation) for children and adults respectively

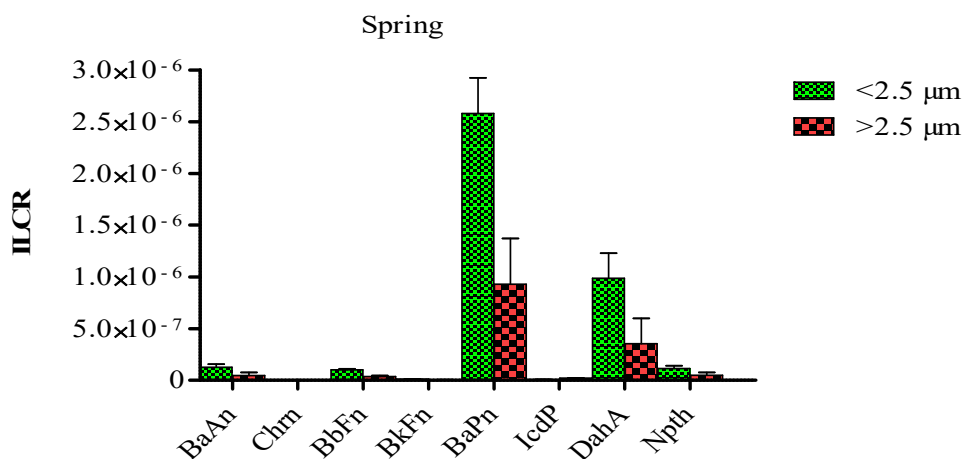


**Fig. 5.4** ILCR associated with < 2.5 and > 2.5 μm in the spring season

**Table 5.5 (a)** Average HQs of PAHs in the summer season

PAHs	RfD (mg kg <sup>-1</sup> day <sup>-1</sup> )	RfC (mg m <sup>-3</sup> )	HQ <sub>C</sub>	HQ <sub>A</sub>
Npth	<sup>a</sup> 2.00 × 10 <sup>-2</sup>	<sup>a</sup> 3.00 × 10 <sup>-3</sup>	3.90 × 10 <sup>-4</sup>	4.99 × 10 <sup>-4</sup>
Acen	<sup>a</sup> 6.00 × 10 <sup>-2</sup>	-	2.12 × 10 <sup>-8</sup>	6.78 × 10 <sup>-9</sup>
Fluo	<sup>a</sup> 4.00 × 10 <sup>-2</sup>	-	8.21 × 10 <sup>-8</sup>	2.63 × 10 <sup>-8</sup>
Anth	<sup>a</sup> 3.00 × 10 <sup>-1</sup>	-	1.06 × 10 <sup>-8</sup>	3.40 × 10 <sup>-9</sup>
Flun	<sup>a</sup> 4.00 × 10 <sup>-2</sup>	-	1.34 × 10 <sup>-7</sup>	4.28 × 10 <sup>-8</sup>
Pym	<sup>a</sup> 3.00 × 10 <sup>-2</sup>	-	2.09 × 10 <sup>-7</sup>	6.72 × 10 <sup>-8</sup>
HI = ΣHQ <sub>i</sub>			3.90 × 10 <sup>-4</sup>	4.99 × 10 <sup>-4</sup>

**Table 5.5 (b)** Average ILCR of PAHs in the summer season

PAHs	Unit risk (μg m <sup>-3</sup> ) <sup>-1</sup>	SF <sub>O</sub> (mg kg <sup>-1</sup> day <sup>-1</sup> ) <sup>-1</sup>	SF <sub>C</sub> (mg kg <sup>-1</sup> day <sup>-1</sup> ) <sup>-1</sup>	SF <sub>A</sub> (mg kg <sup>-1</sup> day <sup>-1</sup> ) <sup>-1</sup>	ILCR <sub>C</sub>	ILCR <sub>A</sub>
BaAn	<sup>b</sup> 6.00 × 10 <sup>-5</sup>	<sup>b</sup> 1.00 × 10 <sup>-1</sup>	9.00 × 10 <sup>-5</sup>	1.95 × 10 <sup>-4</sup>	4.46 × 10 <sup>-8</sup>	1.24 × 10 <sup>-7</sup>
Chrn	<sup>b</sup> 6.00 × 10 <sup>-7</sup>	<sup>b</sup> 1.00 × 10 <sup>-3</sup>	9.00 × 10 <sup>-7</sup>	1.95 × 10 <sup>-6</sup>	5.42 × 10 <sup>-10</sup>	1.50 × 10 <sup>-9</sup>
BbFn	<sup>b</sup> 6.00 × 10 <sup>-5</sup>	<sup>b</sup> 1.00 × 10 <sup>-1</sup>	9.00 × 10 <sup>-5</sup>	1.95 × 10 <sup>-4</sup>	3.53 × 10 <sup>-8</sup>	9.79 × 10 <sup>-8</sup>
BkFn	<sup>b</sup> 6.00 × 10 <sup>-6</sup>	<sup>b</sup> 1.00 × 10 <sup>-2</sup>	9.00 × 10 <sup>-6</sup>	1.95 × 10 <sup>-5</sup>	3.71 × 10 <sup>-9</sup>	1.03 × 10 <sup>-8</sup>
BaPn	<sup>a</sup> 6.00 × 10 <sup>-4</sup>	<sup>a</sup> 1.00 × 10 <sup>0</sup>	9.00 × 10 <sup>-4</sup>	1.95 × 10 <sup>-3</sup>	9.04 × 10 <sup>-7</sup>	2.51 × 10 <sup>-6</sup>
IcdP	<sup>b</sup> 6.00 × 10 <sup>-5</sup>	<sup>b</sup> 1.00 × 10 <sup>-1</sup>	9.00 × 10 <sup>-5</sup>	1.95 × 10 <sup>-4</sup>	2.02 × 10 <sup>-8</sup>	5.60 × 10 <sup>-8</sup>
DahA	<sup>b</sup> 6.00 × 10 <sup>-4</sup>	<sup>b</sup> 1.00 × 10 <sup>0</sup>	9.00 × 10 <sup>-4</sup>	1.95 × 10 <sup>-3</sup>	3.78 × 10 <sup>-7</sup>	1.05 × 10 <sup>-6</sup>
Npth	<sup>c</sup> 3.40 × 10 <sup>-5</sup>	-	5.10 × 10 <sup>-5</sup>	1.11 × 10 <sup>-4</sup>	3.98 × 10 <sup>-8</sup>	1.11 × 10 <sup>-7</sup>

<sup>a</sup>Source: Integrated Risk Information System (IRIS),

<sup>b</sup>Source: WHO/TEF Value based on a toxicity equivalent factor from the WHO or US EPA

<sup>c</sup>Source: California Environmental Protection Agency (CalEPA)

The information regarding RfD, RfC, unit risk and SF<sub>O</sub> prescribed by the IRIS and WHO/TEF are also available at the Risk Assessment Information System (RAIS)

SF<sub>O</sub> is the oral slope factor. SF<sub>C</sub> and SF<sub>A</sub> are the corresponding slope factors (inhalation) for children and adults respectively

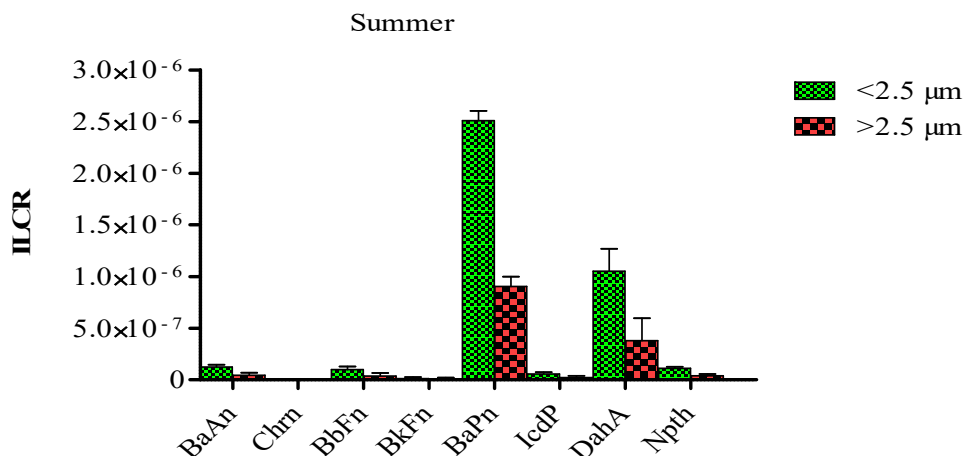


**Fig 5.5** ILCR associated with < 2.5 and > 2.5 μm in the summer season

## [5.2] Correlation matrices among PAHs and carbonaceous species

The Pearson correlation of particulate bound PAHs and carbonaceous species was carried out for all the seasons through the statistical software XLSTAT 7.5.2 version. Correlation matrices among PAHs (Barra et al., 2009; Wang et al., 2011; Masih et al., 2012; Liu et al., 2013), and among PAHs and carbons (Park et al., 2002; Agarwal et al., 2009; Duan et al., 2012; Daso et al., 2016) have already been observed by researchers. Again, significant correlation between PAHs and carbons have also been observed by various researchers (Wheatley & Sadhra, 2004; Sheesley et al., 2008; Yang et al., 2008; Li et al., 2013). In this work, correlations with  $\sim 0.5$  are shown in bold throughout the Tables 5.6 - 5.10. In monsoon season (Table 5.6), where values with  $\geq 0.5$  are represented as good correlation, but good correlation was observed among the following compounds/ species: Npth and Phtn (0.848), Npth and BaPn (0.715), Npth and TC (0.684), Phtn and Acen (0.827), Phtn and Pynr (0.709), Phtn and BbFn (0.610), Phtn and DahA (0.514), Phtn and EC (0.575), Acnp and Fluo (0.941), Acnp and BkFn (0.743), Acnp and DahA (0.739), Acen and Flun (0.536), Acen and BghiP (0.760), Acen and OC (0.581), Fluo and BaAn (0.579), Fluo and BaPn (0.766), Anth and Pynr (0.796), Anth and BkFn (0.901), Anth and IcdP (0.559), Pynr and Chrn (0.598), Pynr and BaPn (0.628), Pynr and TC (0.541), Flun and BbFn (0.511), Flun and EC (0.877), Chrn and BghiP (0.790), Chrn and IcdP (0.580), BaAn and DahA (0.635), BaAn and OC (0.668), BbFn and TC (0.951), BkFn and BaPn (0.786), BghiP and EC (0.710), DahA and OC (0.753) and, TC and EC (0.622) respectively.

In case of autumn season (Table 5.7), good correlations were obtained among the following species: Npth and Acnp (0.781), Npth and DahA (0.519), Npth and EC (0.757), Phtn and Flun (0.566), Acnp and Acen (0.641), Acnp and Pynr (0.836), Acnp and BaPn (0.542), Acnp and OC (0.633), Acen and Chrn (0.640), Acen and BkFn (0.684), Acen and IcdP (0.553), Fluo and Anth (0.739), Fluo and DahA (0.627), Anth and Pynr (0.513), Anth and BaPn (0.607), Pynr and BaAn (0.709), Chrn and BghiP (0.728), Chrn and IcdP (0.650), BaAn and TC (0.855), BkFn and DahA (0.876), BaPn and TC (0.625), BghiP and TC (0.543), and DahA and IcdP (0.732) respectively.

From the Table 5.8 (winter season), significant correlations of the PAHs and carbonaceous species were: Npth and Phtn (0.958), Npth and Pynr (0.697), Npth and Chrn (0.520), Npth and TC (0.687), Phtn and OC (0.681), Acnp and Fluo (0.766), Acnp and Flun

(0.517), Acnp and BghiP (0.542), Acnp and EC (0.872); Acen and Anth (0.564), Acen and BbFn (0.650), Acen and TC (0.502), Fluo and Chrn (0.984), Anth and Flun (0.793), Anth and BkFn (0.531), Pynr and BaAn (0.619), Pynr and OC (0.529), Flun and BaPn (0.673), Flun and IcdP (0.727), Flun and TC (0.560), Chrn and BaAn (0.529), BaAn and DahA (0.876), BaAn and EC (0.626), BbFn and BkFn (0.854), BbFn and TC (0.729), BkFn and IcdP (0.689), BaPn and EC (0.778) IcdP and EC (0.767) and, EC and OC (0.571) respectively.

During spring (Fig. 5.9), good correlations among the PAHs and carbonaceous load was observed. These were Npth and Phtn (0.675), Npth and Anth (0.688), Npth and BaPn (0.851), Npth and TC (0.569), Phtn and Acen (0.867), Phtn and Pynr (0.714), Acnp and Flun (0.831), Acnp and BbFn (0.547), Acnp and OC (0.625), Acen and Pynr (0.827), Acen and BaAn (0.763), Acen and EC (0.572), Fluo and Chrn (0.535), Fluo and BkFn (0.987), Fluo and DahA (0.567), Anth and Flun (0.869), Anth and BghiP (0.525), Anth and TC (0.757), Pynr and Chrn (0.989), Flun and BbFn (0.878), Flun and IcdP (0.559), Chrn and TC (0.857), BkFn and BaPn (0.976), BkFn and BghiP (0.563), BaPn and IcdP (0.642) and, TC and EC (0.589) respectively.

In summer season (Table 5.10), following PAHs and carbonaceous load were found to have good correlations: Npth and Acnp (0.746), Npth and Pynr (0.567), Npth and BaPn (0.568), Npth and TC (0.587), Phtn and Chrn (0.647); Phtn and EC (0.503), Acnp and Anth (0.809), Acnp and BbFn (0.918), Acnp and DahA (0.750), Acnp and OC (0.696), Acen and Flun (0.917), Acen and BkFn (0.520), Fluo and Anth (0.980), Fluo and DahA (0.657), Anth and BaAn (0.739), Pynr and BghiP (0.747), Flun and BaAn (0.565), Flun and OC (0.530), Chrn and IcdP (0.525), BaAn and BaPn (0.713), BbFn and BkFn (0.935); BkFn and TC (0.817), BaPn and EC (0.542), and IcdP and OC (0.686) respectively.

By taking mean values of concentrations of the PAHs and carbonaceous loads throughout the years; the correlation matrices obtained are given in Table 5.11. Species; which were observed to be a good correlations ( $\geq 5$ ) throughout the years were as follows: Npth and Acnp (0.649), Npth and Flun (0.972), Npth and BghiP (0.545), Npth and EC (0.678), Phtn and Acnp (0.616), Phtn and BbFn (0.512), Phtn and BaPn (0.838), Phtn and TC (0.545), Acnp and TC (0.632), Acen and EC (0.653), Fluo and BaAn (0.654), Fluo and IcdP (0.993), Fluo and OC (0.636), Pynr and BghiP (0.510), Pynr and DahA (0.607), Flun and BbFn (0.653), Flun and TC (0.735), Chrn and BaPn (0.548), BaAn and BghiP (0.654), BbFn and IcdP (0.523) and BghiP and EC (0.559) respectively.



**Table 5.6** Correlation matrix of PAHs and carbonaceous load in the monsoon season

	Npth	Phtn	Acnp	Acen	Fluo	Anth	Pyrn	Flun	Chrn	BaAn	BbFn	BkFn	BaPn	BghiP	DahA	IcdP	TC	EC	OC
Npth	1																		
Phtn	<b>0.848</b>	1																	
Acnp	0.485	0.383	1																
Acen	<i>0.317</i>	<b>0.827</b>	0.057	1															
Fluo	0.110	<i>0.453</i>	<b>0.941</b>	<i>-0.421</i>	1														
Anth	0.007	-0.564	<i>0.439</i>	0.206	0.350	1													
Pyrn	0.302	<b>0.709</b>	0.170	0.274	-0.012	<b>0.796</b>	1												
Flun	-0.120	0.158	0.273	<b>0.536</b>	0.326	<i>0.349</i>	0.237	1											
Chrn	0.319	0.284	<i>0.363</i>	0.412	0.203	0.325	<b>0.598</b>	<i>0.246</i>	1										
BaAn	0.408	<i>0.308</i>	0.253	<i>-0.433</i>	<b>0.579</b>	0.538	0.193	0.361	0.433	1									
BbFn	0.382	<b>0.610</b>	-0.274	0.365	<i>0.282</i>	-0.165	<i>0.271</i>	<b>0.511</b>	<i>0.134</i>	0.348	1								
BkFn	0.286	0.174	<b>0.743</b>	0.299	0.371	<b>0.901</b>	-0.779	0.317	-0.249	0.186	<i>0.194</i>	1							
BaPn	<b>0.715</b>	-0.446	<i>0.426</i>	-0.116	<b>0.766</b>	0.133	<b>0.628</b>	<i>-0.163</i>	0.406	0.059	0.395	<b>0.786</b>	1						
BghiP	0.339	0.125	0.322	<b>0.760</b>	-0.218	<i>0.124</i>	0.155	0.469	<b>0.790</b>	<i>-0.104</i>	0.202	0.269	0.173	1					
DahA	-0.137	<b>0.514</b>	<b>0.739</b>	<i>0.025</i>	0.167	-0.065	0.075	0.145	<i>-0.651</i>	<b>0.635</b>	-0.175	<i>-0.828</i>	0.032	0.137	1				
IcdP	0.086	<i>-0.356</i>	0.397	-0.027	0.332	<b>0.559</b>	<i>-0.238</i>	-0.098	<b>0.580</b>	0.326	0.018	-0.260	0.163	<i>-0.643</i>	0.083	1			
TC	<b>0.684</b>	0.411	0.254	0.346	<i>0.083</i>	0.035	<b>0.541</b>	0.062	-0.213	-0.121	<b>0.951</b>	0.045	<i>-0.988</i>	0.039	<i>-0.543</i>	0.327	1		
EC	<i>0.476</i>	<b>0.575</b>	-0.068	0.083	0.125	0.178	0.057	<b>0.877</b>	<i>0.091</i>	-0.026	0.086	0.467	0.052	<b>0.710</b>	0.067	<b>0.622</b>	-0.316	1	
OC	0.265	0.091	0.423	<b>0.581</b>	-0.066	<i>0.397</i>	0.034	-0.696	0.344	<b>0.668</b>	0.127	0.072	0.490	<i>-0.356</i>	<b>0.753</b>	0.053	<i>0.017</i>	0.095	1

*In italics, significant values (except diagonal) at the level of significance alpha=0.050 (two-tailed test)*

Values with >0.5 are shown bold

**Table 5.7** Correlation matrix of PAHs and carbonaceous load in the autumn

	Npth	Phtn	Acnp	Acen	Fluo	Anth	Pyrn	Flun	Chrn	BaAn	BbFn	BkFn	BaPn	BghiP	DahA	IcdP	TC	EC	OC
Npth	1																		
Phtn	<i>0.244</i>	1																	
Acnp	<b>0.781</b>	-0.235	1																
Acen	0.257	0.153	<b>0.641</b>	1															
Fluo	0.310	0.188	<i>-0.006</i>	-0.122	1														
Anth	0.214	<i>-0.130</i>	-0.198	0.076	<b>0.739</b>	1													
Pyrn	0.485	0.289	<b>0.836</b>	0.334	-0.225	<b>0.513</b>	1												
Flun	0.153	<b>0.566</b>	-0.044	-0.399	0.078	<i>-0.915</i>	-0.109	1											
Chrn	0.382	0.216	-0.233	<b>0.640</b>	0.356	0.107	0.206	<i>0.222</i>	1										
BaAn	0.217	0.478	-0.145	0.215	<i>0.048</i>	0.322	<b>0.709</b>	-0.102	0.241	1									
BbFn	<i>0.138</i>	0.433	0.035	-0.145	<i>0.005</i>	0.149	-0.245	0.492	-0.614	-0.260	1								
BkFn	0.279	-0.171	-0.086	<b>0.684</b>	-0.357	-0.175	0.390	<i>0.302</i>	-0.555	-0.273	0.235	1							
BaPn	0.076	0.154	<b>0.542</b>	<i>-0.200</i>	-0.292	<b>0.607</b>	-0.213	-0.423	-0.202	<i>0.073</i>	0.141	<i>0.127</i>	1						
BghiP	0.289	-0.026	<i>-0.251</i>	0.145	-0.071	0.057	0.142	0.256	<b>0.728</b>	-0.141	0.396	-0.085	-0.155	1					
DahA	<b>0.519</b>	0.037	0.264	0.022	<b>0.627</b>	<i>-0.549</i>	0.043	0.071	0.251	-0.598	-0.587	<b>0.876</b>	0.416	0.331	1				
IcdP	0.098	0.163	-0.059	<b>0.553</b>	-0.114	0.063	0.174	-0.144	<b>0.650</b>	0.130	0.067	0.068	0.279	0.065	<b>0.732</b>	1			
TC	0.494	-0.119	0.147	0.041	<i>0.048</i>	-0.132	0.203	-0.210	<i>-0.350</i>	<b>0.855</b>	0.325	0.234	<b>0.625</b>	<i>0.024</i>	-0.173	0.064	1		
EC	<b>0.757</b>	<i>0.072</i>	-0.598	-0.025	0.065	0.438	<i>0.018</i>	0.397	0.496	<i>-0.162</i>	0.028	-0.043	-0.104	-0.154	0.041	<i>0.218</i>	-0.675	1	
OC	0.063	-0.028	<b>0.633</b>	0.098	0.118	0.026	0.434	<i>0.258</i>	-0.206	0.045	0.017	-0.222	<i>0.062</i>	<b>0.543</b>	-0.139	0.079	0.056	0.037	1

*In italics, significant values (except diagonal) at the level of significance alpha=0.050 (two-tailed test)*

Values with >0.5 are shown bold

**Table 5.8** Correlation matrix of PAHs and carbonaceous load in the winter season

	Npth	Phtn	Acnp	Acen	Fluo	Anth	Pyrn	Flun	Chrn	BaAn	BbFn	BkFn	BaPn	BghiP	DahA	IcdP	TC	EC	OC
Npth	1																		
Phtn	<b>0.958</b>	1																	
Acnp	<i>0.067</i>	0.045	1																
Acen	0.036	0.113	<i>0.056</i>	1															
Fluo	0.320	-0.215	<b>0.766</b>	0.145	1														
Anth	-0.137	<i>0.360</i>	0.048	<b>0.564</b>	-0.558	1													
Pyrn	<b>0.697</b>	-0.098	0.108	0.023	0.036	0.161	1												
Flun	0.065	0.451	<b>0.517</b>	0.209	0.270	<b>0.793</b>	<i>0.012</i>	1											
Chrn	<b>0.520</b>	0.260	0.254	-0.675	<b>0.984</b>	-0.546	0.137	-0.664	1										
BaAn	<i>0.268</i>	0.145	-0.294	-0.845	0.053	-0.047	<b>0.619</b>	0.127	<b>0.529</b>	1									
BbFn	0.092	-0.355	0.376	<b>0.650</b>	-0.354	0.192	0.056	0.245	0.156	0.237	1								
BkFn	0.271	0.274	0.075	<i>0.195</i>	0.187	<b>0.531</b>	<i>-0.478</i>	<i>0.165</i>	0.433	-0.522	<b>0.854</b>	1							
BaPn	0.499	0.260	<i>0.393</i>	0.581	0.058	-0.041	0.133	<b>0.673</b>	<i>-0.056</i>	0.329	<i>0.256</i>	-0.533	1						
BghiP	-0.640	0.351	<b>0.542</b>	-0.267	<i>-0.047</i>	0.255	0.491	-0.547	0.098	<i>0.164</i>	0.031	0.410	0.390	1					
DahA	0.243	-0.067	-0.067	0.325	0.013	0.178	-0.982	0.269	0.175	<b>0.876</b>	-0.308	<i>0.319</i>	-0.247	0.038	1				
IcdP	-0.081	<i>0.425</i>	0.354	-0.464	0.324	<i>0.097</i>	0.123	<b>0.727</b>	-0.246	-0.350	0.067	<b>0.689</b>	0.178	<i>-0.512</i>	0.473	1			
TC	<b>0.687</b>	0.098	0.067	<b>0.513</b>	-0.247	0.521	-0.246	<b>0.560</b>	-0.323	<i>0.011</i>	<b>0.729</b>	-0.051	0.353	0.210	0.009	<i>0.239</i>	1		
EC	<i>0.079</i>	0.146	<b>0.872</b>	0.086	0.151	0.324	0.099	<i>-0.296</i>	0.218	<b>0.626</b>	-0.044	<i>0.265</i>	<b>0.778</b>	0.155	0.227	<b>0.767</b>	-0.664	1	
OC	0.106	<b>0.681</b>	-0.683	<i>0.070</i>	0.198	0.074	<b>0.529</b>	0.352	0.057	0.163	0.206	0.617	-0.024	<i>0.437</i>	0.052	-0.201	0.183	<b>0.571</b>	1

*In italics, significant values (except diagonal) at the level of significance alpha=0.050 (two-tailed test)*

Values with >0.5 are shown bold

**Table 5.9** Correlation matrix of PAHs and carbonaceous load in the spring season

	Npth	Phtn	Acnp	Acen	Fluo	Anth	Pyrn	Flun	Chrn	BaAn	BbFn	BkFn	BaPn	BghiP	DahA	IcdP	TC	EC	OC
Npth	1																		
Phtn	<b>0.675</b>	1																	
Acnp	0.117	0.280	1																
Acen	0.340	<b>0.867</b>	<i>0.230</i>	1															
Fluo	0.359	0.127	-0.533	0.312	1														
Anth	<b>0.688</b>	0.200	0.162	0.036	0.069	1													
Pyrn	<i>0.006</i>	<b>0.714</b>	0.354	<b>0.827</b>	0.242	0.018	1												
Flun	0.214	-0.933	<b>0.831</b>	0.102	<i>0.300</i>	<b>0.869</b>	<i>0.026</i>	1											
Chrn	0.384	0.494	0.226	0.091	<b>0.535</b>	0.217	<b>0.989</b>	-0.647	1										
BaAn	0.323	0.095	0.400	<b>0.763</b>	-0.013	<i>0.376</i>	0.073	0.339	0.054	1									
BbFn	0.030	0.388	<b>0.547</b>	<i>-0.422</i>	0.246	-0.257	0.168	<b>0.878</b>	-0.227	0.421	1								
BkFn	-0.654	0.225	0.006	0.052	<b>0.987</b>	0.034	-0.215	-0.055	<i>0.183</i>	-0.252	<i>0.008</i>	1							
BaPn	<b>0.851</b>	0.076	0.029	0.137	-0.023	0.341	0.065	<i>0.213</i>	0.465	0.327	-0.513	<b>0.976</b>	1						
BghiP	0.237	-0.033	0.270	-0.251	<i>0.144</i>	<b>0.525</b>	0.311	0.147	0.285	0.498	0.065	<b>0.563</b>	0.236	1					
DahA	0.068	0.296	0.348	0.434	<b>0.567</b>	-0.320	<i>0.226</i>	-0.251	0.617	<i>-0.065</i>	0.189	-0.531	<i>0.077</i>	0.164	1				
IcdP	0.487	0.211	-0.025	0.323	0.081	-0.458	0.032	<b>0.559</b>	-0.226	0.071	0.062	0.243	<b>0.642</b>	0.212	<i>-0.734</i>	1			
TC	<b>0.569</b>	-0.062	<i>0.014</i>	0.036	0.054	<b>0.757</b>	-0.024	0.136	<b>0.857</b>	0.238	-0.316	<i>0.027</i>	-0.325	0.058	0.456	0.325	1		
EC	<i>0.268</i>	0.473	0.166	<b>0.572</b>	<i>0.005</i>	0.223	0.342	0.293	<i>0.046</i>	0.038	0.240	0.435	0.610	-0.365	0.032	-0.064	<b>0.589</b>	1	
OC	0.053	0.079	<b>0.625</b>	<i>0.103</i>	0.092	0.129	0.060	<i>-0.094</i>	0.363	<b>0.754</b>	0.018	0.063	-0.264	0.433	0.121	<i>0.0317</i>	0.414	-0.520	1

*In italics, significant values (except diagonal) at the level of significance alpha=0.050 (two-tailed test)*

Values with >0.5 are shown bold

**Table 5.10** Correlation matrix of PAHs and carbonaceous load in the summer season

	Npth	Phtn	Acnp	Acen	Fluo	Anth	Pyrn	Flun	Chrn	BaAn	BbFn	BkFn	BaPn	BghiP	DahA	IcdP	TC	EC	OC
Npth	1																		
Phtn	0.453	1																	
Acnp	<b>0.746</b>	0.023	1																
Acen	-0.241	<i>0.360</i>	<i>0.015</i>	1															
Fluo	-0.553	0.151	0.320	0.143	1														
Anth	<i>0.038</i>	0.324	<b>0.809</b>	-0.118	<b>0.980</b>	1													
Pyrn	<b>0.567</b>	-0.065	-0.146	<i>0.237</i>	0.242	0.216	1												
Flun	0.043	0.316	-0.453	<b>0.917</b>	<i>-0.964</i>	<i>0.302</i>	-0.360	1											
Chrn	0.165	<b>0.647</b>	0.184	0.059	0.219	-0.134	0.249	0.223	1										
BaAn	0.084	0.233	0.021	0.373	0.362	<b>0.739</b>	<i>0.187</i>	<b>0.565</b>	<i>0.373</i>	1									
BbFn	0.025	-0.760	<b>0.918</b>	-0.041	0.205	0.247	0.089	-0.120	0.208	-0.151	1								
BkFn	0.385	<i>0.149</i>	-0.341	<b>0.520</b>	-0.089	0.076	-0.204	<i>-0.084</i>	-0.295	0.008	<b>0.935</b>	1							
BaPn	<b>0.568</b>	<i>-0.652</i>	0.267	0.036	-0.539	<i>0.188</i>	0.357	0.073	0.117	<b>0.713</b>	-0.015	<i>0.077</i>	1						
BghiP	0.332	0.025	0.016	0.287	0.058	-0.321	<b>0.747</b>	0.263	-0.326	<i>0.162</i>	0.059	-0.786	-0.083	1					
DahA	-0.471	0.009	<b>0.750</b>	0.027	<b>0.657</b>	0.059	-0.018	0.183	<i>0.009</i>	0.070	0.417	0.061	0.245	0.256	1				
IcdP	<i>0.065</i>	0.411	0.323	-0.778	<i>0.031</i>	-0.362	0.328	0.489	<b>0.525</b>	-0.333	<i>0.026</i>	0.113	0.017	0.498	<i>-0.678</i>	1			
TC	<b>0.587</b>	0.052	-0.076	0.256	0.165	0.217	0.007	<i>-0.245</i>	0.067	0.146	-0.151	<b>0.817</b>	<i>-0.056</i>	-0.019	0.290	0.419	1		
EC	0.047	<b>0.503</b>	0.124	-0.099	0.498	<i>0.387</i>	0.446	0.018	0.243	<i>0.043</i>	0.396	0.216	<b>0.542</b>	0.045	0.365	-0.196	0.391	1	
OC	0.238	<i>0.097</i>	<b>0.696</b>	0.313	<i>0.325</i>	0.029	<i>0.178</i>	<b>0.530</b>	-0.024	0.478	0.126	<i>0.034</i>	0.138	<i>0.371</i>	0.068	<b>0.686</b>	<i>-0.014</i>	-0.781	1

*In italics, significant values (except diagonal) at the level of significance alpha=0.050 (two-tailed test)*

Values with >0.5 are shown bold

**Table 5.11** Correlation matrix of PAHs and carbonaceous load throughout the study

	Npth	Phtn	Acnp	Acen	Fluo	Anth	Pyrn	Flun	Chrn	BaAn	BbFn	BkFn	BaPn	BghiP	DahA	IcdP	TC	EC	OC
Npth	1																		
Phtn	-0.375	1																	
Acnp	<b>0.649</b>	<b>0.616</b>	1																
Acen	<i>0.205</i>	0.037	<i>0.354</i>	1															
Fluo	0.238	<i>0.343</i>	0.012	-0.046	1														
Anth	-0.059	0.171	-0.357	<i>0.265</i>	0.197	1													
Pyrn	<i>0.376</i>	0.092	<i>0.454</i>	0.184	-0.246	<i>0.250</i>	1												
Flun	<b>0.972</b>	-0.308	0.353	-0.578	0.056	-0.162	-0.276	1											
Chrn	0.433	<i>0.321</i>	0.130	0.315	-0.027	0.337	0.139	0.088	1										
BaAn	0.022	0.053	0.246	0.020	<b>0.654</b>	-0.461	<i>0.242</i>	-0.167	0.172	1									
BbFn	0.270	<b>0.512</b>	-0.300	0.153	0.095	<b>0.797</b>	-0.443	<b>0.653</b>	0.031	-0.025	1								
BkFn	<i>0.368</i>	-0.030	0.065	0.492	0.256	0.174	0.323	0.009	-0.146	<i>0.235</i>	0.239	1							
BaPn	0.065	<b>0.838</b>	0.431	-0.007	0.158	0.241	0.169	-0.188	<b>0.548</b>	0.064	0.345	-0.132	1						
BghiP	<b>0.545</b>	0.217	<i>0.179</i>	0.147	-0.491	-0.100	<b>0.510</b>	-0.217	-0.075	<b>0.654</b>	-0.009	-0.619	0.462	1					
DahA	0.307	<i>0.001</i>	-0.114	0.338	0.164	0.325	<b>0.607</b>	0.139	0.277	-0.374	0.452	<i>0.053</i>	0.023	-0.165	1				
IcdP	-0.526	0.167	0.025	-0.192	<b>0.993</b>	0.135	<i>0.018</i>	0.318	0.029	<i>0.193</i>	-0.096	<b>0.523</b>	-0.506	0.034	0.417	1			
TC	<i>0.035</i>	<b>0.545</b>	<b>0.632</b>	0.318	0.028	-0.460	0.071	<b>0.735</b>	-0.013	-0.145	0.423	-0.063	0.038	0.257	-0.026	<i>0.124</i>	1		
EC	<b>0.678</b>	0.086	<i>0.041</i>	<b>0.653</b>	<i>0.325</i>	0.055	0.326	0.061	<i>0.324</i>	0.399	<i>0.150</i>	0.206	0.017	<b>0.559</b>	<i>0.398</i>	-0.043	-0.219	1	
OC	0.322	0.006	<i>0.451</i>	0.106	<b>0.636</b>	0.131	0.212	<i>0.304</i>	0.057	0.414	<b>0.711</b>	<i>0.139</i>	0.234	-0.489	0.265	0.061	0.315	<i>0.204</i>	1

*In italics, significant values (except diagonal) at the level of significance alpha=0.050 (two-tailed test)*

Values with >0.5 are shown bold

## *Conclusion*

## *Conclusion*

---

The following conclusions can be drawn from the present study:

Total carbons were found highest at the site GBD, whereas it was found lowest at JNU. TC load was found in the order as  $GBD > FBD > CPL > GGN > JNU$ . EC and OC were also found in the following order:  $GBD > FBD > CPL > GGN > JNU$ .

The relative abundances of TC, EC and OC with sites in different seasons showed the following order:  $TC > OC > EC$ . Except monsoon season, all the sites contributed relatively higher amount of carbonaceous load regardless the site. Relative order of abundances of carbon was:  $JNU < GGN < CPL < FBD < GBD$ .

Fine particles possessed higher amount of carbons in comparison to coarse particles. Again, it was also observed that winter registered higher amount of carbonaceous load, whereas monsoon season registered lower contributions.

In case of PAHs, the relative abundances (average concentrations) was observed in the following order:  $GBD > FBD > GGN > CPL > JNU$ . An opposite trend of variation of carbons and PAHs were observed between the sites CPL and GGN. The seasonal variation of PAHs showed that the mean concentration of PAHs was lower in the monsoon season but it was found higher during the winter season.

Higher average concentrations were observed for the compounds namely BaPn, Npth, Phtn Pym, Flun and Chrn throughout the study and they showed the following order of concentration:  $BaPn > Npth > Pym > Phtn > Flun > Chrn$ . The rest of other PAHs contributed relatively lower in concentrations, but it was seen that the compounds Acnp, Fluo and BbFn were equally distributed (in terms of average concentrations) throughout the analyses.

The ring wise distributions of PAHs were observed among all the sites and in all the seasons. Npth (a 2-rings PAH) was found with higher amounts at all the sites and size ranges of particles, for which its average concentration across all the seasons was comparatively higher. In this work, similar to the compound Npth; Phtn (a 3-rings PAH), Pym (a 4-rings PAH) and BaPn (a 5-rings PAHs) had contributed relatively higher amount across the sites and seasons. But, the mean concentrations of the PAHs regarding the 3-rings (such as Phtn, Acnp, Acen, Fluo and



Anth), 4-rings (such as Pyn, Flun, Chr and BaAn), 5-rings (such as BbFn, BkFn and BaPn) and 6-rings (such as BghiP, DahA and IcdP) contributed similar variation of concentrations throughout the sites and seasons.

The concentration of PAHs were found highly distributed in fine mode ( $< 2.5 \mu\text{m}$ ) particles, and relatively lower in the coarse mode ( $> 2.5 \mu\text{m}$ ) particles regardless the site and season. The compound Acen and IcdP were found with lower concentration among all the PAHs at all the sites and in all the seasons throughout the analyses.

Winter had the highest PMs concentration among all the seasons. It was observed that among PMs, fine particles ( $<2.5 \mu\text{m}$ ) found to be more than coarse ( $> 2.5 \mu\text{m}$ ) in all the seasons.

Regression and correlation of PMs with the meteorological parameters (temperature, relative humidity, wind speed and dew point) showed a significant relationship with relative humidity. Again, significant relations were observed between EC vs OC, TC vs EC, OC vs TC and, PAHs vs TC, OC, EC.

Source apportionments of PAHs were carried out by applying the PCA. The average contributions of different sources were in the following order: diesel and gasoline  $>$  diesel, gasoline and coal  $>$  gasoline and wood  $>$  coal and wood. Diagnostic ratio of PAHs and, ratio of carbonaceous species were also applied for source identification of PAHs and carbon. It was revealed that PAHs were emitted mainly from diesel, gasoline, natural gas, coal and biomass burning. Again, from the ratio of OC/EC and TC/EC, it was also concluded that carbonaceous species were emitted from vehicular activities and coal burning.

Health risk assessments of PAHs were also carried out in terms of HQ and ILCR for both children and adults. HQs were quantified for the compounds Npth, Acen, Fluo, Anth, Flun and Pyn. Again, ILCR was observed for the compounds BaAn, Chr, BbFn, BkFn, BaPn, IcdP, DahA and Npth. The corresponding HQ was found highest for Npth in all the seasons. ILCR associated with BaPn and DahA was comparatively higher for both children and adults among the observed PAHs.

Higher carcinogenic risks were also observed to be associated with BaPn and DahA regarding  $< 2.5$  and  $> 2.5 \mu\text{m}$  particle size. It was concluded that the carcinogenicity of PAHs

fell below and within the range of ILCR (i.e.,  $10^{-6}$  to  $10^{-4}$ ). Similar conclusion was also drawn for ILCR between the fine and coarse mode particles.

Pearson's correlation was carried out among PAHs and carbonaceous load. Significant correlations were observed between the PAH compounds and carbonaceous species. This inferred the probability of similar emission sources among the species.

## *References*

## References

---

- Abdel-Shafy, H. I., & Mansour, M. S. (2016). A review on polycyclic aromatic hydrocarbons: source, environmental impact, effect on human health and remediation. *Egyptian Journal of Petroleum*, 25(1), 107-123.
- Abdallah, M. A. E., & Atia, N. N. (2014). Atmospheric concentrations, gaseous–particulate distribution, and carcinogenic potential of polycyclic aromatic hydrocarbons in Assiut, Egypt. *Environmental Science and Pollution Research*, 21(13), 8059-8069.
- Agarwal, T., Khillare, P. S., Shridhar, V., & Ray, S. (2009). Pattern, sources and toxic potential of PAHs in the agricultural soils of Delhi, India. *Journal of Hazardous Materials*, 163(2), 1033-1039.
- Akyüz, M., & Çabuk, H. (2008). Particle-associated polycyclic aromatic hydrocarbons in the atmospheric environment of Zonguldak, Turkey. *Science of the Total Environment*, 405(1), 62-70.
- Akyüz, M., & Çabuk, H. (2009). Meteorological variations of PM<sub>2.5</sub>/PM<sub>10</sub> concentrations and particle-associated polycyclic aromatic hydrocarbons in the atmospheric environment of Zonguldak, Turkey. *Journal of Hazardous Materials*, 170(1), 13-21.
- Albuquerque, M., Coutinho, M., & Borrego, C. (2016). Long-term monitoring and seasonal analysis of polycyclic aromatic hydrocarbons (PAHs) measured over a decade in the ambient air of Porto, Portugal. *Science of the Total Environment*, 543, 439-448.
- Albuquerque, M., Coutinho, M., & Borrego, C. (2016). Long-term monitoring and seasonal analysis of polycyclic aromatic hydrocarbons (PAHs) measured over a decade in the ambient air of Porto, Portugal. *Science of the Total Environment*, 543, 439-448.
- Aldabe, J., Elustondo, D., Parra, A., Foan, L., Simon, V., Santamaría, J. M., & Santamaría, C. (2012). Polycyclic Aromatic Hydrocarbons (PAHs) sampled in aerosol phase at different sites of the Western Pyrenees in Navarra (Spain). *Environmental Engineering & Management Journal (EEMJ)*, 11(6).
- Alves, C. A., Vicente, A. M. P., Gomes, J., Nunes, T., Duarte, M., & Bandowe, B. A. M. (2016). Polycyclic aromatic hydrocarbons (PAHs) and their derivatives (oxygenated-PAHs, nitrated-PAHs and azaarenes) in size-fractionated particles emitted in an urban road tunnel. *Atmospheric Research*, 180, 128-137.
- Amador-Muñoz, O., Villalobos-Pietrini, R., Miranda, J., & Vera-Avila, L. E. (2011). Organic compounds of PM<sub>2.5</sub> in Mexico Valley: spatial and temporal patterns, behavior and sources. *Science of the Total Environment*, 409(8), 1453-1465.
- Anastasopoulos, A. T., Wheeler, A. J., Karman, D., & Kulka, R. H. (2012). Intraurban concentrations, spatial variability and correlation of ambient polycyclic aromatic hydrocarbons (PAH) and PM<sub>2.5</sub>. *Atmospheric Environment*, 59, 272-283.

- Arnott, W. P., Zielinska, B., Rogers, C. F., Sagebiel, J., Park, K., Chow, J., ... & Sarofim, A. (2005). Evaluation of 1047-nm photoacoustic instruments and photoelectric aerosol sensors in source-sampling of black carbon aerosol and particle-bound PAHs from gasoline and diesel powered vehicles. *Environmental Science & Technology*, 39(14), 5398-5406.
- ATSDR, 2005. Toxicology profile for polyaromatic hydrocarbons. ATSDR's Toxicological Profiles on CD-ROM, CRC Press, Boca Raton, FL.
- Augusto, S., Pereira, M. J., Máguas, C., & Branquinho, C. (2013). A step towards the use of biomonitors as estimators of atmospheric PAHs for regulatory purposes. *Chemosphere*, 92(5), 626-632.
- Avino, P., Brocco, D., Lepore, L., & Ventrone, I. (2000). Distribution of elemental carbon (EC) and organic carbon (OC) in the atmospheric aerosol particles of Rome. *Journal of Aerosol Science*, 31, 364-365.
- Bae, M. S., Schauer, J. J., Turner, J. R., & Hopke, P. K. (2009). Seasonal variations of elemental carbon in urban aerosols as measured by two common thermal-optical carbon methods. *Science of the total Environment*, 407(18), 5176-5183
- Barra, R., Quiroz, R., Saez, K., Araneda, A., Urrutia, R., & Popp, P. (2009). Sources of polycyclic aromatic hydrocarbons (PAHs) in sediments of the Biobio River in south central Chile. *Environmental Chemistry Letters*, 7(2), 133-139.
- Baumard, P., Budzinski, H., & Garrigues, P. (1998). Polycyclic aromatic hydrocarbons in sediments and mussels of the western Mediterranean Sea. *Environmental Toxicology and Chemistry*, 17(5), 765-776.
- Behera, S. N., & Sharma, M. (2015). Spatial and seasonal variations of atmospheric particulate carbon fractions and identification of secondary sources at urban sites in North India. *Environmental Science and Pollution Research*, 22(17), 13464-13476.
- Bisht, D. S., Dumka, U. C., Kaskaoutis, D. G., Pipal, A. S., Srivastava, A. K., Soni, V. K., ... & Tiwari, S. (2015). Carbonaceous aerosols and pollutants over Delhi urban environment: Temporal evolution, source apportionment and radiative forcing. *Science of the Total Environment*, 521, 431-445.
- Blanchard, C. L., Chow, J. C., Edgerton, E. S., Watson, J. G., Hidy, G. M., & Shaw, S. (2014). Organic aerosols in the southeastern United States: speciated particulate carbon measurements from the SEARCH network, 2006–2010. *Atmospheric Environment*, 95, 327-333.
- Blomqvist, P., McNamee, M. S., Stec, A. A., Gylestam, D., & Karlsson, D. (2014). Detailed study of distribution patterns of polycyclic aromatic hydrocarbons and isocyanates under different fire conditions. *Fire and Materials*, 38(1), 125-144.
- Boehm, P. D. (2010). 15 Polycyclic Aromatic Hydrocarbons (PAHs). *Environmental forensics: Contaminant specific guide*, 313.

- Bojes, H. K., & Pope, P. G. (2007). Characterization of EPA's 16 priority pollutant polycyclic aromatic hydrocarbons (PAHs) in tank bottom solids and associated contaminated soils at oil exploration and production sites in Texas. *Regulatory Toxicology and Pharmacology*, 47(3), 288-295.
- Booyens, W., Van Zyl, P. G., Beukes, J. P., Ruiz-Jimenez, J., Kopperi, M., Riekkola, M. L., ... & Vakkari, V. (2015). Size-resolved characterisation of organic compounds in atmospheric aerosols collected at Welgegund, South Africa. *Journal of Atmospheric Chemistry*, 72(1), 43-64.
- Bortey-Sam, N., Ikenaka, Y., Akoto, O., Nakayama, S. M., Yohannes, Y. B., Baidoo, E., ... & Ishizuka, M. (2015). Levels, potential sources and human health risk of polycyclic aromatic hydrocarbons (PAHs) in particulate matter (PM<sub>10</sub>) in Kumasi, Ghana. *Environmental Science and Pollution Research*, 22(13), 9658-9667.
- Bourotte, C., Forti, M. C., Taniguchi, S., Bicego, M. C., & Lotufo, P. A. (2005). A wintertime study of PAHs in fine and coarse aerosols in São Paulo city, Brazil. *Atmospheric Environment*, 39(21), 3799-3811.
- Brachtl, M. V., Durant, J. L., Perez, C. P., Oviedo, J., Sempertegui, F., Naumova, E. N., & Griffiths, J. K. (2009). Spatial and temporal variations and mobile source emissions of polycyclic aromatic hydrocarbons in Quito, Ecuador. *Environmental Pollution*, 157(2), 528-536.
- Briggs, D. J., Collins, S., Elliott, P., Fischer, P., Kingham, S., Lebret, E., ... & Van Der Veen, A. (1997). Mapping urban air pollution using GIS: a regression-based approach. *International Journal of Geographical Information Science*, 11(7), 699-718.
- Briggs, D. J., Collins, S., Elliott, P., Fischer, P., Kingham, S., Lebret, E., ... & Van Der Veen, A. (1997). Mapping urban air pollution using GIS: a regression-based approach. *International Journal of Geographical Information Science*, 11(7), 699-718.
- Brook, R. D., Brook, J. R., & Rajagopalan, S. (2003). Air pollution: the "Heart" of the problem. *Current Hypertension Reports*, 5(1), 32-39.
- Budzinski, H., Jones, I., Bellocq, J., Pierard, C., & Garrigues, P. H. (1997). Evaluation of sediment contamination by polycyclic aromatic hydrocarbons in the Gironde estuary. *Marine chemistry*, 58(1-2), 85-97.
- Cachier, H., Bremond, M. P., & Buat-Ménard, P. (1989). Determination of atmospheric soot carbon with a simple thermal method. *Tellus B*, 41(3), 379-390.
- Cai, T., Zhang, Y., Fang, D., Shang, J., Zhang, Y., & Zhang, Y. (2017). Chinese vehicle emissions characteristic testing with small sample size: Results and comparison. *Atmospheric Pollution Research*, 8(1), 154-163.

- Cancio, J. A. L., Castellano, A. V., Martín, S. S., & Rodríguez, J. F. S. (2004). Size distributions of PAHs in ambient air particles of two areas of Las Palmas de Gran Canaria. *Water, Air, and Soil Pollution*, 154(1-4), 127-138.
- Cao, J. J., Lee, S. C., Chow, J. C., Watson, J. G., Ho, K. F., Zhang, R. J., ... & Zou, S. C. (2007). Spatial and seasonal distributions of carbonaceous aerosols over China. *Journal of Geophysical Research: Atmospheres*, 112(D22).
- Cao, J. J., Lee, S. C., Ho, K. F., Zhang, X. Y., Zou, S. C., Fung, K., ... & Watson, J. G. (2003). Characteristics of carbonaceous aerosol in Pearl River Delta Region, China during 2001 winter period. *Atmospheric Environment*, 37(11), 1451-1460.
- Caricchia, A. M., Chiavarini, S., & Pezza, M. (1999). Polycyclic aromatic hydrocarbons in the urban atmospheric particulate matter in the city of Naples (Italy). *Atmospheric Environment*, 33(23), 3731-3738.
- Cetin, B., Ozturk, F., Keles, M., & Yurdakul, S. (2017). PAHs and PCBs in an Eastern Mediterranean megacity, Istanbul: Their spatial and temporal distributions, air-soil exchange and toxicological effects. *Environmental Pollution*, 220, 1322-1332.
- Chakraborty, D., & Mondal, N. K. (2017). Assessment of Health Risk of Children from Traditional Biomass Burning in Rural Households. *Exposure and Health*, 1-12.
- Chang, K. F., Fang, G. C., Chen, J. C., & Wu, Y. S. (2006). Atmospheric polycyclic aromatic hydrocarbons (PAHs) in Asia: a review from 1999 to 2004. *Environmental Pollution*, 142(3), 388-396.
- Chen, S. J., Liao, S. H., Jian, W. J., & Lin, C. C. (1997). Particle size distribution of aerosol carbons in ambient air. *Environment International*, 23(4), 475-488.
- Cheung, K. L., Polidori, A., Ntziachristos, L., Tzamkiozis, T., Samaras, Z., Cassee, F. R., ... & Sioutas, C. (2009). Chemical characteristics and oxidative potential of particulate matter emissions from gasoline, diesel, and biodiesel cars. *Environmental Science & Technology*, 43(16), 6334-6340.
- Chou, C. K., Lee, C. T., Cheng, M. T., Yuan, C. S., Chen, S. J., Wu, Y. L., ... & Liu, S. C. (2010). Seasonal variation and spatial distribution of carbonaceous aerosols in Taiwan. *Atmospheric Chemistry and Physics*, 10(19), 9563-9578.
- Chow, J. C., Watson, J. G., Lowenthal, D. H., Egami, R. T., Solomon, P. A., Thuillier, R. H., ... & Ranzieri, A. (1998). Spatial and temporal variations of particulate precursor gases and photochemical reaction products during SJVAQS/AUSPEX ozone episodes. *Atmospheric Environment*, 32(16), 2835-2844.
- Churg, A., & Brauer, M. (1997). Human lung parenchyma retains PM<sub>2.5</sub>. *American Journal of Respiratory and Critical Care Medicine*, 155(6), 2109-2111.

- Currie, L. A., Klouda, G. A., Benner, B. A., Garrity, K., & Eglinton, T. I. (1999). Isotopic and molecular fractionation in combustion; three routes to molecular marker validation, including direct molecular 'dating' (GC/AMS). *Atmospheric Environment*, 33(17), 2789-2806.
- Dab, W., Medina, S., Quenel, P., Le Moullec, Y., Le Tertre, A., Thelot, B., ... & Ferry, R. (1996). Short term respiratory health effects of ambient air pollution: results of the APHEA project in Paris. *Journal of Epidemiology and Community Health*, 50(Suppl 1), s42-s46.
- Daisey, J. M., Leyko, M. A., & Kneip, T. J. (1979). Source identification and allocation of polynuclear aromatic hydrocarbon compounds in the New York City aerosol: methods and applications. Polynuclear Aromatic Hydrocarbons. *Ann Arbor Science, Ann Arbor*, 201-215.
- Dallarosa, J. B., Teixeira, E. C., Pires, M., & Fachel, J. (2005). Study of the profile of polycyclic aromatic hydrocarbons in atmospheric particles (PM<sub>10</sub>) using multivariate methods. *Atmospheric Environment*, 39(35), 6587-6596.
- Dan, M., Zhuang, G., Li, X., Tao, H., & Zhuang, Y. (2004). The characteristics of carbonaceous species and their sources in PM<sub>2.5</sub> in Beijing. *Atmospheric Environment*, 38(21), 3443-3452.
- Daso, A. P., Akortia, E., & Okonkwo, J. O. (2016). Concentration profiles, source apportionment and risk assessment of polycyclic aromatic hydrocarbons (PAHs) in dumpsite soils from Agbogbloshie e-waste dismantling site, Accra, Ghana. *Environmental Science and Pollution Research*, 23(11), 10883-10894.
- De la Campa, A. S., Pio, C., De la Rosa, J. D., Querol, X., Alastuey, A., & González-Castanedo, Y. (2009). Characterization and origin of EC and OC particulate matter near the Doñana National Park (SW Spain). *Environmental Research*, 109(6), 671-681.
- Del Vento, S., & Dachs, J. (2007). Influence of the surface microlayer on atmospheric deposition of aerosols and polycyclic aromatic hydrocarbons. *Atmospheric Environment*, 41(23), 4920-4930.
- Delfino, R. J., Staimer, N., Tjoa, T., Arhami, M., Polidori, A., Gillen, D. L., ... & Sioutas, C. (2010). Association of biomarkers of systemic inflammation with organic components and source tracers in quasi-ultrafine particles. *Environmental Health Perspectives*, 118(6), 756-762.
- Demircioglu, E., Sofuoglu, A., & Odabasi, M. (2011). Particle-phase dry deposition and air-soil gas exchange of polycyclic aromatic hydrocarbons (PAHs) in Izmir, Turkey. *Journal of Hazardous Materials*, 186(1), 328-335.
- Denby, B., Horálek, J., Walker, S. E., Eben, K., & Fiala, J. (2005). Interpolation and assimilation methods for European scale air quality assessment and mapping. *Part I: Review and Recommendations. European Topic Centre on Air and Climate Change Technical Paper*, 7.



- Di Vaio, P., Coccoziello, B., Corvino, A., Fiorino, F., Frecentese, F., Magli, E., ... & Severino, B. (2016). Level, potential sources of polycyclic aromatic hydrocarbons (PAHs) in particulate matter (PM<sub>10</sub>) in Naples. *Atmospheric Environment*, *129*, 186-196.
- Dickhut, R. M., Canuel, E. A., Gustafson, K. E., Liu, K., Arzayus, K. M., Walker, S. E., . . . & MacDonald, E. H. (2000). Automotive sources of carcinogenic polycyclic aromatic hydrocarbons associated with particulate matter in the Chesapeake Bay region. *Environmental Science & Technology*, *34*(21), 4635–4640.
- Didyk, B. M., Simoneit, B. R., Pezoa, L. A., Riveros, M. L., & Flores, A. A. (2000). Urban aerosol particles of Santiago, Chile:: organic content and molecular characterization. *Atmospheric Environment*, *34*(8), 1167-1179.
- Ding, L. C., Ke, F., Wang, D. K., Dann, T., & Austin, C. C. (2009). A new direct thermal desorption-GC/MS method: Organic speciation of ambient particulate matter collected in Golden, BC. *Atmospheric Environment*, *43*(32), 4894-4902.
- Duan, F. K., He, K. B., Ma, Y. L., Yang, F. M., Yu, X. C., Cadle, S. H., ... & Mulawa, P. A. (2006). Concentration and chemical characteristics of PM<sub>2.5</sub> in Beijing, China: 2001–2002. *Science of the Total Environment*, *355*(1), 264-275.
- Duan, F., Liu, X., Yu, T., & Cachier, H. (2004). Identification and estimate of biomass burning contribution to the urban aerosol organic carbon concentrations in Beijing. *Atmospheric Environment*, *38*(9), 1275-1282.
- Duan, J., Tan, J., Wang, S., Chai, F., He, K., & Hao, J. (2012). Roadside, Urban, and Rural comparison of size distribution characteristics of PAHs and carbonaceous components of Beijing, China. *Journal of Atmospheric Chemistry*, *69*(4), 337-349.
- Dubey, J., Kumari, K. M., & Lakhani, A. (2015). Chemical characteristics and mutagenic activity of PM<sub>2.5</sub> at a site in the Indo-Gangetic plain, India. *Ecotoxicology and Environmental Safety*, *114*, 75-83.
- Duval, M. M., & Friedlander, S. K. (1981). Source resolution of polycyclic aromatic hydrocarbons in the Los Angeles atmosphere application of a CMB with first-order decay. *United States Environmental Protection Agency, Washington, DC*.
- El-Mubarak, A. H., Rushdi, A. I., Al-Mutlaq, K. F., Bazeyad, A. Y., Simonich, S. L., & Simoneit, B. R. (2014). Identification and source apportionment of polycyclic aromatic hydrocarbons in ambient air particulate matter of Riyadh, Saudi Arabia. *Environmental Science and Pollution Research*, *21*(1), 558-567.
- Fan, Z. L., Chen, X. C., Lui, K. H., Ho, S. S. H., Cao, J. J., Lee, S. C., ... & Ho, K. F. (2017). Relationships between Outdoor and Personal Exposure of Carbonaceous Species and Polycyclic

- Aromatic Hydrocarbons (PAHs) in Fine Particulate Matter (PM<sub>2.5</sub>) at Hong Kong. *Aerosol and Air Quality Research*, 17(3), 666-679.
- Fang, G. C., Chang, C. N., Wu, Y. S., Fu, P. P. C., Yang, I. L., & Chen, M. H. (2004). Characterization, identification of ambient air and road dust polycyclic aromatic hydrocarbons in central Taiwan, Taichung. *Science of the Total Environment*, 327(1), 135-146.
- Fang, G. C., Wu, Y. S., Chen, J. C., Chang, C. N., & Ho, T. T. (2006). Characteristic of polycyclic aromatic hydrocarbon concentrations and source identification for fine and coarse particulates at Taichung Harbor near Taiwan Strait during 2004–2005. *Science of the Total Environment*, 366(2), 729-738.
- Fang, M. D., Lee, C. L., Jiang, J. J., Ko, F. C., & Baker, J. E. (2012). Diffusive exchange of PAHs across the air–water interface of the Kaohsiung Harbor lagoon, Taiwan. *Journal of Environmental Management*, 110, 179-187.
- Filzmoser, P., Hron, K., & Reimann, C. (2009). Principal component analysis for compositional data with outliers. *Environmetrics*, 20(6), 621-632.
- Finardi, S., Radice, P., Cecinato, A., Gariazzo, C., Gherardi, M., & Romagnoli, P. (2015). Seasonal variation of PAHs concentration and source attribution through diagnostic ratios analysis. *Urban Climate*.
- Fine, P. M., Cass, G. R., & Simoneit, B. R. (2002). Chemical characterization of fine particle emissions from the fireplace combustion of woods grown in the southern United States. *Environmental Science & Technology*, 36(7), 1442-1451.
- Fon, T. Y. W., Noriatsu, O., & Hiroshi, S. (2007). Polycyclic aromatic hydrocarbons (PAHs) in the aerosol of Higashi Hiroshima, Japan: pollution scenario and source identification. *Water, Air, and Soil Pollution*, 182(1-4), 235-243.
- Fountoukis, C., Butler, T., Lawrence, M. G., van der Gon, H. D., Visschedijk, A. J. H., Charalampidis, P., ... & Pandis, S. N. (2014). Impacts of controlling biomass burning emissions on wintertime carbonaceous aerosol in Europe. *Atmospheric Environment*, 87, 175-182.
- Fraser, M. P., Lakshmanan, K., Fritz, S. G., & Ubanwa, B. (2002). Variation in composition of fine particulate emissions from heavy-duty diesel vehicles. *Journal of Geophysical Research: Atmospheres*, 107(D21).
- Fromme, H., Oddoy, A., Piloty, M., Krause, M., & Lahrz, T. (1998). Polycyclic aromatic hydrocarbons (PAH) and diesel engine emission (elemental carbon) inside a car and a subway train. *Science of the Total Environment*, 217(1), 165-173.
- Gabriel, K. R. (1971). The biplot graphic display of matrices with application to principal component analysis. *Biometrika*, 453-467.

- Galarneau, E. (2008). Source specificity and atmospheric processing of airborne PAHs: Implications for source apportionment. *Atmospheric Environment*, 42 (35), 8139–8149.
- Gargava, P., & Rajagopalan, V. (2015). Source apportionment studies in six Indian cities—drawing broad inferences for urban PM<sub>10</sub> reductions. *Air Quality, Atmosphere & Health*. DOI 10.1007/s11869-015-0353-4.
- Gatari, M. J., & Boman, J. (2003). Black carbon and total carbon measurements at urban and rural sites in Kenya, East Africa. *Atmospheric Environment*, 37(8), 1149-1154.
- Gelencsér, A. (2005). *Carbonaceous aerosol* (Vol. 30). Springer Science & Business Media.
- Geng, H., Jung, H. J., Park, Y., Hwang, H., Kim, H., Kim, Y. J., ... & Ro, C. U. (2009a). Morphological and chemical composition characteristics of summertime atmospheric particles collected at Tokchok Island, Korea. *Atmospheric Environment*, 43(21), 3364-3373.
- Geng, H., Park, Y., Hwang, H., Kang, S., & Ro, C. U. (2009b). Elevated nitrogen-containing particles observed in Asian dust aerosol samples collected at the marine boundary layer of the Bohai Sea and the Yellow Sea. *Atmospheric Chemistry and Physics*, 9(18), 6933-6947.
- Gnauk, T., Müller, K., van Pinxteren, D., He, L. Y., Niu, Y., Hu, M., & Herrmann, H. (2008). Size-segregated particulate chemical composition in Xinken, Pearl River Delta, China: OC/EC and organic compounds. *Atmospheric Environment*, 42(25), 6296-6309.
- Godec, R., Čačković, M., Šega, K., & Bešlić, I. (2012). Winter mass concentrations of carbon species in PM<sub>10</sub>, PM<sub>2.5</sub> and PM<sub>1</sub> in zagreb air, Croatia. *Bulletin of Environmental Contamination and Toxicology*, 89(5), 1087-1090.
- Golobočanin, D. D., Škrbić, B. D., & Miljević, N. R. (2004). Principal component analysis for soil contamination with PAHs. *Chemometrics and Intelligent Laboratory Systems*, 72(2), 219-223.
- Gonçalves, C., Evtugina, M., Alves, C., Monteiro, C., Pio, C., & Tomé, M. (2011). Organic particulate emissions from field burning of garden and agriculture residues. *Atmospheric Research*, 101(3), 666-680.
- Gonçalves, C., Evtugina, M., Alves, C., Monteiro, C., Pio, C., & Tomé, M. (2011). Organic particulate emissions from field burning of garden and agriculture residues. *Atmospheric Research*, 101(3), 666-680.
- Guo, H., Lee, S. C., Ho, K. F., Wang, X. M., & Zou, S. C. (2003). Particle-associated polycyclic aromatic hydrocarbons in urban air of Hong Kong. *Atmospheric Environment*, 37(38), 5307-5317.
- Gupta, A. K., Nag, S.,p & Mukhopadhyay, U. K. (2006). Characterisation of PM<sub>10</sub>, PM<sub>2.5</sub> and benzene soluble organic fraction of particulate matter in an urban area of Kolkata, India. *Environmental Monitoring and Assessment*, 115(1), 205-222.

- Gurjar, B. R., Jain, A., Sharma, A., Agarwal, A., Gupta, P., Nagpure, A. S., & Lelieveld, J. (2010). Human health risks in megacities due to air pollution. *Atmospheric Environment*, 44(36), 4606-4613.
- Halsall, C. J., Coleman, P. J., Davis, B. J., Burnett, V., Waterhouse, K. S., Harding-Jones, P., & Jones, K. C. (1994). Polycyclic aromatic hydrocarbons in UK urban air. *Environmental Science & Technology*, 28(13), 2380-2386.
- Han, B., Bai, Z., Guo, G., Wang, F., Li, F., Liu, Q., ... & Hu, Y. (2009). Characterization of PM<sub>10</sub> fraction of road dust for polycyclic aromatic hydrocarbons (PAHs) from Anshan, China. *Journal of Hazardous Materials*, 170(2), 934-940.
- Han, B., Ding, X., Bai, Z., Kong, S., & Guo, G. (2011). Source analysis of particulate matter associated polycyclic aromatic hydrocarbons (PAHs) in an industrial city in northeastern China. *Journal of Environmental Monitoring*, 13(9), 2597-2604.
- Han, Y., Cao, J., Chow, J. C., Watson, J. G., An, Z., Jin, Z., ... & Liu, S. (2007). Evaluation of the thermal/optical reflectance method for discrimination between char-and soot-EC. *Chemosphere*, 69(4), 569-574.
- Harrison, R. M. & Yin, J. (2000). Particulate matter in the atmosphere: which particle properties are important for its effects on health? *The Science of the Total Environment* 249 (2000) 85-101.
- Harvey, R. G. (1991). *Polycyclic aromatic hydrocarbons: chemistry and carcinogenicity*. CUP Archive.
- Hasheminassab, S., Daher, N., Schauer, J. J. & Sioutas, C. (2013). Source apportionment and organic compound characterization of ambient ultrafine particulate matter (PM) in the Los Angeles Basin. *Atmospheric Environment*, 79, 529-539.
- Hassanvand, M. S., Naddafi, K., Faridi, S., Nabizadeh, R., Sowlat, M. H., Momeniha, F., ... & Niazi, S. (2015). Characterization of PAHs and metals in indoor/outdoor PM<sub>10</sub>/PM<sub>2.5</sub>/PM<sub>1</sub> in a retirement home and a school dormitory. *Science of the Total Environment*, 527, 100-110.
- Hassine, S. B., Hammami, B., Ameer, W. B., El Megdiche, Y., Barhoumi, B., & Driss, M. R. (2014). Particulate polycyclic aromatic hydrocarbons (PAH) in the atmosphere of Bizerte City, Tunisia. *Bulletin of Environmental Contamination and Toxicology*, 93(3), 375-382.
- Hazarika, N., & Srivastava, A. (2017). Estimation of risk factor of elements and PAHs in size-differentiated particles in the National Capital Region of India. *Air Quality, Atmosphere & Health*, 10(4), 469-482.
- Hazarika, N., Jain, V. K., Srivastava, A. (2015). Source identification and metallic profiles of size-segregated particulate matters at various sites in Delhi. *Environmental Monitoring and Assessment*, (2015) 187:602. DOI 10.1007/s10661-015-4809-7.

- Hazarika, N., Srivastava, A., & Das, A. (2017). Quantification of particle bound metallic load and PAHs in urban environment of Delhi, India: Source and toxicity assessment. *Sustainable Cities and Society*, 29, 58-67.
- He, M., Zheng, J., Yin, S., & Zhang, Y. (2011). Trends, temporal and spatial characteristics, and uncertainties in biomass burning emissions in the Pearl River Delta, China. *Atmospheric Environment*, 45(24), 4051-4059.
- Heal, M. R. (2014). The application of carbon-14 analyses to the source apportionment of atmospheric carbonaceous particulate matter: a review. *Analytical and Bioanalytical Chemistry*, 406(1), 81-98.
- Herngren, L., Goonetilleke, A., Ayoko, G. A., & Mostert, M. M. (2010). Distribution of polycyclic aromatic hydrocarbons in urban stormwater in Queensland, Australia. *Environmental Pollution*, 158(9), 2848-2856.
- Hitzenberger, R., Ctyroky, P., Berner, A., Turšič, J., Podkrajšek, B., & Grgić, I. (2006). Size distribution of black (BC) and total carbon (TC) in Vienna and Ljubljana. *Chemosphere*, 65(11), 2106-2113.
- Ho, K. F., Cao, J. J., Harrison, R. M., Lee, S. C., & Bau, K. K. (2004). Indoor/outdoor relationships of organic carbon (OC) and elemental carbon (EC) in PM<sub>2.5</sub> in roadside environment of Hong Kong. *Atmospheric Environment*, 38(37), 6327-6335.
- Ho, K. F., Lee, S. C., Jimmy, C. Y., Zou, S. C., & Fung, K. (2002). Carbonaceous characteristics of atmospheric particulate matter in Hong Kong. *Science of the Total Environment*, 300(1), 59-67.
- Hoek, G., Beelen, R., De Hoogh, K., Vienneau, D., Gulliver, J., Fischer, P., & Briggs, D. (2008). A review of land-use regression models to assess spatial variation of outdoor air pollution. *Atmospheric Environment*, 42(33), 7561-7578.
- Hong, H., Yin, H., Wang, X., & Ye, C. (2007). Seasonal variation of PM<sub>10</sub>-bound PAHs in the atmosphere of Xiamen, China. *Atmospheric Research*, 85(3), 429-441.
- Hoseini, M., Yunesian, M., Nabizadeh, R., Yaghmaeian, K., Ahmadkhaniha, R., Rastkari, N., ... & Naddafi, K. (2016). Characterization and risk assessment of polycyclic aromatic hydrocarbons (PAHs) in urban atmospheric Particulate of Tehran, Iran. *Environmental Science and Pollution Research*, 23(2), 1820-1832.
- Hu, J., Liu, C. Q., Zhang, G. P., & Zhang, Y. L. (2012). Seasonal variation and source apportionment of PAHs in TSP in the atmosphere of Guiyang, Southwest China. *Atmospheric Research*, 118, 271-279.
- Hu, Y., Wang, Y., Wang, Z. S., Wang, D. Z., & Li, Y. (2013). Hierarchical Clustering Assisted Human Health Risk Assessment of PAHs in a Typical Oilfield, China. In *Applied Mechanics and Materials* (Vol. 316, pp. 501-504). Trans Tech Publications.

- Huang, H., Ho, K. F., Lee, S. C., Tsang, P. K., Ho, S. S. H., Zou, C. W., ... & Xu, H. M. (2012). Characteristics of carbonaceous aerosol in PM<sub>2.5</sub>: Pearl Delta River region, China. *Atmospheric Research*, *104*, 227-236.
- Huang, L., & Wang, G. (2014). Chemical characteristics and source apportionment of atmospheric particles during heating period in Harbin, China. *Journal of Environmental Sciences*, *26*(12), 2475-2483.
- Huang, X. F., Xue, L., Tian, X. D., Shao, W. W., Sun, T. L., Gong, Z. H., ... & He, L. Y. (2013). Highly time-resolved carbonaceous aerosol characterization in Yangtze River Delta of China: composition, mixing state and secondary formation. *Atmospheric Environment*, *64*, 200-207.
- Huboyo, H. S., Tohno, S., & Cao, R. (2011). Indoor PM<sub>2.5</sub> characteristics and CO concentration related to water-based and oil-based cooking emissions using a gas stove. *Aerosol and Air Quality Research*, *11*(4), 401-411.
- Hussain, K., Rahman, M., Prakash, A., & Hoque, R. R. (2015). Street dust bound PAHs, carbon and heavy metals in Guwahati city—seasonality, toxicity and sources. *Sustainable Cities and Society*, *19*, 17–25.
- IARC (2013): Outdoor air pollution a leading environmental cause of cancer deaths.
- IARC Monographs on the evaluation of carcinogenic risks to humans, Volume 109 (2016).
- IARC Some non-heterocyclic polycyclic aromatic hydrocarbons and some related exposures. Volume 92 (2010)
- Ielpo, P., Fermo, P., Comite, V., Mastroianni, D., Viviano, G., Salerno, F., & Tartari, G. (2016). Chemical characterization of biomass fuel particulate deposits and ashes in households of Mt. Everest region (NEPAL). *Science of the Total Environment*, *573*, 751-759.
- Inomata, Y., Kajino, M., Sato, K., Ohara, T., Kurokawa, J. I., Ueda, H., ... & Akimoto, H. (2013). Source contribution analysis of surface particulate polycyclic aromatic hydrocarbon concentrations in northeastern Asia by source–receptor relationships. *Environmental Pollution*, *182*, 324-334.
- Jaiprakash., Habib, G., (2017). Chemical and optical properties of PM<sub>2.5</sub> from on-road operation of light duty vehicles in Delhi city. *Science of the Total Environment*, *586*, 900-916.
- Jamhari, A. A., Sahani, M., Latif, M. T., Chan, K. M., Tan, H. S., Khan, M. F., & Tahir, N. M. (2014). Concentration and source identification of polycyclic aromatic hydrocarbons (PAHs) in PM<sub>10</sub> of urban, industrial and semi-urban areas in Malaysia. *Atmospheric Environment*, *86*, 16-27.
- Jeng, H. A. (2010). Chemical composition of ambient particulate matter and redox activity. *Environmental Monitoring and Assessment*, *169*(1-4), 597-606.

- Jerrett, M., Arain, A., Kanaroglou, P., Beckerman, B., Potoglou, D., Sahuvaroglu, T., ... & Giovis, C. (2005). A review and evaluation of intraurban air pollution exposure models. *Journal of Exposure Science and Environmental Epidemiology*, 15(2), 185-204.
- Ji, D., Zhang, J., He, J., Wang, X., Pang, B., Liu, Z., ... & Wang, Y. (2016). Characteristics of atmospheric organic and elemental carbon aerosols in urban Beijing, China. *Atmospheric Environment*, 125, 293-306.
- Jimoda, L.A (2012). Effects of particulate matter on human health, the ecosystem, climate and materials: A Review. Series: Working and Living Environmental Protection Vol. 9, No 1, 2012, pp. 27 – 44.
- Jin, T., Lu, K., Liu, S., Zhao, S., Qu, L., & Xu, X. (2017). Chemical Characteristics of Particulate Matter Emission from a Heavy-Duty Diesel Engine Using ETC Cycle Dynamometer Test. *Aerosol and Air Quality Research*, 17(2), 406-411.
- Jin, T., Qu, L., Liu, S., Gao, J., Wang, J., Wang, F., ... & Xu, X. (2014). Chemical characteristics of particulate matter emitted from a heavy duty diesel engine and correlation among inorganic and PAH components. *Fuel*, 116, 655-661.
- Jones, G. S., Jones, A., Roberts, D. L., Stott, P. A., & Williams, K. D. (2005). Sensitivity of global-scale climate change attribution results to inclusion of fossil fuel black carbon aerosol. *Geophysical Research Letters*, 32(14).
- Kam, W., Liacos, J. W., Schauer, J. J., Delfino, R. J., & Sioutas, C. (2012). Size-segregated composition of particulate matter (PM) in major roadways and surface streets. *Atmospheric Environment*, 55, 90-97.
- Kameda, Y., Shirai, J., Komai, T., Nakanishi, J., & Masunaga, S. (2005). Atmospheric polycyclic aromatic hydrocarbons: size distribution, estimation of their risk and their depositions to the human respiratory tract. *Science of the Total Environment*, 340(1), 71-80.
- Kang, F., Mao, X., Wang, X., Wang, J., Yang, B., & Gao, Y. (2017). Sources and health risks of polycyclic aromatic hydrocarbons during haze days in eastern China: A 1-year case study in Nanjing City. *Ecotoxicology and Environmental Safety*, 140, 76-83.
- Karar, K., & Gupta, A. K. (2007). Source apportionment of PM<sub>10</sub> at residential and industrial sites of an urban region of Kolkata, India. *Atmospheric Research*, 84(1), 30-41.
- Kaupp, H., & McLachlan, M. S. (2000). Distribution of polychlorinated dibenzo-P-dioxins and dibenzofurans (PCDD/Fs) and polycyclic aromatic hydrocarbons (PAHs) within the full size range of atmospheric particles. *Atmospheric Environment*, 34(1), 73-83.
- Kaur, S., Senthilkumar, K., Verma, V. K., Kumar, B., Kumar, S., Katnoria, J. K., & Sharma, C. S. (2013). Preliminary analysis of polycyclic aromatic hydrocarbons in air particles (PM<sub>10</sub>) in Amritsar,

- India: sources, apportionment, and possible risk implications to humans. *Archives of Environmental Contamination and Toxicology*, 65(3), 382-395.
- Kavouras, I. G., Koutrakis, P., Tsapakis, M., Lagoudaki, E., Stephanou, E. G., Von Baer, D., & Oyola, P. (2001). Source apportionment of urban particulate aliphatic and polynuclear aromatic hydrocarbons (PAHs) using multivariate methods. *Environmental Science & Technology*, 35(11), 2288–2294.
- Ke, C. L., Gu, Y. G., & Liu, Q. (2017). Polycyclic Aromatic Hydrocarbons (PAHs) in Exposed-Lawn Soils from 28 Urban Parks in the Megacity Guangzhou: Occurrence, Sources, and Human Health Implications. *Archives of Environmental Contamination and Toxicology*, 72(4), 496-504.
- Ke, L., Ding, X., Tanner, R. L., Schauer, J. J., & Zheng, M. (2007). Source contributions to carbonaceous aerosols in the Tennessee Valley Region. *Atmospheric Environment*, 41(39), 8898-8923.
- Kempton, R. A. (1984). The use of biplots in interpreting variety by environment interactions. *The Journal of Agricultural Science*, 103(01), 123-135.
- Khalili, N. R., Scheff, P. A., & Holsen, T. M. (1995). PAH source fingerprints for coke ovens, diesel and gasoline engines, highway tunnels, and wood combustion emissions. *Atmospheric Environment*, 29(4), 533-542.
- Kim, B. M., Lee, S. B., Kim, J. Y., Kim, S., Seo, J., Bae, G. N., & Lee, J. Y. (2016). A multivariate receptor modeling study of air-borne particulate PAHs: Regional contributions in a roadside environment. *Chemosphere*, 144, 1270-1279.
- Kim, K. H., Jahan, S. A., Kabir, E., & Brown, R. J. (2013). A review of airborne polycyclic aromatic hydrocarbons (PAHs) and their human health effects. *Environment International*, 60, 71-80.
- Koerber, R., Bayona, J. M., & Niessner, R. (1999). Determination of benzo [a] pyrene diones in air particulate matter with liquid chromatography mass spectrometry. *Environmental Science & Technology*, 33(10), 1552-1558.
- Kong, S., Ding, X., Bai, Z., Han, B., Chen, L., Shi, J., & Li, Z. (2010). A seasonal study of polycyclic aromatic hydrocarbons in PM<sub>2.5</sub> and PM<sub>2.5-10</sub> in five typical cities of Liaoning Province, China. *Journal of Hazardous Materials*, 183(1), 70-80.
- Kourtchev, I., Ruuskanen, T., Maenhaut, W., Kulmala, M., & Claeys, M. (2005). Observation of 2-methyltetrols and related photo-oxidation products of isoprene in boreal forest aerosols from Hyttiälä, Finland. *Atmospheric Chemistry and Physics*, 5(10), 2761-2770.
- Křůmal, K., Mikuška, P., & Večeřa, Z. (2015). Monosaccharide anhydrides, monocarboxylic acids and OC/EC in PM<sub>1</sub> aerosols in urban areas in the Czech Republic. *Atmospheric Pollution Research*, 6(6), 917-927.



- Kulkarni, P., & Venkataraman, C. (2000). Atmospheric polycyclic aromatic hydrocarbons in Mumbai, India. *Atmospheric Environment*, 34(17), 2785-2790.
- Kumar, A., & Deshmukh, S. U. (2010). Elemental and Organic Carbon in Ambient Air of a Major Indian Urban Community. *Bulletin of Environmental Contamination and Toxicology*, 84(3), 319-321.
- Kumar, P., Gulia, S., Harrison, R. M., & Khare, M. (2017b). The influence of odd–even car trial on fine and coarse particles in Delhi. *Environmental Pollution*, 225, 20-30.
- Kumar, S., Aggarwal, S. G., Fu, P. Q., Kang, M., Sarangi, B., Sinha, D., & Kotnala, R. K. (2017a). Size-segregated sugar composition of transported dust aerosols from Middle-East over Delhi during March 2012. *Atmospheric Research*, 189, 24-32.
- Laden, F., Neas, L. M., Dockery, D. W., & Schwartz, J. (2000). Association of fine particulate matter from different sources with daily mortality in six US cities. *Environmental Health Perspectives*, 108(10), 941.
- Lai, I. C., Chang, Y. C., Lee, C. L., Chiou, G. Y., & Huang, H. C. (2013). Source identification and characterization of atmospheric polycyclic aromatic hydrocarbons along the southwestern coastal area of Taiwan—with a GMDH approach. *Journal of Environmental Management*, 115, 60-68.
- Lavanchy, V. M. H., Gäggeler, H. W., Nyeki, S., & Baltensperger, U. (1999). Elemental carbon (EC) and black carbon (BC) measurements with a thermal method and an aethalometer at the high-alpine research station Jungfraujoch. *Atmospheric Environment*, 33(17), 2759-2769
- Lee, B. K., & Lee, C. H. (2008). Analysis of acidic components, heavy metals and PAHS of particulate in the Changwon–Masan area of Korea. *Environmental Monitoring and Assessment*, 136(1-3), 21-33.
- Lee, C. L., Huang, H. C., Wang, C. C., Sheu, C. C., Wu, C. C., Leung, S. Y., ... & Jiang, H. (2016). A new grid-scale model simulating the spatiotemporal distribution of PM<sub>2.5</sub>-PAHs for exposure assessment. *Journal of Hazardous Materials*, 314, 286-294.
- Legendre, P., & Gallagher, E. D. (2001). Ecologically meaningful transformations for ordination of species data. *Oecologia*, 129(2), 271-280.
- Lewandowska, A., Falkowska, L., Murawiec, D., Pryputniewicz, D., Burska, D., & Beldowska, M. (2010). Elemental and organic carbon in aerosols over urbanized coastal region (southern Baltic Sea, Gdynia). *Science of the Total Environment*, 408(20), 4761-4769.
- Li, J., Wang, G., Aggarwal, S. G., Huang, Y., Ren, Y., Zhou, B., ... & Zhang, R. (2014 a). Comparison of abundances, compositions and sources of elements, inorganic ions and organic compounds in atmospheric aerosols from Xi'an and New Delhi, two megacities in China and India. *Science of the Total Environment*, 476, 485-495.

- Li, J., Zhang, G., Li, X. D., Qi, S. H., Liu, G. Q., & Peng, X. Z. (2006a). Source seasonality of polycyclic aromatic hydrocarbons (PAHs) in a subtropical city, Guangzhou, South China. *Science of the Total Environment*, 355(1), 145-155.
- Li, R. J., Kou, X. J., Geng, H., Dong, C., & Cai, Z. W. (2014 b). Pollution characteristics of ambient PM<sub>2.5</sub>-bound PAHs and NPAHs in a typical winter time period in Taiyuan. *Chinese Chemical Letters*, 25(5), 663-666.
- Li, X. H., Liu, X. F., Shan, F. U., Cheng, H. X., & Xu, X. B. (2006b). Polycyclic aromatic hydrocarbon in urban soil from Beijing, China. *Journal of Environmental Sciences*, 18(5), 944-950.
- Li, X., Kong, S., Yin, Y., Li, L., Yuan, L., Li, Q., ... & Chen, K. (2016a). Polycyclic aromatic hydrocarbons (PAHs) in atmospheric PM<sub>2.5</sub> around 2013 Asian Youth Games period in Nanjing. *Atmospheric Research*, 174, 85-96.
- Li, X., Wang, S., Duan, L., Hao, J., Li, C., Chen, Y., & Yang, L. (2007). Particulate and trace gas emissions from open burning of wheat straw and corn stover in China. *Environmental Science & Technology*, 41(17), 6052-6058.
- Li, Y., Cao, J., Li, J., Zhou, J., Xu, H., Zhang, R., & Ouyang, Z. (2013). Molecular distribution and seasonal variation of hydrocarbons in PM<sub>2.5</sub> from Beijing during 2006. *Particuology*, 11(1), 78-85.
- Li, Y., Liu, J., Cao, Z., Lin, C., & Yang, Z. (2010). Spatial distribution and health risk of heavy metals and polycyclic aromatic hydrocarbons (PAHs) in the water of the Luanhe River Basin, China. *Environmental Monitoring and Assessment*, 163(1), 1-13.
- Li, Y., Liu, X., Liu, M., Li, X., Meng, F., Wang, J., ... & Qin, Y. (2016b). Investigation into atmospheric PM<sub>2.5</sub>-borne PAHs in Eastern cities of China: concentration, source diagnosis and health risk assessment. *Environmental Science: Processes & Impacts*, 18(5), 529-537.
- Li, Z., Sjodin, A., Porter, E. N., Patterson, D. G., Needham, L. L., Lee, S., ... & Mulholland, J. A. (2009). Characterization of PM<sub>2.5</sub>-bound polycyclic aromatic hydrocarbons in Atlanta. *Atmospheric Environment*, 43(5), 1043-1050.
- Liaud, C., Dintzer, T., Tschamber, V., Trouve, G., & Le Calvé, S. (2014). Particle-bound PAHs quantification using a 3-stages cascade impactor in French indoor environments. *Environmental Pollution*, 195, 64-72.
- Liaud, C., Millet, M., & Le Calvé, S. (2015). An analytical method coupling accelerated solvent extraction and HPLC-fluorescence for the quantification of particle-bound PAHs in indoor air sampled with a 3-stages cascade impactor. *Talanta*, 131, 386-394.
- Lima, A. L. C., Farrington, J. W., & Reddy, C. M. (2005). Combustion-derived polycyclic aromatic hydrocarbons in the environment—a review. *Environmental Forensics*, 6(2), 109-131.

- Lin, C. C., Chen, S. J., Huang, K. L., Hwang, W. I., Chang-Chien, G. P., & Lin, W. Y. (2005). Characteristics of metals in nano/ultrafine/fine/coarse particles collected beside a heavily trafficked road. *Environmental Science & Technology*, 39(21), 8113-8122.
- Lin, J. J. (2002). Characterization of the major chemical species in PM<sub>2.5</sub> in the Kaohsiung City, Taiwan. *Atmospheric Environment*, 36(12), 1911-1920.
- Lin, J. J., & Tai, H. S. (2001). Concentrations and distributions of carbonaceous species in ambient particles in Kaohsiung City, Taiwan. *Atmospheric Environment*, 35(15), 2627-2636.
- Lin, N., Chen, Y., Du, W., Shen, G., Zhu, X., Huang, T., ... & Liu, G. (2016). Inhalation exposure and risk of polycyclic aromatic hydrocarbons (PAHs) among the rural population adopting wood gasifier stoves compared to different fuel-stove users. *Atmospheric Environment*, 147, 485-491.
- Liu, A., Duodu, G. O., Mummullage, S., Ayoko, G. A., & Goonetilleke, A. (2017). Hierarchy of factors which influence polycyclic aromatic hydrocarbons (PAHs) distribution in river sediments. *Environmental Pollution*, 223, 81-89.
- Liu, D., Xu, Y., Chaemfa, C., Tian, C., Li, J., Luo, C., & Zhang, G. (2014). Concentrations, seasonal variations, and outflow of atmospheric polycyclic aromatic hydrocarbons (PAHs) at Ningbo site, Eastern China. *Atmospheric Pollution Research*, 5(2), 203-209.
- Liu, G., Bi, R., Wang, S., Li, F., & Guo, G. (2013). The use of spatial autocorrelation analysis to identify PAHs pollution hotspots at an industrially contaminated site. *Environmental Monitoring and Assessment*, 185(11), 9549-9558.
- Liu, Y., Wang, S., Lohmann, R., Yu, N., Zhang, C., Gao, Y., ... & Ma, L. (2015). Source apportionment of gaseous and particulate PAHs from traffic emission using tunnel measurements in Shanghai, China. *Atmospheric Environment*, 107, 129-136.
- Liu, Y., Zhu, L., & Shen, X. (2001). Polycyclic aromatic hydrocarbons (PAHs) in indoor and outdoor air of Hangzhou, China. *Environmental Science & Technology*, 35(5), 840-844.
- Lu, T., Huang, Z., Cheung, C. S., & Ma, J. (2012). Size distribution of EC, OC and particle-phase PAHs emissions from a diesel engine fueled with three fuels. *Science of the Total Environment*, 438, 33-41.
- Lu, W., Yang, L., Chen, J., Wang, X., Li, H., Zhu, Y., ... & Wang, W. (2016). Identification of concentrations and sources of PM<sub>2.5</sub>-bound PAHs in North China during haze episodes in 2013. *Air Quality, Atmosphere & Health*, 9(7), 823-833.
- Lu, W., Yang, L., Chen, J., Wang, X., Li, H., Zhu, Y., ... & Wang, W. (2016). Identification of concentrations and sources of PM<sub>2.5</sub>-bound PAHs in North China during haze episodes in 2013. *Air Quality, Atmosphere & Health*, 9(7), 823-833.

- Mandalakis, M., Tsapakis, M., Tsoga, A., & Stephanou, E. G. (2002). Gas–particle concentrations and distribution of aliphatic hydrocarbons, PAHs, PCBs and PCDD/Fs in the atmosphere of Athens (Greece). *Atmospheric Environment*, 36(25), 4023-4035.
- Mantis, J., Chaloulakou, A., & Samara, C. (2005). PM<sub>10</sub>-bound polycyclic aromatic hydrocarbons (PAHs) in the Greater Area of Athens, Greece. *Chemosphere*, 59(5), 593-604.
- Mantis, J., Chaloulakou, A., & Samara, C. (2005). PM<sub>10</sub>-bound polycyclic aromatic hydrocarbons (PAHs) in the Greater Area of Athens, Greece. *Chemosphere*, 59(5), 593-604.
- Martellini, T., Giannoni, M., Lepri, L., Katsoyiannis, A., & Cincinelli, A. (2012). One year intensive PM<sub>2.5</sub> bound polycyclic aromatic hydrocarbons monitoring in the area of Tuscany, Italy. Concentrations, source understanding and implications. *Environmental Pollution*, 164, 252-258.
- Martín, F., Palomino, I., & Vivanco, M. G. (2010). Application of a method for combining measured data and modelling results in air quality assessment in Spain. *Física de la Tierra*, 21, 65-78.
- Martins, L. D., da Silva Júnior, C. R., Solci, M. C., Pinto, J. P., Souza, D. Z., Vasconcellos, P., ... & de Andrade, J. B. (2012). Particle emission from heavy-duty engine fuelled with blended diesel and biodiesel. *Environmental Monitoring and Assessment*, 184(5), 2663-2676.
- Masih, J., Singhvi, R., Taneja, A., Kumar, K., & Masih, H. (2012). Gaseous/particulate bound polycyclic aromatic hydrocarbons (PAHs), seasonal variation in North central part of rural India. *Sustainable Cities and Society*, 3, 30–36.
- Mastral, A. M., López, J. M., Callén, M. S., Garcí a T., Murillo, R., & Navarro, M. V. (2003). Spatial and temporal PAH concentrations in Zaragoza, Spain. *Science of the Total Environment*, 307(1), 111-124.
- Megido, L., Negral, L., Castrillón, L., Marañón, E., Fernández-Nava, Y., & Suárez-Peña, B. (2016). Traffic tracers in a suburban location in northern Spain: relationship between carbonaceous fraction and metals. *Environmental Science and Pollution Research*, 23(9), 8669-8678.
- Melnyk, A., Dettlaff, A., Kuklińska, K., Namieśnik, J., & Wolska, L. (2015). Concentration and sources of polycyclic aromatic hydrocarbons (PAHs) and polychlorinated biphenyls (PCBs) in surface soil near a municipal solid waste (MSW) landfill. *Science of the Total Environment*, 530, 18-27.
- Minguillón, M. C., Arhami, M., Schauer, J. J., & Sioutas, C. (2008). Seasonal and spatial variations of sources of fine and quasi-ultrafine particulate matter in neighborhoods near the Los Angeles–Long Beach harbor. *Atmospheric Environment*, 42(32), 7317-7328.
- Mirivel, G., Riffault, V., & Galloo, J. C. (2010). Simultaneous determination by ultra-performance liquid chromatography–atmospheric pressure chemical ionization time-of-flight mass spectrometry of nitrated and oxygenated PAHs found in air and soot particles. *Analytical and Bioanalytical Chemistry*, 397(1), 243-256.

- Mitchell, E. J. S., Coulson, G., Butt, E. W., Forster, P. M., Jones, J. M., & Williams, A. (2017). Heating with Biomass in the United Kingdom: Lessons from New Zealand. *Atmospheric Environment*, *152*, 431-454.
- Miyazaki, Y., Aggarwal, S. G., Singh, K., Gupta, P. K., & Kawamura, K. (2009). Dicarboxylic acids and water-soluble organic carbon in aerosols in New Delhi, India, in winter: Characteristics and formation processes. *Journal of Geophysical Research: Atmospheres*, *114*(D19).
- Mohanraj, R., Solaraj, G., & Dhanakumar, S. (2011). PM<sub>2.5</sub> and PAH concentrations in urban atmosphere of Tiruchirappalli, India. *Bulletin of Environmental Contamination and Toxicology*, *87*(3), 330-335.
- Moon, K. J., Han, J. S., Ghim, Y. S., & Kim, Y. J. (2008). Source apportionment of fine carbonaceous particles by positive matrix factorization at Gosan background site in East Asia. *Environment International*, *34*(5), 654-664.
- Narváez, R. F., Hoepner, L., Chillrud, S. N., Yan, B., Garfinkel, R., Whyatt, R., ... & Miller, R. L. (2008). Spatial and temporal trends of polycyclic aromatic hydrocarbons and other traffic-related airborne pollutants in New York City. *Environmental Science & Technology*, *42*(19), 7330.
- Neff, J. M., Stout, S. A., & Gunster, D. G. (2005). Ecological risk assessment of polycyclic aromatic hydrocarbons in sediments: identifying sources and ecological hazard. *Integrated Environmental Assessment and Management*, *1*(1), 22-33.
- Nguyen, D. L., Kim, J. Y., Ghim, Y. S., & Shim, S. G. (2015). Influence of regional biomass burning on the highly elevated organic carbon concentrations observed at Gosan, South Korea during a strong Asian dust period. *Environmental Science and Pollution Research*, *22*(5), 3594-3605.
- Ni, M., Yang, G., Wang, S., Wang, X., Xiao, G., Zheng, C., ... & Cen, K. (2016). Experimental investigation on the characteristics of ash layers in a high-temperature wire-cylinder electrostatic precipitator. *Separation and Purification Technology*, *159*, 135-146.
- Norman, R. E., Carpenter, D. O., Scott, J., Brune, M. N., & Sly, P. D. (2013). Environmental exposures: an underrecognized contribution to noncommunicable diseases. *Reviews on Environmental Health*, *28*(1), 59-65.
- Noth, E. M., Hammond, S. K., Biging, G. S., & Tager, I. B. (2011). A spatial-temporal regression model to predict daily outdoor residential PAH concentrations in an epidemiologic study in Fresno, CA. *Atmospheric Environment*, *45*(14), 2394-2403.
- Noth, E. M., Hammond, S. K., Biging, G. S., & Tager, I. B. (2011). A spatial-temporal regression model to predict daily outdoor residential PAH concentrations in an epidemiologic study in Fresno, CA. *Atmospheric Environment*, *45*(14), 2394-2403.

- Novembre, J., & Stephens, M. (2008). Interpreting principal component analyses of spatial population genetic variation. *Nature genetics*, 40(5), 646-649.
- Okuda, T., Naoi, D., Tenmoku, M., Tanaka, S., He, K., Ma, Y., ... & Zhang, D. (2006). Polycyclic aromatic hydrocarbons (PAHs) in the aerosol in Beijing, China, measured by aminopropylsilane chemically-bonded stationary-phase column chromatography and HPLC/fluorescence detection. *Chemosphere*, 65(3), 427-435.
- Ono-Ogasawara, M., & Myojo, T. (2011). A proposal of method for evaluating airborne MWCNT concentration. *Industrial Health*, 49(6), 726-734.
- Pachauri, T., Singla, V., Satsangi, A., Lakhani, A., & Kumari, K. M. (2013). Characterization of carbonaceous aerosols with special reference to episodic events at Agra, India. *Atmospheric Research*, 128, 98-110.
- Padhi, B. K., Adhikari, A., Satapathy, P., Patra, A. K., Chandel, D., & Panigrahi, P. (2016). Predictors and respiratory depositions of airborne endotoxin in homes using biomass fuels and LPG gas for cooking. *Journal of Exposure Science and Environmental Epidemiology*. Nature.com
- Panda, S., Sharma, S. K., Mahapatra, P. S., Panda, U., Rath, S., Mahapatra, M., ... & Das, T. (2016). Organic and elemental carbon variation in PM<sub>2.5</sub> over megacity Delhi and Bhubaneswar, a semi-urban coastal site in India. *Natural Hazards*, 80(3), 1709-1728.
- Pant, P., Baker, S. J., Goel, R., Guttikunda, S., Goel, A., Shukla, A., & Harrison, R. M. (2016). Analysis of size-segregated winter season aerosol data from New Delhi, India. *Atmospheric Pollution Research*, 7(1), 100-109.
- Pant, P., Baker, S. J., Shukla, A., Maikawa, C., Pollitt, K. J. G., & Harrison, R. M. (2015b). The PM<sub>10</sub> fraction of road dust in the UK and India: Characterization, source profiles and oxidative potential. *Science of the Total Environment*, 530, 445-452.
- Pant, P., Habib, G., Marshall, J. D., & Peltier, R. E. (2017). PM<sub>2.5</sub> exposure in highly polluted cities: A case study from New Delhi, India. *Environmental Research*, 156, 167-174.
- Pant, P., Shukla, A., Kohl, S. D., Chow, J. C., Watson, J. G., & Harrison, R. M. (2015a). Characterization of ambient PM<sub>2.5</sub> at a pollution hotspot in New Delhi, India and inference of sources. *Atmospheric Environment*, 109, 178-189.
- Park, J. S., Wade, T. L., & Sweet, S. T. (2002). Atmospheric deposition of PAHs, PCBs, and organochlorine pesticides to Corpus Christi Bay, Texas. *Atmospheric Environment*, 36(10), 1707-1720.
- Park, S. S., Bae, M. S., Schauer, J. J., Ryu, S. Y., Kim, Y. J., Cho, S. Y., & Kim, S. J. (2005). Evaluation of the TMO and TOT methods for OC and EC measurements and their characteristics in PM<sub>2.5</sub> at an urban site of Korea during ACE-Asia. *Atmospheric Environment*, 39(28), 5101-5112.

- Park, S. S., Kim, Y. J., & Fung, K. (2001). Characteristics of PM<sub>2.5</sub> carbonaceous aerosol in the Sihwa industrial area, Korea. *Atmospheric Environment*, 35(4), 657-665.
- Park, S. S., Kim, Y. J., & Kang, C. H. (2002). Atmospheric polycyclic aromatic hydrocarbons in Seoul, Korea. *Atmospheric Environment*, 36(17), 2917-2924.
- Park, S. S., Kim, Y. J., & Kang, C. H. (2007). Polycyclic aromatic hydrocarbons in bulk PM<sub>2.5</sub> and size-segregated aerosol particle samples measured in an urban environment. *Environmental Monitoring and Assessment*, 128(1-3), 231-240.
- Pathak, A. K., Yadav, S., Kumar, P., & Kumar, R. (2013). Source apportionment and spatial-temporal variations in the metal content of surface dust collected from an industrial area adjoining Delhi, India. *Science of the Total Environment*, 443, 662-672.
- Pengchai, P., Chantara, S., Sopajaree, K., Wangkarn, S., Tengcharoenkul, U., & Rayanakorn, M. (2009). Seasonal variation, risk assessment and source estimation of PM<sub>10</sub> and PM<sub>10</sub>-bound PAHs in the ambient air of Chiang Mai and Lamphun, Thailand. *Environmental Monitoring and Assessment*, 154(1), 197-218.
- Pies C, Hoffmann B, Petrowsky J, Yang Y, Ternes TA, Hofmann T (2008) Characterization and source identification of polycyclic aromatic hydrocarbons (PAHs) in river bank soils. *Chemosphere* 72:1594– 1601.
- Pietrogrande, M. C., Bacco, D., Ferrari, S., Ricciardelli, I., Scotto, F., Trentini, A., & Visentin, M. (2016). Characteristics and major sources of carbonaceous aerosols in PM<sub>2.5</sub> in Emilia Romagna Region (Northern Italy) from four-year observations. *Science of the Total Environment*, 553, 172-183.
- Pistocchi, A., Sarigiannis, D. A., & Vizcaino, P. (2010). Spatially explicit multimedia fate models for pollutants in Europe: state of the art and perspectives. *Science of the Total Environment*, 408(18), 3817-3830.
- Pongpiachan, S., Hattayanone, M., Choochuay, C., Mekmok, R., Wuttijak, N., & Kettranakul, A. (2015). Enhanced PM<sub>10</sub> bounded PAHs from shipping emissions. *Atmospheric Environment*, 108, 13-19.
- Poor, N., Tremblay, R., Kay, H., Bhethanabotla, V., Swartz, E., Luther, M., & Campbell, S. (2004). Atmospheric concentrations and dry deposition rates of polycyclic aromatic hydrocarbons (PAHs) for Tampa Bay, Florida, USA. *Atmospheric Environment*, 38(35), 6005-6015.
- Pope III, C. A., & Dockery, D. W. (2006). Health effects of fine particulate air pollution: lines that connect. *Journal of the Air & Waste Management Association*, 56(6), 709-742.
- Potapova, M., Desianti, N., & Enache, M. (2016). Potential effects of sediment contaminants on diatom assemblages in coastal lagoons of New Jersey and New York States. *Marine Pollution Bulletin*, 107(2), 453-458.

- Pozo, K., Estellano, V. H., Harner, T., Diaz-Robles, L., Cereceda-Balic, F., Etcharren, P., ... & Vergara-Fernández, A. (2015). Assessing Polycyclic Aromatic Hydrocarbons (PAHs) using passive air sampling in the atmosphere of one of the most wood-smoke-polluted cities in Chile: the case study of Temuco. *Chemosphere*, *134*, 475-481.
- Prabhakaran, D., Roy, A., Praveen, P. A., Ramakrishnan, L., Gupta, R., Amarchand, R., ... & Tandon, N. (2017). 20-Year Trend of Cardiovascular Disease Risk Factors: Urban and Rural National Capital Region of Delhi, India. *Global Heart*.
- Querol, X., Alastuey, A., Moreno, T., Viana, M. M., Castillo, S., Pey, J., ... & Dos Santos, S. G. (2008). Spatial and temporal variations in airborne particulate matter (PM<sub>10</sub> and PM<sub>2.5</sub>) across Spain 1999–2005. *Atmospheric Environment*, *42*(17), 3964-3979.
- Rajput, N., & Lakhani, A. (2009). PAHs and their carcinogenic potencies in diesel fuel and diesel generator exhaust. *Human and Ecological Risk Assessment*, *15*(1), 201-213.
- Rajput, P., & Sarin, M. M. (2014). Polar and non-polar organic aerosols from large-scale agricultural-waste burning emissions in Northern India: implications to organic mass-to-organic carbon ratio. *Chemosphere*, *103*, 74-79.
- Rajput, P., Sarin, M. M., Sharma, D., & Singh, D. (2014). Atmospheric polycyclic aromatic hydrocarbons and isomer ratios as tracers of biomass burning emissions in Northern India. *Environmental Science and Pollution Research*, *21*(8), 5724-5729.
- Rajput, P., Sarin, M., & Kundu, S. S. (2013). Atmospheric particulate matter (PM<sub>2.5</sub>), EC, OC, WSOC and PAHs from NE–Himalaya: abundances and chemical characteristics. *Atmospheric Pollution Research*, *4*(2), 214-221.
- Ram, K., & Sarin, M. M. (2015). Atmospheric carbonaceous aerosols from Indo-Gangetic Plain and Central Himalaya: impact of anthropogenic sources. *Journal of Environmental Management*, *148*, 153-163.
- Ram, K., Sarin, M. M., & Hegde, P. (2008). Atmospheric abundances of primary and secondary carbonaceous species at two high-altitude sites in India: Sources and temporal variability. *Atmospheric Environment*, *42*(28), 6785-6796.
- Ramanathan, V., Ramana, M. V., Roberts, G., Kim, D., Corrigan, C., Chung, C., & Winker, D. (2007). Warming trends in Asia amplified by brown cloud solar absorption. *Nature*, *448*(7153), 575-578.
- Ravindra, K., Bencs, L., Wauters, E., De Hoog, J., Deutsch, F., Roekens, E., ... & Van Grieken, R. (2006). Seasonal and site-specific variation in vapour and aerosol phase PAHs over Flanders (Belgium) and their relation with anthropogenic activities. *Atmospheric Environment*, *40*(4), 771-785.



- Ravindra, K., Bencs, L., Wauters, E., De Hoog, J., Deutsch, F., Roekens, E., ... & Van Grieken, R. (2006). Seasonal and site-specific variation in vapour and aerosol phase PAHs over Flanders (Belgium) and their relation with anthropogenic activities. *Atmospheric Environment*, 40(4), 771-785.
- Ravindra, K., Sokhi, R., & Van Grieken, R. (2008). Atmospheric polycyclic aromatic hydrocarbons: source attribution, emission factors and regulation. *Atmospheric Environment*, 42(13), 2895-2921.
- Ravindra, K., Wauters, E., & Van Grieken, R. (2007). Poster 34 Spatial and temporal variations in particulate Polycyclic Aromatic Hydrocarbon (PAH) levels over Menen (Belgium) and their relation with air mass trajectories. *Developments in Environmental Science*, 6, 838-841.
- Ray, S., Khillare, P. S., Agarwal, T., & Shridhar, V. (2008). Assessment of PAHs in soil around the International Airport in Delhi, India. *Journal of Hazardous Materials*, 156(1), 9-16.
- Righini, G., Cappelletti, A., Ciucci, A., Cremona, G., Piersanti, A., Vitali, L., & Ciancarella, L. (2014). GIS based assessment of the spatial representativeness of air quality monitoring stations using pollutant emissions data. *Atmospheric Environment*, 97, 121-129.
- Rogge, W. F., Hildemann, L. M., Mazurek, M. A., Cass, G. R., & Simoneit, B. R. (1993a). Sources of fine organic aerosol. 2. Noncatalyst and catalyst-equipped automobiles and heavy-duty diesel trucks. *Environmental Science & Technology*, 27(4), 636-651.
- Rogge, W. F., Hildemann, L. M., Mazurek, M. A., Cass, G. R., & Simoneit, B. R. (1993b). Sources of fine organic aerosol. 4. Particulate abrasion products from leaf surfaces of urban plants. *Environmental Science & Technology*, 27(13), 2700-2711.
- Roy, D., Gautam, S., Singh, P., Singh, G., Das, B. K., & Patra, A. K. (2016). Carbonaceous species and physicochemical characteristics of PM<sub>10</sub> in coal mine fire area—a case study. *Air Quality, Atmosphere & Health*, 9(4), 429-437.
- Roy, D., Seo, Y. C., Sinha, S., Bhattacharya, A., Singh, G., & Biswas, P. K. (2017). Human health risk exposure with respect to particulate-bound polycyclic aromatic hydrocarbons at mine fire-affected coal mining complex. *Environmental Science and Pollution Research*, 1-17.
- Russell, A. G., & Brunekreef, B. (2009). A focus on particulate matter and health.
- Sachdeva, K., Narayanan, P., & Arora, P. (2013). Assessment of carbon fractions of aerosols collected under gravity settling at two different heights in the Delhi region. *Urban Climate*, 5, 104-111.
- Safai, P. D., Raju, M. P., Rao, P. S. P., & Pandithurai, G. (2014). Characterization of carbonaceous aerosols over the urban tropical location and a new approach to evaluate their climatic importance. *Atmospheric Environment*, 92, 493-500.
- Salam, A., Bauer, H., Kassim, K., Ullah, S. M., Puxbaum, H., 2003. Aerosol chemical of a mega-city in Southeast Asia (Dhaka—Bangladesh). *Atmospheric Environment*, 37, 2517–2528.

- Salam, A., Ullah, M. B., Islam, M. S., Salam, M. A., & Ullah, S. M. (2013). Carbonaceous species in total suspended particulate matters at different urban and suburban locations in the Greater Dhaka region, Bangladesh. *Air Quality, Atmosphere & Health*, 6(1), 239-245.
- Salvador, P., Artíñano, B., Viana, M. M., Querol, X., Alastuey, A., González-Fernández, I., & Alonso, R. (2011). Spatial and temporal variations in PM<sub>10</sub> and PM<sub>2.5</sub> across Madrid metropolitan area in 1999–2008. *Procedia Environmental Sciences*, 4, 198-208.
- Samara, C., Voutsas, D., Kouras, A., Eleftheriadis, K., Maggos, T., Saraga, D., & Petrakakis, M. (2014). Organic and elemental carbon associated to PM<sub>10</sub> and PM<sub>2.5</sub> at urban sites of northern Greece. *Environmental Science and Pollution Research*, 21(3), 1769-1785.
- Sarkar, S., & Khillare, P. S. (2011). Association of polycyclic aromatic hydrocarbons (PAHs) and metallic species in a tropical urban atmosphere–Delhi, India. *Journal of Atmospheric Chemistry*, 68(2), 107-126.
- Sarkar, S., & Khillare, P. S. (2013). Profile of PAHs in the inhalable particulate fraction: source apportionment and associated health risks in a tropical megacity. *Environmental Monitoring and Assessment*, 185, 1119-1213.
- Sarkar, S., Khillare, P. S., Jyethi, D S., Hasan, A., & Parween, M., (2010). Chemical speciation of respirable suspended particulate matter during a major firework festival in India. *Journal of Hazardous Materials* 184, 321-330
- Sarti, E., Pasti, L., Scaroni, I., Casali, P., Cavazzini, A., & Rossi, M. (2017). Determination of n-alkanes, PAHs and nitro-PAHs in PM<sub>2.5</sub> and PM<sub>1</sub> sampled in the surroundings of a municipal waste incinerator. *Atmospheric Environment*, 149, 12-23.
- Satsangi, A., Pachauri, T., Singla, V., Lakhani, A., & Kumari, K. M. (2012). Organic and elemental carbon aerosols at a suburban site. *Atmospheric Research*, 113, 13-21.
- Schwartz, J. (1994a). Air pollution and hospital admissions for the elderly in Birmingham, Alabama. *American Journal of Epidemiology*, 139(6), 589-598.
- Schwartz, J. (1994b). Air pollution and hospital admissions for the elderly in Detroit, Michigan. *American Journal of Respiratory and Critical Care Medicine*, 150(3), 648-655.
- Schwartz, J. (1994c). PM<sub>10</sub> ozone, and hospital admissions for the elderly in Minneapolis-St. Paul, Minnesota. *Archives of Environmental Health: An International Journal*, 49(5), 366-374.
- See, S. W., & Balasubramanian, R. (2008). Chemical characteristics of fine particles emitted from different gas cooking methods. *Atmospheric Environment*, 42(39), 8852-8862.
- Seinfeld, J.H., Pandis, S.N (1998). Atmospheric chemistry and physics. Air Pollution to Climate Change. Wiley, New York. (1360 pp.).

- Seinfeld, J.H., Pandis, S.N (2006). Atmospheric Chemistry and Physics: From Air Pollution to Climate Change, 2nd Edition. John Wiley & Sons, New York.
- Sharma, H., Jain, V. K., & Khan, Z. H. (2007). Characterization and source identification of polycyclic aromatic hydrocarbons (PAHs) in the urban environment of Delhi. *Chemosphere*, 66(2), 302-310.
- Sharma, S. K., Mandal, T. K., Saxena, M., Sharma, A., Datta, A., & Saud, T. (2014). Variation of OC, EC, WSIC and trace metals of PM<sub>10</sub> in Delhi, India. *Journal of Atmospheric and Solar-Terrestrial Physics*, 113, 10-22.
- Sharma, S. K., Mandal, T. K., Saxena, M., Sharma, A., Datta, A., & Saud, T. (2014). Variation of OC, EC, WSIC and trace metals of PM<sub>10</sub> in Delhi, India. *Journal of Atmospheric and Solar-Terrestrial Physics*, 113, 10-22.
- Sharma, S. K., Mandal, T. K., Shenoy, D. M., Bardhan, P., Srivastava, M. K., Chatterjee, A., ... & Ghosh, S. K. (2015). Variation of Stable Carbon and Nitrogen Isotopic Composition of PM<sub>10</sub> at Urban Sites of Indo Gangetic Plain (IGP) of India. *Bulletin of Environmental Contamination and Toxicology*, 95 (5), 661-669.
- Sharma, S. K., Sharma, A., Saxena, M., Choudhary, N., Masiwal, R., Mandal, T. K., & Sharma, C. (2016). Chemical characterization and source apportionment of aerosol at an urban area of Central Delhi, India. *Atmospheric Pollution Research*, 7(1), 110-121.
- Sheesley, R. J., Schauer, J. J., Smith, T. J., Garshick, E., Laden, F., Marr, L. C., & Molina, L. T. (2008). Assessment of diesel particulate matter exposure in the workplace: freight terminals. *Journal of Environmental Monitoring*, 10(3), 305-314.
- Shihua, Q., Jun, Y., Gan, Z., Jiamo, F., Guoying, S., Zhishi, W., ... & Yunshun, M. (2001). Distribution of polycyclic aromatic hydrocarbons in aerosols and dustfall in Macao. *Environmental Monitoring and Assessment*, 72(2), 115-127.
- Shirmohammadi, F., Hasheminassab, S., Saffari, A., Schauer, J. J., Delfino, R. J., & Sioutas, C. (2016). Fine and ultrafine particulate organic carbon in the Los Angeles basin: trends in sources and composition. *Science of the Total Environment*, 541, 1083-1096.
- Sicre, M. A., Marty, J. C., Saliot, A., Aparicio, X., Grimalt, J., & Albaiges, J. (1987). Aliphatic and aromatic hydrocarbons in the Mediterranean aerosol. *International Journal of Environmental Analytical Chemistry*, 29(1-2), 73-94.
- Silva, F. S., Cristale, J., André, P. A., Saldiva, P. H., & Marchi, M. R. (2010). PM<sub>2.5</sub> and PM<sub>10</sub>: the influence of sugarcane burning on potential cancer risk. *Atmospheric Environment*, 44(39), 5133-5138.

- Simcik, M. F., Eisenreich, S. J., & Liroy, P. J. (1999). Source apportionment and source/sink relationships of PAHs in the coastal atmosphere of Chicago and Lake Michigan. *Atmospheric Environment*, 33(30), 5071–5079.
- Singh, D. K., & Gupta, T. (2016). Effect through inhalation on human health of PM<sub>1</sub> bound polycyclic aromatic hydrocarbons collected from foggy days in northern part of India. *Journal of Hazardous Materials*, 306, 257-268.
- Singh, D. P., Gadi, R., Mandal, T. K., Saud, T., Saxena, M., & Sharma, S. K. (2013). Emissions estimates of PAH from biomass fuels used in rural sector of Indo-Gangetic Plains of India. *Atmospheric Environment*, 68, 120-126.
- Singh, R., Kulshrestha, M. J., Kumar, B., & Chandra, S. (2015). Impact of anthropogenic emissions and open biomass burning on carbonaceous aerosols in urban and rural environments of Indo-Gangetic Plain. *Air Quality, Atmosphere & Health*. DOI 10.1007/s11869-015-0377-9.
- Singh, T., Khillare, P. S., Shridhar, V., & Agarwal, T. (2008). Visibility impairing aerosols in the urban atmosphere of Delhi. *Environmental Monitoring and Assessment*, 141(1), 67-77.
- Singla, V., Pachauri, T., Satsangi, A., Kumari, K. M., & Lakhani, A. (2012). Characterization and mutagenicity assessment of PM<sub>2.5</sub> and PM<sub>10</sub> PAH at Agra, India. *Polycyclic Aromatic Compounds*, 32(2), 199-220.
- Sioutas, C., Delfino, R. J., & Singh, M. (2005). Exposure assessment for atmospheric ultrafine particles (UFPs) and implications in epidemiologic research. *Environmental Health Perspectives*, 947-955.
- Sitaras, I. E., & Siskos, P. A. (2008). The role of primary and secondary air pollutants in atmospheric pollution: Athens urban area as a case study. *Environmental Chemistry Letters*, 6(2), 59-69.
- Škrbić, B., & Đurišić-Mladenović, N. (2010). Chemometric interpretation of heavy metal patterns in soils worldwide. *Chemosphere*, 80(11), 1360-1369.
- Slezakova, K., Castro, D., Delerue-Matos, C., da Conceição Alvim-Ferraz, M., Morais, S., & do Carmo Pereira, M. (2013). Impact of vehicular traffic emissions on particulate-bound PAHs: Levels and associated health risks. *Atmospheric Research*, 127, 141-147.
- Spindler, G., Grüner, A., Müller, K., Schlimper, S., & Herrmann, H. (2013). Long-term size-segregated particle (PM<sub>10</sub>, PM<sub>2.5</sub>, PM<sub>1</sub>) characterization study at Melpitz--influence of air mass inflow, weather conditions and season. *Journal of Atmospheric Chemistry*, 70(2), 165-195.
- Spindler, G., Müller, K., Brüggemann, E., Gnauk, T., & Herrmann, H. (2004). Long-term size-segregated characterization of PM<sub>10</sub>, PM<sub>2.5</sub>, and PM<sub>1</sub> at the IfT research station Melpitz downwind of Leipzig (Germany) using high and low-volume filter samplers. *Atmospheric Environment*, 38(31), 5333-5347.

- Srivastava, A., & Jain, V. K. (2007a). Seasonal trends in coarse and fine particle sources in Delhi by the chemical mass balance receptor model. *Journal of Hazardous Materials*, 144(1), 283-291.
- Srivastava, A., & Jain, V. K. (2007b). Size distribution and source identification of total suspended particulate matter and associated heavy metals in the urban atmosphere of Delhi. *Chemosphere*, 68(3), 579-589.
- Srivastava, A., Gupta, S., & Jain, V. K. (2008). Source apportionment of total suspended particulate matter in coarse and fine size ranges over Delhi. *Aerosol and Air Quality Research* 8(2), 188-200.
- Srivastava, A., Gupta, S., & Jain, V. K. (2009). Winter-time size distribution and source apportionment of total suspended particulate matter and associated metals in Delhi. *Atmospheric Research*, 92(1), 88-99.
- Stogiannidis, E., & Laane, R. (2015). Source characterization of polycyclic aromatic hydrocarbons by using their molecular indices: an overview of possibilities. In *Reviews of Environmental Contamination and Toxicology* (pp. 49-133). Springer International Publishing.
- Sudheer, A. K., Aslam, M. Y., Upadhyay, M., Rengarajan, R., Bhushan, R., Rathore, J. S., ... & Kumar, S. (2016). Carbonaceous aerosol over semi-arid region of western India: Heterogeneity in sources and characteristics. *Atmospheric Research*, 178, 268-278.
- Sudheer, A. K., Aslam, M. Y., Upadhyay, M., Rengarajan, R., Bhushan, R., Rathore, J. S., ... & Kumar, S. (2016). Carbonaceous aerosol over semi-arid region of western India: Heterogeneity in sources and characteristics. *Atmospheric Research*, 178, 268-278.
- Sun, P., Bao, M., Li, F., Cao, L., Wang, X., Zhou, Q., ... & Tang, H. (2015). Sensitivity and Identification Indexes for Fuel Oils and Crude Oils Based on the Hydrocarbon Components and Diagnostic Ratios Using Principal Component Analysis (PCA) Biplots. *Energy & Fuels*, 29(5), 3032-3040.
- Szabó, J., Nagy, A. S., & Erdős, J. (2015). Ambient concentrations of PM<sub>10</sub>, PM<sub>10</sub>-bound polycyclic aromatic hydrocarbons and heavy metals in an urban site of Győr, Hungary. *Air Quality, Atmosphere & Health*, 8(2), 229-241.
- Taiwo, A. M., Harrison, R. M., & Shi, Z. (2014). A review of receptor modelling of industrially emitted particulate matter. *Atmospheric Environment*, 97, 109-120.
- Tang, X. L., Bi, X. H., Sheng, G. Y., Tan, J. H., & Fu, J. M. (2006). Seasonal variation of the particle size distribution of n-alkanes and polycyclic aromatic hydrocarbons (PAHs) in urban aerosol of Guangzhou, China. *Environmental Monitoring and Assessment*, 117(1-3), 193-213.
- Thornhill, D. A., Foy, B. D., Herndon, S. C., Onasch, T. B., Wood, E. C., Zavala, M., ... & Marr, L. C. (2008). Spatial and temporal variability of particulate polycyclic aromatic hydrocarbons in Mexico City. *Atmospheric Chemistry and Physics*, 8(12), 3093-3105.

- Thurston, G. D., & Spengler, J. D. (1985). A quantitative assessment of source contributions to inhalable particulate matter pollution in metropolitan Boston. *Atmospheric Environment* (1967), 19(1), 9-25.
- Tiwari, S., Dumka, U. C., Kaskaoutis, D. G., Ram, K., Panicker, A. S., Srivastava, M. K., ... & Pandey, A. K. (2016). Aerosol chemical characterization and role of carbonaceous aerosol on radiative effect over Varanasi in central Indo-Gangetic Plain. *Atmospheric Environment*, 125, 437-449.
- Tiwari, S., Srivastava, A. K., Bisht, D. S., Safai, P. D., & Parmita, P. (2013). Assessment of carbonaceous aerosol over Delhi in the Indo-Gangetic Basin: characterization, sources and temporal variability. *Natural Hazards*, 65(3), 1745-1764.
- Tobiszewski, M., & Namieśnik, J. (2012). PAH diagnostic ratios for the identification of pollution emission sources. *Environmental Pollution*, 162, 110-119.
- Tongo, I., Ezemonye, L., & Akpeh, K. (2017). Distribution, characterization, and human health risk assessment of polycyclic aromatic hydrocarbons (PAHs) in Ovia River, Southern Nigeria. *Environmental Monitoring and Assessment*, 189(6), 247.
- Trivedi, D. K., Ali, K., & Beig, G. (2014). Impact of meteorological parameters on the development of fine and coarse particles over Delhi. *Science of the Total Environment*, 478, 175-183.
- Tue, N. M., Takahashi, S., Suzuki, G., Viet, P. H., Subramanian, A., Bulbule, K. A., ... & Tanabe, S. (2014). Methylated and unsubstituted polycyclic aromatic hydrocarbons in street dust from Vietnam and India: Occurrence, distribution and in vitro toxicity evaluation. *Environmental Pollution*, 194, 272-280.
- Turpin, B. J., & Lim, H. J. (2001). Species contributions to PM<sub>2.5</sub> mass concentrations: Revisiting common assumptions for estimating organic mass. *Aerosol Science & Technology*, 35(1), 602-610.
- Tyagi, S., Tiwari, S., Mishra, A., Singh, S., Hopke, P. K., Singh, S., & Attri, S. D. (2017). Characteristics of absorbing aerosols during winter foggy period over the National Capital Region of Delhi: Impact of planetary boundary layer dynamics and solar radiation flux. *Atmospheric Research*.
- United States Environmental Protection Agency (1989). Risk assessment guidance for superfund. Volume I. Human health evaluation manual (part A). EPA 540-1-89-002, Office of Emergency and Remedial Response. US EPA, Washington.
- United States Environmental Protection Agency, (1998). Integrated Risk Information System (IRIS), available at: [www.epa.gov](http://www.epa.gov). Washington, DC, US Environmental Protection Agency.
- United States Environmental Protection Agency, (2012). <http://www.epa.gov/reg3hwmd/risk/human>.
- US EPA (1997). Air risk assessment work plan. Air and Radiation Division, Tristate, EPA, Washington, 1997.

- Valavanidis, A., Fiotakis, K., Vlachogianni, T (2008). Airborne Particulate Matter and Human Health: Toxicological Assessment and Importance of Size and Composition of Particles for Oxidative Damage and Carcinogenic Mechanisms. *Journal of Environmental Science and Health Part C*, 26:339–362, 2008.
- Vardar, N., & Noll, K. E. (2003). Atmospheric PAH concentrations in fine and coarse particles. *Environmental Monitoring and Assessment*, 87(1), 81-92.
- Vardar, N., & Noll, K. E. (2003). Atmospheric PAH concentrations in fine and coarse particles. *Environmental Monitoring and Assessment*, 87(1), 81-92.
- Vasilakos, C., Levi, N., Maggos, T., Hatzianestis, J., Michopoulos, J., & Helmis, C. (2007). Gas–particle concentration and characterization of sources of PAHs in the atmosphere of a suburban area in Athens, Greece. *Journal of Hazardous Materials*, 140(1), 45-51.
- Vicente, E. D., Duarte, M. A., Calvo, A. I., Nunes, T. F., Tarelho, L. A. C., Custódio, D., ... & Alves, C. A. (2015). Influence of operating conditions on chemical composition of particulate matter emissions from residential combustion. *Atmospheric Research*, 166, 92-100.
- Villalobos, A. M., Amonov, M. O., Shafer, M. M., Devi, J. J., Gupta, T., Tripathi, S. N., ... & Schauer, J. J. (2015). Source apportionment of carbonaceous fine particulate matter (PM<sub>2.5</sub>) in two contrasting cities across the Indo–Gangetic Plain. *Atmospheric Pollution Research*, 6(3), 398-405.
- Villar-Vidal, M., Lertxundi, A., de Dicastillo, M. M. L., Alvarez, J. I., Santa Marina, L., Ayerdi, M., ... & Ibarluzea, J. (2014). Air Polycyclic Aromatic Hydrocarbons (PAHs) associated with PM<sub>2.5</sub> in a North Cantabric coast urban environment. *Chemosphere*, 99, 233-238.
- Vineis, P., Stringhini, S., & Porta, M. (2014). The environmental roots of non-communicable diseases (NCDs) and the epigenetic impacts of globalization. *Environmental Research*, 133, 424-430.
- Vodička, P., Schwarz, J., Cusack, M., & Ždímal, V. (2015). Detailed comparison of OC/EC aerosol at an urban and a rural Czech background site during summer and winter. *Science of the Total Environment*, 518, 424-433.
- Vojtisek-Lom, M., Pechout, M., Dittrich, L., Beránek, V., Kotek, M., Schwarz, J., ... & Topinka, J. (2015). Polycyclic aromatic hydrocarbons (PAH) and their genotoxicity in exhaust emissions from a diesel engine during extended low-load operation on diesel and biodiesel fuels. *Atmospheric Environment*, 109, 9-18.
- Vuković, G., Urošević, M. A., Razumenić, I., Kuzmanoski, M., Pergal, M., Škrivanj, S., & Popović, A. (2014). Air quality in urban parking garages (PM<sub>10</sub>, major and trace elements, PAHs): instrumental measurements vs. active moss biomonitoring. *Atmospheric Environment*, 85, 31-40.

- Wang, G., Cheng, S., Li, J., Lang, J., Wen, W., Yang, X., & Tian, L. (2015a). Source apportionment and seasonal variation of PM<sub>2.5</sub> carbonaceous aerosol in the Beijing-Tianjin-Hebei Region of China. *Environmental Monitoring and Assessment*, 187(3), 1-13.
- Wang, J., Geng, N. B., Xu, Y. F., Zhang, W. D., Tang, X. Y., & Zhang, R. Q. (2014). PAHs in PM<sub>2.5</sub> in Zhengzhou: concentration, carcinogenic risk analysis, and source apportionment. *Environmental Monitoring and Assessment*, 186(11), 7461-7473.
- Wang, J., Ho, S. S. H., Ma, S., Cao, J., Dai, W., Liu, S., ... & Han, Y. (2016). Characterization of PM<sub>2.5</sub> in Guangzhou, China: uses of organic markers for supporting source apportionment. *Science of the Total Environment*, 550, 961-971.
- Wang, J., Li, X., Jiang, N., Zhang, W., Zhang, R., & Tang, X. (2015). Long term observations of PM<sub>2.5</sub>-associated PAHs: comparisons between normal and episode days. *Atmospheric Environment*, 104, 228-236.
- Wang, W., Huang, M. J., Kang, Y., Wang, H. S., Leung, A. O., Cheung, K. C., & Wong, M. H. (2011). Polycyclic aromatic hydrocarbons (PAHs) in urban surface dust of Guangzhou, China: status, sources and human health risk assessment. *Science of the Total Environment*, 409(21), 4519-4527.
- Wang, X., Cheng, H., Xu, X., Zhuang, G., & Zhao, C. (2008). A wintertime study of polycyclic aromatic hydrocarbons in PM<sub>2.5</sub> and PM<sub>2.5-10</sub> in Beijing: assessment of energy structure conversion. *Journal of Hazardous Materials*, 157(1), 47-56.
- Wang, Y., Li, P. H., Li, H. L., Liu, X. H., & Wang, W. X. (2010). PAHs distribution in precipitation at Mount Taishan: China. Identification of sources and meteorological influences. *Atmospheric Research*, 95(1), 1-7.
- Wang, Y., Li, P. H., Li, H. L., Liu, X. H., & Wang, W. X. (2010). PAHs distribution in precipitation at Mount Taishan: China. Identification of sources and meteorological influences. *Atmospheric Research*, 95(1), 1-7.
- Wang, Y., Li, Q., Wang, S., Wang, Y., Luo, C., Li, J., & Zhang, G. (2015b). Seasonal and diurnal variations of atmospheric PAHs and OCPs in a suburban paddy field, South China: impacts of meteorological parameters and sources. *Atmospheric Environment*, 112, 208-215.
- Wang, Z., & Stout, S. (2010). *Oil spill environmental forensics: fingerprinting and source identification*. Academic Press.
- Watson, J.G., Chow, J.C., Houck, J.E., (2001). PM<sub>2.5</sub> chemical source profiles for vehicle exhaust, vegetative burning, geological material, and coal in Northwestern Colorado during 1995. *Chemosphere* 43, 1141-1151.



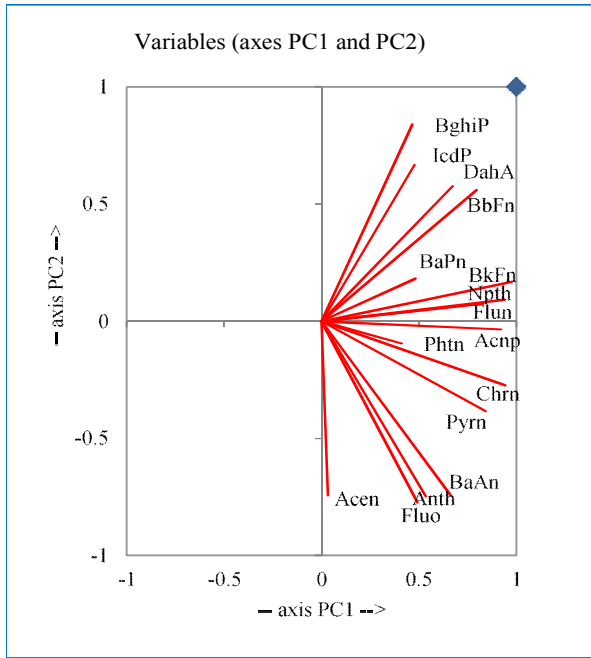
- Wheatley, A. D., & Sadhra, S. (2004). Occupational exposure to diesel exhaust fumes. *Annals of Occupational Hygiene*, 48(4), 369-376.
- WHO (2006). Health risks of particulate matter from long-range trans-boundary air pollution.
- WHO (2015). India: first to adapt the Global Monitoring Framework on noncommunicable diseases (NCDs).
- WHO (2016). WHO's Urban Ambient Air Pollution database - Update 2016
- WHO, India (2014). World Health Organization - Noncommunicable Diseases (NCD) Country Profiles, 2014.
- Wong, D. W., Yuan, L., & Perlin, S. A. (2004). Comparison of spatial interpolation methods for the estimation of air quality data. *Journal of Exposure Science and Environmental Epidemiology*, 14(5), 404-415.
- World Health Organization (2006). *Air quality guidelines: global update 2005: particulate matter, ozone, nitrogen dioxide, and sulfur dioxide*.
- Wu, D., Wang, Z., Chen, J., Kong, S., Fu, X., Deng, H., ... & Wu, G. (2014). Polycyclic aromatic hydrocarbons (PAHs) in atmospheric PM<sub>2.5</sub> and PM<sub>10</sub> at a coal-based industrial city: implication for PAH control at industrial agglomeration regions, China. *Atmospheric Research*, 149, 217-229.
- Xia, Z., Duan, X., Tao, S., Qiu, W., Liu, D., Wang, Y., ... & Song, Y. (2013). Pollution level, inhalation exposure and lung cancer risk of ambient atmospheric polycyclic aromatic hydrocarbons (PAHs) in Taiyuan, China. *Environmental Pollution*, 173, 150-156.
- Xu Y, Bahadur R, Zhao C, RubyLeung L (2013) Estimating the radiative forcing of carbonaceous aerosols over California based on satellite and ground observations. *Journal of Geophysical Research: Atmospheres* 118:11–148. doi:10.1002/jgrd.50835
- Xu, H., Guinot, B., Niu, X., Cao, J., Ho, K. F., Zhao, Z., ... & Liu, S. (2015a). Concentrations, particle-size distributions, and indoor/outdoor differences of polycyclic aromatic hydrocarbons (PAHs) in a middle school classroom in Xi'an, China. *Environmental Geochemistry and Health*, 37(5), 861-873.
- Xu, H., Ho, S. S. H., Gao, M., Cao, J., Guinot, B., Ho, K. F., ... & Zheng, C. (2016). Microscale spatial distribution and health assessment of PM<sub>2.5</sub>-bound polycyclic aromatic hydrocarbons (PAHs) at nine communities in Xi'an, China. *Environmental Pollution*, 218, 1065-1073.
- Xu, Z., Wen, T., Li, X., Wang, J., & Wang, Y. (2015b). Characteristics of carbonaceous aerosols in Beijing based on two-year observation. *Atmospheric Pollution Research*, 6(2), 202-208.
- Yan, C., Zheng, M., Yang, Q., Zhang, Q., Qiu, X., Zhang, Y., ... & Zhu, Y. (2015). Commuter exposure to particulate matter and particle-bound PAHs in three transportation modes in Beijing, China. *Environmental Pollution*, 204, 199-206.

- Yang, F., Brook, J., He, K., Duan, F., & Ma, Y. (2010). Temporal variability in fine carbonaceous aerosol over two years in two megacities: Beijing and Toronto. *Advances in Atmospheric Sciences*, 27(3), 705.
- Yang, F., Huang, L., Duan, F., Zhang, W., He, K., Ma, Y., ... & Cheng, Y. (2011). Carbonaceous species in PM<sub>2.5</sub> at a pair of rural/urban sites in Beijing, 2005–2008. *Atmospheric Chemistry and Physics*, 11(15), 7893-7903.
- Yang, H., Yu, J. Z., Ho, S. S. H., Xu, J., Wu, W. S., Wan, C. H., ... & Wang, L. (2005). The chemical composition of inorganic and carbonaceous materials in PM<sub>2.5</sub> in Nanjing, China. *Atmospheric Environment*, 39(20), 3735-3749.
- Yang, T. T., Hsu, C. Y., Chen, Y. C., Young, L. H., Huang, C. H., & Ku, C. H. (2017). Characteristics, Sources, and Health Risks of Atmospheric PM<sub>2.5</sub>-Bound Polycyclic Aromatic Hydrocarbons in Hsinchu, Taiwan. *Aerosol and Air Quality Research*, 17(2), 563-573.
- Yang, Y., Ligouis, B., Pies, C., Grathwohl, P., & Hofmann, T. (2008). Occurrence of coal and coal-derived particle-bound polycyclic aromatic hydrocarbons (PAHs) in a river floodplain soil. *Environmental Pollution*, 151(1), 121-129.
- Yin, H. L., Qiu, C. Y., Ye, Z. X., Li, S. P., & Liang, J. F. (2015). Seasonal variation and source apportionment of organic tracers in PM<sub>10</sub> in Chengdu, China. *Environmental Geochemistry and Health*, 37(1), 195-205.
- Yttri, K. E., Simpson, D., Nøjgaard, J. K., Kristensen, K., Genberg, J., Stenström, K., ... & Offenberg, J. H. (2011). Source apportionment of the summer time carbonaceous aerosol at Nordic rural background sites. *Atmospheric Chemistry and Physics*, 11(24), 13339-13357.
- Yu, S., Dennis, R. L., Bhawe, P. V., & Eder, B. K. (2004). Primary and secondary organic aerosols over the United States: estimates on the basis of observed organic carbon (OC) and elemental carbon (EC), and air quality modeled primary OC/EC ratios. *Atmospheric Environment*, 38(31), 5257-5268.
- Yunker, M. B., Macdonald, R. W., Vingarzan, R., Mitchell, R. H., Goyette, D., & Sylvestre, S. (2002). PAHs in the Fraser River basin: a critical appraisal of PAH ratios as indicators of PAH source and composition. *Organic Geochemistry*, 33(4), 489-515.
- Zhang, F., Xu, L., Chen, J., Chen, X., Niu, Z., Lei, T., ... & Zhao, J. (2013). Chemical characteristics of PM<sub>2.5</sub> during haze episodes in the urban of Fuzhou, China. *Particuology*, 11(3), 264-272.
- Zhang, S., Zhang, W., Wang, K., Shen, Y., Hu, L., & Wang, X. (2009). Concentration, distribution and source apportionment of atmospheric polycyclic aromatic hydrocarbons in the southeast suburb of Beijing, China. *Environmental Monitoring and Assessment*, 151(1-4), 197-207.

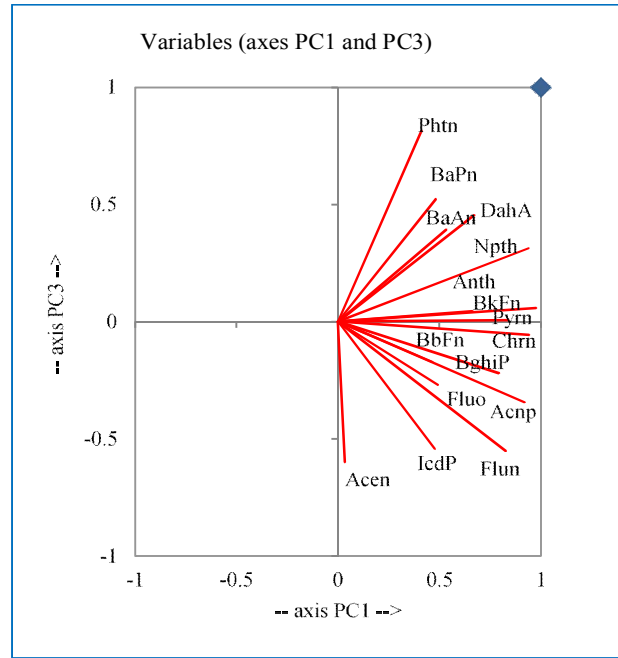
- Zhang, X. Y., Wang, Y. Q., Niu, T., Zhang, X. C., Gong, S. L., Zhang, Y. M., & Sun, J. Y. (2012). Atmospheric aerosol compositions in China: spatial/temporal variability, chemical signature, regional haze distribution and comparisons with global aerosols. *Atmospheric Chemistry and Physics*, 12(2), 779-799.
- Zhou, H., He, J., Zhao, B., Zhang, L., Fan, Q., Lü, C., ... & Yuan, Y. (2016). The distribution of PM<sub>10</sub> and PM<sub>2.5</sub> carbonaceous aerosol in Baotou, China. *Atmospheric Research*, 178, 102-113.

## *Appendices*

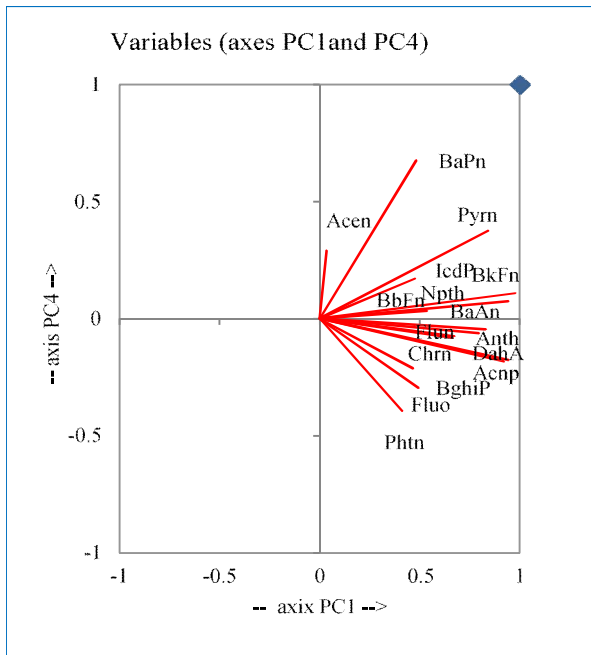
Appendices



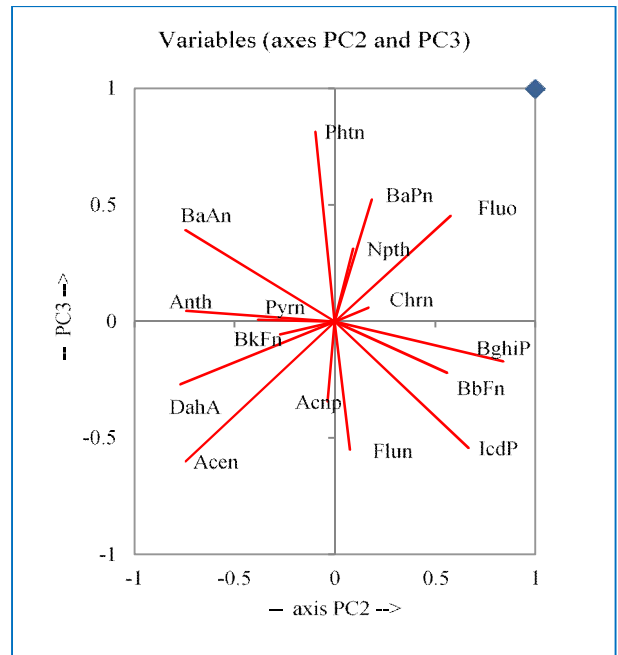
a.



b.

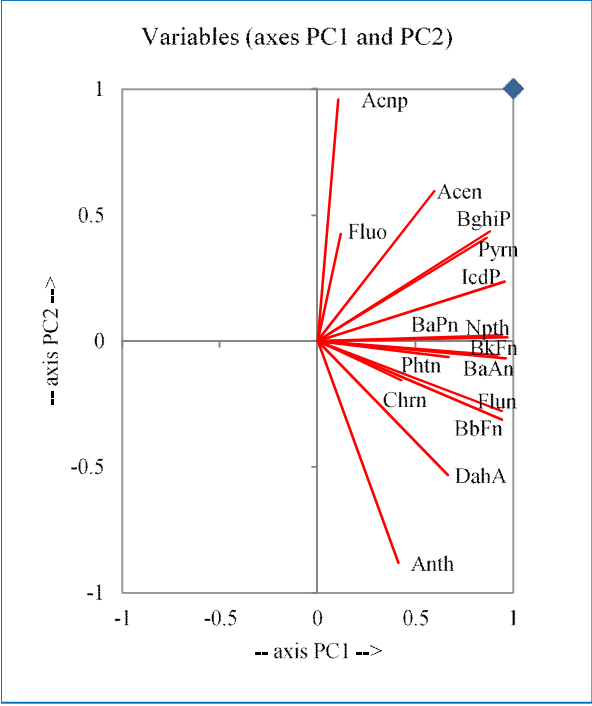


c.

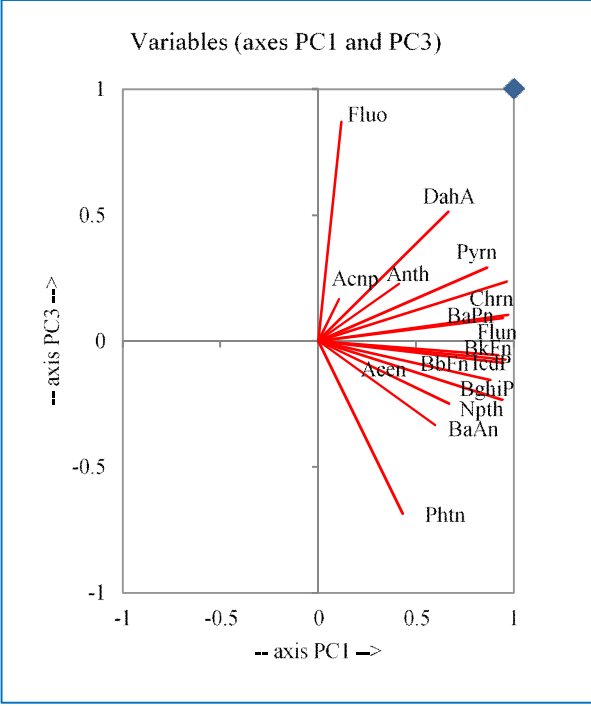


d.

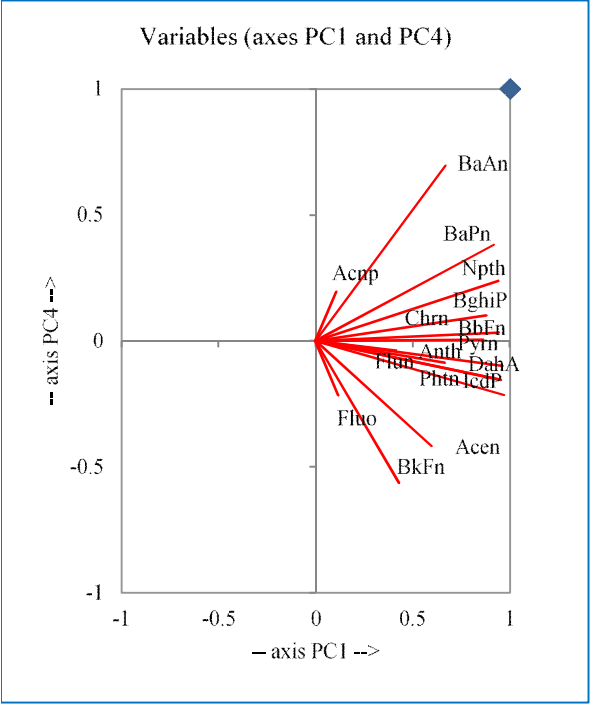
**Fig A1** Biplots between a. PC1 vs PC2, b. PC1 vs PC3, c. PC1 vs PC4 and d. PC2 vs PC3 in the monsoon season



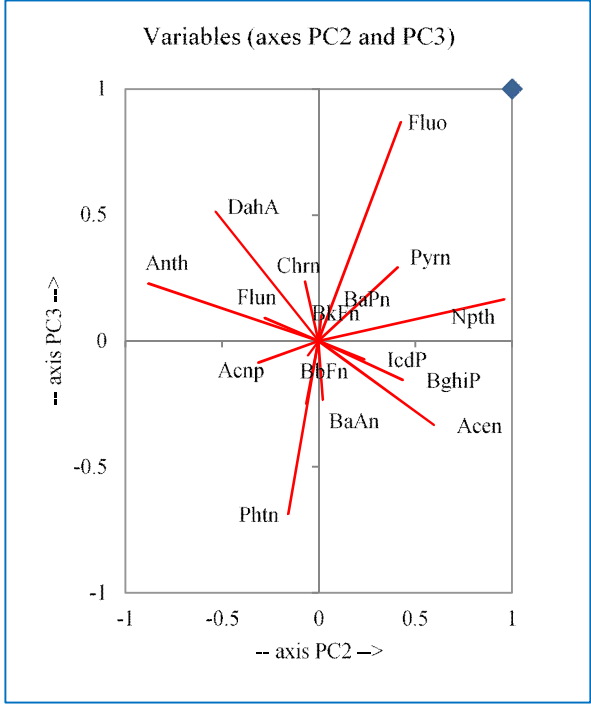
a.



b.

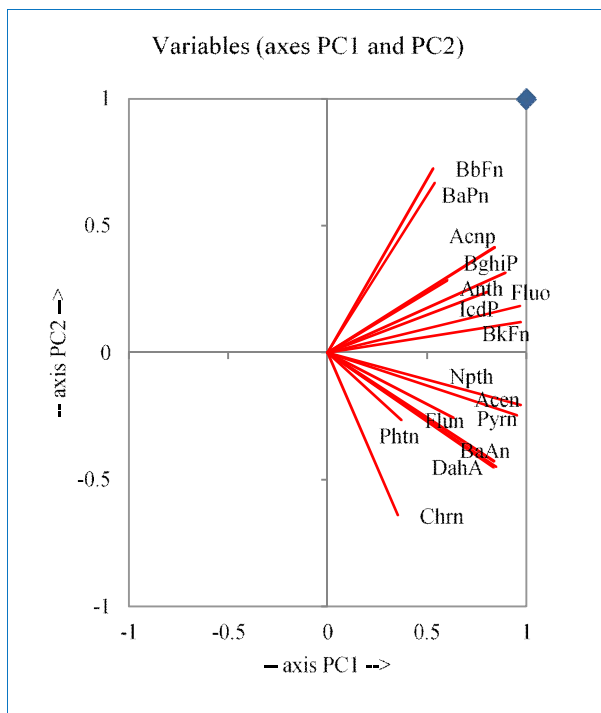


c.

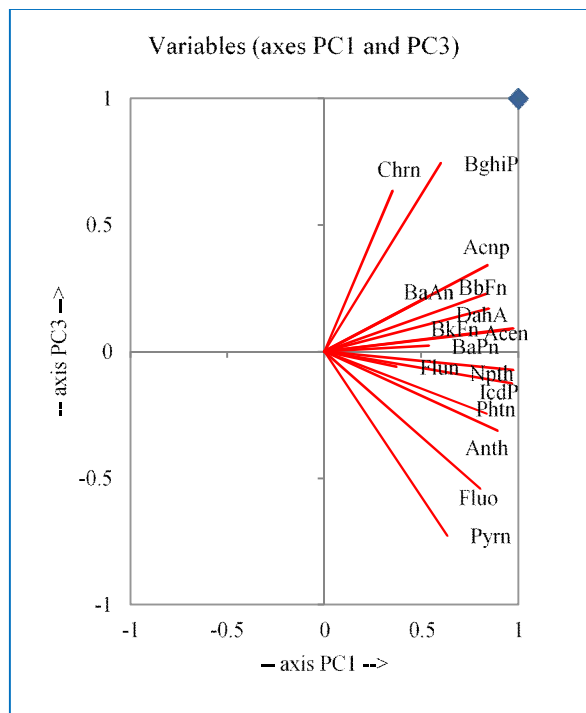


d.

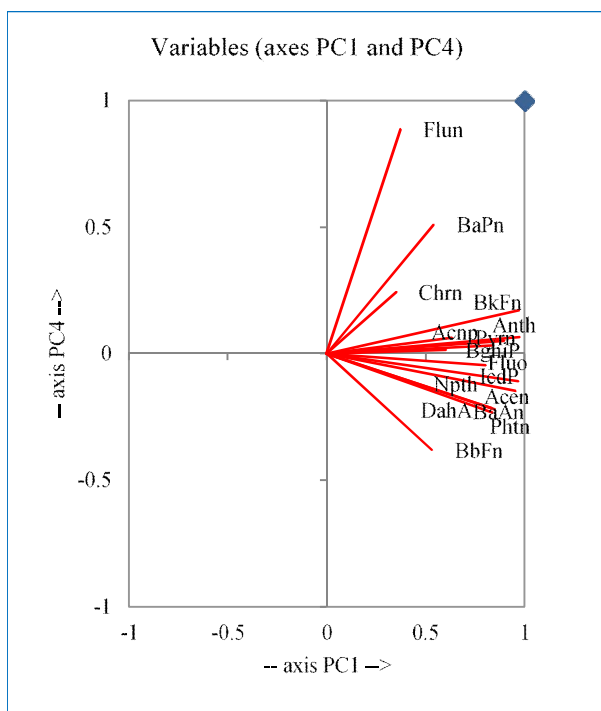
**Fig A2** Biplots between a. PC1 vs PC2, b. PC1 vs PC3, c. PC1 vs PC4 and d. PC2 vs PC3 in the autumn season



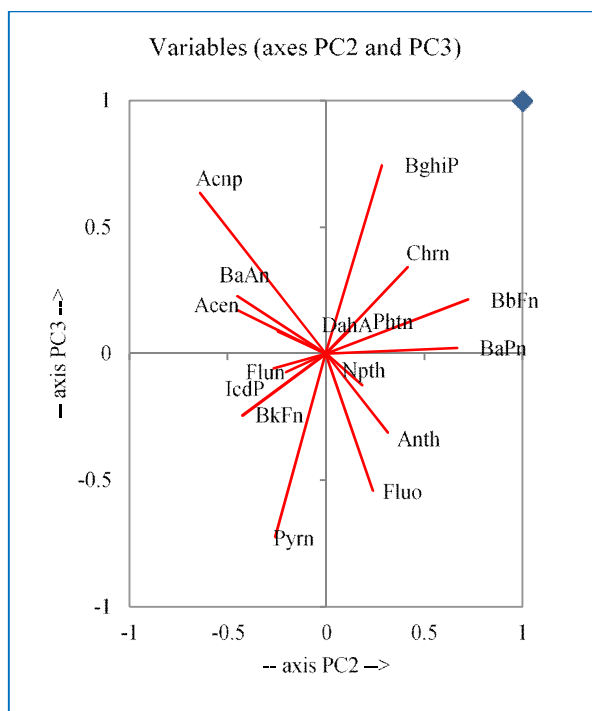
a.



b.

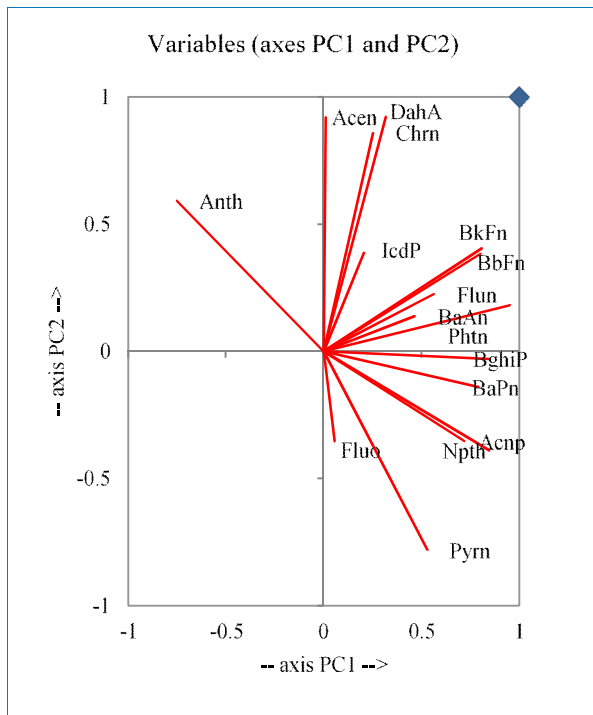


c.

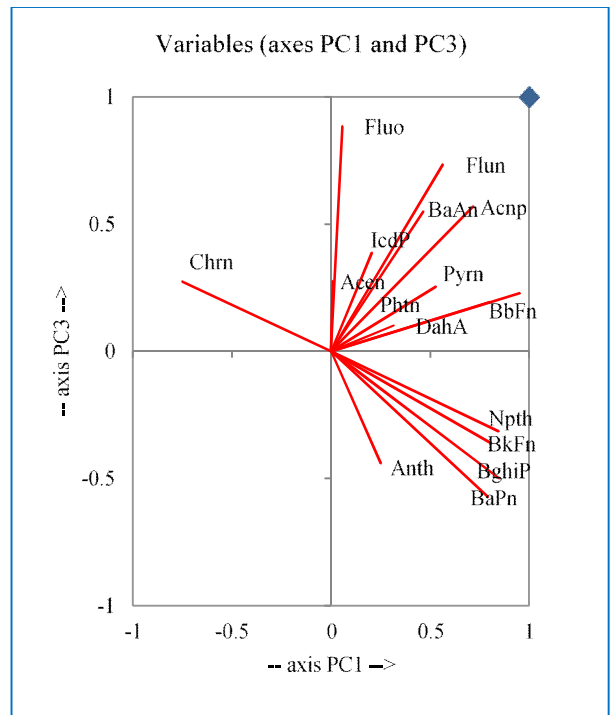


d.

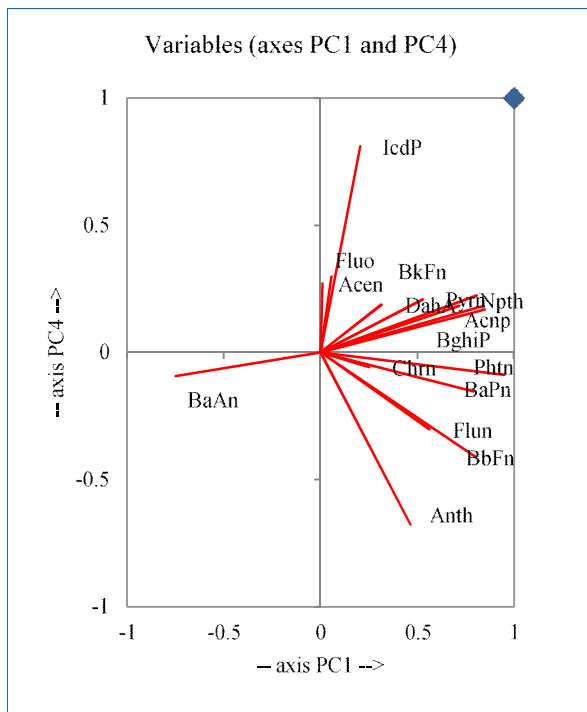
**Fig A3** Biplots between a. PC1 vs PC2, b. PC1 vs PC3, c. PC1 vs PC4 and d. PC2 vs PC3 in the winter season



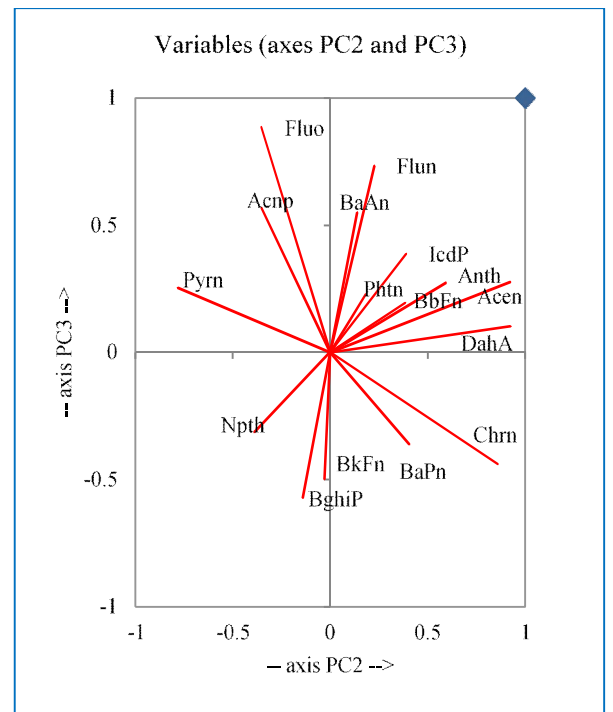
a.



b.



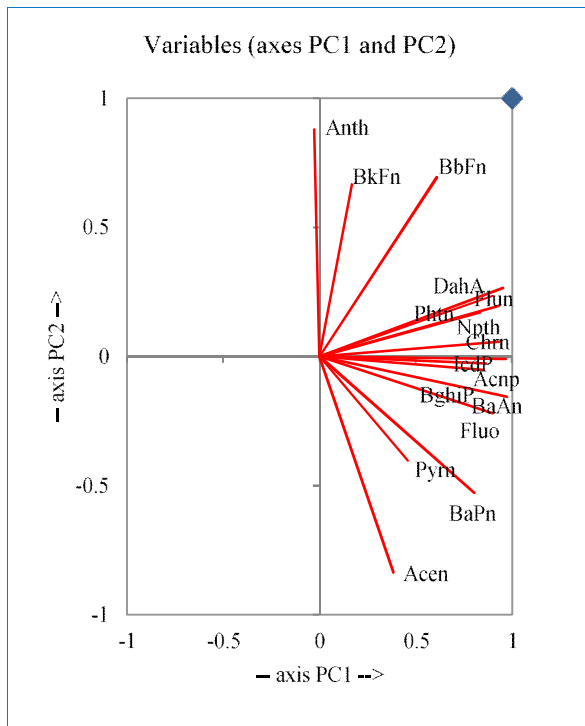
c.



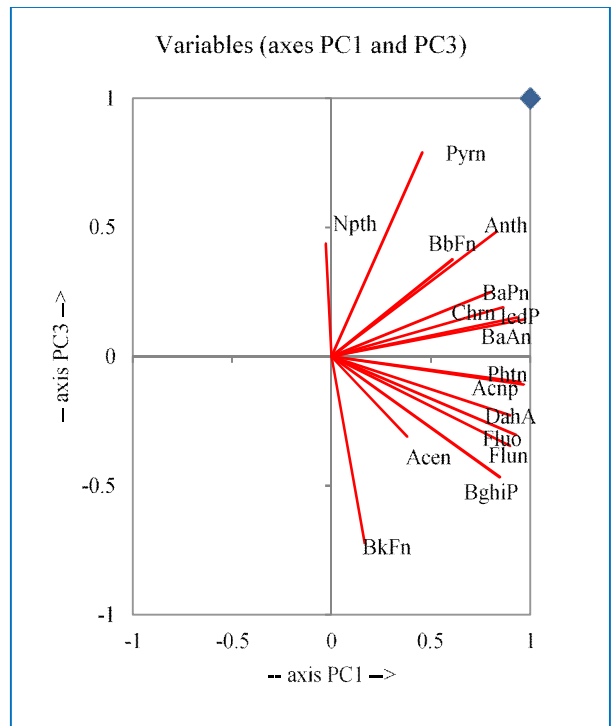
d.

**Fig A4** Biplots between a. PC1 vs PC2, b. PC1 vs PC3, c. PC1 vs PC4 and d. PC2 vs PC3 in the spring season

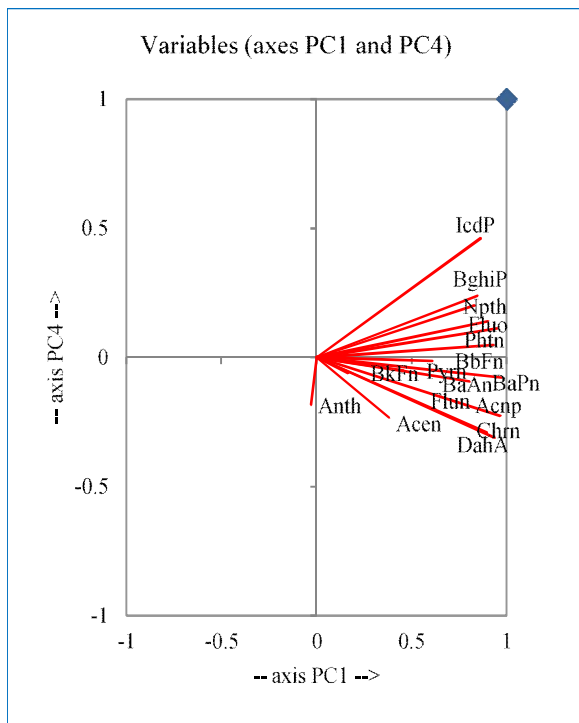




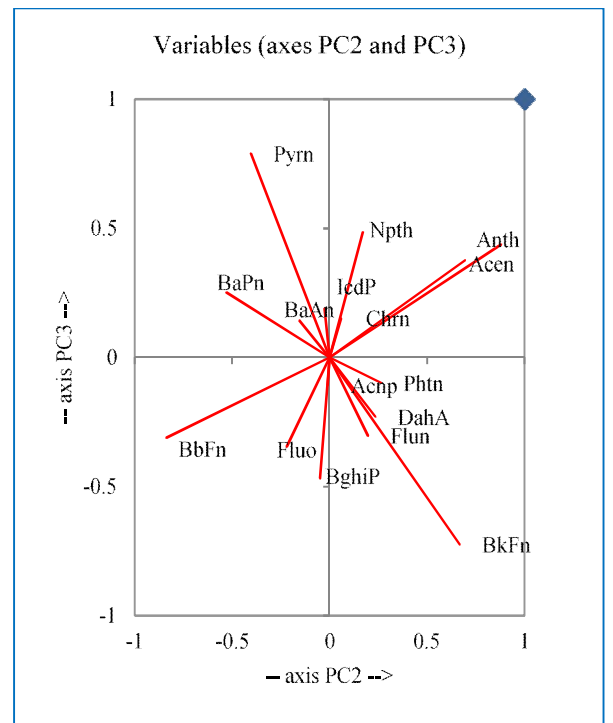
a.



b.

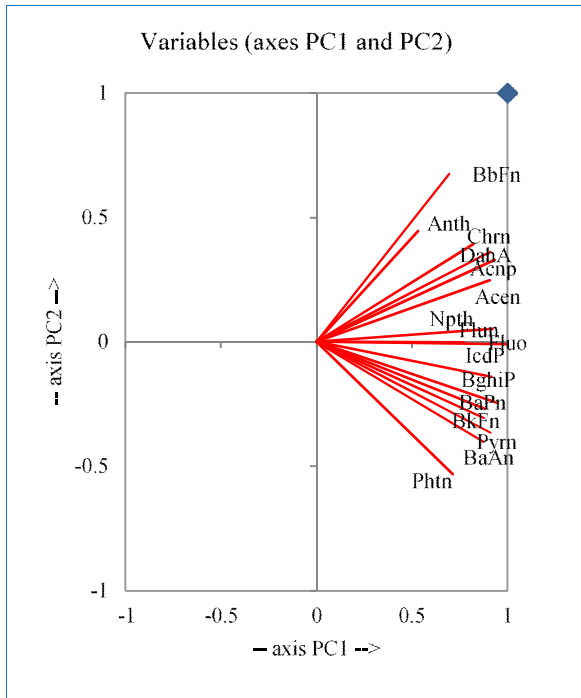


c.

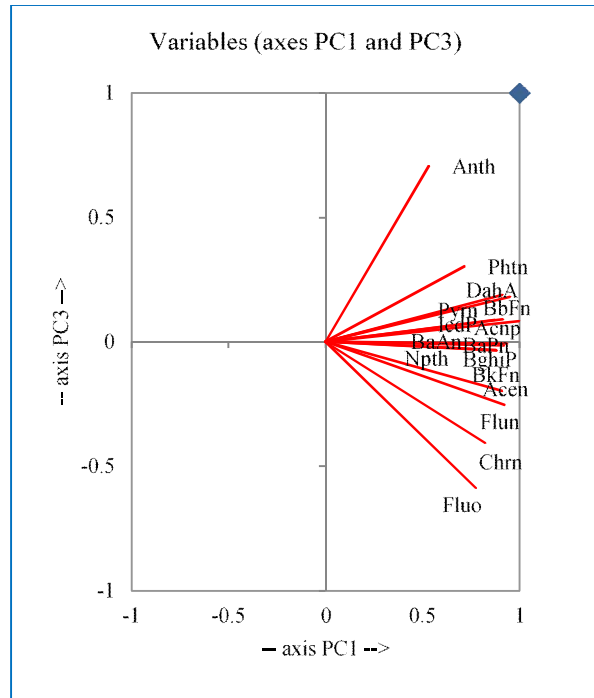


d.

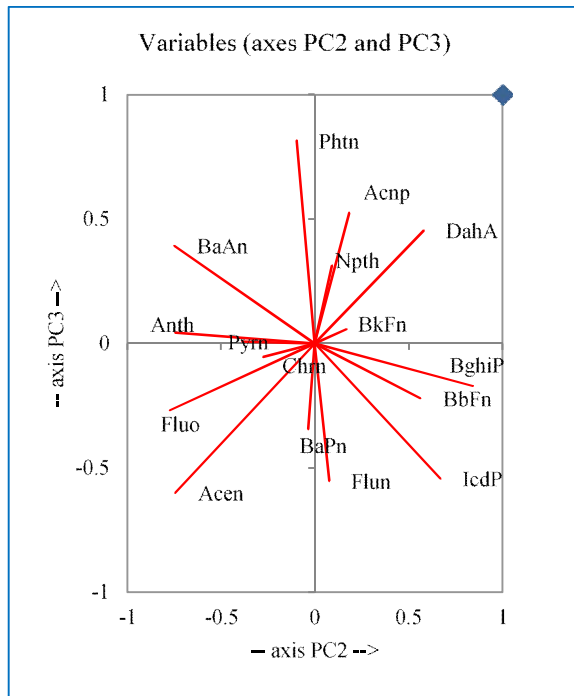
**Fig A5** Biplots between a. PC1 vs PC2, b. PC1 vs PC3, c. PC1 vs PC4 and d. PC2 vs PC3 in the summer season



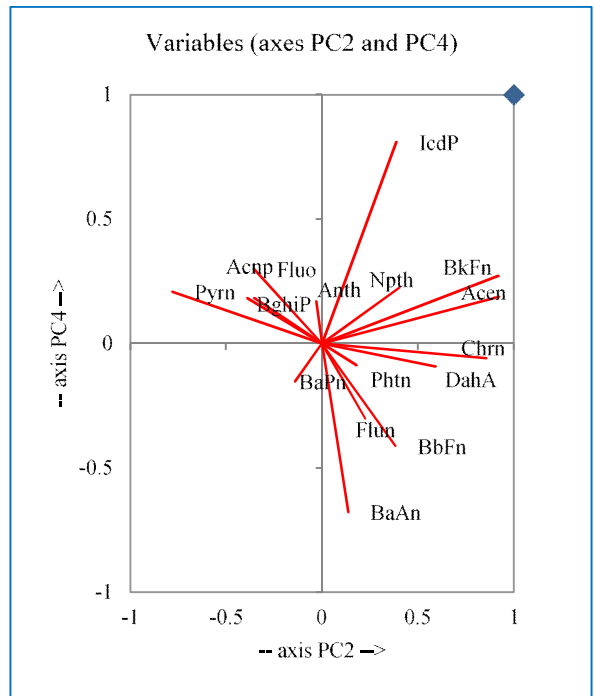
a.



b.



c.



d.

**Fig A6** Biplots between a. PC1 vs PC2, b. PC1 vs PC3, c. PC1 vs PC4 and d. PC2 vs PC3 throughout the study period

## *Publications*

# Estimation of risk factor of elements and PAHs in size-differentiated particles in the National Capital Region of India

Naba Hazarika<sup>1</sup> · Arun Srivastava<sup>1</sup>

Received: 13 May 2016 / Accepted: 19 September 2016  
© Springer Science+Business Media Dordrecht 2016

**Abstract** Size-differentiated particulate matters (viz. fine and coarse) were analyzed for quantification of elements and associated polycyclic aromatic hydrocarbons with energy dispersive X-ray fluorescence and gas chromatography-mass spectrometry techniques for the samples collected through Dekati PM<sub>10</sub> impactor and Sioutas five-stage cascade impactor from five different sites of the National Capital Region, India for the year 2014–2015. The dominant sources of elements were crustal origin and diverse man-made activities revealed by principal component analysis, while for polycyclic aromatic hydrocarbons, it was attributed to be emitted from vehicular fuels, combustion processes (such as coal, wood, and biomass burning) and petrogenic sources indicated by molecular diagnostic ratios. Chronic health risk assessment was also observed for the species: elements and polycyclic aromatic hydrocarbons. The observed hazard quotient of an individual species was less than unity, but the hazard index of the species was found to be greater than unity.

**Keywords** Particulate matters · Elements and PAHs · Source identification · Hazard index

## Introduction

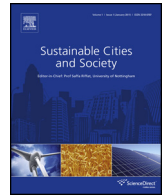
Particulate matters (PMs) of size-segregated have been studied widely due to their great impact on human health.

✉ Naba Hazarika  
naba1612@gmail.com

✉ Arun Srivastava  
srivastava02@hotmail.com

<sup>1</sup> Laboratory No. 302, School of Environmental Sciences, Jawaharlal Nehru University, New Delhi 110067, India

The chemistry of respirable suspended particulates shows larger health effects on human due to its potential penetrating power into the lungs causing lung dysfunctions which in turn cause long-term as well as short-term effects such as respiratory and cardiovascular abnormalities (Shridhar et al. 2010; Hazarika et al. 2015). The particles having size range <2.5 μm have been established as more detrimental than the size range <10 μm due to their depositional characteristics in the respiratory system (Villar-Vidal et al. 2014). Besides the relationship of inhalation of PMs and health effects, the other properties such as biological, chemical, and physical are also important factors on the effects of PMs on human health which has been observed by the epidemiological studies (Manousakas et al. 2014). Up to now, elements (metals and non-metals) and polycyclic aromatic hydrocarbons (PAHs) adhered with PMs have also been studied at various sites of the capital of India (Sarkar et al. 2010; Sarkar and Khillare 2011; Singh et al. 2011) and throughout the globe (Valavanidis et al. 2008; Szabó et al. 2015) due to their complex chemistry in ambient atmosphere. Further, excluding metallic abundances, only the PAHs of particle phase are also carried out in different parts of the world up to the present (Martins et al. 2013; Ré et al. 2015). The rapid growth of urbanization, vehicular transportation, and industrialization in Delhi and the National Capital Region (NCR) are the key factors for the changing air quality. In case of Delhi, the government was the key initiator for policymaking, while the Supreme Court of India has suggested the government to implement air policies effectively. The World Bank and the Central Pollution Control Board (CPCB) already announced the possible decrease in the concentration level of suspended particles in 2005. For obtaining the sustainability regarding air pollution and issue of urban transport, the National Urban Transport Policy (NUTP) was



# Quantification of particle bound metallic load and PAHs in urban environment of Delhi, India: Source and toxicity assessment



Naba Hazarika\*, Arun Srivastava\*, Arunangshu Das

School of Environmental Sciences, Jawaharlal Nehru University, New Delhi 110067, India

## ARTICLE INFO

### Article history:

Received 1 July 2016

Received in revised form

20 November 2016

Accepted 23 November 2016

Available online 25 November 2016

### Keywords:

Particulate matters

Metals/metalloids

PAHs

Source identification (PCA)

Excess cancer risk

## ABSTRACT

The present investigation was carried out to observe the concentration variation of metals/metalloids and Polycyclic Aromatic Hydrocarbons (PAHs) associated with size-segregated particles and its probable emission sources along with the toxicity level in urban environment from the capital of India. Energy Dispersive X-ray Fluorescence (EDXRF) and Gas Chromatography-Mass Spectrometry (GC-MS) techniques were applied for the quantification of metals/metalloids and PAHs in fine (<2.5 μm) and coarse (>2.5 μm) mode particles for the samples collected from four different sensitive sites in Delhi (India) during the year 2012–13. The observed load of metals/metalloids as well as PAHs predominated the fine mode particles, while it was lesser in coarse mode particles regardless the sites. Among metals/metalloids; Si had the highest average percentage contribution (~14%), and similarly Benzo[a]pyrene had highest average percentage contribution (~23%) among PAHs. Source apportionment of metals/metalloids and PAHs were carried out by applying the Principal Component Analysis (PCA). Crustal re-suspension, vehicular transportations and industrial activities were found to be the major sources of metals/metalloids; while vehicular emission, burning of biomass and coal were the responsible factors for PAHs. Molecular Diagnostic Ratio (MDR) also showed similar emission sources of PAHs. Excess cancer risk were observed for Ni, As and Pb; where As had the highest inhalation carcinogenic risk.

© 2016 Elsevier Ltd. All rights reserved.

## 1. Introduction

Polycyclic Aromatic Hydrocarbons (PAHs) and metals/metalloids associated with particulate matters have been given importance long since due to their adverse health effects on human. Transport of particles, their dry and wet deposition in ambient atmosphere affect living beings and are related to anthropogenic and natural activities (Calvo et al., 2013). The intrinsic connection between metals/metalloids and PAHs can put serious dimensions in the dynamic behaviour i.e., residence time, transportation pattern and health effects in a particular region. PAHs; which are known to be ubiquitous pollutants in the environment are site specific, where anthropogenic activities and meteorological parameters play an important role in determining their levels throughout the season (Birgul & Tasdemir, 2015; Ma et al., 2013; Ravindra et al., 2006; Yadav, Tandon, & Attri, 2013a; Yin, Qiu, Ye, Li, & Liang, 2015). Spatial and temporal variability of pollutants is seasonal and the colder season registers

considerably higher levels of particulate bound species (such as metals/metalloids, PAHs etc.). At present, incomplete combustion of organic materials are the main causes of emission of PAHs which are linked with vast use of wood and/or biomass, coal, oil, gas etc. (Alebić-Juretić, 2015; Tobiszewski & Namieśnik, 2012; WHO, 2000; Wang, Chen, Yang, Qiao, & Tian, 2007). Because of the rise of PAHs in ambient air, a larger size of population gets exposed to the perils of toxicity of emission (Villar-Vidal et al., 2014).

Different approaches have been made to analyze the metals/metalloids and PAHs content present in various size ranges of particulate matters viz. PM<sub>2.5</sub>, PM<sub>10</sub> or both at various locations in India (Sarkar & Khillare, 2011; Sarkar, Khillare, Jyethi, Hasan, & Parween, 2010; Singh, Gadi, & Mandal, 2011) and abroad (Dallarosa, Teixeira, Meira, & Wiegand, 2008; Ercan and Dinçer, 2016; Gaga et al., 2012; Jeng, 2010; Minguillón et al., 2012; Szabó, Nagy, & Erdős, 2015; Tolis et al., 2015; Vuković et al., 2014). To investigate the source apportionment and/or risk assessments of particulate bound species; efforts have been made so far (Hieu & Lee, 2010; Massey, Kulshrestha, & Taneja, 2013; Sarkar & Khillare, 2011). Researchers have also focused on ultrafine mode of particles for their major role in the indoor and/or outdoor environments (Afshari, Matson, & Ekberg, 2005; Géhin, Ramalho, & Kirchner, 2008; Kumar et al., 2014; Levy, Dumyahn, & Spengler, 2002;

\* Corresponding authors.

E-mail addresses: [naba1612@gmail.com](mailto:naba1612@gmail.com) (N. Hazarika), [srivastava02@hotmail.com](mailto:srivastava02@hotmail.com) (A. Srivastava).

# Source identification and metallic profiles of size-segregated particulate matters at various sites in Delhi

Naba Hazarika · V. K. Jain · Arun Srivastava

Received: 13 March 2015 / Accepted: 12 August 2015 / Published online: 29 August 2015  
© Springer International Publishing Switzerland 2015

**Abstract** A study of elemental composition in the ambient air of Delhi was carried out in the monsoon, winter and summer seasons at four different sites from August 2012 to April 2013 in the size ranges <1, 1–2.5, 2.5–10 and >10  $\mu\text{m}$  using “Dekati PM10” impactor. At each site, three samples were collected and were analyzed by energy-dispersive X-ray fluorescence (EDXRF). The presence of elements was found to be very common and highly concentrated in aerosol particles at all the sites, which are Na, Al, Si, K, Ca, Zn and Ba. Total suspended particulate matters (TSPMs) of fine particles were found high in comparison to coarse particles at all seasons. The TSPM of fine particles was found to be varied in the range from 303.6 to 416.2  $\mu\text{g}/\text{m}^3$ . Similarly, the range of coarse TSPM was observed from 162.9 to 262.8  $\mu\text{g}/\text{m}^3$ . Correlation matrices were observed between fine (size ranges <1 and 1–2.5  $\mu\text{m}$ ) and coarse (size ranges 2.5–10 and >10  $\mu\text{m}$ ) size particles for all elements with seasons. Source apportionments of elements were carried out using MS Excel 2010 through XLSTAT software. The source apportionments between fine and coarse particles were carried out through factor analysis and dominated sources found to be crustal re-suspension and industrial activities.

**Keywords** Aerosols · Fine particles · Coarse particles · Source apportionment · EDXRF

## Introduction

Particulate matters  $\text{PM}_{10}$ ,  $\text{PM}_{2.5}$  and  $\text{PM}_{10}$  have been playing a major role in the atmosphere by making their chemistry adhered with elements. The particulate matters of the size ranges from  $\text{PM}_1$  to  $\text{PM}_{2.5}$  have a history of long-term and short-term effects on human health resulting with asthma, coughing and sneezing, heart attack, cancer, etc. which, in turn, follow chronic or acute effects (Niu et al. 2010; Shridhar et al. 2010). The meteorological parameters and diverse sources, which vary with time and space, determine the concentration of aerosols in the ambient atmosphere (Pipal et al. 2011; Lowenthal et al. 2014; Odeshi et al. 2014). The emission of toxic heavy metals has been increasing day by day due to rapid increase in number of industries worldwide, which, in turn, increases the health risk of the civilization. In the present scenario, crustal re-suspension is assumed to be an important factor in the environment for the elements like Ca, Mg, etc. (Jain et al. 2000; Das et al. 2006; Pekey et al. 2013), but vehicular traffic and industrial activities are also the responsible factors which have been reported so far (Lopes et al. 2006; Morawska et al. 2008; Chatterjee et al. 2012; Mansha et al. 2012; Yarkin et al. 2012; Pekey and Dogan 2013). The presence of elements in size-segregated particulate matters of fine and coarse mode particles with different seasons varies due to

---

N. Hazarika · V. K. Jain · A. Srivastava (✉)  
School of Environmental Sciences, Jawaharlal Nehru University,  
New Delhi 110067, India  
e-mail: srivastava02@hotmail.com

A. Srivastava  
e-mail: a\_srivastava@mail.jnu.ac.in



ISSN NO. 2320-5407

Journal homepage: <http://www.journalijar.com>

INTERNATIONAL JOURNAL  
OF ADVANCED RESEARCH

## RESEARCH ARTICLE

## SEM-EDX analysis of size segregated particulate matter in Allahabad located in north India

Rajesh Kushwaha, Naba Hazarika, Arun Srivastava\*

School of Environmental Sciences, Jawaharlal Nehru University, New Delhi-110067, India.

**Manuscript Info****Manuscript History:**

Received: 14 June 2013  
Final Accepted: 23 June 2013  
Published Online: July 2013

**Key words:**

Particulate matter,  
particulate morphology,  
size fraction, metals,  
SEM-EDX, Allahabad.

**Abstract**

Aerosol samples of size ranges  $PM_{<1}$ ,  $PM_{1-2.5}$ ,  $PM_{2.5-10}$ , and  $PM_{\geq 10}$  were collected from urban and rural area of Allahabad. The average mass concentration of  $PM_{<1}$  was  $85.87 \pm 37.45 \mu\text{g}/\text{m}^3$ ,  $PM_{1-2.5}$   $51.14 \pm 9.48 \mu\text{g}/\text{m}^3$ ,  $PM_{2.5-10}$   $44.25 \pm 15.35 \mu\text{g}/\text{m}^3$  and  $PM_{\geq 10}$  was  $46.22 \pm 17.03 \mu\text{g}/\text{m}^3$  at urban site while at rural site it was found  $PM_{<1}$   $65.51 \pm 20.24 \mu\text{g}/\text{m}^3$ ,  $PM_{1-2.5}$   $50.91 \pm 9.45 \mu\text{g}/\text{m}^3$ ,  $PM_{2.5-10}$   $48.7 \pm 6.25 \mu\text{g}/\text{m}^3$  and  $PM_{\geq 10}$   $25.08 \pm 14.60 \mu\text{g}/\text{m}^3$ . Scanning electron microscopy–energy dispersive X-ray analysis (SEM-EDX) was used to understand the differences in morphology, elemental composition of particulate matters viz.  $PM_{<1}$ ,  $PM_{1-2.5}$ ,  $PM_{2.5-10}$  and  $PM_{\geq 10}$  respectively. The SEM micrograph, size segregated aerosol was different at the two sites. It was observed that SEM-EDX is a useful method to identify the source of emission of particulate matter. The results revealed concentration of pollution is site specific but largely because of industry, vehicular activities, crustal dust and soil.

Copy Right, IJAR, 2013;. All rights reserved.

**Introduction**

Solid or liquid particles or both dispersed in gaseous medium, found in air are termed as aerosol [Reist, 1933; Vincent, 1989]. Atmospheric aerosol consists of particle of both natural and anthropogenic origins. It is now well established that the element from natural sources are generally found in the coarse particle whereas element emitted from anthropogenic activities are associated with fine particles (Seinfeld, 1986). The importance of atmospheric aerosols is because of their impact on human health (Dockery, *et al.*, 1993), ability to scatter light, thereby affecting visibility, and their role in global climate change (Seinfeld, 1986). Most importantly, the particle size distribution of aerosols is vital for an accurate and reliable assessment of their impact on human health (Fernandez, *et al.*, 2001). This is due to the degree of respiratory penetration retention, which is a direct function of the aerodynamic diameter of these particles. It has been found that particles  $>30 \mu\text{m}$  in aerodynamic diameter have a low probability of entering the nasal passage of humans. Particles with diameter  $>5 \mu\text{m}$  are usually filtered in the nose. Particles with  $<1-2 \mu\text{m}$  diameter predominantly get deposited in the alveolar region of the lung during

normal breathing (Mccornac, 1971). The size distribution of particles and its associated metals, which are important from the viewpoint of identification of the source of pollution and their adverse impact on human health [Espinoza, *et al.*, 2001; Haywood, *et al.*, 1997]. In addition, particles size characteristic of aerosol also affect cloud physics [Muller, *et al.*, 1999; Haywood, and Ramaswamy, 1998]. In the past, several investigations have been carried out on the measurements of size distribution of aerosol and associated elemental concentration in urban areas (Kushwaha, *et al.*, 2012; Infante, and Acosta, 1991; Spengler, and Thurston, 1983; Zoller, *et al.*, 1974). Size distribution of atmospheric particles where heavy metals are associated, plays a very important role not only due to their toxicity when inhaled, but also because they control the extent to which metals may be dispersed via atmospheric transportation. The elevated metal concentration can pose serious risk to human health. Therefore, the determination of metal levels is usually limited to estimating the concentration of a number of metals in TSP, although these measurements can give some indication of the general pollution level in an area (Fernandez, *et al.*, 2000). Earlier studies have indicated that the rate of



## TRAFFIC RELATED AEROSOL EXPOSURE AND THEIR RISK ASSESSMENT OF ASSOCIATED METALS IN DELHI, INDIA

Rajesh Kushwaha, Naba Hazarika and Arun Srivastava\*

School of Environmental Sciences, Jawaharlal Nehru University

New Delhi 110067, India

Tel (+91-9958257889) and Fax (+91-2671502)

\*Corresponding author: srivastava02@hotmail.com

### Abstract

A pilot study was carried out in New Delhi, India, to assess the level of traffic related aerosol exposure, individually and associated metals. These investigations also try to formulate their risk assessment using different modes of transport on a typical journey to work route and compared Bus, Auto-rickshaws and Bike (Two Wheelers) during the journey. The inhalable particulate matter monitored in winter period and also evaluated the potential health risk due to inhalation in the study. The exposure of Particulate matter was observed maximum in the Bike ( $502 \pm 176.38 \mu\text{gm}^{-3}$ ) and minimum in the Auto-rickshaw ( $208.15 \pm 61.38 \mu\text{gm}^{-3}$ ). In case of human exposure to metals (viz. Cu, Cd, Mn, Pb, Ni, Co, Cr, Fe, Zn), it was mostly exposed by Fe, Zn and Co and least exposed by Cd, Cr and Pb. Human health risk was estimated based on exposure and dosage response. The assessment of particulate-bound elements was calculated by assuming exposure of 6 h. The findings indicated that the exposure to particulate bound elements have relatively more adverse health effects.

Key words: Inhalable Aerosol, Personal Exposure, Metals, Risk Assessment, Hazardous Quotient

### Introduction

Vehicles are a major source of pollutants in Delhi; the daily pollution load has increased from 1,450 tons in 1991 to 3,000 metric tons in 1997 (MoEF, 1997). The share of the transport sector has increased from 64% to 67% during the same period while that of the industrial sector (including power plants) has decreased from 29% to 25% (MoEF, 1997). Suspended particulate matter is one of the most critical air pollutants in India, especially in Delhi; millions of people breathe air with high concentrations of dreaded pollutants. The air is highly polluted in terms of suspended particulate matter in most cities especially in Delhi (Prasad et al., 2003; Kushwaha et al., 2012). It is estimated the incidence of mortality and morbidity in different groups in India is due to exposure to  $\text{PM}_{10}$ . These impacts translated into economic values. The results indicated 2.5 million premature deaths and total morbidity and mortality costs ranges from Rs 885 billion to 4250 billion annually region wide. Urban air pollution is estimated to cause 250,000 death and billions of cases respiratory illnesses



# Estimation of bioaerosol in indoor environment in the university library of Delhi

Bipasha Ghosh,<sup>1</sup> Himanshu Lal,<sup>2</sup> Rajesh Kushwaha,<sup>2</sup> Naba Hazarika,<sup>2</sup> Arun Srivastava<sup>2,\*</sup> and Vinod Kumar Jain<sup>2</sup>

<sup>1</sup>Indira Gandhi Academy of Environmental Education Research and Ecoplanning  
Jiwaji University  
Gwalior 474011, India

<sup>2</sup>School of Environmental Sciences  
Jawaharlal Nehru University  
New Delhi 110067, India

**Key Words:** Bioaerosol, library environment, source identification, allergic fungi, indoor air quality

## ABSTRACT

Ambient levels of viable bioaerosol (fungi, Gram positive and negative bacteria) were measured in Central Library, Jawaharlal Nehru University, New Delhi during July 2011 to October 2012. Study was done at five indoor sites [basement, reading hall, 3rd, 4th and 5th floors] and one outdoor. Air samples were drawn into standard petri dishes using Buck Bio-culture pump at a flow rate of 40 L min<sup>-1</sup> for 1 min. This study reveals interesting relationship between the concentration of fungal spores and bacteria in relation to both environmental and human factor. Most observed fungal species detected in the samples were *Rhizopus oryzae*, *Aspergillus nidulans* and *Aspergillus flavus*. Specific bacterial identification was not possible but Gram staining followed by microscopic analysis helped in deriving the different shapes of bacteria collected. *Bacillus* and *Coccus* were found maximally. Indoor/Outdoor ratio above 1 for fungal spores signified higher source in the indoor environment at different sections. In indoor environment highest fungal concentration was found in Basement (3140 colony-forming units (CFU) m<sup>-3</sup>) while lowest in 3rd floor (2560 CFU m<sup>-3</sup>). In case of bacterial concentration both Gram negative and positive bacteria were found maximum in the Reading Hall (792 and 696 CFU m<sup>-3</sup>, respectively) while lowest in 3rd floor (475 and 437 CFU m<sup>-3</sup>, respectively). Higher bacterial counts were primarily attributed to the number of library occupants. High concentration may be due to larger rate of shedding of human skin cells, microbes released from respiratory tract and transport of microbes from floor surfaces on suspended particles.

## INTRODUCTION

As a generic class of airborne pollutants, particulate matter usually associated with compounds of biological origin is often termed as "Bioaerosol". This definition includes all airborne microorganisms regardless of viability or ability to be recovered by culture; it comprises whole microorganisms as well as fractions, biopolymers and products from all varieties of living things [1]. Bioaerosols may consist of pathogenic or non-pathogenic, live or dead fungi and bacteria, bacterial endotoxins, mycotoxins, peptidoglycans,  $\beta$  (1,3)-glucans, viruses, high molecular weight allergens, pollens, etc. [2].

Bioaerosols may originate from almost any natural or man-made surface and each source may give rise to an entirely unique assemblage of air microbes. Different environments that are mainly bioaerosol sensitive are animal housing [3], composting and dumping sites [4], ceilings and walls of indoor surfaces [5], saw mills [6], and food processing and manufacturing plants [7]. Poor indoor air quality has been shown to cause several health hazards. In many indoor environments airborne bacteria, fungi and their fragments may fall into respirable size range that can penetrate deep into human lungs (< 10  $\mu$ m) [8,9]. The presence of undesirable bioaerosols is often associated with sick building syndrome (SBS) and building related illnesses [10]. Sources include furnishings and building materi-

\*Corresponding author  
Email: srivastava02@hotmail.com